

UNIVERSITY OF LATVIA

Faculty of Biology



Anna Kiršteina

DOCTORAL THESIS

**THE IMMUNOPROTECTIVE AND DIAGNOSTIC POTENTIAL OF
INFLUENZA VIRUS HAEMAGGLUTININ STALK DOMAIN FOR
DEVELOPMENT OF NOVEL VACCINE PROTOTYPES**

Promotion to the degree of Doctor of Biology

Molecular Biology

Supervisor: Dr. biol. Andris Kazāks

Riga, 2022

The work of this doctoral thesis was carried out at the Latvian Biomedical Research and Study Centre from 2017 to 2021.



Latvian Biomedical
Research and Study Centre
research and education in biomedicine from genes to human

NATIONAL
DEVELOPMENT
PLAN 2020



EUROPEAN UNION
European Regional
Development Fund

INVESTING IN YOUR FUTURE

The research was supported by the EU Seventh Framework Programme for research (No. 602,437), ERDF grant (No. 1.1.1.1/16/A/054), Egide (Osmosis project No. 39719WH), State Education and Development Agency of Latvia (Osmosis project No. LV-FR/2018/2), European Research Council (ERC-2015-CoG GA 648974 to GP), CNRS (IR-RMN FR3050), EC (project iNext GA 653706), and Equipex contracts (ANR-10-EQPX-47-01; ANR-15-CE29-0022-01).

Form of the thesis: collection of research papers in biology, subfield – molecular biology.

Supervisor: Dr. biol. Andris Kazāks

Reviewers:

- 1) Dr. biol. Andris Dišlers, Latvian Biomedical Research and Study Centre
- 2) Dr. biol. Andris Zeltiņš, Latvian Biomedical Research and Study Centre
- 3) Dr. rer. nat., prof. Rainer Ulrich, Federal Research Institute for Animal Health, Greifswald, Germany

The thesis will be defended at the public session of the Doctoral Committee of Biology, University of Latvia, at 11:00 on June 9st, 2022 at Latvian Biomedical Research and Study Centre, Ratsupites Str. k-1.

The thesis is available at the Library of the University of Latvia, Kalpaka blv. 4.

This thesis is accepted for the commencement of the degree of Doctor of Biology on April 21st, 2022 by the Doctoral Committee of Biology, University of Latvia.

Chairman of the Doctoral Committee: _____ / Dr. biol., prof. Kaspars Tārs /

Secretary of the Doctoral Committee: _____ / Dr. biol. Daina Eze /

© University of Latvia, 2022

© Anna Kiršteina, 2022

ABSTRACT

The effectiveness of current influenza vaccination strategies is challenged by the high mutation rates and antigenic flexibility of influenza viruses. More effective vaccination options are needed to protect the vulnerable risk groups against seasonal outbreaks and to improve pandemic preparedness. Targeting evolutionarily conserved influenza proteins could improve cross-reactive immunity and alleviate the burden of annual vaccine component reformulation. The conventional vaccines mainly target the immunodominant head domain of influenza surface protein hemagglutinin (HA). However, constant antigenic evolution of the head domain allows the virus to escape the pre-existing antibody responses. HA stalk domain, on the other hand, is evolving much more slowly. It is therefore relatively well conserved across influenza subtypes and targeted by broadly protective antibody responses.

The aim of this study was to develop an influenza vaccine candidate that includes a virus-like particle (VLP) displayed HA stalk antigen in its native trimeric form. We analyzed several stalk antigens in their free and VLP displayed state for their potency to induce cross-reactive antibody responses and to protect against various influenza virus infections in mice. All vaccine proteins were recombinantly produced in microbial expression systems, resulting in high yields of the target protein. While VLP displayed linear stalk was immunogenic and induced cross-reactive antibody responses, it did not contain conformational epitopes associated with potent protection against disease symptoms. Free stalk antigen served as a useful tool to assess stalk-specific immunity in the pre-pandemic sera of people with occupational contact to swine. Genetic fusion of stalk and bacteriophage coat protein genes yielded soluble aggregates, but chemical VLP functionalization resulted in successful particle display. Employing X-ray crystallography and magic angle spinning solid-state nuclear magnetic resonance, we observed preservation of the trimeric post-fusion folding state in both free and VLP-coupled forms of stalk antigens. Although VLP displayed stalk antigen induced potent cross-reactive antibody in mice, it was unable to protect against lethal influenza challenges. Simultaneous display of the stalk antigen and a triplet M2 protein ectodomain on the same particle broadened the immune mechanisms and increased vaccine-induced protective effect. The multimeric VLPs afforded robust protection against standard heterologous and heterosubtypic influenza challenges, as well as high-dose homologous influenza infection. Our results herein indicate that a combined application of genetic and modular functionalization to expose two different conserved influenza antigens on a single particle is a promising approach for the development of a multivalent broadly protective influenza vaccine.

KOPSAVILKUMS

Gripas vīrusu mutēšanas ātrums un antigēnu mainība samazina šobrīd licencēto gripas vakcīnu efektivitāti. Lai aizsargātu riska grupas pret sezonālajiem gripas uzliesmojumiem un uzlabotu gatavību pandēmijām, ir nepieciešamas jaunas vakcinācijas stratēģijas. Vakcīna, kas mērķēta pret konservatīviem gripas vīrusa proteīniem, varētu paplašināt inducēto imunitāti un novērst nepieciešamību pēc ikgadējas vakcīnas komponentu atjaunošanas. Šī brīža vakcīnu darbība galvenokārt tiek mērķēta pret gripas vīrusa virsmas proteīna hemaglutinīna (HA) imunodominanto galvas domēnu. Nepārtraukta galvas domēna epitopu evolūcija ļauj vīrusam izvairīties no esošajām antivielu reakcijām. HA stalka domēnam raksturīga daudz zemāka mainība. HA stalks ir salīdzinoši konservatīvs starp dažādiem gripas vīrusa apakštipiem, un pret to mērķēta plaši aizsargājošu antivielu iedarbība.

Šī pētījuma mērķis bija izstrādāt gripas vakcīnas kandidātu, eksponējot HA stalka trimēru tā natīvajā trimēra konformācijā uz vīrusiem līdzīgo daļiņu (VLP) virsmas. Mēs salīdzinājām vairākus stalka antigēnus brīvā un uz VLP eksponētā formā pēc to spējas pelēs inducēt plaši iedarbīgas antivielu atbildes un pasargāt pret dažādu gripas vīrusu infekcijām. Visi vakcīnu proteīni tika rekombinanti producēti mikrobiālās ekspresijas sistēmās, iegūstot augstu mērķa proteīna iznākumu. Lai gan uz VLP eksponēts lineārs stalks bija imunogēns un izsauca plašu antivielu atbildi, tas nesaturēja konformacionālus epitopus, kas ir saistīti ar spēcīgu aizsardzību pret slimības simptomiem. Stalka antigēns tika izmantots, lai noteiktu stalka specifisko imunitāti serumā, kas pirms pandēmijas iegūts no cūkkopības darbiniekiem. Ģenētiski sapludinot stalka peptīda un VLP bakteriofāgu apvalka proteīnu gēnus, tika iegūti šķīstoši agregāti, savukārt ķīmiskas konjugācijas rezultātā stalks tika eksponēts uz VLP virsmas. Izmantojot rentgenstaru kristalogrāfiju un kodolu magnētisko rezonansi ar griešanu zem maģiskā leņķa, tika novērota stalka antigēnu zema pH trimēra formas saglabāšanās gan brīvā, gan VLP-saistītā formā. Lai gan uz VLP virsmas eksponēts stalka domēns pelēs izsauca spēcīgu un plašu antivielu atbildi, tas nepasargāja pret letālām gripas vīrusu infekcijām. Uz vienas daļiņas vienlaicīgi eksponējot gan stalku, gan trīskāršu M2 proteīna ektodomēnu tika panākta imūno mehānismu dažādošana un palielināts vakcīnas aizsargājošais efekts. Multimēriskās VLP nodrošināja stabilu aizsardzību pret standarta heterologu un heterosubtipisku gripas vīrusu infekcijām, kā arī homologu lielas devas gripas vīrusa infekciju. Mūsu rezultāti liecina, ka ģenētiskās un modulārās funkcionalizācijas pieeju apvienošana, lai uz vienas daļiņas eksponētu divus dažādus konservatīvus gripas antigēnus, ir daudzsoļa pieeja multimēriskās plaši aizsargājošas gripas vakcīnas izstrādē.

TABLE OF CONTENTS

ABBREVIATIONS	7
INTRODUCTION	8
1. LITERATURE OVERVIEW	9
1.1 Influenza virus	9
1.1.1 General characteristics of influenza	9
1.1.2 Influenza diversity	11
1.1.3 Influenza plasticity	12
1.2 Influenza A virion.....	15
1.2.1. Virion structure and proteins	15
1.2.2 The structure and functions of influenza HA	19
1.3 Limitations of conventional vaccination strategies	22
1.4 Novel vaccination strategies and broadly protective influenza vaccines	26
1.4.1 General considerations to obtain vaccines that are more effective	26
1.4.2 Broadly protective vaccines targeting internal influenza proteins	27
1.4.3 Broadly protective vaccines targeting influenza surface proteins	28
1.5 VLP-based vaccination strategies.....	34
1.5.1 General characteristics of VLPs	34
1.5.2 Variety of VLP sources and their production systems	34
1.5.3 The basis of VLP immunogenicity	36
1.5.4 Types of VLPs and their modification possibilities	38
2. MATERIALS AND METHODS.....	41
2.1 Plasmid construction.....	41
2.2 Plasmid DNA amplification and insert confirmation.....	42
2.3 Antigen expression	43
2.4 Protein purification.....	45
2.5 Coupling of HA stalk antigens to VLPs	48
2.6 Protein crystallization and structure determination	48
2.7 Enzyme-linked immunosorbent assay (ELISA).....	49
2.8 Statistical analyses	51
3. RESULTS	52
3.1 Production and purification of chimeric HBc virus-like particles carrying influenza virus LAH domain as vaccine candidates.....	52

3.2 Structure and applications of novel influenza HA tri-stalk protein for evaluation of HA stem-specific immunity	64
3.3 Construction and Immunogenicity of a Novel Multivalent Vaccine Prototype Based on Conserved Influenza Virus Antigens	81
3.4 Structural Analysis of an Antigen Chemically Coupled on Virus-Like Particles in Vaccine Formulation	105
4. DISCUSSION.....	112
5. CONCLUSIONS	120
6. THESIS.....	121
7. PUBLICATIONS	122
8. APPROBATION OF THE RESEARCH	123
9. ACKNOWLEDGEMENTS AND FUNDING	124
REFERENCES.....	125
APPENDICES	145

ABBREVIATIONS

- 3M2e – a triple M2e peptide;
A/pH1N1 – influenza A virus from the H1N1 subtype causing the 2009 pandemic;
ADCC – antibody-dependent cellular cytotoxicity;
ADCP – antibody-dependent cell-mediated phagocytosis;
AP/tri-stalk – phage AP205 coat protein VLPs displaying a tri-stalk antigen;
APC – antigen-presenting cell;
AP-M2e – phage AP205 coat protein VLPs displaying a 3M2e antigen;
AP-M2e/tri-stalk – phage AP205 coat protein VLPs displaying a 3M2e antigen and a tri-stalk antigen;
BSA – bovine serum albumin;
CDC – complement-dependent cytotoxicity;
cRNA – complementary RNA;
DC – dendritic cell;
DMSO – dimethyl sulfoxide;
EDTA – ethylenediaminetetraacetic acid;
ELISA – enzyme-linked immunosorbent assay;
Fc γ -Rs – Fc gamma receptors;
HA – hemagglutinin;
HBc – hepatitis B virus core;
IL-1 β – interleukin 1 beta;
IPTG – isopropyl β -D-1-thiogalactopyranoside;
IV – influenza vaccine;
K1-K1 – tandem core HBc VLPs displaying lysine linkers in both MIRs;
LAH – long alpha helix;
LAH1-PP7 – fusion protein of LAH3 and phage PP7 coat protein;
LAH3-HBc – tandem core HBc VLPs displaying LAH3 in MIR 1 and lysine linker in MIR 2;
M1 – matrix protein 1;
M2 – matrix protein 2 ion channel;
M2e – the ectodomain of M2 ion channel protein;
MAS-NMR – magic angle spinning solid-state nuclear magnetic resonance;
MHC – major histocompatibility complex;
MIR – major insertion region;
NA – neuraminidase;
NEP – nuclear export protein, formerly NS2;
NK-cells – natural killer cells;
NP – nucleoprotein;
NS1 – non-structural protein 1;
OD – optical density;
ORF – open reading frame;
PA – polymerase acidic protein;
PB1 – polymerase basic protein 1;
PB2 – polymerase basic protein 2;
PBS – phosphate-buffered Saline;
PCR – polymerase chain reaction;
PDB – protein data bank;
PEG – polyethyleneglycol;
rHA – recombinant full-length hemagglutinin;
RNP – ribonucleoprotein;
SATA – N-succinimidyl S acetylthioacetate;
SDS/PAGE – sodium dodecyl sulfate polyacrylamide gel electrophoresis;
SMPH – succinimidyl-6-((b-maleimidopropionamido)-hexanoate;
TAE – Tris acetate-EDTA buffer;
TNF α – tumor necrosis factor alpha;
VLP – virus like particle;
WHO – World Health Organization

INTRODUCTION

With the annual morbidity affecting 10-20% of the world's population, seasonal influenza virus remains a major disturbance to health care and the global economy. Adverse disease reactions can cause severe complications that can result in long-term consequences and death, particularly in people with underlying chronic conditions or extreme age. An effective vaccine should prevent excessive mortality. Yet, the genetic variability of influenza viruses interferes with current influenza vaccine effectiveness and raises concerns about the possibility of an emerging influenza pandemic, which could be only a few mutations away. The ongoing Sars-CoV-2 virus pandemic has emphasized that even with vaccines developed at record-breaking speed, there is no way to prevent millions of deaths during the months of vaccine testing, approval, and distribution process. The current influenza vaccine manufacturing technologies are either slow and mutation-prone or unable to produce sufficient doses for the global society, and they cannot compete with virus variability. Therefore, a broadly effective and cheap influenza vaccine remains an urgent, yet unsolved public health challenge.

One of the ways to outrun the constant influenza variability is to target its evolutionary conserved epitopes, thereby aiming for a broad spectrum of the induced immunity. Influenza virus hemagglutinin (HA) is the major vaccine- or infection- included antibody target. While its head domain tends to change under immune pressure, the stalk domain is structurally conserved and draws interest as a potential component for a broadly protective vaccine if properly presented to the immune system. Virus-like particles (VLPs) represent a potent and safe, yet relatively cheap platform for target antigen display as they embody the key morphological and immunological features of viruses without causing the infection: (1) high-density repetitive epitopes; (2) particulate nature; (3) ability to induce cellular and humoral immunity.

The aim of the study was to develop an influenza vaccine candidate that includes a VLP-displayed HA stalk antigen in its native trimeric form.

The tasks of the study:

- 1) Construct, express, and purify HA stalk-based vaccine candidates in their free and VLP-displayed form;
- 2) Perform structural studies of HA stalk antigens in their free and VLP-displayed form;
- 3) Assess the vaccine candidate immunogenicity and cross-reactivity in mice;
- 4) Evaluate the potency of the selected vaccine candidates to induce protective immunity in mice against homologous and heterologous influenza viruses.

1. LITERATURE OVERVIEW

1.1 Influenza virus

1.1.1 General characteristics of influenza

Human influenza is a communicable acute respiratory viral infection affecting the upper and lower airways (Fukuyama & Kawaoka, 2011). Influenza epidemics occur during the colder seasons in both hemispheres. Seasonal transmission patterns are less pronounced in the tropical countries where the virus spreads throughout the year (Tamerius et al., 2013). Despite the fact that the influenza virus has been known to mankind for almost 100 years, the annual morbidity incidence in a typical year is estimated to affect between 10-20% of the human population of which 3-5 million cases are registered as severe (Somes et al., 2018; WHO, 2018). Influenza kills as much as 290-650 thousand people each year, remaining as one of the leading causes of death caused by infectious diseases (CDC, 2021b; Iuliano et al., 2018). Subsequent side effects are an overwhelming impact on health care systems worldwide, work and school time losses, and a considerable direct and indirect socioeconomic disruption estimated to reach billions of euros every year (Preaud et al., 2014; Putri et al., 2018). Although the recent Sars-Cov-2 pandemic prevention measures have reduced influenza transmission to a historically low level, health experts predict the virus might preserve its regular seasonal transmission patterns once the restrictions are lifted (Jones, 2020; Olsen et al., 2020).

The potent spread of the influenza virus is based on its wide mode of transmission – respiratory droplets (particles $>10\ \mu\text{m}$) and aerosols (particles $<5\ \mu\text{m}$) are shed during coughing, sneezing, or talking of the infected patient and they may linger in the air and rapidly infect the epithelial cells of the respiratory tract of the nearby people. Alternatively, transmission can occur by means of direct contacts or fomites (Killingley & Nguyen-Van-Tam, 2013). Influenza viruses primarily replicate in the epithelial cells of the mammalian respiratory tract and in the epithelial cells of the avian intestinal tract (Krammer et al., 2018). Viral incubation usually lasts 1-2 days (C. Paules & Subbarao, 2017). An infected person may transmit the virus even before the first symptoms of the disease appear, but the viral shedding typically peaks in the first two days of clinical illness and correlates with disease severity (Ip et al., 2016). Virus replication results in cell death of human pulmonary epithelial and immune cells with pro-inflammatory and immunopathology implications (Downey et al., 2018). The clinical presentation of influenza varies from asymptomatic to mild to severe; the mild manifestations are usually easily manageable and the disease is limited to the upper respiratory tract presenting typical symptoms

such as cough, fever, fatigue, sore throat, myalgia, headache, runny nose, ocular and gastrointestinal symptoms (Downey et al., 2018; Fukuyama & Kawaoka, 2011; Krammer et al., 2018; C. Paules & Subbarao, 2017).

The World Health Organization and local authorities recommend annual vaccination for patients prone to severe complications after influenza infection as it can substantially reduce disease severity (WHO, 2018). These complications are associated with pathologic changes in the airways and include but are not limited to hemorrhagic bronchitis, primary viral and secondary bacterial pneumonia, as well as a variety of non-respiratory complications such as viral myocarditis and viral encephalitis or exacerbation of underlying chronic diseases, and they can lead to acute respiratory or heart failure, and death (Morris et al., 2017; Piroth et al., 2021; Sellers et al., 2017). While all age groups can be affected, patients at the highest risk of developing serious adverse reactions are children under the age of two and elderly, pregnant people, health care workers, and immunocompromised people or those with underlying respiratory, cardiovascular, metabolic, oncologic, and other comorbidities (Coleman et al., 2018; Piroth et al., 2021). The highest mortality during the seasonal outbreaks is observed among seniors over 65 years of age, and population aging suggests that the number of lethal cases will increase in the future (Acosta et al., 2019; Iuliano et al., 2018; Paget et al., 2019). However, most infections occur in children, and it is estimated that up to 111 thousand annual influenza-associated deaths affect children under the age of five. The lack of pre-existing immunity against influenza is therefore also associated with increased morbidity and fatalities (Acosta et al., 2019; Iuliano et al., 2018; Nair et al., 2011; Somes et al., 2018). Most influenza-related fatalities are reported in low- and middle-income countries, linked with limited access to vaccines and health care (Coleman et al., 2018; Iuliano et al., 2018; Nair et al., 2011; Paget et al., 2019).

In the case of epidemiological likelihood, influenza is primarily clinically diagnosed (WHO, 2018). However, due to the similarity of influenza disease to the clinical manifestations of other respiratory pathogen infections, the definitive diagnosis requires more specific testing, such as serological, immunological, or molecular diagnosis, particularly important upon the risk of serious complications (Merckx et al., 2017; Nie et al., 2014; Sakai-Tagawa et al., 2017). Several neuraminidase inhibitors, such as oseltamivir, zanamivir, and peramivir, are available to treat or prevent influenza; however, due to resistance of circulating viruses and various adverse effects, most of these antivirals are used only to treat severely ill patients after a careful risk assessment and rarely – for prophylaxis (Duwe, 2017). Adamantane group drugs that block the M2 ion channel of type A influenza are no longer recommended for influenza treatment due

to the high resistance (Duwe, 2017; Gubareva et al., 2010). Yet, a number of potent antivirals that inhibit influenza neuraminidase (laninamivir octanoate) or RNA polymerase (baloxavir marboxil, T-705 ribofuranosyltriphosphate), or block the viral attachment by removing influenza receptors on host cells (DAS181) have been shown to be highly effective, especially when used early after disease onset (Furuta et al., 2013; Malakhov et al., 2006; Omoto et al., 2018; A. Watanabe et al., 2010).

1.1.2 Influenza diversity

Influenza viruses belong to the *Orthomyxoviridae* family, characterized by the fragmented negative-strand RNA genome. The family includes distinct influenza viruses, phylogenetically divided in genera, and they are commonly referred to as type A, B, C, and D influenza (Asha & Kumar, 2019; ICTV, 2020; Krammer et al., 2018). Only type A and B influenza viruses pose a major risk to human health as they cause seasonal epidemics with high rates of morbidity and fatality (WHO, 2018). Being mainly a human pathogen, the influenza C virus can also infect other mammals – dogs, cattle, and swine. Although most people are exposed to type C influenza at least once during childhood, the virus is known to generally cause upper respiratory disease with mild cold-like symptoms. Lower respiratory infections are also reported, especially in children younger than two years of age; yet, they are rare (Sederdahl & Williams, 2020). Type D influenza virus is a recently identified pathogen that primarily affects cattle and swine; however, it poses a potential threat for interspecies transmission (Asha & Kumar, 2019; Hause et al., 2013).

Type A influenza viruses are divided into subtypes based on the distinct antigenic characteristics of their major surface glycoproteins hemagglutinin (HA) and neuraminidase (NA) – a total of 18 different HA (H1-H18) and 11 NA (N1-N11) variants have been identified so far (Tong et al., 2012, 2013). The HA proteins are further classified into two groups according to the phylogeny of the HA protein and the structure and antigenicity of the HA stalk (group 1: H1, H2, H5, H6, H8, H9, H11, H12, H13, H16, H17, and H18; group 2: H3, H4, H7, H10, H14, and H15) (Joyce et al., 2016; Russell et al., 2004). Influenza A viruses have a wide host tropism – humans, wild and domestic birds, swine, horses, dogs and cats, marine mammals, and bats – with wild aquatic bird populations considered the primary reservoir for influenza A viruses. Unlike human influenza, avian influenza is transmitted fecal-orally, therefore, high-density poultry houses are at great risk of becoming influenza virus replication incubators (Munster et al., 2007; Yoon et al., 2014). Despite the great diversity, only three of the HA subtypes (H1, H2, and H3) and two NA subtypes (N1 and N2) have been sustainably circulating

in the human population, with A/H1N1 and A/H3N2 causing the most recent outbreaks (Krammer et al., 2018; T. Watanabe et al., 2014; WHO, 2018). Predominating circulation of the A/H3N2 subtype is associated with higher mortality, especially among the senior population; however, during seasons dominated by the A/H1N1 subtype people under 65 years of age are more severely affected (L. Li et al., 2018; Paget et al., 2019). Influenza B viruses have a much more limited host range, and they mainly infect humans. However, there are reports of spillover to other species, such as swine, seals, and horses (Kawano et al., 1978; Osterhaus et al., 2000; Ran et al., 2015). Two antigenically distinct influenza B lineages (Yamagata and Victoria) have evolved and now co-circulate in the human population, with higher prevalence among pediatric population and young adults (Caini et al., 2015; L. Jennings et al., 2018; WHO, 2018). Although the incidence is variable, influenza B accounts for approximately 22.6% of the isolated respiratory samples across different influenza seasons (Caini et al., 2015). Influenza viruses have a standard nomenclature – they are named according to the virus type, host species and location of isolation, isolate number and year of isolation, and, only for type A influenza, HA and NA subtype (Krammer et al., 2018).

1.1.3 Influenza plasticity

An important aspect of influenza viruses is that they are genetically labile and promptly accumulate mutations, resulting in major antigenic changes and immune evasion. Yearly influenza epidemics arise through a gradual process called antigenic drift when nucleotide mutations and amino acid substitutions accumulate in the antigenic sites of NA and HA genes of influenza A and B viruses (Figure 1) (Bedford et al., 2015; Rambaut et al., 2008; Webster et al., 1992). It occurs due to continuous antibody-mediated selective pressure and a low-fidelity RNA polymerase that lacks proofreading activity during replication (Webster et al., 1992; Wong et al., 2013). Mutations mainly occur around the receptor-binding sites as they are primarily recognized by neutralizing antibodies, and the structural plasticity of NA and HA proteins tolerates these substitutions without functional impairment (Caton et al., 1982; Wiley et al., 1981; R. Xu et al., 2010). As a result, the pre-existing immunity and previous vaccine compositions are much less effective thereby promoting viral transmission (Belongia et al., 2016; Kirkpatrick et al., 2018; Wong et al., 2013). A faster rate of antigenic drift, as well as more frequent and fatal epidemics, are associated with the A/H3N2 virus as compared to the co-circulating A/H1N1 and type B influenza viruses (Bedford et al., 2015).

The segmented influenza virus genome and its wide host tropism allow for introduction of novel virus variants or swapping of genome fragments between two or more influenza strains

from different animals during a simultaneous infection of the same host cell (Neumann & Kawaoka, 2019; Saunders-Hastings & Krewski, 2016). This event, referred to as antigenic shift and restricted to type A influenza, occurs rarely and unpredictably, and can produce a reassortant influenza subtype with novel combinations of NA and HA proteins (Figure 1). Such divergent antigenic combinations can drastically change the immune system's ability to recognize and fight the virus (Krammer et al., 2018; C. Paules & Subbarao, 2017). Pigs, quails, and bats have been reported as potent sources for influenza re-assortment as they express the complete set of sialylated receptors compatible with binding both avian and human influenza viruses (α 2,3-galactose linked sialic acid receptors and α 2,6-galactose linked sialic acid receptors respectively) (Chothe et al., 2017; Nelli et al., 2010; H. Wan & Perez, 2006). If such influenza strain sustains the ability of human-to-human transmission, a pandemic can arise (Potter, 2001; Saunders-Hastings & Krewski, 2016; Taubenberger & Morens, 2006).

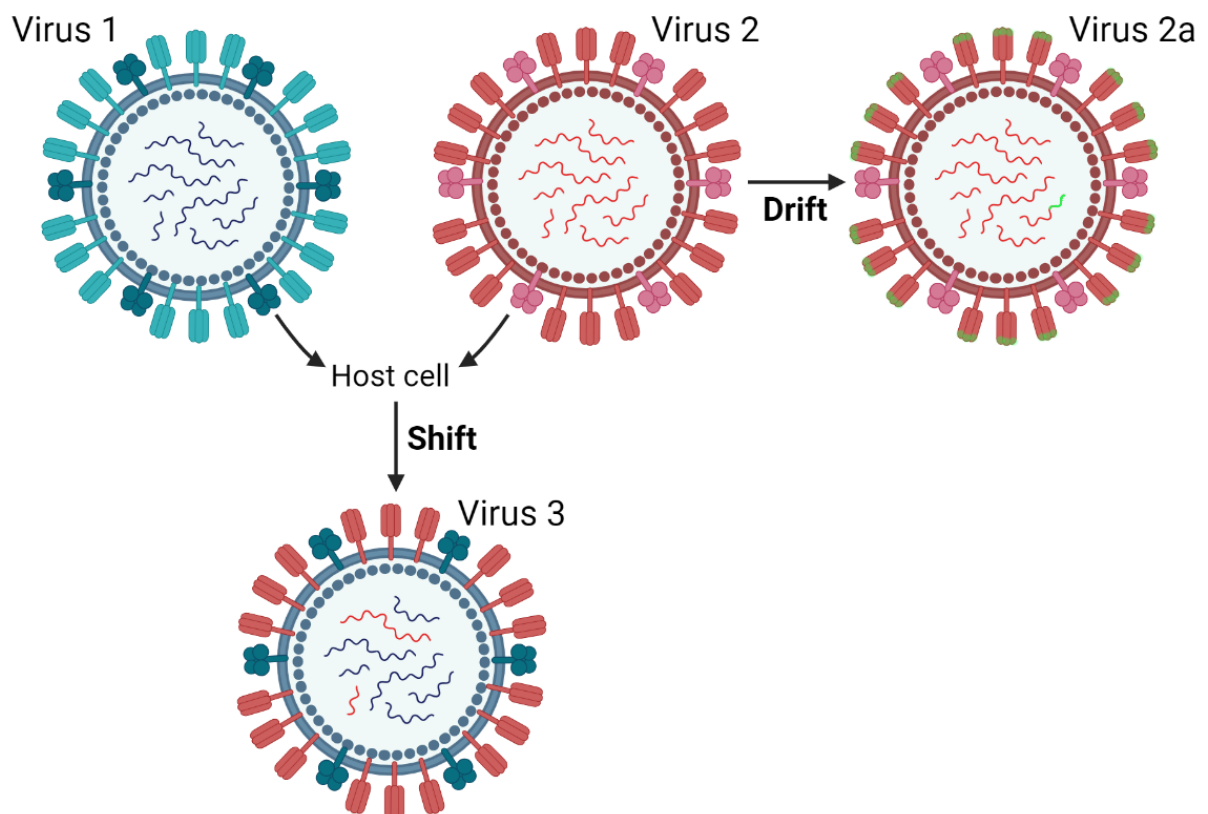


Figure 1. Antigenic shift and antigenic drift of influenza viruses. Antigenic shift: co-infection of the same host cell with a human and zoonotic influenza virus can result in the interchange of viral genome segments and the emergence of a novel influenza virus that is potentially spreading in the immunologically naïve society. Antigenic drift: accumulation of minor antigenic mutations in HA and NA genes to avoid immune recognition. The figure was created in BioRender.

Since the beginning of the 20th century, the influenza virus has jumped the species barrier four times causing a global pandemic and claiming millions of lives. Three influenza pandemics

occurred in the last century – in 1918 a novel A/H1N1 virus emerged directly from waterfowl, but in 1957 (A/H2N2) and 1968 (A/H3N2) the virus re-assorted between human and avian hosts (Potter, 2001; Saunders-Hastings & Krewski, 2016; Taubenberger & Morens, 2006). The 1918 pandemic is still considered one of the deadliest pandemics in recorded history as it infected as much as half of the global population and killed 50-100 million people worldwide, hampering population growth for the next decade (Potter, 2001; Taubenberger & Morens, 2006). After each pandemic, the causative virus continued to circulate in humans displacing the previous seasonal strains (Sutton, 2018). In the last influenza pandemic in 2009, the pandemic virus arose from re-assortment of four different viral subtypes of avian, swine, and human origin, and the pandemic A/H1N1 virus (A/pH1N1) is now circulating in society as a seasonal influenza virus (Saunders-Hastings & Krewski, 2016; WHO, 2018; York & Donis, 2013). Notably, the vaccines for A/pH1N1 became available only after the first waves of the pandemic influenza had peaked (Broadbent & Subbarao, 2011). A shift of morbidity and mortality toward younger ages has been observed during these pandemics, with extreme mortality among young adults and hospitalization rates of children up to seven times higher than during seasonal outbreaks (Loo & Gale, 2007; Shanks & Brundage, 2012; Shrestha et al., 2011; Simonsen et al., 1998). Immunologically naive hosts are at higher risk due to a lack of little or no pre-existing immune cross-protection; furthermore, potent immune systems can quickly become excessively stimulated or dysregulated in response to the virus, thus leading to tissue and organ damage (Loo & Gale, 2007; Shanks & Brundage, 2012).

With the increased globalization process – international travel, living in densely populated urban areas, and close contact with animals, especially poultry and swine – infectious diseases are emerging at an unprecedented rate (Rohr et al., 2019; Saunders-Hastings & Krewski, 2016). Therefore, of further concern are several influenza strains with a pandemic potential that have been circulating in domestic and wild animals with sporadic non-sustained human outbreaks. Zoonotic influenza of H1, H3, H5, H7, H9, and H10 subtypes have occasionally caused infections in humans in recent years, with the highly pathogenic avian H5 and H7 strains often causing severe disease and high rate of fatalities (Dandagi & Byahatti, 2011; Harfoot & Webby, 2017; Peacock et al., 2019; Sutton, 2018; T. Watanabe et al., 2014; Zhao et al., 2020). Furthermore, the world's first human infection with the avian influenza of H10N3 subtype was registered mid-2021 in China; however, the risk of a large-scale spread is considered to be low (WHO, 2021b). No direct human-to-human transmission has been registered for these viruses, indicating that further changes are necessary for adaption to spread into the human population. However, only several mutations were necessary for the avian H5N1

to acquire sustained transmission between ferrets, animals that are often used as models for human influenza infection; a similar experiment has been carried out in guinea pigs as well (Linster et al., 2014; Zhang et al., 2013). As there is no way to predict when, where, and which influenza subtype will cause the next outbreak or pandemic, these zoonotic viruses remain on the watch list for a high pandemic potential. Furthermore, the high evolution rate of influenza viruses in combination with the large number of influenza A subtypes and the two influenza B lineages requires constant surveillance and risk assessment (Neumann & Kawaoka, 2019).

1.2 Influenza A virion

1.2.1. Virion structure and proteins

Morphologically, influenza A viruses are enveloped pleomorphic particles that can either adapt spherical or elliptical shape, on average 120 nm in diameter, or form filamentous virions that are approximately 100 nm in diameter but can reach over 30 μm (A. Harris et al., 2006; Seladi-Schulman et al., 2013). The filamentous virions are predominantly isolated from *in vivo* samples during clinical infection while spherical forms are mainly produced in laboratory settings, e.g. passaging in eggs (Seladi-Schulman et al., 2013). The host-derived lipid bilayer of influenza virus, formed during nascent particle budding, envelops segmented negative-sense single-stranded RNA genome (Figure 2) (Dou et al., 2018; A. Harris et al., 2006). The influenza virus life cycle can be roughly divided into three steps: (1) virus attachment to the host cell via HA; (2) viral entry into the cell by endocytosis and replication; (3) viral assembly and progeny virus release. Replication of the viral RNA occurs in the nucleus of the host cell through a positive-sense intermediate – complementary RNA (cRNA), but the transcription results in positive-sense mRNAs that are transported to the cytoplasm for viral protein synthesis (Krammer et al., 2018).

The viral envelope embeds three integral membrane proteins and overlays the matrix and viral interior containing influenza genome (Dou et al., 2018; A. Harris et al., 2006). Influenza virus matrix is made of a helical layer of matrix 1 (M1) protein, one of the most abundant influenza proteins that constitute the viral shell and closely associates with the viral envelope (Selzer et al., 2020). M1 anchors the viral surface proteins within the envelope and interacts with the viral genome; it has a critical role for virion stability and pH-dependent RNA genome release as well as progeny virus budding (Rossman & Lamb, 2011; Selzer et al., 2020). Each genome segment is packed in a distinct filamentous ribonucleoprotein particle (RNP) in a complex with nucleoprotein (NP) and heterotrimeric RNA-dependent RNA polymerase and

acts as an independent transcription-replication unit (Gallagher et al., 2017; Pflug et al., 2017). NP is a positively charged arginine-rich protein that oligomerizes and encapsidates the negatively charged phosphate backbone of the viral genome for RNA transcription, replication, and packaging, and it takes part in the RNP complex nuclear transport (Portela & Digard, 2002). Each RNP complex adopts a shape of a flexible rod where two anti-parallel RNA strands are coated with NP, with bases exposed to the solvent (Baudin et al., 1994; Pflug et al., 2017). The RNP loops at one end, but the non-coding termini of the viral RNA form a short duplex region at the other end. This partially complementary highly conserved region binds the RNA polymerase and acts as a promoter sequence (Arranz et al., 2012; Dou et al., 2018). The RNA polymerase is a complex that consists of polymerase acidic protein (PA), and two polymerase basic proteins (PB1 and PB2) and it catalyzes RNA replication and transcription in infected cells (Boivin et al., 2010). During the viral replication, the newly synthesized RNA polymerase complex and NP are imported into the host cell nucleus to further promote the viral RNA replication and transcription rate (Krammer et al., 2018).

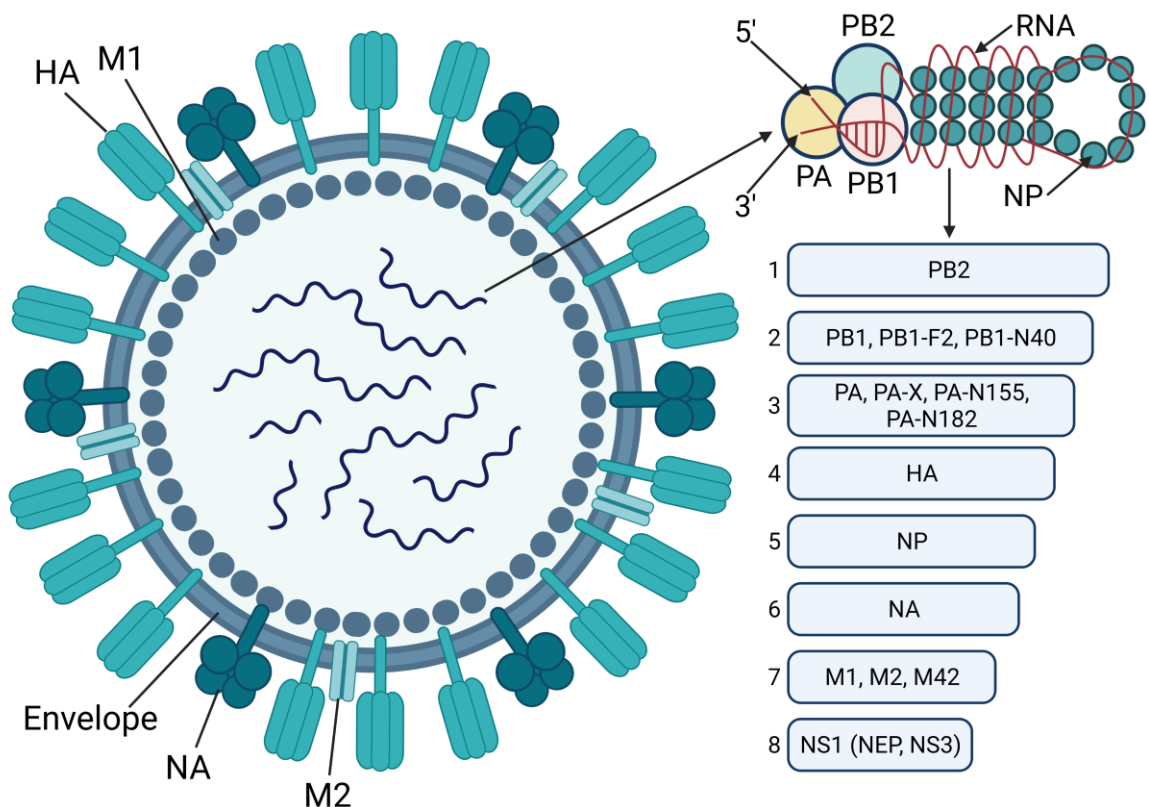


Figure 2. Scheme of influenza A virion. Influenza A virus is an enveloped negative-sense RNA virus. The 8 single-stranded RNA segments are numbered from the longest to shortest and encode for: (1) – PB2 (polymerase basic protein 2); (2) – PB1 (polymerase basic protein 1), PB1-N40, PB1-F2; (3) – PA (polymerase acidic protein), PA-X, PA-N155, PA-N182; (4) – HA (hemagglutinin); (5) – NP (nucleoprotein); (6) – NA (neuraminidase); (7) – M1 (matrix 1 protein), M2 (ion channel matrix 2 protein), M42; (8) – NS1 (non-structural protein 1), NEP (nuclear export protein), NS3. The figure was adapted from (Vasin et al., 2014) and created in BioRender.

The two major influenza antigenic determinants are viral surface spikes – glycoproteins neuraminidase (NA) and hemagglutinin (HA) (Gamblin & Skehel, 2010). HA is the predominant protein on the influenza surface, with the HA:NA ratio of approximately 5:1 for most influenza viruses (Getie-Kebtie et al., 2013). Both HA and NA are considered crucial factors of infectivity, pathogenicity, transmissibility, host specificity; furthermore, recently it was discovered that these proteins also act as motile machinery moving the viral particles on a cell surface and enhancing virus infection (Sakai et al., 2017). A third integral membrane protein is the less abundant matrix protein 2 ion channel (M2) (Kolpe et al., 2017).

HA is a homo-trimeric influenza surface protein that is essential for the first stages of the viral infection cycle – receptor binding and host cell entry through the host cell membrane as for other enveloped viruses (Wiley & Skehel, 1987). The functional role of HA in cells as well as the various conformations it adapts during the host cell entry process are described below. NA is a homo-tetrameric transmembrane viral glycoprotein that visually resembles a knob-like structure, with an enzyme active site located at the center of each monomer (Colman et al., 1983). It is one of the main antibody targets; however, immune pressure leads to constant accumulation of mutations in NA protein antigenic sites allowing to escape protective immunity and to produce drug-resistant mutants (Duwe, 2017). NA promotes infection through its enzymatic activity as it cleaves off the terminal sialic acid residues by which the virus HA becomes trapped on the mucosal surfaces of host respiratory tract, thereby releasing the virus and helping it to reach the host cells (Cohen et al., 2013). Furthermore, NA protein allows for the mature progeny virus release from infected cells as it also catalyzes the cleavage of the sialic acid from the HA cellular receptors of the budding virion and the cell surface receptors while preventing virion aggregation (Gamblin & Skehel, 2010). NA activity is associated with facilitated virus transmission since non-aggregated virions are more likely to be spread via aerosols (Lakdawala et al., 2011).

M2 is a homo-tetrameric multifunctional influenza surface protein consisting of four 97 amino acid α -helices, and each of them can be divided into 3 parts – a highly conserved and unstructured N-terminal ectodomain, a single-pass hydrophobic transmembrane domain, and a C-terminal tail (Kwon & Hong, 2016; Lamb et al., 1985). Only a few M2 proteins are incorporated into the mature virions; however, it is relatively abundant in the virus infected cell membranes (Lamb et al., 1985; Zebedee & Lamb, 1988). M2 primarily functions as a proton-selective ion channel that is required for the viral genome uncoating (Pinto et al., 1992). Shortly after the virus enters the host cell the M2 is destabilized by the acidic environment of the endosomes thereby enabling the flux of protons into the virion interior (Pinto et al., 1992;

Schnell & Chou, 2008). That, in turn, weakens the interactions between M1 protein and RNP in the viral core (Pinto et al., 1992). The acidic conditions facilitate the conformational changes of the HA protein, causing fusion between the viral and endosomal membranes, and, as a result, the RNPs are released into the cytosol (Benton et al., 2020). M2 protein also participates in virus assembly and mature virion budding. The C-terminal tail of M2 interacts with the M1 protein at the site of viral budding, and this interaction is important for the efficient virion assembly and production of infectious viral particles (B. J. Chen et al., 2008). Furthermore, M2e protein alters the membrane curvature during virus budding and mediates the membrane scission to release the progeny virus particles (Rossman et al., 2010). Finally, M2 protein helps influenza virus to evade autophagy and enhance the stability and yield of viral progeny, thereby promoting viral transmission (Beale et al., 2014; Gannagé et al., 2009).

There are several additional influenza proteins that are generally not found in the virion or are present in very small amounts but are abundantly expressed in the virus-infected host cells. The non-structural protein 1 (NS1) is a multifunctional, yet non-essential viral protein that antagonizes host immune system responses by inhibition of interferon activity and modulates host gene expression and viral replication cycle (Hale et al., 2008; Kochs et al., 2007). Nuclear export protein (NEP, formerly termed NS2), an alternative splicing product of the same gene segment as NS1, interacts with M1 protein and nucleoporins and helps to catalyze the export of newly synthesized viral RNA from the cell nucleus to the cytoplasm (Lamb & Choppin, 1979; Paterson & Fodor, 2012). PB1-F2 is a product of an alternative open reading frame from the PB1 gene translated as the result of leaky ribosomal scanning (W. Chen et al., 2001). PB1-F2 is a pathogenicity factor that is expressed in many, but not all influenza A viruses, and has been present in all the pandemic influenza strains (W. Chen et al., 2001; Varga & Palese, 2011). Being the smallest known influenza protein, PB1-F2 has a substantial role in viral pathogenicity via pro-apoptotic and anti-interferon mechanisms, as well as a role in polymerase activity regulation (Mazur et al., 2008; Varga & Palese, 2011). PB1-N40 is an N-terminally truncated form of the PB1-F2 that controls the balance between PB1 and PB1-F2 gene expression (Wise et al., 2009). PA-X is expressed from the PA gene segment due to ribosomal frame-shifting and it functions to repress cellular gene expression and modulate viral virulence (Jagger et al., 2012). Relatively recently additional products of PA gene have been identified – PA-N155 and PA-N182 proteins that are N-terminally truncated forms of PA as the result of leaky ribosomal scanning and likely fulfill some functions in the viral replication (Muramoto et al., 2013). M42 and NS3 proteins are alternative splicing products of genome segments 7 and 8 respectively. M42 is an isoform of the M2 ion channel with an antigenically

distinct ectodomain that can functionally replace the M2 (Wise et al., 2012). NS3 is potentially associated with adaptation to mouse host (Selman et al., 2012). Furthermore, a putative NEG8 protein encoded by genomic segment 8 has also been predicted (Clifford et al., 2009).

1.2.2 The structure and functions of influenza HA

The HA protein is first expressed as a fusion-incapable precursor protein in a monomeric form called HA0; it is cotranslationally translocated across the rough endoplasmic reticulum where protein folding into trimers occurs (Braakman et al., 1991; Gething et al., 1986). The HA0 undergoes post-translational N-linked glycosylation, an important aspect for protein folding, and stability, as well as for receptor-binding, antigenicity, and immune evasion (P. Kim et al., 2018). The trimers are selectively transported to the cell surface via the Golgi complex. The precursor protein must be cleaved into disulfide-bonded HA1 and HA2 subunits by cellular proteases to yield infectious viral particles and it most often occurs during viral budding or infection or in the trans-Golgi compartment (Copeland et al., 1986; Zhirnov et al., 2002). A major structural rearrangement after the cleavage is the relocation of the highly conserved N-terminus of HA2, referred to as fusion peptide, from the bottom of the cleavage loop to the interior of the trimer (Cross et al., 2009). The proteolytically activated mature HA at neutral pH conditions adapts the so-called pre-fusion conformation that projects 135 Å off the membrane (Figure 3) (Wiley & Skehel, 1987; Wilson et al., 1981). The pre-fusion HA trimer consists of two structurally distinct regions – a receptor-binding globular, membrane-distal head, formed by the middle part of HA1 polypeptide and a long, extended membrane-proximal fusogenic stalk, formed primarily by the HA2 chain and N- and C-termini of the HA1 polypeptide (Carr et al., 1997; Wilson et al., 1981).

The immunodominant globular head is the primary target of antibody responses and a subject of constant antigenic drift (Kirkpatrick et al., 2018; R. Xu et al., 2010). It consists primarily of an antiparallel 8-strand β -sheet with two looped out regions between strands 1-2 and 3-4 and includes a receptor-binding domain and a vestigial esterase domain (Wilson et al., 1981). The receptor-binding site is a shallow pocket located at the membrane-distal tip of each head domain monomer and the residues forming the face of the pocket are highly conserved (Gamblin et al., 2004; Weis et al., 1988; Wilson et al., 1981). Antibody binding epitopes that surround the receptor-binding pocket and include parts of the monomer tip and esterase domain are much more variable (F. L. Raymond et al., 1986; R. Xu et al., 2010). The main role of the head domain is to adhere the virus to the epithelial cells of the host's respiratory tract by attaching to sialic acid receptors on the host cell surface. As a result, the influenza virus is taken

up into an endosome by receptor-mediated endocytosis (Carr et al., 1997; Wiley & Skehel, 1987). As briefly mentioned above, different influenza virus strains preferably bind receptors with different sialyl linkages at the C-2 position determining the viral host specificity – avian viruses preferentially bind to α 2,3-galactose linked sialic acid receptors, while the human and swine viruses bind α 2,6-galactose linked sialic acid receptors (Nelli et al., 2010).

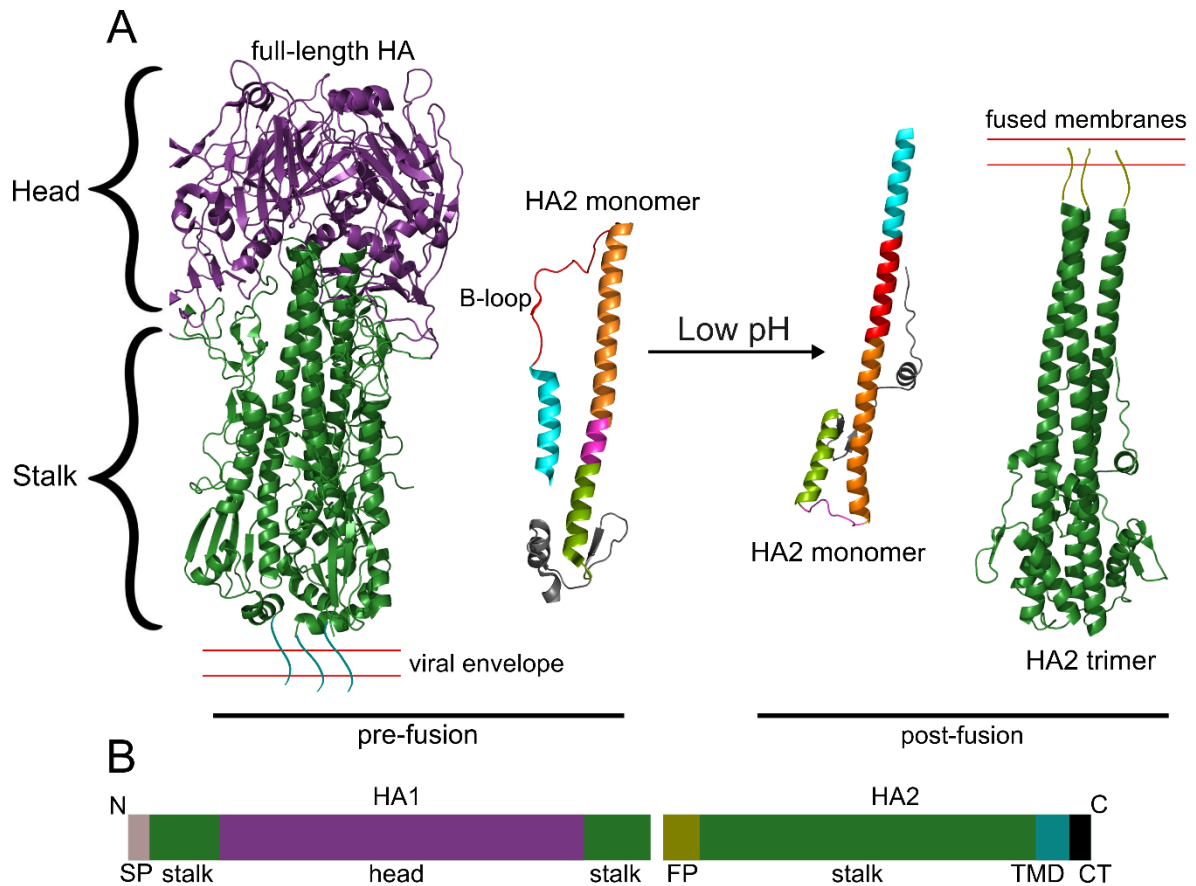


Figure 3. The structure of influenza virus hemagglutinin (HA). **(A)** The three-dimensional structure of the influenza A (subtype H3) HA protein in its pre-fusion (PDB ID: 1MQL) and post-fusion (PDB ID: 1HTM) conformations. The HA structure is shown in a cartoon representation with the head domain in purple and stalk domain in green. The HA2 monomer is color-coded by segments from the N- to the C- terminus (cyan, red, orange, magenta, green, and grey). **(B)** A linear scheme of the HA molecule. The stalk domain (green) is formed primarily by the HA2 polypeptide and by the N- and C-termini of HA1. The head domain (purple) spans the middle part of the HA1 polypeptide. There is a signal peptide (SP) at the N-terminus of the HA1, a fusion peptide (FP) at the N-terminus of the HA2, and a transmembrane domain (TMD) and cytoplasmic tail (CT) at the C-terminus of HA2.

The stalk domain mediates the viral and endosomal membrane fusion and contains a C-terminal transmembrane helix that anchors the HA protein in the viral membrane and an N-terminal fusion peptide of each HA2 polypeptide (Gamblin et al., 2004; Wiley & Skehel, 1987; Wilson et al., 1981). A long α -helix and a shorter antiparallel α -helix of HA2 polypeptide form a hairpin structure connected with an extended region referred to as B-loop. Three such

identical hairpins twist around each other to form a triple-stranded left-handed coiled-coil core structure, with the short α -helices packing in the grooves along its membrane-proximal side (Di Lella et al., 2016; Wilson et al., 1981). The three long α -helices form a cavity at the bottom of the molecule where the hydrophobic N-terminal HA2 fusion peptide tightly packs (Wiley & Skehel, 1987; Wilson et al., 1981). The fusion peptide has a crucial role in triggering the cell and membrane fusion as well as manipulating the target membrane curvature and it is highly conserved (Cross et al., 2009; Daniels et al., 1985; Smrt et al., 2015). The membrane-proximal base of the protein is formed by a compact, globular antiparallel 5-strand β -sheet structure and a short α -helix formed by the C-terminus of HA2 polypeptide that anchors each monomer in the viral membrane followed by a short cytosolic tail (Wilson et al., 1981).

The acidification of the endosome environment triggers large-scale conformational rearrangement in the pre-fusion HA protein with at least a few intermediate conformations. That, in turn, induces HA-mediated pH-dependent membrane fusion necessary to deliver the viral genome into the host cell for replication (Carr et al., 1997; J. Gao et al., 2020; R. Xu & Wilson, 2011). The pre-fusion state is metastable meaning that the HA2 subunit is held in this state by the stabilizing interactions of the surrounding HA1 subunit and the fusion peptide, but the acidification or removal of HA1 polypeptide leads to HA2 adapting the thermodynamically more stable fusogenic state (Carr et al., 1997; Garcia et al., 2015; R. Xu & Wilson, 2011). However, the fusogenic conformational changes of the HA2 subunit are likely to be independent of the HA head (J. Gao et al., 2020). As the pH approaches approximately 5.0-6.0, the fusion process is initiated (Daniels et al., 1985).

Although several fusion models are proposed, the major conformational changes in these models coincide (Benton et al., 2020; Di Lella et al., 2016; J. Gao et al., 2020). First, the protonation of the fusion peptide and its surrounding residues results in the liberation of the previously sequestered peptide from its hydrophobic pocket (Daniels et al., 1985; Garcia et al., 2015). The acidification causes the HA1 polypeptide to dissociate from the HA2 part except for a disulfide bond that flexibly links both polypeptides; it happens as the surface charge of HA1 changes and several salt bridge and hydrogen bond contacts are weakened upon protonation (Daniels et al., 1985; Y. Zhou et al., 2014). Under the acidic conditions, the HA2 polypeptide undergoes two major antigenic changes – (1) the initially unstructured B-loop converts to a helix extending the coiled-coil core and (2) the residues 106–112 of the central long α -helix transition to a loop (Bullough et al., 1994; Carr et al., 1997; Park et al., 2003; R. Xu & Wilson, 2011). The helix-to-loop transition causes the fusion membranes to come in close contact and dimple so that the fusion can occur (Park et al., 2003). Furthermore, the extended

form drives the conformational change to a lower-energy ‘spring-loaded’ state and the boomerang-shaped fusion peptide is inserted into the target cell membrane, locating the N- and C- termini of HA2 polypeptide in opposing membranes (Benton et al., 2020; Carr et al., 1997; R. Xu & Wilson, 2011).

Packing of the C-terminal “leashes” into the grooves of the coiled coil is necessary to mediate the lipid mixing stage (Benton et al., 2020; J. Chen et al., 1999; Park et al., 2003). The trimeric HA forms a zipper-like structure by bringing together the N- and C-terminal anchors (the boomerang-shaped fusion peptide and the transmembrane domain) and collapsing the extended intermediate. That results in hemifusion or lipid mixing of the outer layer of viral and endosomal membranes. Then the inner leaflets of both membranes are also merged, forming a fusion pore that allows for the viral genome entry into the host cell (Benton et al., 2020; J. Chen et al., 1999; Park et al., 2003; Smrt et al., 2015). The newly formed post-fusion HA conformation is energetically more favorable and the fusogenic changes are therefore irreversible. Each monomer of the post-fusion HA consists of a long α -helix, a short antiparallel α helix, and an unstructured loop region connecting the two helices. Together they form an extended six-helix bundle structure or a trimer of hairpins with the fusion peptide and transmembrane domain located at the same trimer end (Bullough et al., 1994; Garcia et al., 2015; Wiley & Skehel, 1987; R. Xu & Wilson, 2011). The structure of post-fusion HA is shown in Figure 3.

1.3 Limitations of conventional vaccination strategies

Although social distancing, global travel restrictions, and use of surgical masks and respirators in public places have dramatically reduced influenza transmission during the Sars-Cov-2 pandemic, these preventive approaches are not sustainable because of their restrictive nature (Olsen et al., 2020). There is no doubt that surgical masks and respirators will continue to be used in healthcare settings after the Sars-Cov-2 pandemic due to their high degree of protection; however, other measures are necessary to control influenza spread in the general public (C. Paules & Subbarao, 2017). Development of the first experimental military influenza vaccine (IV) in 1940s, soon after human influenza virus was first isolated from acute-stage patient throat washings, was an important scientific achievement (CDC, 2019; W. Smith et al., 1933). A few years later, in 1945, the first inactivated IV was licensed for use in civilians (CDC, 2019). Due to the influenza virus resistance to many of the available antiviral medications, seasonal IV still remains the recommended measure to control influenza virus transmission and

to reduce influenza-related morbidity and mortality (Duwe, 2017; WHO, 2018). Vaccination reduces the disease severity, the likelihood of severe complications, and therefore – hospital admissions, which are particularly significant aspects for the risk group patients, and IV can protect infants during the first six months of life with the immunity passed from a vaccinated mother (Giles et al., 2018; WHO, 2018). Yet, even though various IVs have been available for human use for decades, the actual seasonal IV effectiveness is suboptimal. It depends upon various factors and fluctuates across the seasons between the infection viruses, age and risk groups, and vaccine compositions, from approximately 19 to 60%, with the lowest effectiveness observed in the elderly population (Bedford et al., 2015; Belongia et al., 2016; CDC, 2021a; Gouma et al., 2020).

There are three types of seasonal IVs, commercially available in various countries, which contain inactivated (e.g. whole-virion, split-virion, and subunit vaccines) or live-attenuated influenza viruses, or recombinant HA protein. They all show good safety profiles and high efficacy against well-matched influenza viruses, while affording low to moderate protection against antigenically distinct influenza strains (CDC, 2021a; Gouma et al., 2020; WHO, 2018). All three licensed vaccine types are multivalent, covering antigenic components from two influenza A strains (A/pH1N1 and A/H3N2) and from one or both influenza B lineages (Victoria and/or Yamagata) anticipated to circulate in the next outbreak (WHO, 2018). As one of the influenza B lineages included in the vaccine confers little or no protection against the other influenza B lineage, quadrivalent vaccines are strongly advised to provide broader protection against influenza B viruses (Belshe, 2010).

The global annual seasonal IV production capacity is estimated at around 1.5 billion doses; yet, the actual number of vaccine doses produced and distributed is probably much lower (Palache et al., 2017; Sparrow et al., 2021). Although the influenza disease burden is higher in low- and middle-income countries, the majority of vaccines are manufactured and distributed in the developed countries (Bresee et al., 2018; McLean et al., 2016). In addition, as a measure of pandemic preparedness, several mock-up vaccines have been developed against different influenza subtypes that have pandemic potential (Soema et al., 2015). The estimated maximum global vaccine supply in a potential pandemic is 8.31 billion doses of a monovalent vaccine; however, more realistic scenarios propose no more than 4.15 billion doses of pandemic vaccine, with two doses required to induce protective immunity (Sparrow et al., 2021).

Seasonal IVs target the hypervariable viral surface proteins HA and NA and predominantly elicit neutralizing antibodies against the immunodominant HA head domain (Gamblin & Skehel, 2010; Krammer, 2019). As described above, the influenza virus and, in

particular, the globular head of the HA protein, is highly plastic and mutable and undergoes continuous antigenic drift and occasional antigenic shift, abrogating neutralizing antibody-binding affinity (Bedford et al., 2015; Kirkpatrick et al., 2018; Neumann & Kawaoka, 2019). Current IVs have to be reformulated and re-administered periodically to match the fast-evolving influenza strains and to maintain vaccine effectiveness (Kirkpatrick et al., 2018; WHO, 2018). Recommendations on seasonal IV content are updated twice a year by WHO, once in each hemisphere, based on global influenza surveillance, accumulation of viral sequences in public databases, and predictive computational cartography models for the antigenic evolution (WHO, 2021a; Yamayoshi & Kawaoka, 2019a). It takes place at least six months prior the upcoming influenza epidemic to accommodate production, calibration and quality assurance of large quantities of IVs (Gerdil, 2003). Vaccine candidate strain selection issues cause antigenic mismatches between the circulating viruses and prognosed vaccine components, therefore unpredictably and significantly diminishing vaccine effectiveness (Bedford et al., 2015; Belongia et al., 2016; CDC, 2021a). For example, the selected type B IV strains differ from the predominantly circulating lineage by 25-50% (Caini et al., 2015).

Due to the relatively low production costs and considerable production capacity, seasonal IV production is mostly performed by passaging the virus in the allantoic fluid of embryonated chicken eggs, accounting for 88% of the global IV market in 2018 (J.-R. Chen et al., 2020; Rajaram et al., 2020). Exceptions are several cell-culture based vaccines, e.g. inactivated virus subunit vaccines grown in mammalian cells, and recombinant HA vaccines produced in insect-cell based system (J.-R. Chen et al., 2020; Cox et al., 2015). Growing the human virus in eggs can adversely influence virus replication and evolution, as there are crucial differences between the human and avian tissue. Influenza HA binds the host cell receptors via host-specific sialic acid residues (α 2,6-linkage for human cells and α 2,3-linkage for avian cells) (Nelli et al., 2010). The selective environment, driven by the adaptation of human virus to grow in eggs during multiple passages, can cause mutations in the receptor binding-subunit of HA. These egg-adaptive mutations can detrimentally affect HA antigenicity and alter the match between the vaccine and seed strains, thereby contributing to the decline in immune protection from vaccination (Rajaram et al., 2020; D. D. Raymond et al., 2016; Skowronski et al., 2014; Wu et al., 2017).

Influenza virus replication in eggs is highly unpredictable and varies greatly between the strains – while high propagation yields are observed for some strains, others, e.g., A/H3N2, replicate poorly in eggs and it can be difficult to achieve sufficient viral titers (Rajaram et al., 2020; Yamayoshi & Kawaoka, 2019a). Highly pathogenic avian influenza strains, such as

A/H5N1, are lethal to avian tissue and cannot be efficiently propagated in an egg-based system (Pérez Rubio & Eiros, 2018; Pillet et al., 2018). The timeline of traditional egg-based vaccine production, including testing and distribution, can stretch more than 6 months during which novel mutations can arise; this process is too lengthy to promptly protect society against a novel pandemic strain, especially if several more months are necessary to reach a maximum production capacity (Sparrow et al., 2021; Yamayoshi & Kawaoka, 2019a). The continuous supply of pathogen-free fertilized eggs requires planning even a year in advance, hence an off-season pandemic or an outbreak of avian influenza or other poultry diseases can compromise plentiful egg supply and delay vaccine production (Sparrow et al., 2021). In addition, patients with previous anaphylactic reactions and egg allergies have an increased risk of adverse reactions to vaccines produced in eggs due to residual egg protein (Klimek et al., 2017).

Vaccine production in cultured cell-lines overcomes some of the issues as the cell supply can be stockpiled in advance and has a lower risk of contamination; in some cases, the product lacks egg-adaptive mutations, and, therefore, has sometimes been associated with better vaccine effectiveness (Barr et al., 2018; J.-R. Chen et al., 2020; Manini et al., 2017). For most mammalian cell-based vaccines there is still the need for the time consuming process of vaccine seed strain selection for virus production in mammalian cells during which people are left unprotected against the emerging virus (J.-R. Chen et al., 2020; Manini et al., 2017). Due to the challenging and expensive scale-up of mammalian cell-based vaccine production, low virus yields are achievable resulting in fairly high production costs (J.-R. Chen et al., 2020). Insect-based environment provides an efficient and stable platform for HA protein production and potentially offers shorter production cycles than the fertilized egg system; however, as an emerging technology, is not widely used yet (Cox et al., 2015). Therefore, the use of cell-culture-based seasonal vaccines is currently limited.

Conventional IV effectiveness is significantly affected by the strength and longevity of the host immunity. Immune responses elicited by conventional vaccination strategies do not confer durable protection, therefore, an annual booster dose is required for optimal protection (Young et al., 2018). Immune senescence, characterized by the age-associated decline of immune responses, can lead to reduced vaccine effectiveness in elderly patients, especially during the A/H3N2 dominated outbreaks (Belongia et al., 2016; N. D. Lambert et al., 2012). Influenza immunological imprinting is a concept that implies that not only the virulence of the circulating strain but also pre-existing exposure to influenza viruses may influence the immunological responses to subsequent influenza infections and vaccination (Acosta et al., 2019). Hence, it opens a prospect to enhance vaccine effectiveness and durability when properly

researched. The addition of adjuvants and higher doses of immunization antigen are also applied to boost the immunity of risk-group patients, especially pediatric patients and older adults; however, such measures will not confer protection against newly emerging influenza viruses (Clark et al., 2009; DiazGranados et al., 2014).

1.4 Novel vaccination strategies and broadly protective influenza vaccines

1.4.1 General considerations to obtain vaccines that are more effective

Novel vaccination strategies that are seeking ways to avoid limitations of conventional IVs by means of innovative approaches or platforms are currently extensively studied in different phases of preclinical and clinical trials. These technologies include recombinant influenza proteins and virus-like particles (VLPs), nucleic acid-based vaccines, viral vector vaccines delivering foreign influenza proteins, and others (Carter et al., 2019; Cummings et al., 2014; Feldman et al., 2019; Liebowitz et al., 2020; Lindgren et al., 2017). While these technologies pave a promising way for more effective vaccines, they largely rely on eukaryotic expression systems, characterized by lower yields and higher costs than the prokaryotic cells (Owczarek et al., 2019). Hence, to date, none of these vaccines have been approved for human use. Furthermore, these experimental vaccination strategies often fail to confer broad protection against antigenically distinct viruses. As there is no way to precisely predict the antigenic evolution of the large number of influenza strains, even fast-producible and more effective approaches with improved manufacturing capacity might not be sufficient to rapidly fight emerging influenza viruses and mitigate the disease burden.

A broadly protective IV is an unmet, yet urgent public health need; currently, many laboratories around the world focus their resources and research to develop such a vaccine (Appendix 1). A truly universal vaccine should confer at least 75% protection against symptoms caused by group 1 and group 2 influenza A virus infections, and the protection must last for at least one year (C. I. Paules et al., 2017). Vaccines targeting conserved influenza proteins hold a great promise toward such a cross-protective and durable IV capable to defend against homologous viruses and antigenically drifted and shifted virus variants with a pandemic potential (Krammer, 2016; Saelens, 2019). Furthermore, the possibility to recombinantly mass-produce and stockpile vaccine components could tremendously benefit both the economy and public health. Various evolutionary conserved influenza epitopes have been studied as components of such universal vaccine for several decades, and they are present both inside (parts of M1, PB1, and NP, and others) and on the surface of the influenza virion (the receptor

binding subunit of HA, enzymatic site of NA, HA stalk, and the ectodomain of M2) (Kaminski & Lee, 2011; Yamayoshi & Kawaoka, 2019b). Conserved influenza antigens are mostly immuno-subdominant or internal and therefore generally induce non-sterilizing immunity. However, even though neutralizing antibodies can effectively prevent viral entry and release, they also drive antibody-mediated immune pressure promoting selection of virus escape mutants (Kirkpatrick et al., 2018; Tsuchiya et al., 2001). Furthermore, unlike the non-neutralizing antibody responses, the sterilizing mechanisms rapidly eliminate the infection virus and may prevent induction of adaptive heterosubtypic immune responses (Bodewes et al., 2010; Choi et al., 2020).

1.4.2 Broadly protective vaccines targeting internal influenza proteins

Although internal influenza proteins do not elicit robust antibody responses after infection or vaccination with seasonal vaccines, the conserved regions of these proteins have gained substantial interest from researchers as potential components of a broadly protective vaccine. The internal M1 and NP proteins contain T-cell reactive regions that are highly conserved among influenza A strains, but in the case of PB1, epitopes are shared among both influenza A and B viruses (L. Y.-H. Lee et al., 2008; Terajima et al., 2013). The M1 and NP proteins show around 90% amino-acid sequence identity between a variety of influenza A human and avian strains (L. Y.-H. Lee et al., 2008). These conserved antigens induce cross-reactive antibodies that mainly target infected cells by Fc-dependent effector mechanisms (Kaminski & Lee, 2011). Furthermore, the conserved T-cell reactive regions of these proteins are targeted by cytotoxic T-lymphocytes, inducing broad cross-reactive responses, based primarily on the CD8+ T-cells, even in the absence of antibodies (Epstein et al., 2005; Woodland, 2003; D. Zhou et al., 2010). These internal proteins have been successfully applied in several vaccine candidates to induce protection against homologous and heterologous virus strains (Appendix 1). Activated CD8+ cytotoxic T-cells kill virus-infected cells and promote clearance of the virus, and can thereby reduce disease severity and adverse complications, and prevent mortality and re-infection (Woodland, 2003). While CD4+ T-cells have not been as thoroughly investigated as CD8+ T-cells and antibody responses in regard to IVs, both levels of CD8+ T-cells and B-cells seem to be dependent on CD4+ T-cells (Wilkinson et al., 2012; Woodland, 2003). Since immune senescence is known to result in age-related decline of antibody responses, cell-based responses have been shown to correlate with better protective immunity in the elderly (McElhaney et al., 2006). However, as the conserved T-cell reactive regions are not displayed on the virion surface

and therefore do not induce neutralizing antibody responses, vaccines containing these epitopes induce infection-permissive immunity (Kaminski & Lee, 2011).

Other relatively conserved internal influenza proteins, such as the rest of RNA polymerase subunits (PA and PB2), NS1, NEP, and the PB1 RNA reading frame shift product PB1-F2, also induce antibody reactions after influenza infections. However, due to limited cross-reactivity, rapidly dropping antibody titers, and even proviral activity, their protective efficacy is much less studied (Crowe et al., 2006; Kaminski & Lee, 2011; Kuo et al., 2010). A vaccine targeting a single internal protein is therefore not considered a potent approach to replace current vaccination strategies (Woodland, 2003).

1.4.3 Broadly protective vaccines targeting influenza surface proteins

Mechanisms of M2e-induced protection

Although the whole M2 protein shares relatively high sequence homology between type A influenza viruses, most attempts to induce broadly protective immune responses have been based on its 23 residues long N-terminal ectodomain (M2e) (Mezhenskaya et al., 2019; Saelens, 2019). The relatively slow evolution of the M2e sequence can be explained by the information stored in its coding genome segment. The gene fragment encoding for the first nine amino-acid residues of the M2e overlaps with the N-terminus of the M1 protein in the same open reading frame, and this fragment is almost absolutely conserved (Ito et al., 1991). The remaining M2e residues and the C-terminus of M1 are also encoded by the same nucleotides, but in different open reading frames, and therefore show higher variability (Ito et al., 1991; Saelens, 2019). Since M2e-specific antibody responses induced by natural infection or conventional vaccines are negligible, the selective immune pressure on this epitope is most likely very low (Black et al., 1993; Kolpe et al., 2017). When properly displayed, M2e has been shown to induce potent humoral and cellular immunity across a variety of influenza strains; hence, it is not surprising that it has been described in many publications as an attractive target for a broadly protective IV (Appendix 1). Various technologies and platforms are being tested to increase the immunogenicity of M2e, e.g. fusion proteins, prime-boost regimens, nucleic-acid vaccines, plasmid and viral vectors, particulate structures, and adjuvants. Because of the slight differences between M2e residues 10-24 of different influenza strains, inclusion of several M2e consensus sequences of different origins in the vaccine can increase cross-reactivity between influenza A viruses (Mezhenskaya et al., 2019). The functional influenza B ortholog of M2 protein, named BM2, has a significantly different sequence, and its ectodomain is only 7 amino-acid residues long, which is probably too short to induce potent protective immunity (Saelens, 2019).

The broad immunoprotective potential of M2e is mainly based on its ability to elicit durable, yet non-neutralizing antibody responses. While the anti-M2e antibodies do not inhibit the viral entry into host cells, therefore inducing infection-permissive immunity, multiple experiments have demonstrated that anti-M2e antibodies confer significant cross-protective immunity *in vivo* (El Bakkouri et al., 2011; Fu et al., 2009). Monoclonal anti-M2e antibodies have been shown to protect animals from lethal influenza infections both prophylactically and therapeutically, and the M2e-induced protective immunity can be transferred to naïve animals by immune serum (Jegerlehner et al., 2004; Kolpe et al., 2018; Mozdzanowska et al., 1999; Ramos et al., 2015; R. Wang et al., 2008). Despite the sparse occurrence of M2e on virions, anti-M2e antibodies strongly bind the abundant M2e on virus-infected cells (Figure 4) (El Bakkouri et al., 2011; Mezhenskaya et al., 2019; Zebedee & Lamb, 1988). The anti-M2e immune complexes mediate humoral protection mainly via antibody-mediated Fc-receptor dependent effector mechanisms such as antibody-dependent cellular cytotoxicity (ADCC), antibody-dependent cell-mediated phagocytosis (ADCP), and complement-dependent cytolysis (CDC), resulting in the elimination and/or phagocytosis of influenza virus-infected cells before progeny virus budding (El Bakkouri et al., 2011; Kolpe et al., 2017; Y.-N. Lee et al., 2014; Nimmerjahn & Ravetch, 2005). A balance between activating and inhibitory Fc gamma receptors (Fcγ-Rs) sets a threshold for triggering sustained effector functions by IgG antibodies. In turn, differences in IgG subclasses and their varying binding affinity to Fcγ-Rs affect their ability to mediate effector responses, contributing to their efficacy during viral infections (Nimmerjahn & Ravetch, 2005). It has been demonstrated, that Fcγ-Rs on alveolar macrophages are essential for M2e-specific protection (El Bakkouri et al., 2011). There are contradictory findings on whether natural killer (NK) cells and complement are essential for elimination of infected cells, but it is highly possible that both play an accessory role in M2e-induced protection (Jegerlehner et al., 2004; Simhadri et al., 2015; Tompkins et al., 2007; R. Wang et al., 2008).

Although different studies report inconsistencies in vaccine induced M2e-specific T-cell responses, it has been demonstrated that T-cell immunity can contribute to increased virus clearance and faster recovery, as well as reduced disease severity and long-term protection (Eliasson et al., 2008, 2018; M.-C. Kim et al., 2014; Y.-N. Lee et al., 2014; Tompkins et al., 2007). Both M2e-specific CD4⁺ and CD8⁺ T-cells seem to be involved in virus clearance via cytotoxicity pathways, but CD4⁺ T-cells appear to play a greater role in mediating long-lasting cross-protection (Eliasson et al., 2018; M.-C. Kim et al., 2014; Tompkins et al., 2007; Topham et al., 1997).

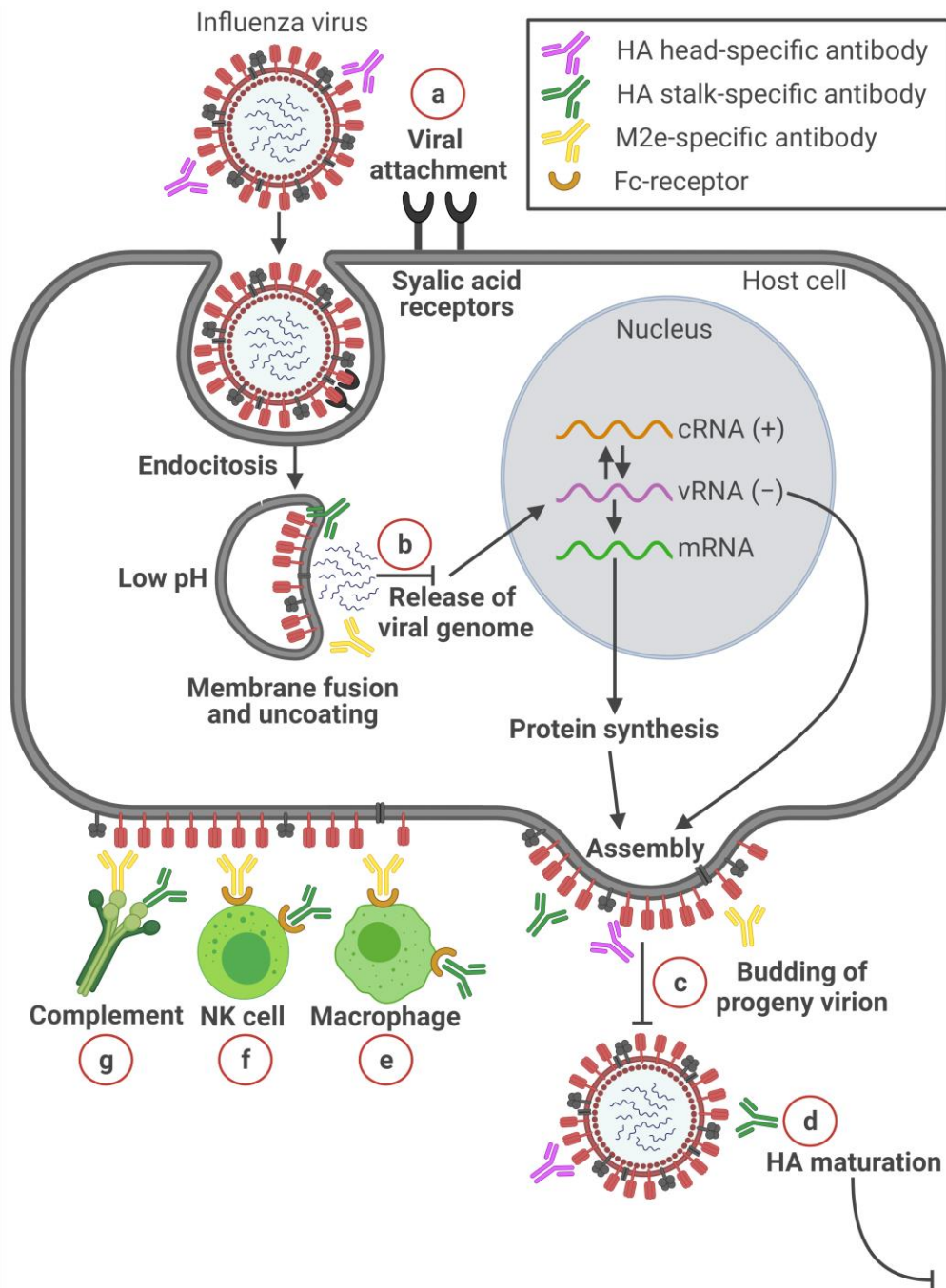


Figure 4. Antibodies against influenza HA and M2e. Conventional influenza vaccines primarily elicit antibody responses against the HA head that (a) neutralize by blocking the viral attachment to host cell. Antibodies targeting HA-stalk can (b) prevent the viral and endosomal membrane fusion by sterically inhibiting the conformational changes of HA2. Alternatively, M2e specific antibodies can constrain the proton transport into the endosome thereby preventing the pH-dependent structural changes in the HA. Head-, stalk- and M2e-reactive antibodies (c) can interfere with virus budding thereby reducing the production of progeny virus, but stalk-specific antibodies (d) may inhibit HA maturation by blocking the protease cleavage site on the HA0 polypeptide. Stalk- and M2e-reactive antibodies can also mediate protection through (e) antibody-dependent cell-mediated phagocytosis, (f) antibody-dependent cellular cytotoxicity, and (g) complement-dependent cytotoxicity. cRNA - complementary RNA; vRNA – viral RNA; NK – natural killer cells. The figure was adapted from (Krammer, 2019; L. C. Lambert & Fauci, 2010) and created in BioRender.

While M2e vaccines produce potent immune responses in animal models, the M2e-induced immunity in early-phase clinical trials has been relatively poor at generating and maintaining sufficient levels of protection in humans – at least when compared with vaccines that induce sterilizing protection. It is likely that the M2e will not be the only component of an IV that will substitute the conventional vaccines; therefore, the use of multiple components in a single vaccine to induce a broad and lasting protective immunity is now under consideration in many laboratories (Appendix 1) (Kolpe et al., 2017; Saelens, 2019).

HA stalk-specific immunity

Unlike the immunodominant, yet fast-evolving head domain of HA protein, its membrane-proximal stalk domain exhibits high conservation in its sequence and structure. This is because the immuno-subdominant HA stalk evolves significantly slower than its head domain, and the stalk-targeted selective pressure is not aided to evade neutralizing-antibody responses (Kirkpatrick et al., 2018). Yet, the stalk region contains several vulnerable sites targeted by broadly reactive immune responses – both neutralizing and infection-permissive antibodies (Bernstein et al., 2020; Corti et al., 2011; Ellebedy & Ahmed, 2012). Isolated from mice and humans, they significantly protect animals from diverse influenza virus challenges and have been shown to correlate with protection in human populations (Corti et al., 2010, 2011; Dreyfus et al., 2012; Ekiert et al., 2009; Kashyap et al., 2010; Ng et al., 2019; Okuno et al., 1993; Wu & Wilson, 2018). Most of these monoclonal antibodies are known to recognize conserved HA epitopes across the same influenza subtype or group based on structural differences between group 1 and group 2 HA stalk, but antibodies that cross-react between groups have also been isolated (Corti et al., 2010, 2011; Ekiert et al., 2009, 2011; Friesen et al., 2014; Joyce et al., 2016; Kallewaard et al., 2016; Kashyap et al., 2008; Lang et al., 2017; G.-M. Li et al., 2012; Okuno et al., 1993; Russell et al., 2004; Sui et al., 2009; Yamayoshi et al., 2017). Furthermore, a conserved epitope that is shared in both type A and B influenza has been discovered as well (Dreyfus et al., 2012).

Antibodies against the HA stalk are mostly hetero-reactive (Yamayoshi & Kawaoka, 2019b). They can possess broad specificity and neutralization potency resulting from extracellular inhibition of the progeny virion release and prevention of the proteolytic activation of HA trimer (Figure 4) (Brandenburg et al., 2013; Yamayoshi et al., 2017). Anti-stalk antibodies can also inhibit neuraminidase functionality through steric hindrance or neutralize the virus intracellularly by blocking the viral fusion machinery during viral entry (Brandenburg et al., 2013, 2013; Okuno et al., 1993). However, stalk-specific antibody-mediated suppression

of virus replication largely relies on effector functions, such as ADCC, ADCP, and CDC, resulting in effector cell activation and clearance of virus-infected cells (DiLillo et al., 2014, 2016). Antibodies mediating effector functions are known to induce broader protective responses; however, they exhibit different levels of effector activity, probably, due to the distinct structures they target and varying antibody affinity for the Fc-receptors (DiLillo et al., 2014; Srivastava et al., 2013). These non-neutralizing functions can be mediated by distinct infection-permissive antibodies or to increase the potency of neutralizing antibodies (Adachi et al., 2019; DiLillo et al., 2014; Jegaskanda et al., 2014; Srivastava et al., 2013).

Following the discovery of such cross-reactive antibodies, the challenge now is to develop an IV candidate that can elicit these antibodies at sufficiently high amounts to confer protection against heterosubtypic viruses. The first hardship is the weak immune responses targeting the HA stalk after infection and vaccination with seasonal vaccines due to the immunodominant properties of HA head (Margine et al., 2013; Zost et al., 2019). Steric hindrance and antibody inaccessibility have been considered as the possible causes of the stalk immune sub-dominance (Steel et al., 2010). Despite the close packing of HA stalk on the viral membrane and steric shielding by the HA head, the stalk domain has been shown to be accessible to broadly neutralizing antibodies (A. K. Harris et al., 2013). Yet, removal or masking of the immuno-dominant globular HA head epitopes can lead to increased stalk-directed antibody levels as it allows the immune system to focus on the stalk domain (Eggink et al., 2014; Krammer, 2016).

Therefore, another prerequisite to creating a potent broadly protective vaccine is generating a stable stalk antigen that structurally resembles the full length HA, as correct structural conformation of target epitopes can be crucial to induce a strong immune response (Jegerlehner et al., 2013; Krammer, 2015). Due to the metastable nature of HA trimer, removal of its head and transmembrane domains disrupts the pre-fusion conformation and results in reduced antibody binding affinity or even loss of many cross-reactive antibody binding epitopes (J. Chen et al., 1995; Impagliazzo et al., 2015; Wilson et al., 1981). Although even linear epitopes have been shown to confer protection against lethal infections, it is usually associated with the display of significant disease symptoms (S. Chen et al., 2015; Ramirez et al., 2018). Most of the broadly reactive antibodies are conformation-specific and show optimal binding when the HA stalk is in its native pre-fusion conformation, blocking conformational rearrangements necessary for membrane fusion. For example, well-characterized antibodies MEDI8852, CR6261, and C179 bind highly conserved regions in the membrane-proximal pre-fusion stalk comprised of HA1 and HA2 (Dreyfus et al., 2013; Ekiert et al., 2009; Kallewaard

et al., 2016). Even slight changes in antigen structure compared to the full-length HA stalk can result in weaker antibody binding affinity (Bommakanti et al., 2012; Mallajosyula et al., 2014). However, the post-fusion stalk antigen too is sufficient to protect against lethal challenge with distinct influenza viruses from both group 1 and 2 (Adachi et al., 2019). Adachi et al. demonstrated that in the stable post-fusion conformation of HA stalk its long-alpha helix is exposed to the immune system and elicits robust and durable cross-reactive antibody responses.

Various approaches have been proposed to elicit potent anti-stalk antibody responses (Appendix 1). A promising way to improve the levels of stalk-specific antibodies is priming the conventional vaccine with DNA encoding HA (Ledgerwood et al., 2011; Wei et al., 2010). Several headless-HA constructs, created by removal of entire globular head and subsequent stabilization of the pre-fusion trimeric conformation, have shown promising results in animal models, affording homologous, heterosubtypic and even cross-group protection (Impagliazzo et al., 2015; Mallajosyula et al., 2014; Steel et al., 2010; Valkenburg et al., 2016; Yassine et al., 2015). Vaccines based on hyperglycosylated HA protein, nucleic acid vaccines, synthetic stalk peptides, or VLP displayed stalk epitopes, have also gained substantial scientific interest as potent stimulators of broadly reactive antibody responses (S. Chen et al., 2015; Eggink et al., 2014; Lin et al., 2014; Pardi et al., 2018; Ramirez et al., 2018; Staneková et al., 2011). Another strategy to boost the anti-stalk antibody responses is to use serial immunization with chimeric full-length HA proteins or viruses displaying chimeric HAs that contain the same stalk and divergent head domains (Krammer et al., 2013; Nachbagauer et al., 2015). A promising chimeric-HA vaccine candidate from Nachbagauer et al. has recently finished phase 1 clinical trials, demonstrating strong, durable, and functional immune responses against the HA stalk (Nachbagauer et al., 2021).

Conserved regions of HA and NA head domains

Due to the antigenic evolution of immunodominant NA and HA epitopes, their induced immunity is the most potent against antigenically-matched viruses (Eichelberger & Wan, 2015). Although the enzyme active site of NA protein is comprised of highly conserved amino acids and has been shown to bind some broadly reactive antibodies, the NA-induced immunity is infection-permissive and appear to be less effective than HA- or M2- specific immunity (Choi et al., 2020; Eichelberger & Wan, 2015; Mozdzanowska et al., 1999; Sandbulte et al., 2007). Similarly, some epitopes of the otherwise hypervariable HA head, such as the sialic acid receptor binding pocket, are also relatively conserved, and several broadly neutralizing head-binding antibodies have been discovered (Bangaru et al., 2019; Ekiert et al., 2012; Thornburg

et al., 2016; Zhu et al., 2013). Yet, their cross-reactivity is mostly restricted within a subtype or shows limited heterosubtypic binding. Therefore, even though the immune responses towards the immunodominant HA and NA are more robust than those to less immunogenic M2e or HA stem, the conserved regions of NA and HA head have gained little interest by researchers as potential components of a broadly effective IV.

1.5 VLP-based vaccination strategies

1.5.1 General characteristics of VLPs

The structural proteins of many viruses are capable of autonomous self-assembly into VLPs – globular, icosahedral, or rod-shaped, almost crystal-like nanoscale arrays, generally ranging from 20 to 200 nm in size, which is analogous to the size of the corresponding viruses (Bachmann & Jennings, 2010; Syomin & Ilyin, 2019). They act as scaffolds presenting a large number of functional and/or immunological epitopes in a highly repetitive manner (D. M. Smith et al., 2013a). Acting as empty viral shells, VLPs possess many key characteristics of the original pathogen including close resemblance of the morphology, uniformity and high symmetry, predictable immunological properties, and stability at wide pH and temperature ranges and over different chemical environments (Ma et al., 2012a; Pushko et al., 2013; D. M. Smith et al., 2013b). Yet, these protein shells are devoid of the viral genome, vital for replication and infection, and therefore are proved as generally safe and highly immunogenic platforms for vaccine development (Ma et al., 2012a; Pushko et al., 2013). Due to their immune response enhancing properties, high manufacturing yields, and cost-effective and fast production that allows for a candidate vaccine generation as fast as 3 weeks after the release of sequence information, VLPs are considered as potent multimeric carriers for immunologically weak influenza epitopes (Landry et al., 2010; Nooraei et al., 2021).

1.5.2 Variety of VLP sources and their production systems

The genes encoding VLP shells have been derived from a vast diversity of pathogenic viral precursors, including animal and plant viruses, as well as bacteriophages and yeast Ty retrotransposons (Balke & Zeltins, 2020; Curcio et al., 2015; Liekniņa et al., 2019; Qian et al., 2020). VLPs vary greatly in their structural complexity. They may be composed of one or more capsid proteins, arranged in a single or several layers. The structural proteins can be embedded within a phospholipid bilayer, derived from the host cell membrane, or the lipid bilayer can be enveloped around the protein shell (Figure 5) (Jeong & Seong, 2017; Lua et al., 2014).

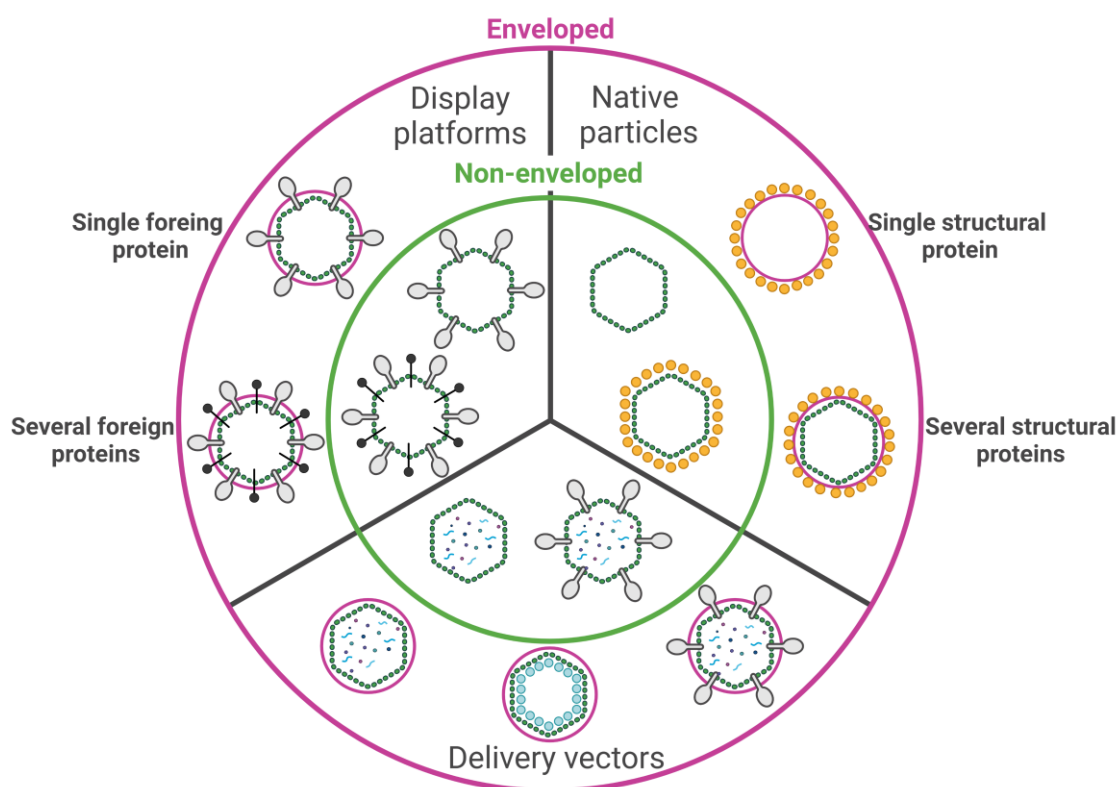


Figure 5. Structural and functional versatility of virus-like particles. The figure was created in BioRender.

VLPs can be rapidly produced in a variety of hosts, both prokaryotic and eukaryotic – bacteria, yeast, plant, insect, and mammalian cells – as well as cell-free expression systems, chosen depending on the structural and antigenic complexity of the particles (Bahar et al., 2021; Bundy & Swartz, 2011; Gopal & Schneemann, 2018; Huang et al., 2017; Jeong & Seong, 2017; H. J. Kim & Kim, 2017; Scotti & Rybicki, 2013). The pET expression platform based on *Escherichia coli* cells is extensively applied in VLP research due to its easy low-cost use. However, antigen expression in the *E. coli* platform is at large limited to produce simple VLPs, composed of a single capsid protein. This system lacks eukaryotic post-translational modifications and often fails to produce correct disulfide bonds, and therefore frequently yields misfolded or insoluble proteins with decreased stability, reduced biological activity, and impaired immunogenicity (Huang et al., 2017; Walsh & Jefferis, 2006). Also, one must take into account the presence of bacterial endotoxins, which can induce a pyrogenic response and even trigger a septic shock in mammalian hosts. Therefore, endotoxins need to be removed during the VLP purification process or endotoxin-free *E. coli* strains can be used instead (Mamat et al., 2015). Alternatively, the most commonly used eukaryotic expression cells are yeasts, such as *Saccharomyces cerevisiae*, *Pichia pastoris*, or *Hansenula polymorpha*, which offer low-cost production of simple VLPs and provide un-complex eukaryotic post-translational modifications (H. J. Kim & Kim, 2017).

1.5.3 The basis of VLP immunogenicity

Mimicking of the origin pathogen dimensions and surface geometry provides adjuvant-like activity and allows the VLPs to effectively penetrate into the lymph and stimulate potent immune response with balanced humoral and cellular components (Gomes et al., 2017; D. M. Smith et al., 2013b). A single T=3 symmetry VLP presents 180 copies of the target protein, a T=7 symmetry capsid carries as much as 415 protein copies, but the M13 bacteriophage VLP is assembled from approximately 2700 coat proteins (Basnak et al., 2010; Ma et al., 2012b; H. Xu et al., 2018). The highly repetitive nature of VLP antigens, ordered approximately at 5-10 nm intervals, can directly stimulate innate immunity by recognition of pathogen-associated molecular patterns (Austyn, 2016; Bachmann & Zinkernagel, 1997; Dintzis et al., 1982). It facilitates the crosslinking of B-cell receptors, thereby reducing the signaling threshold required for T-cell independent B-cell activation (Bachmann & Zinkernagel, 1997; Carroll & Isenman, 2012; Jegerlehner et al., 2002). Molecules of the complement system, pentraxins, and natural antibodies are the key components mediating the humoral innate immune responses (Bottazzi et al., 2010; Carroll & Isenman, 2012; Palma et al., 2018). These macromolecules are multimeric and therefore can effectively interact with particulate structures with multivalent surface antigen organization, such as the exterior of viruses, which can therefore provide much stronger immune responses than antigen alone (Zabel et al., 2013). The repetitive antigen shell of the VLPs, therefore, prompts and amplifies the binding of natural IgM antibodies and pentraxins as well as fixation of the components of the complement cascade, thus promoting their opsonization and uptake by lymph node resident antigen-presenting cells (APCs), especially the dendritic cells (DCs), through pattern-recognition receptors (Bachmann & Jennings, 2010; Bottazzi et al., 2010).

VLP uptake leads to DC maturation – further antigen internalization decreases, antigen-processing proteolytic machinery is upregulated and peptide-major histocompatibility complex (MHC) molecules are expressed on the cell surface at high levels (Austyn, 2016). DC activation induces pro-inflammatory cytokine production (such as TNF α and IL-1 β) that, in turn, recruit more DCs and upregulate proteolysis in the DCs enhancing the VLP antigen presentation (Fiebiger et al., 2001). It is an essential step for initiation of the adaptive responses as mature DCs present the VLP antigens to lymphocytes, particularly T-cells, leading to CD4+ T-helper cell activation via the MHC class II presentation, CD8+ T-cell responses via the MHC class I presentation, and further B-cell stimulation (Figure 6) (Bachmann & Jennings, 2010; Gomes et al., 2017; Nooraei et al., 2021; Tao et al., 2019).

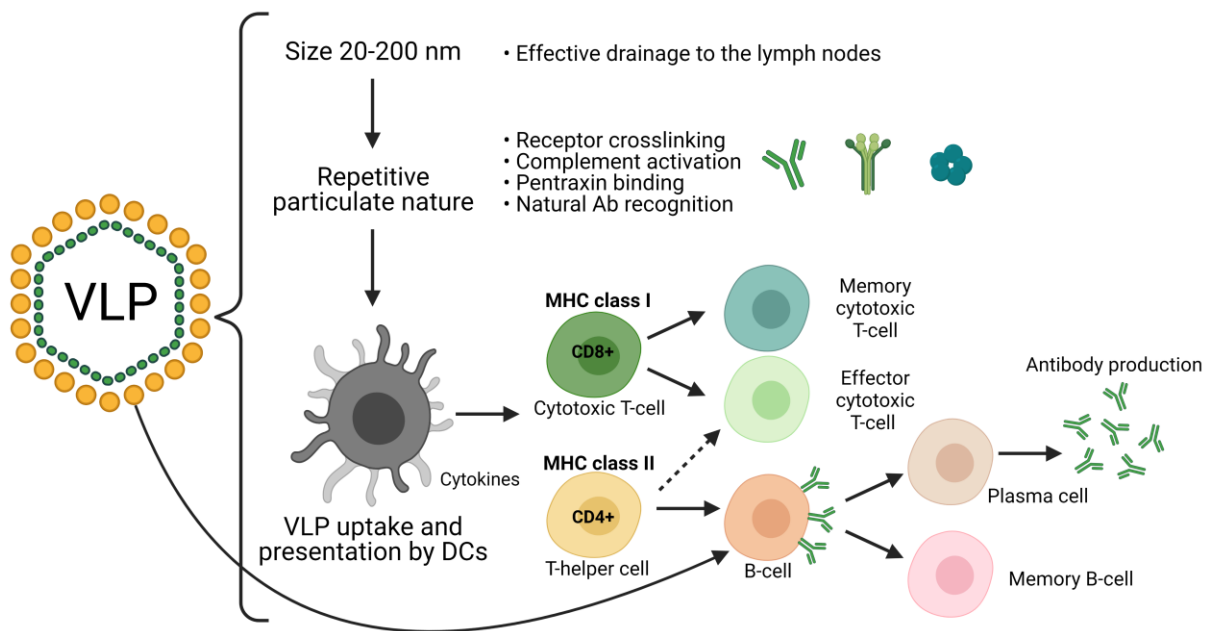


Figure 6. Immune responses to VLPs. The VLP size and particulate nature ensure effective drainage into the lymph nodes and enhances interactions with the multimeric components of the humoral immune system (crosslinking of B-cell receptors, binding of pentraxins and natural antibodies, and activation of the complement system). That, in turn, promotes unspecific VLP internalization by the dendritic cells (DCs), following VLP processing, DC maturation, and cytokine production that stimulates differentiation of other cells, such as T-cells. As a result, the processed VLP is presented by class I and II major histocompatibility complexes (MHC) for detection by CD8⁺ and CD4⁺ T-cells. Cellular and cytotoxic responses are driven by peptide-MHC I complex presentation by DCs to cytotoxic T-cells that, in turn, differentiate into memory and effector cytotoxic T-cells. T-helper cells also secrete cytokines that upregulate antigen presentation by DCs and assist effector cytotoxic T-cells. The humoral immune response is initiated by peptide-MHC II complex presentation by DCs to T-helper cells. T-helper cells interact with B-cells that differentiate into long-lived memory B-cells or in plasma cells that produce antibodies. The figure was adapted from (Bachmann & Jennings, 2010; Nooraei et al., 2021; Tao et al., 2019) and created in BioRender.

It has been shown that the optimal antigen dimensions for internalization and retention in lymph nodes and subsequent uptake by APCs, in particular the DCs, are 20-200 nm, matching most VLPs (Fifis et al., 2004; Manolova et al., 2008; Reddy et al., 2006). The particulate geometry and size of VLPs are thereby critical features predisposing these particles to rapid and efficient drainage into lymphatic circulation where they are preferentially collected by DCs and macrophages, followed by B-cell follicular delivery (Batista & Harwood, 2009; G. T. Jennings & Bachmann, 2008; Jia et al., 2012; Manolova et al., 2008; Reddy et al., 2006). That in turn promotes direct interaction with B-cells triggering antibody responses and contributing to the generation of memory B-cells and long-lived plasma cells (Barrington et al., 2002; Phan et al., 2009). APC interactions are dependent on other VLP properties as well, such as shape, charge, and hydrophobicity or hydrophilicity of particle surface, the technique of antigen presentation

and their conformation, ligands for Toll-like receptors, etc., thus, by modulating these factors, the particle immune recognition and processing can be enhanced even further (Ahsan et al., 2002; Gomes et al., 2017; G. T. Jennings & Bachmann, 2008). For example, viruses and many of their successor VLPs require nucleic acid for the shell assembly process (Perlmutter & Hagan, 2015). This encapsulated nucleic acid is derived from the host and therefore without any infectious potential and it can be replaced or modified. It acts as an adjuvant and promotes the APC uptake and triggers the binding of pattern recognition receptors, such as Toll-like receptors, thereby stimulating cytokine signaling and enhancing immune responses (Gomes et al., 2017; Hua & Hou, 2013; Perlmutter & Hagan, 2015).

1.5.4 Types of VLPs and their modification possibilities

Many of the versatile VLPs are suitable for bioengineering and can be modified to carry antigens of a heterologous origin, packaged in the particle or exposed on the VLP surface, and transport different therapeutic or diagnostic agents, such as oligonucleotides, cell-targeting moieties, probes, adjuvants or drugs, as cargos; it is even possible to simultaneously display desired epitopes and encapsulate adjuvants (Gomes et al., 2017; Ma et al., 2012b). For the creation of vaccines, both unmodified and chimeric VLPs have been extensively investigated.

Usually, VLPs consisting of unmodified authentic virus proteins are likely vaccine candidates against the parent virus itself, as they preserve the native conformation of the origin antigens, displayed in a highly dense arrangement, thereby eliciting stronger immune responses than individual antigens (Pushko et al., 2013; Syomin & Ilyin, 2019). Since the first recombinant VLP vaccine against hepatitis B virus became commercially available in 1986, VLPs have developed into an attractive vaccinology platform (Pushko et al., 2013). So far, several native VLP vaccines have been approved for both human and animal use, including numerous vaccines against hepatitis B virus and vaccines against human papillomavirus, hepatitis E virus, and a pilot project for a malaria vaccine, and many more are currently under investigation in both preclinical and clinical trials (Atcheson et al., 2021; Qian et al., 2020). Despite the structural complexity and production issues of native influenza VLPs, numerous such vaccine candidates have entered human clinical studies and have shown to induce potent immune responses (Appendix 2). Yet, regardless of the numerous successes, the expression of many pathogen-derived VLPs and their purification to yield a stable product is difficult and often unproductive (Lua et al., 2014). Furthermore, they are mostly based on HA head or NA proteins and therefore do not entirely eliminate the need for frequent reformulations of the vaccine composition. Indeed, native VLPs lack the ability to selectively display specific

conserved epitopes and therefore rarely induce broad immune responses (Schwarz & Douglas, 2015).

This disadvantage can be circumvented as the VLP shell can also be modified to carry antigens of a foreign source in a multivalent manner, yielding chimeric particles. Under the desirable conditions, the displayed epitopes assume similar immunological properties as the particulate platform (Bachmann & Jennings, 2010; Pushko et al., 2013). Most often, the production of chimeric particles is an empirical and time-consuming process. Yet, with the advances in protein engineering tools, continuously accumulating structural data and computational models of both the viral capsids and target antigens, and the aid of high-quality 3D data imaging programs, any VLP modifications can be significantly alleviated (Jeong & Seong, 2017). It is even possible to obtain VLPs displaying several foreign epitopes (Syomin & Ilyin, 2019). VLP decoration can be pursued either by genetic manipulations or by modular approach (M. T. Smith et al., 2013).

Antigen presentation via the genetic fusion technique requires the substitution or integration of target sequence inserts into the capsid protein surface sites using mainstream molecular biology techniques (Bachmann & Jennings, 2010; Pushko et al., 2013). The gene of the desired antigen is directly attached to the capsid protein gene and expressed as a single fusion protein, which is a substantial benefit from the manufacturing perspective, rendering it a rather commonly used strategy for obtaining chimeric VLPs (Chackerian, 2007). This technique, however, is typically restricted by the limitations of insert size and ensuring the correct fold of both the capsid protein and the displayed antigen (Ma et al., 2012b; Taylor et al., 2000). Indeed, fusion-protein capsid assembly is prone to errors. Foreign sequences longer than a few dozen amino acids, oligomeric inserts, large protein volume, and high positive charge, incorrectly selected insert site, display antigens with high hydrophobicity or a high ratio of β -strands, and interactions with cellular proteins can cause detrimental interactions, significantly impairing the stability, folding and assembly of particles. That, in turns, triggers aggregation and insolubility, and thus, diminished immunogenicity (Billaud et al., 2005; Chackerian, 2007; Koho et al., 2015; Ma et al., 2012b; Zlotnick, 1994). Misfolded display antigens induce ineffective antibodies, and therefore scientists often choose to insert linear epitopes that do not bind conformation-specific antibodies (S. Chen et al., 2015; Jegerlehner et al., 2013; Ramirez et al., 2018). Furthermore, the fusion-VLP technique is not always applicable as the shell and display antigens can require different post-translational modifications and therefore – different expression systems (Brune et al., 2016).

In the chemical functionalization technique, the VLP and display antigen are expressed and purified separately in a modular approach and then covalently coupled *in vitro*. Although the modular functionalization is more complex in terms of production, as it adds an additional step in VLP assembly, it bypasses the folding constraints, insert size limitations, assembly issues, and incompatible post-translational modifications, and therefore is often favored (Koho et al., 2015; M. T. Smith et al., 2013). The coupling of diverse conformational epitopes and even full-length proteins is possible, increasing the likelihood of broadly reactive antibody responses (Röhn et al., 2006). Furthermore, the VLP shell proteins can be produced and purified in advance, accelerating the vaccine manufacturing time, increasing pandemic preparedness, and allowing to prepare a vaccine platform for multiple targets simultaneously (Brune & Howarth, 2018; Jegerlehner et al., 2013). Bifunctional crosslinking reagents usually couple the surface-exposed nucleophilic amino acid side chains of the VLP and display antigen. The most common approach is to link the primary amine from lysine or N-terminus of the VLP with thiol of the antigen, derived from the native or inserted sequence cysteines or introduced by chemical reagents, such as 2-iminothiolane or N-succinimidyl S-acetylthioacetate (Ma et al., 2012b; M. T. Smith et al., 2013; Thermo Scientific, 2021). The abundant primary amines offer a suitable scaffold for high-density antigen presentation; however, the occurring coupling reaction is random and lacks density control and site-specific decoration, and therefore is difficult to predict or analyze (Brune & Howarth, 2018; M. T. Smith et al., 2013). Excessive antigenic display can oppress the functional properties of the VLP shell and even distort the native fold of proteins or cause precipitation of the product (Brune & Howarth, 2018; Carrico et al., 2012). Antigen display by chemical coupling can also result in incomplete or uneven decoration (Brune & Howarth, 2018). The reactive side chain moieties of glutamic acid, aspartic acid, tyrosine, and unnatural amino acids can also be used to form covalent bonds between the shell and target antigens, possibly offering a scaffold for more specific functionalization (Brune & Howarth, 2018; M. T. Smith et al., 2013). Alternatively, VLPs can be decorated using other covalent decoration methods, such as the SpyTag/SpyCatcher technology, sortase, and split inteins, or by exploiting the non-covalent interactions, such as histidine-nickel affinity, or biotin-streptavidin display, or others (Brune et al., 2016; Chackerian et al., 2006; Koho et al., 2015; Ma et al., 2012b; Shah & Muir, 2014; Tang et al., 2016).

Chimeric influenza VLPs have been extensively investigated in both preclinical and clinical trials (Appendix 3). Yet, despite the decades of research, none of these vaccine candidates has been licensed for human use.

2. MATERIALS AND METHODS

2.1 Plasmid construction

HA stalk antigens. Two conserved HA2 polypeptide fragments with sequences that overlap at the C-terminus were used in our experiments – a sequence encoding the long-alpha helix (LAH) (coding for HA residues 418–474) and an N-terminally extended LAH sequence (coding for HA residues 403-474), both derived from the pandemic influenza A virus strain A/Luxembourg/43/2009 (H1N1) (GenBank Accession No FN423713.1). The product of the second, N-terminally extended gene is referred to as tri-stalk protein. These sequences were PCR-amplified and inserted into the high-copy pETDuet-1 expression vector (Novagen) between *NcoI* and *BspTI* restriction sites. Briefly, the expression vectors and PCR-amplified target genes were digested with compatible restriction enzymes and analyzed via 1% agarose gel electrophoresis in standard 1× TAE buffer. Analyzed under the ultraviolet light, the desired fragments were isolated from the ethidium bromide-containing gel with GeneJET Gel Extraction Kit (Thermo Fisher Scientific). The purified fragments were subsequently ligated into the target vector with T4 DNA ligase (Thermo Fisher Scientific) following the manufacturer's instructions.

3M2e. A third highly-conserved influenza A protein used in our experiments was a triple 72-residue M2e peptide (3M2e), comprised of three 24-residue M2e variants from different influenza A virus subtypes (Table 1). The 3M2e gene was supplied cloned in an expression ready pET24a(+) vector (BioCat GmbH). As the 3M2e gene was initially designed for chemical coupling, it also contains an N-terminal 6× polyhistidine tag and a cleavage site for the TEV protease, as well as a C-terminal cysteine and an EAAAK linker.

Table 1. Amino acid sequence of the 3M2e peptide used in our experiments

Reference virus	Amino acid sequence
H1N1 (A/Puerto Rico/8/1934) – fragment 1	MSLLTEVETP IRNEWGSRSNGSSD
H1N9 (A/duck/Yunnan/1282/2007) – fragment 2	MSLLTEVETP TRNGWGSKNGSSD
H3N2 (A/swine/Quebec/1262080/2010) – fragment 3	MSLLTEVETP TRNEWESSNGSSD

*Cysteines in the original sequence were substituted with Serines (bold) to avoid disulfide-bond formation.

Variable amino acids marked in red.

Native VLP proteins. For the *Acinetobacter* phage AP205 (referred to as AP) VLP production and for the *Escherichia* virus Q-beta (Qβ) VLP production, their coat protein genes (GenBank Accession No NC_002700.2 and AY099114.1, respectively) were PCR-amplified and cloned in the pETDuet-1 plasmid between *NcoI* and *PstI* restriction sites. Another *NheI*

restriction site was introduced before the STOP codon for the AP construct. The expression plasmids were prepared as described above.

AP-M2e. To yield chimeric AP-M2e fusion gene, a 72-residue sequence encoding the 3M2e peptide was PCR-amplified, adding *NheI* and *PstI* restriction sites and additional STOP codon, and ligated into a *NheI/PstI* digested AP-pETDuet-1 vector at the C-terminus of the AP205 coat protein gene.

LAH1-PP7. To create chimeric LAH1-PP7 fusion gene, the C-terminus of the *Pseudomonas* phage PP7 coat protein (GenBank Accession No NC_001628.1) encoding gene was fused with H1 LAH sequence, separated by a short GSG-encoding linker, and cloned into a pETDuet-1 vector as described for the AP-M2e protein.

K1-K1. A sequence encoding hepatitis B virus core (HBc) hetero-tandem construct was supplied by GeneArt (Life Technologies), with codon usage optimized for expression in yeasts (Peyret et al., 2015). The construct encoded for an HBc dimer, where a C-terminally truncated 149-residue HBc monomer (referred to as Core 1) was fused with a full-length 185-residue HBc monomer (referred to as Core 2), covalently linked with a 7×GGS linker. This gene included a lysine codon between flexible glycine linkers in both major insertion regions (MIRs), and unique restriction sites were introduced in both MIRs by silent mutations up- and downstream the lysine linkers (*XbaI/NotI* sites in Core 1 and *EcoRI/NheI* in Core 2, respectively). The construct was cloned into a pPICZC expression vector (Invitrogen) between *AgeI* restriction sites, yielding an expression plasmid for a fusion protein, referred to as K1-K1.

LAH3-HBc. To create chimeric LAH3-HBc protein, the K1-K1 linker of Core 1 was first cut out using the *XbaI* and *NotI* restriction sites, while the Core 2 remained unchanged. A yeast-optimized sequence encoding the LAH (referred to as LAH3) comprising of HA residues 420–474 from influenza A virus strain A/Hong Kong/1/1968 (H3N2) (GenBank Accession No AAK51718) was supplied by GeneArt. The digested vector and LAH3 sequence were ligated as described above.

2.2 Plasmid DNA amplification and insert confirmation

For plasmid DNA amplification, except the HBc constructs, the competent *E. coli* XL1-Blue cells (Stratagene) were transformed with the recombinant plasmid of interest using a heat-shock of +42°C degrees according to the manufacturer's instructions. The transformation mixture was plated on selective LB-medium agar plates supplemented with ampicillin (100 µg/mL) and incubated overnight at +37°C. Individual colonies were inoculated into 4 mL of

2×TY medium supplemented with ampicillin (50 µg/mL) and grown overnight at +37°C on a shaker. Plasmid DNA was isolated and purified with GeneJET Plasmid Miniprep Kit (Thermo Fisher Scientific) following the manufacturer's instructions. Selection of the positive plasmid clones was performed by a restriction analysis with compatible restriction enzymes and subsequent 1% agarose gel electrophoresis, following confirmation by Sanger DNA sequencing with BigDye Terminator v3.1 Cycle Sequencing Kit (Thermo Fisher Scientific) following the manufacturer's instructions.

The recombinant K1-K1 and LAH3-HBc constructs were digested with *PmeI* restriction enzyme to yield linearized vectors for transformation in electrocompetent *P. pastoris* KM71H cells (Thermo Fisher Scientific) by electroporation at 1.2 kV (Electroporator 2510). 96-well plates were filled with liquid YPD medium supplemented with zeocin (0.2 mg/mL for the first 48 h and 2 mg/mL for the following 48 h) for high copy number clone selection. The highest optical density cultures at OD_{A600} were selected and seeded on YPD-medium agar plates to yield single-cell colonies. Insert copy number was analyzed using quantitative real time PCR based on the zeocin gene. As clones with multiple integrated expression units have been proven to yield optimal target protein expression, the clone with the highest copy number (50 ± 2) was isolated and used to generate a Research Cell Bank (in BMGY-medium in 30% (v/v) glycerol, OD_{A600} = 25.0) (Nordén et al., 2011).

2.3 Antigen expression

All proteins, except the HBc constructs, were overexpressed in a two-step T7 promoter-regulated bacterial expression system. The recombinant plasmids of interest were transformed in competent *E. coli* BL21(DE3) cells (Stratagene) using a heat-shock of +42°C degrees according to the manufacturer's instructions. The transformation mixture was seeded on selective LB-medium agar plates as described above. Several colonies were inoculated into a selective LB-medium. The primary culture was grown overnight at +37°C and then added to a selective 2×TY medium, not exceeding 5-10% of the total culture volume. To produce U-¹³C, ¹⁵N-labeled free LAH protein, expression was performed in the following medium: Na₂HPO₄ (6 g/L), K₂HPO₄ (3 g/L), NaCl (2.5 g/L), ¹⁵NH₄Cl (1 g/L), U-¹³C D-glucose (2 g/L), 1 M CaCl₂ (100 µL/L), 1 M MgSO₄ (2.5 mg/L), 6% thiamine (33.33 µL/L), biotin (1 µg/L), ampicillin (500 µg/L). The expression culture was incubated at +37°C under continuous shaking conditions until OD_{A540} reached 0.6-0.8 (corresponding to the mid-log phase). Target protein gene expression was promptly induced with isopropyl-β-thiogalactopyranoside (1 mM

for the HA stalk proteins' and 3M2e expression cells and 0.1 mM for the VLPs). HA LAH and tri-stalk, as well as 3M2e expression cells were then grown for another 3-4 h at +37°C, while for the AP205, AP-M2e and Q β VLP expression cells the incubation temperature was lowered to +20°C and the cultivation was continued for another 16-18 h.

For K1-K1 and LAH3-HBc gene expression, 1.8 mL of Cell Bank suspension was seeded in 2 \times 2 L baffled Nalgene® shake-flasks containing 250 mL of BMGY-medium and incubated until the OD_{A600} reached 15-20. The culture was then used to inoculate a 30 L BIOSTAT Cplus bioreactor (Sartorius) at 5% of the total volume. The bioreactor was filled with 10 L of Basal Salts medium (Table 2) supplemented with PTM1 trace salts (Table 3) per liter of Basal Salts medium.

Table 2. The composition of the basal salts medium per liter

Component	Amount
85% phosphoric acid	26.7 mL
CaSO ₄	0.93 g
K ₂ SO ₄	18.2 g
MgSO ₄ ·7H ₂ O	14.9 g
KOH	4.13 g
glycerol	40 g
PTM1 trace salts solution	4.35 mL

Table 3. The composition of the PTM1 trace salts solution per liter

Component	Amount
CuSO ₄ ·5H ₂ O	6.0 g
KI	0.08 g
MnSO ₄ ·H ₂ O	3.0 g
Na ₂ MoO ₄ ·2H ₂ O	0.2 g
H ₃ BO ₃	0.02 g
ZnCl ₂	20.0 g
FeCl ₃	13.7 g
CoCl ₂ ·6H ₂ O	0.9 g
H ₂ SO ₄	5.0 mL
biotin	0.2 g

After inoculation, the bioreactor was first run in batch-mode. The dissolved oxygen tension was maintained at 30%, the pH range – between 4.75–5.0, and the pre-induction temperature – at 30 \pm 0.1°C. The fed-batch induction phase was prompted 28.5 h after inoculation because of depletion of the carbon source (indicated by 20% drop in carbon evolution rate and a spike in dissolved oxygen tension). This phase was maintained for 48 h at a fixed flowrate of 50 mL/h. The induction media contained methanol for K1-K1 induction and 50% (v/v) glycerol and methanol at a 60:40 ratio for LAH3-HBc induction supplemented with 12 mL of PTM1 trace salts per liter of media. To prevent foamation, PEG-2000 was added

during fermentation. 48 h after the induction, the fermentation culture was cooled to 12°C to minimize proteolytic activity.

Cells or fermentation broth were harvested by low-speed centrifugation for 30 min at +4°C and stored frozen at -20° C. The production and solubility of target proteins were analyzed by sodium dodecyl sulphate–polyacrylamide gel electrophoresis (SDS/PAGE) with a 4% stacking and 15% separating polyacrylamide gel stained with Coomassie blue.

2.4 Protein purification

Purification of the HA tri-stalk antigen and LAH antigen were done in the same way. First, expression cells were resuspended in buffer A (20 mM Tris-HCl (pH 8.0) and 100 mM NaCl) (6 mL of buffer per 1 g of cells) and disrupted by sonication on ice, followed by clearance of the insoluble cell debris by centrifugation at 18,000 × g for 30 min at +4°C. Supernatant was decanted, heated to +55°C for 30 min, subsequently cooled to the room temperature (RT), and clarified by centrifugation at 16,000 × g for 15 min at RT. A three-step chromatography process was used to purify the HA tri-stalk antigen. First, the soluble fraction was applied to a weak anion-exchange column HiPrep 16/10 DEAE FF (20 mL, GE Healthcare), pre-equilibrated with buffer A. Column-bound protein was eluted with a linear salt gradient of 0.1-0.6 M NaCl in buffer A at 4 mL/min. Fractions containing the protein of interest were then pooled and diluted twice with 20 mM Tris-HCl (pH 8.0), and loaded on a strong anion-exchange column MonoQ 5/50 GL (1 mL, GE Healthcare), pre-equilibrated with buffer A. Column-bound protein was linearly eluted with 0.1-0.5 M NaCl in buffer A at 1 mL/min, and subsequently passed through a size-exclusion Superdex 200 10/300 GL matrix (20 mL, GE Healthcare) in 20 mM Tris-HCl (pH 8.0) and 200 mM NaCl buffer at 0.5 mL/min. Only fractions from the second peak were pooled as they corresponded to the molecular weight of trimeric protein.

To purify the 3M2e protein, expression cells were lysed as described above, except for the buffer B that contained 20 mM Tris-HCl (pH 8.0) and 300 mM NaCl. Two step chromatography process was then applied – first, the supernatant was passed through a metal affinity chromatography HisTrap™ FF column (1 mL, GE Healthcare), pre-equilibrated with buffer B containing 10 mM imidazole. Column-bound protein was linearly eluted with 0.1-0.5 M imidazole in buffer B, and subsequently passed through a size-exclusion Superdex 200 10/300 GL matrix in 20 mM Tris-HCl (pH 8.0) and 200 mM NaCl buffer at 0.5 mL/min.

To purify the LAH1-PP7 chimeric protein, cells were lysed as described above, with an additional lysis step: the insoluble debris was washed twice with lysis buffer A, and an

additional sonication step was performed in buffer A, supplemented with 0.25 M urea. Following the low speed centrifugation, the supernatant was loaded onto a Superdex 200 10/300 GL matrix (20 mL) in buffer A and fractions containing the chimeric LAH1-PP7 protein were pooled.

Lysis of AP205, AP-M2e, and Q β VLPs expression cells was performed as described above for the HA stalk proteins. Initial purification of these VLPs was performed by ammonium sulphate precipitation and thermal treatment. Solid ammonium sulphate was added gradually to the cleared supernatant under mild stirring conditions until 40% of saturation was reached, and the solution was incubated for 1 h at +4°C. The precipitated protein was collected by centrifugation at 16,000 \times g for 15 min at RT, and dissolved in minimal amount of 20 mM Tris-HCl (pH 8.0) buffer. Subsequently, the mixture was incubated at +55°C for 30 min to remove thermally unstable contaminants, following cooldown to RT and clarification by centrifugation at 16,000 \times g for 15 min at RT.

The purification of AP205 VLPs was performed with three subsequent chromatography columns. First, the cleared supernatant was loaded on a Sepharose 4 FF size-exclusion column (130 mL, GE Healthcare), pre-equilibrated with buffer A, run at 1 mL/min. Pooled fractions containing the target protein were further applied to an anion-exchange Fractogel TMAE (M) matrix (20 mL, Merck KGaA), pre-equilibrated with buffer A. Bound protein was eluted with a linear salt gradient of 0.1-1 M NaCl in buffer A at 3 mL/min. Fractions were again pooled and mixed with ammonium sulphate to 1.5 M final concentration and loaded on a hydrophobic-interaction Fractogel Propyl (S) matrix (20 mL, Merck KGaA), pre-equilibrated with 50 mM NaHPO₄ (pH 7.3) and 1.5 mM ammonium sulphate buffer. Protein was eluted with 25 mM NaHPO₄ (pH 7.3) buffer at 3 mL/min.

To purify the AP-M2e and Q β VLPs, supernatant was first loaded onto a Sepharose 4 FF matrix, pre-equilibrated with buffer A. Pooled fractions were then applied on a Fractogel DEAE (M) anion-exchange matrix (20 mL, Merck KGaA) in buffer A. The column was eluted with a linear gradient of 0.1-1 M NaCl in buffer A at 3 mL/min.

To disrupt the yeast K1-K1 or LAH3-HBc expression cells, they were first resuspended in lysis buffer C, containing lysis buffer A, supplemented with 0.1% Triton X-100, at a proportion of 15% (w/v). Cells were then lysed in four cycles at 10,000 psi with French Press (Thermo Electron), followed by clearance of the insoluble cell debris by centrifugation at 18,000 \times g for 30 min at +4°C.

The K1-K1 was first precipitated with solid ammonium sulphate, added gradually under mild stirring conditions within five minutes until 35% of saturation, and then centrifuged at

18,000 × *g* for 20 min at +4°C. To dissolve the precipitate, minimal amount of 20 mM Tris-HCl (pH 8.0) buffer was added, and the solution was incubated at +55°C for 30 min, following cooldown to RT and clarification by centrifugation at 16,000 × *g* for 15 min at RT. The cleared supernatant was then loaded onto a HiPrep 16/10 DEAE FF column, and the flow-through was collected.

To purify the LAH3-HBc protein, 20 mM Tris-HCl (pH 8.0) and 50% PEG6000 (w/v) solution was added dropwise to the supernatant under mild stirring conditions until 5% of PEG6000 was reached, and the solution was incubated for 1 h at +4°C. The precipitated protein was collected by centrifugation at 18,000 × *g* for 20 min at +4°C, and dissolved in minimal amount of 20 mM Tris-HCl (pH 8.0) and 2 M urea buffer. The solution was loaded onto a Sepharose 4 FF matrix in column buffer D, containing 20 mM Tris-HCl (pH 8.0), 100 mM NaCl and 1 M urea at 1 mL/min. Selected fractions were applied to an anion-exchange Fractogel TMAE (M) matrix, pre-equilibrated with column buffer D. Bound protein was eluted with a linear salt gradient of 0.1-1 M NaCl in buffer D at 3 mL/min. VLP-containing fractions were pooled and dialyzed (10 kDa MWCO membrane) at +4°C against 100× excess of buffer A with two buffer exchanges during the 48 h period. Dialyzed material was collected.

All chromatography steps were performed at RT and controlled by ÄKTA FPLC (Amersham Biosciences), ÄKTA Prime Plus, ÄKTA Avant 25 or ÄKTA Pure (GE Healthcare) chromatography systems. Protein concentration was estimated using Nanodrop (Thermo Scientific) or by the Bradford assay. Protein purity was assessed by SDS/PAGE, and their identity and quality was confirmed with immunoblotting on nitrocellulose membrane and Western Blots. VLP assembly was monitored by native 1% agarose gel electrophoresis in ethidium bromide staining or by transmission electron microscopy (TEM). To visualize the protein samples (5 µL, 0.1–0.5 mg/mL) by TEM, they were adsorbed on Formvar/carbon supported copper 200 grids, briefly washed with 1 mM EDTA solution and for 1 min negatively stained with 1% uranyl acetate. The samples were then analyzed using a JEM-1230 electron microscope (JEOL Ltd.) at 100 kV. Purified proteins were concentrated using Amicon-Ultra centrifugation units (Merck-Millipore) with a cut-off of 10 or 100 kDa. Single use aliquots of the purified proteins were stored frozen at –20°C or slowly frozen at –70°C in a Mr. Frosty™ (Thermo Scientific) container for further use in mice immunizations.

2.5 Coupling of HA stalk antigens to VLPs

For the chemical coupling reaction, the buffer for the reaction proteins was exchanged into phosphate buffered saline (PBS) of pH 7.4 using HiTrap Desalting column (5 mL, GE Healthcare), pre-equilibrated with PBS.

As there are no cysteines in the amino acid sequence of the tri-stalk and LAH antigens (stalk antigens for short), N-succinimidyl S-acetylthioacetate (SATA) reagent was used to add free sulfhydryl groups to the stalk antigen following the manufacturer's protocol (Thermo Scientific). First, the stalk antigen was mixed SATA reagent in dimethyl sulfoxide (DMSO) to reach a 3.3-fold molar excess of SATA over the tri-stalk antigen, adding protected sulfhydryl groups to the protein. The reaction mixture was incubated for 30 min at RT, and then transferred to a Zeba™ Spin desalting column (Thermo Scientific) to remove residual SATA and DMSO according to the manufacturer's instructions. Sulfhydryl groups were de-protected by addition of deacetylation solution (0.5 M hydroxylamine, 25 mM EDTA in PBS (pH 7.2–7.5)) to the SATA-modified antigen at a 1:10 volume ratio. The reaction mixture was incubated for 2 h at RT, and a Zeba Spin desalting column was used to remove any traces of the hydroxylamine.

SATA-coupled HA stalk antigen was immediately conjugated to AP205, AP-M2e, or Q β VLPs via the heterobifunctional cross-linking succinimidyl-6-((b-maleimidopropionamido)-hexanoate (SMPH) crosslinker (Thermo Scientific) following the manufacturer's protocol. Briefly, VLPs were mixed with the SMPH reagent in DMSO at a 10-fold excess of crosslinker to protein, and the mixture was incubated for 30 min at RT. The unreacted crosslinker was removed by desalting in a Zeba Spin column. Next, SMPH-coupled VLPs were mixed with the SATA-coupled stalk antigen at a 1:3 molar ratio and incubated for 30 min at RT, and an Amicon-Ultra 4 filter with a cut-off of 100 kDa was used to remove excess stalk antigen. Coupling efficiency was assessed by SDS/PAGE. Single use aliquots of the coupled proteins were stored frozen at -20°C or slowly frozen at -70°C in a Mr. Frosty™ until use.

2.6 Protein crystallization and structure determination

Protein was concentrated to 10 mg/mL in buffer containing 20 mM Tris-HCl (pH 8.0) and 200 mM NaCl using a 10 kDa cut-off Amicon-Ultra centrifugation unit. Crystallization was performed by the sitting-drop vapor-diffusion setup in 96-well MRC crystallization plates (Molecular Dimensions) using Freedom EVO crystallization robot (TECAN). The preliminary screening of the optimal tri-stalk crystallization conditions was performed using commercial

kits – Clear Strategy Screen I, Structure Screen 1&2 HT-96, PACT Premier™ and JCSG-plus (Molecular Dimensions). Equal amount of protein solution was mixed with precipitant liquid from the well (0.4 or 1 µL for screening and optimized conditions respectively) creating drops. After optimization of crystallization conditions, crystals were obtained at 2.0 M ammonium sulphate and 0.1 M Bis-Tris precipitation solution (pH 5.5). Acquired crystals were soaked briefly in precipitation solution supplemented with 30% glycerol for cryoprotection and then frozen in liquid nitrogen.

The diffraction data were collected at beamline I911-3 of MAX-lab synchrotron (Lund University, Sweden). Data were first processed using programs from the CCP4 software suite. The experimental diffraction images were indexed with MOSFLM (Battye et al., 2011), scaled with SCALA (Evans, 2006), and the phase determination was carried out with molecular replacement in PHASER (McCoy et al., 2007), using the structure of post-fusion HA stalk or the HA tri-stalk as the search model (PDB ID: 1HTM; PDB ID: 6GOL). The initial model was built automatically in BUCCANEER (Cowtan, 2006). Model was further adjusted in COOT (Emsley et al., 2010), following numerous refinement runs in REFMAC (Kovalevskiy et al., 2018). Structure was visualized in COOT and PyMOL (The PyMol Molecular Graphics System, Version 1.8 Schrödinger, LLC).

2.7 Enzyme-linked immunosorbent assay (ELISA)

ELISA conditions varied for each of the original paper. However, indirect ELISA was performed for all the experiments. Briefly, microtitration plates were coated overnight at +4°C with recombinant target proteins or buffer alone to check for the background noise. Plates were washed between steps three times with a buffer containing Tween 20. Free binding sites were blocked with 1% bovine serum albumin (BSA). After incubation and washing, sera were added in three-fold dilutions to triplicate wells, following another incubation and washing. Sera from naïve mice or sera from young children served as the negative control. The bound antibody was detected with color reactions by alkaline phosphatase- or horseradish peroxidase- (HRPO) conjugated antibody and a suitable substrate, and the OD was measured using an ELISA plate reader.

Publication I. To measure the LAH3-HBc induced antibody responses, full-length recombinant HAs (rHAs) from influenza group 1 and 2 (Sino Biological Inc.) were used as coating antigens in 384-well plates (Greiner Bio- One GmbH). Wells were coated with 20 µL of rHAs in 100 mM carbonate buffer (pH 9.6) at 3.5 µg/mL. Alternatively, wells were filled

with carbonate buffer for the background control, or with irrelevant antigens (Cytomegalovirus grade 2 antigen (2 µg/mL), EBV capsid protein (30 ng/mL), or *Toxoplasma gondii* antigen (2 µg/mL)) (Microbix, Mississauga) or HBc VLPs (2 µg/mL) in carbonate buffer that served as the negative control. Plates were incubated overnight at +4°C, and washed with 1% Tween-20 in buffer A (20 mM Tris (pH 8.0) and 100 mM NaCl). Blocking was performed with 1% BSA in buffer A for 2 h at RT, following a washing step. Sera were added in the wells, starting with 100-fold dilution for mouse sera, and incubated for 1.5 h at RT. After washing, alkaline phosphatase conjugated goat anti-mouse IgG (ImTec Diagnostics) was added at 1/750 dilution and incubated for 1.5 h following another washing step. Following 1 h incubation at +37°C, bound antibody was detected with 2-amino-2-methyl-1-propanol Spectromax Plus (Sopachem) at 405 nm.

Publication II. To detect the reactivity of sera from swine workers with tri-stalk protein, ELISA conditions were first optimized using sera from the LAH1-PP7 immunized mice. ELISA was performed as described in publication I with a few changes. First, we conducted a checkerboard titration method. Serial dilutions of the tri-stalk coating antigen (0.15625, 0.3125, 0.625, 1.25, 2.5, 5.0 and 10.0 µg/mL) were tested against diluted sera (starting from 100-fold dilution). Sera from LAH-PP7 immunized mice were used as the positive control and sera from naïve mice – as the negative control. After blocking, alkaline phosphatase-conjugated goat anti-human IgG (Southern Biotech) was added at dilution of 1/1000. Bound-antibody was detected with 4-nitrophenyl phosphate disodium salt hexahydrate (Sigma-Aldrich). The optimal conditions were found to be 1.25 µg/mL of HA tri-stalk as the coating antigen and serum dilution of 1:2700. These conditions were applied to assess the reactivity of human sera to HA tri-stalk. Low-titer sera from children were used as the negative control. Sera were added to blocked wells starting from 300-fold dilution and the rest of ELISA was performed as described above for the testing conditions. Furthermore, to assess the reactivity of mice and human sera with rHAS, a variety of rHAs from influenza A group 1 and 2 viruses were used as coating antigens (Sino Biological Inc.).

Publication III. 96-well microtitration plates (Corning™ CostarCorning Life Sciences) were filled with 50 µL of the coating antigens (HA tri-stalk, 3M2e or rHAs from group 1 or group 2 influenza) at 2 µg/mL, and incubated overnight at +4°C. Washing was performed with 0.05% Tween 20 in PBS. For blocking, 1% bovine serum albumin (BSA) in PBS was added to the wells for 30 min at +37°C. Diluted sera, starting from 1:000 (for IgG and IgG1) or 1:10 (for IgG2a) dilution was added to the wells and incubated for 1 h +37°C, with a following washing step. Then, HRPO-conjugated goat anti-mouse IgG (Sigma-Aldrich) (for IgG antibody) or

primary rabbit anti-mouse IgG1 and IgG2a antibody (Abcam) and secondary HRPO-conjugated goat anti-rabbit IgG (Sigma-Aldrich) (for IgG1 and IgG2a antibody) was added, following incubation for 30 min at +37°C and a subsequent washing step. Bound antibody was detected with 3,3', 5,5';-tetramethylbenzidine substrate (Thermo Scientific) at 450 nm.

2.8 Statistical analyses

Statistical evaluation of data was performed using GraphPad Prism 6.0 software (GraphPad Software Inc.). For the publication II, a one-way ANOVA was applied to analyze the statistical significance of experimental data, followed by the Holm–Bonferroni multiple comparison test. Spearman's rank correlation coefficient was applied to evaluate correlations. For the publication III, a one-way ANOVA was employed to evaluate the statistical significance of immunogenicity data, with an additional Tukey's multiple comparison test to compare the IgG endpoint titers. A log-rank Mantel-Cox test was applied to compare the differences in the survival distributions.

3. RESULTS

3.1 Production and purification of chimeric HBc virus-like particles carrying influenza virus LAH domain as vaccine candidates

Highlights:

- Unlike the unmodified HBc gene, the HBc tandem-core technology of fused core dimers allowed for expression of a soluble LAH3-HBc protein where a hydrophobic LAH monomer from the A/H3N2 HA stalk was inserted in the MIR of one of the core dimers.
- This chimeric protein could be produced in an endotoxin-free *P. pastoris* fermentation system in a bioreactor with a scale-up potential and successfully purified to at least 90% homogeneity yielding assembled VLPs.
- The chimeric LAH3-HBc particles were highly immunogenic in mice and elicited potent antibody responses against group 2 rHAs (H3, H4, H7, H10, H14, and H15) as well as cross-reactive, yet, lower antibody responses against heterologous group 1 rHAs (H1, H2, H5, H9, and H11).

RESEARCH ARTICLE

Open Access



Production and purification of chimeric HBc virus-like particles carrying influenza virus LAH domain as vaccine candidates

Andris Kazaks^{1*}, I-Na Lu², Sophie Farinelle², Alex Ramirez³, Vincenzo Crescente³, Benjamin Blaha⁴, Olotu Ogonah⁴, Tarit Mukhopadhyay⁴, Mapi Perez de Obanos⁵, Alejandro Krimer⁵, Inara Akopjana¹, Janis Bogans¹, Velta Ose¹, Anna Kirsteina¹, Tatjana Kazaka¹, Nicola J. Stonehouse⁶, David J. Rowlands⁶, Claude P. Muller², Kaspars Tars^{1,8} and William M. Rosenberg^{3,7}

Abstract

Background: The lack of a universal influenza vaccine is a global health problem. Interest is now focused on structurally conserved protein domains capable of eliciting protection against a broad range of influenza virus strains. The long alpha helix (LAH) is an attractive vaccine component since it is one of the most conserved influenza hemagglutinin (HA) stalk regions. For an improved immune response, the LAH domain from H3N2 strain has been incorporated into virus-like particles (VLPs) derived from hepatitis B virus core protein (HBc) using recently developed tandem core technology.

Results: Fermentation conditions for recombinant HBc-LAH were established in yeast *Pichia pastoris* and a rapid and efficient purification method for chimeric VLPs was developed to match the requirements for industrial scale-up. Purified VLPs induced strong antibody responses against both group 1 and group 2 HA proteins in mice.

Conclusion: Our results indicate that the tandem core technology is a useful tool for incorporation of highly hydrophobic LAH domain into HBc VLPs. Chimeric VLPs can be successfully produced in bioreactor using yeast expression system. Immunologic data indicate that HBc VLPs carrying the LAH antigen represent a promising universal influenza vaccine component.

Keywords: Virus-like particles, Tandem-core, Influenza vaccine, Long alpha helix, Yeast

Background

Worldwide, influenza epidemics result in excessive morbidity and the deaths of 250,000–500,000 people, annually [1]. Seasonal epidemics and pandemics are caused by group A influenza viruses, which are the main targets of seasonal vaccines. Currently licensed influenza vaccines are effective against homologous viruses, however, these vaccines need to be reformulated for every season on the basis of predictions of the upcoming circulating subtypes. Prediction mismatches can impact vaccine effectiveness, and have significant epidemiological and economical consequences [2]. Moreover,

besides seasonal epidemics, influenza viruses can cause occasional pandemics. Thus, development of a universal influenza vaccine, which would protect against a broad spectrum of influenza viruses, is warranted. Novel attempts to construct such universal vaccines are generally based on conserved antigens from influenza matrix protein 2, as well as from the hemagglutinin (HA) stalk domain [3]. However, these antigens are naturally weak immunogens. Various strategies have been developed to elicit more potent immune responses with broader reactivity upon appropriate presentation to the host immune system [1, 4].

Presentation on the surface of symmetric virus-like particles (VLPs) stands out as one of the most efficient approaches to improve immune responses to weak antigens [5]. A number of attempts have been made to

* Correspondence: andris@biomed.lv

¹Latvian Biomedical Research and Study Centre, Ratsupites 1, Riga LV-1067, Latvia

Full list of author information is available at the end of the article



© The Author(s). 2017 **Open Access** This article is distributed under the terms of the Creative Commons Attribution 4.0 International License (<http://creativecommons.org/licenses/by/4.0/>), which permits unrestricted use, distribution, and reproduction in any medium, provided you give appropriate credit to the original author(s) and the source, provide a link to the Creative Commons license, and indicate if changes were made. The Creative Commons Public Domain Dedication waiver (<http://creativecommons.org/publicdomain/zero/1.0/>) applies to the data made available in this article, unless otherwise stated.

construct broadly protective candidate vaccines based on the conserved extracellular domain of matrix protein 2 (M2e) of influenza A viruses [6–9]. Although these M2e-based VLP vaccine candidates have been successfully tested in animal models, further efficacy studies are needed to demonstrate their protective potential in humans [1]. In addition, many scientists now believe that a universal and broad cross-protective influenza vaccine may require additional components. One such potential candidate is the structurally conserved 55 amino acid-long alpha helix (LAH) of the HA stalk domain.

Here, we incorporated the LAH domain from H3N2 influenza virus into H3c VLPs using novel tandem core technology based on the fusion of two H3c open reading frames to produce a single polypeptide chain. This strategy allows the insertion of large heterologous sequences in one of the two major immunodominant regions (MIR) located at the terminus of each spike, without compromising VLP formation [10]. A chimeric H3c-LAH gene was expressed in yeast *Pichia pastoris*. This expression system is preferred to bacteria because it avoids contamination with bacterial endotoxins. Fermentation and purification conditions compatible with industrial scale-up were established. The VLPs obtained induced a strong and broadly cross-reactive antibody response against several HA protein strains derived from both group 1 and group 2 influenza A virus subtypes in mice. These data indicate that tandem core VLPs carrying the LAH antigen represent a promising universal influenza vaccine component.

Methods

DNA constructions and yeast clone selection

A yeast codon optimized sequence encoding the tandem core construct including lysine linkers in both MIRs was designed and synthesized at GeneArt and cloned in the pPICZC vector (*Invitrogen*) using *Bst*BI and *Age*I restriction sites. Silent mutations were introduced up- and downstream of the two MIRs to create unique restriction sites (*Xba*I/*Not*I in Core 1 and *Eco*RI/*Nhe*I in Core 2). The resulting plasmid pPICZC PHe7 K1,K1 (K1-K1, for short) was used as a template for other MIR insertions. The lysine-encloding linker in Core 1 was replaced by yeast-optimized DNA sequence encoding the 55 amino acid long influenza H3N2 virus (A/Hong Kong/1/1968, Accession № AAK51718) HA stalk domain (corresponding to HA amino acids 420–474), using *Xba*I and *Not*I restriction sites. Resulting pPICZC coHe(LAH3,K1) construct (LAH3-H3c, for short) was linearized with *Pme*I to transform *P. pastoris* KM71H electrocompetent cells via electroporation. High copy number clones were selected in 96 well plates with liquid YPD medium containing 0.2 mg/mL (first 48 h) and 2 mg/mL (following 48 h) of zeocin. Cultures showing highest optical density (OD) at

A = 600 nm were selected and spread on YPD agar plates in order to isolate single cell colonies. Selected clones were analysed for insert copy number by quantitative real time PCR based on the zeocin gene. The highest copy clone was selected and used to generate a Research Cell Bank.

Fermentation conditions for LAH3-H3c

For seed culture, 2 × 250 mL of buffered glycerol-complex medium (BMGY; 1% (w/v) yeast extract, 2% (w/v) peptone, 100 mM potassium phosphate buffer pH 6.0, 1.34% (w/v) YNB, 0.0004% (w/v) biotin, and 1% (v/v) glycerol) was inoculated with 1.8 mL of cell bank suspension (BMGY culture in 30% (v/v) glycerol, OD = 25.0) in 2 L baffled Nalgene® shakeflasks. After 16–18 h the OD of the flask was between 15 and 20 and a 5% transfer volume was used to inoculate the bioreactor.

Invitrogen's fermentation protocol for *Pichia pastoris* Mut^S strains was used to generate experimental material in a 30 L BIOSTAT Cplus bioreactor (Sartorius). The reactor was filled with Basal Salts medium (26.7 mL/L phosphoric acid (85%), 0.93 g/L CaSO₄, 18.2 g/L K₂SO₄, 14.9 g/L MgSO₄·7H₂O, 4.13 g/L KOH, 40 g/L glycerol), plus 4.35 mL PTM₁ trace salts per litre of Basal Salts media to achieve a total starting working volume of 10 L post-inoculation. The PTM₁ trace salts contained: CuSO₄·5H₂O, 6.0 g/L; KI, 0.08 g/L; MnSO₄·H₂O, 3.0 g/L; Na₂MoO₄·2H₂O, 0.2 g/L; H₃BO₃, 0.02 g/L; ZnCl₂, 20.0 g/L; FeCl₃, 13.7 g/L; CoCl₂ · 6H₂O, 0.9 g/L; H₂SO₄, 5.0 mL/L; and biotin, 0.2 g/L.

The bioreactor was run in batch-mode after inoculation. The dissolved oxygen tension (DOT) was maintained at 30% and was controlled in a sequence cascade by agitating the impeller between 400 to 1000 rpm followed by oxygen gas blending in ratio mode at a constant volumetric gas flowrate of 0.51 vvm. The pH range was maintained between 4.75–5.0 and pre-induction temperature at 30 ± 0.1 °C. A 20% drop in carbon evolution rate (CER) and spike in DOT, indicating depletion of carbon source, triggered the fed-batch induction phase. This was observed 28.5 h after bioreactor inoculation.

This fed-batch induction phase was maintained for 48 h at a fixed flowrate of 50 mL/h. The induction media itself is comprised of a 60:40 ratio of 50% (v/v) glycerol and pure methanol respectively, plus 12 mL PTM₁ salts per liter of induction media. PPG2000 was used to prevent extensive foam formation throughout the fermentation. After 48 h of induction the culture was cooled to 12 °C to minimize proteolytic activity. Fermentation broth was harvested at 3000 g, 20 min and 4 °C. The wet pellets were weighed and stored at –20 °C.

Purification and characterization of chimeric VLPs

Yeast cells were resuspended in lysis buffer (20 mM Tris HCl, 100 mM NaCl, 0.1% Triton X-100, pH = 8.0) at a proportion of 15% (w/v) and disrupted by French Press (4 cycles, 10,000 psi). The soluble fraction was separated by centrifugation (30 min, 18,000 g, +4 °C).

For purification of HBc K1-K1 VLPs, solid ammonium sulfate was added until 35% of saturation by continuous stirring for 5 min following centrifugation (20 min, 18,000 g, +4 °C). The precipitate was dissolved in a minimal volume of 20 mM Tris HCl pH = 8.0, subjected to thermal treatment (30 min at 55 °C) and centrifuged again. The supernatant was passed through an anion-exchange HiPrep 16/10 DEAE Fast Flow column and the flow-through fraction was collected. All chromatography runs were monitored and controlled by an ÄKTA FPLC chromatography device (GE Healthcare).

For purification of chimeric LAH3-HBc VLPs, PEG6000 50% solution in 20 mM Tris HCl, pH = 8.0 (w/v) was added dropwise to the cell supernatant under continuous stirring until the final concentration reached 5% (w/v) and incubated 1 h at +4 °C. After centrifugation (20 min, 18,000 g, +4 °C) the precipitate was dissolved in a minimal volume of 20 mM Tris HCl, 2 M urea and loaded onto a size-exclusion Sepharose 4 FF matrix (XK26/40 column, bed height 25 cm) in column buffer A (20 mM Tris HCl, 100 mM NaCl, 1 M urea, pH = 8.0) at V = 1 mL/min. 10 mL fractions were collected and analyzed by native agarose gel, denaturing PAGE, and electron microscopy. Selected fractions were pooled and loaded onto anion-exchange Fractogel EMD TMAE (M) column (Tricorn 10/50 column, 3.5 mL bed volume) equilibrated with column buffer A. Column-bound proteins were eluted with a linear gradient of 10 column volumes using column buffer A containing 1 M NaCl. Fractions containing VLPs were dialyzed (10 kDa MWCO membrane) against 100× excess of 20 mM Tris HCl, 100 mM NaCl, pH = 8.0, with two buffer exchanges, for 48 h at +4 °C. Dialyzed material was pooled and concentrated with Amicon 100 kDa MWCO filter until it reached concentration of about 1 mg/mL. The VLP preparation was aliquoted, slowly frozen at -70 °C in a Mr. Frosty™ container and used for immunization of mice.

Protein concentrations were estimated by the Bradford assay. The purity of protein samples was analyzed by SDS-PAGE according to standard protocols with a 4% stacking and 15% separating polyacrylamide gel (PAAG). To visualize protein bands, the gels were stained with Coomassie Brilliant Blue G-250. Alternatively, separated proteins were transferred onto nitrocellulose membrane and detected by immunoblotting with the monoclonal anti-HBc antibody and the anti-mouse IgG peroxidase conjugate (DAKO). To assess nucleic acid content,

samples were subjected to native 1% agarose gel electrophoresis in TAE buffer (pH = 8.4) for approximately 0.5 h at 5 V/cm. Nucleic acids in the agarose gels were visualized by ethidium bromide staining. A 1 kb DNA ladder (Thermo Fischer Scientific) was used as a marker. For transmission electron microscopy, the protein samples (at c = 0.1–0.5 mg/mL) were adsorbed on carbon-Formvar-coated copper grids and negatively stained with 1% uranyl acetate aqueous solution. The grids were examined with a JEM-1230 electron microscope (JEOL Ltd., Tokyo, Japan) at 100 kV. Electron micrographs were recorded digitally using a side-mounted Morada camera (Olympus - Soft Imaging System GmbH, Munster, Germany) with iTEM software (version 3.2, Soft Imaging System GmbH).

Mouse immunizations

All mouse experiments were performed in accordance with protocols approved by the Animal Welfare Structure of the Minister of Agriculture, Viticulture and the Consumer Protection of the Grand Duchy of Luxembourg (Ref. LNSI-2014-02). Female BALB/c mice were purchased from Harlan Laboratories, Inc. 8-week-old BALB/c mice were immunized using a standard protocol including 3 intraperitoneal injections at 2 weeks interval with 30 µg of chimeric LAH3-HBc VLPs for primary immunisation, and with twice 15 µg for the second and third injection. The antigen was dissolved in 100 µL phosphate buffered saline adjuvanted with 100 µL MF59 (Addavax, Invivogen) containing 20 µg CpG (OD2395 Vaccigrad, Invivogen) totaling 200 µL per injected dose.

Enzyme-linked immunosorbent assay (ELISA)

Influenza-specific IgG in mouse serum was measured by indirect ELISA using the following purified recombinant group 1 and group 2 HA antigens at the given concentrations: A/Texas/36/1991 (Tex91) (H1, 1.5 µg/ml), A/California/4/2009 (Cal09) (H1, 3.5 µg/ml), A/Japan/305/57 (JP57) (H2, 1.25 µg/ml), A/Perth/16/2009 (Perth09) (H3, 0.625 µg/ml), A/Swine/Ontario/01911-1/99 (Onta99) (H4, 1.25 µg/ml), A/Vietnam/1203/04 (VN04) (H5, 1.25 µg/ml), A/Netherlands/219/2003 (Neth03) (H7, 2.5 µg/ml), A/Hong Kong/1073/99 (HK99) (H9, 1.25 µg/ml), A/Jiangxi-Donghu/346/2013 (JX13) (H10, 2.5 µg/ml), A/mallard /Alberta/294/1977 (Alb77) (H11, 1.25 µg/ml), A/mallard/Astrakhan/263/1982 (Astrak82) (H14, 1 µg/ml), and A/duck/AUS/341/1983 (AUS83) (H15, 2 µg/ml) all purchased from *Sino Biological Inc.* Subsaturating coating concentrations were determined with a serum of a mouse sublethally challenged either with pH1N1 (group 1 HA) or H3N2 (group 2 HA) or with specific monoclonal antibodies against HA H1N1, HA H3N2, HA H5N1, HA H7N9 and HA H9N2 from

the same supplier, after coating ELISA plates with three-fold dilution series of each antigen.

Wells of 384-well microtiter plates (Greiner) were coated overnight at 4 °C with 20 µL/well of 3.5 µg/mL purified HA proteins in carbonate buffer (100 mM, pH = 9.6) or with carbonate buffer alone as a background control. Irrelevant antigens (Cytomegalovirus grade 2 antigen, 2 µg/ml; purified EBV capsid protein, 30 ng/ml; *Toxoplasma gondii* antigen, 2 µg/ml; Microbix, Mississauga, Canada) served as negative antigen controls. Reactivity against “empty” HBc VLPs (20 µl per well of 2 µg/ml) was used as positive control. All subsequent steps were performed at room temperature. Wells were washed sequentially in washing buffer (Tris HCl containing 1% Tween 20) and blocked for 2 h with 1% BSA in Tris buffer. After washing, sera (starting with a 100-fold dilution) were added, incubated for 90 min, and washed. Alkaline phosphatase conjugated goat anti-mouse IgG (1/750 dilution, ImTec Diagnostics) was added for 90 min, washed and developed using 2-amino-2-methyl-1-propanol. Absorbance was measured at 405 nm (Spectromax Plus, Sopachem) after 60 min incubation.

Results and discussion

Modification of the HBc gene

The insertion of heterologous sequences into viral structural genes generates chimeric VLPs that can be used as stable nanocontainers for diagnostics, vaccination and gene transfer purposes [11, 12]. The successful assembly of chimeras is dependent on the nature of the insert as

well as its position within the carrier gene. For HBc, the MIR is generally considered as the most promising insertion site of the HBc molecule due to its surface exposure and high insertion capacity [13]. Recently, a number of approaches have been developed for MIR-insertion and the presentation of “difficult” protein sequences including large, charged and/or hydrophobic domains, T-cell epitopes, and cell-receptor ligands. These strategies include the SplitCore [14], the use of a non-covalent “binding-tag” peptide [15], and the tandem core technology. The latter is based on a genetically fused HBc dimer that can assemble in correctly folded HBc VLPs [16] while accommodating large heterologous sequences [10].

Previously, we have demonstrated that the yeast *P. pastoris* system is well suited for high-level of synthesis and purification of wild-type HBc VLPs expressed from a cloned HBc monomer gene [17]. The current study is based on so called hetero-tandem core, where a C-terminally truncated HBc monomer gene (Core 1, 149 aa) was genetically fused via a GGSx7 linker with a full-length HBc monomer gene (Core 2, 185 aa) to form a covalently linked dimer. To further explore the potential of this HBc carrier, we introduced into each MIR two short sequences encoding a lysine codon flanked on both sides by flexible glycine linkers (Fig. 1a). Such surface-exposed lysine residues can be efficiently used for chemical coupling of peptides containing reactive SH groups provided by free cysteine residues [18]. The resulting construct K1-K1 was transformed in yeast *P. pastoris*. The selected clone containing multiple

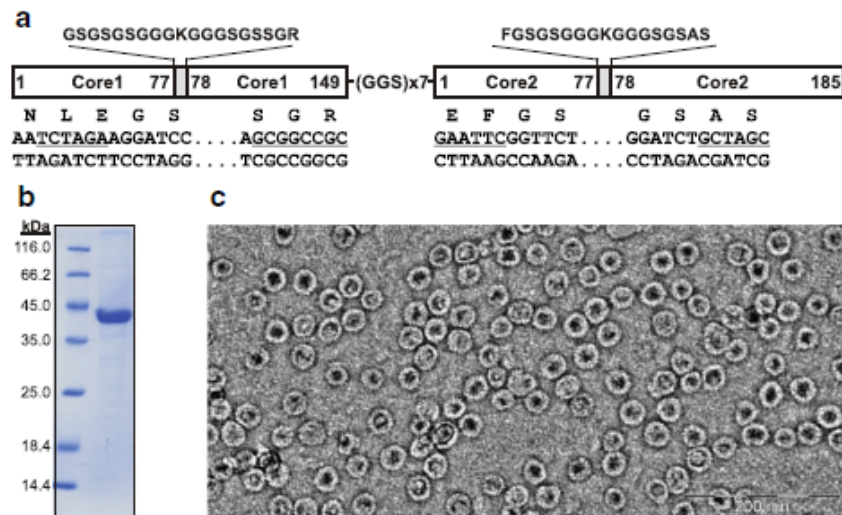
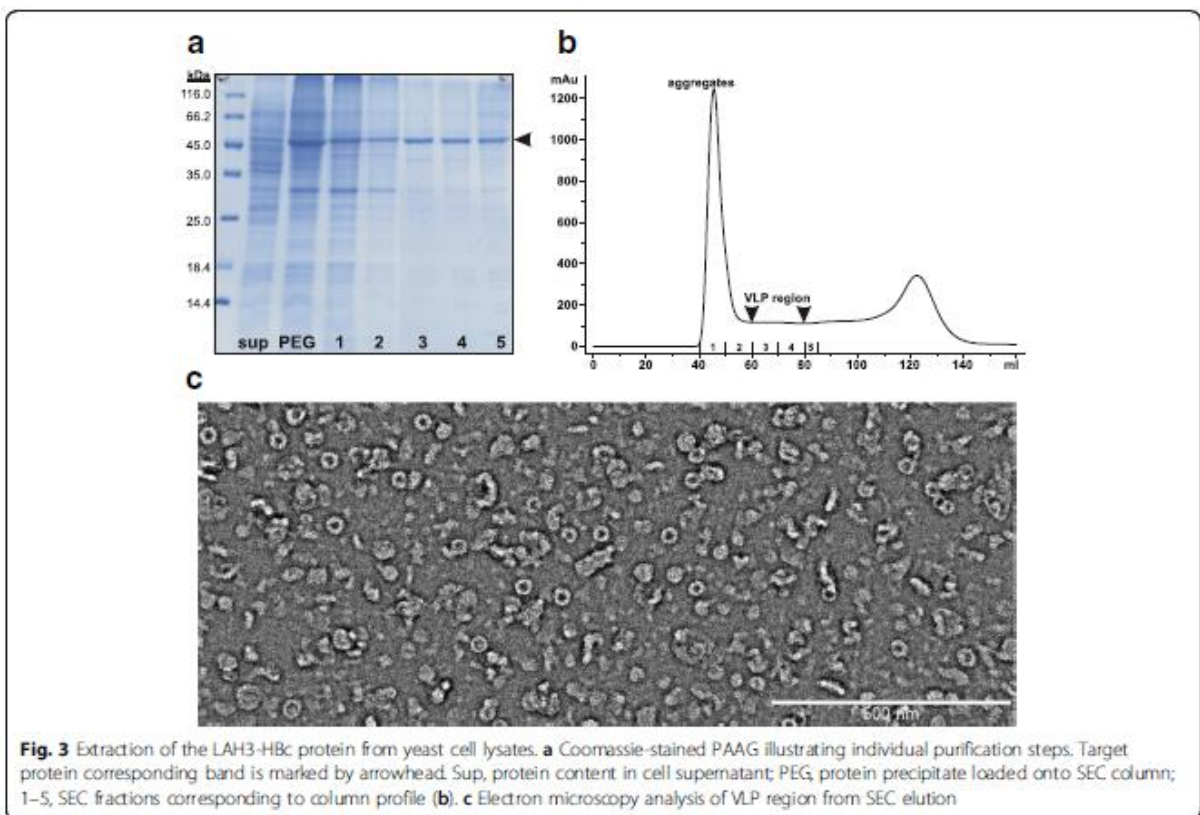
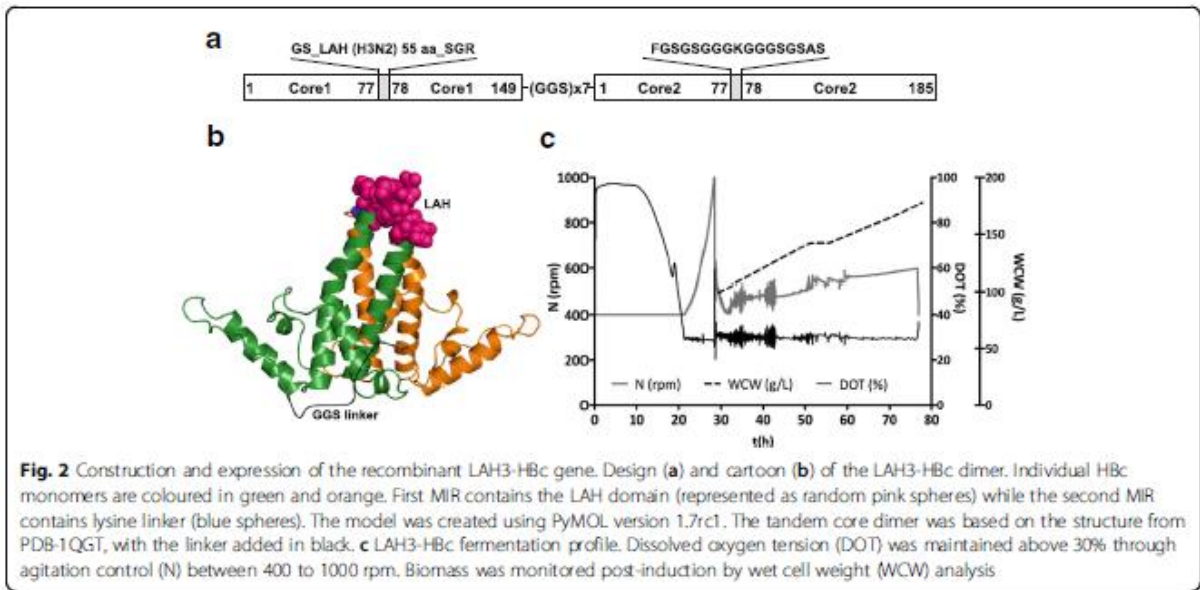


Fig. 1 a Design of the HBc K1-K1 construct. Amino acid sequences of inserted lysine linkers are shown in upper part. Below, introduced unique restriction sites at both ends of the linkers (*Xba*I/*Not*I in Core1 and *Eco*RV/*Nhe*I in Core2) are underlined. Purified K1-K1 VLPs were characterized by Coomassie-stained PAAG (**b**) and electron microscopy (**c**)

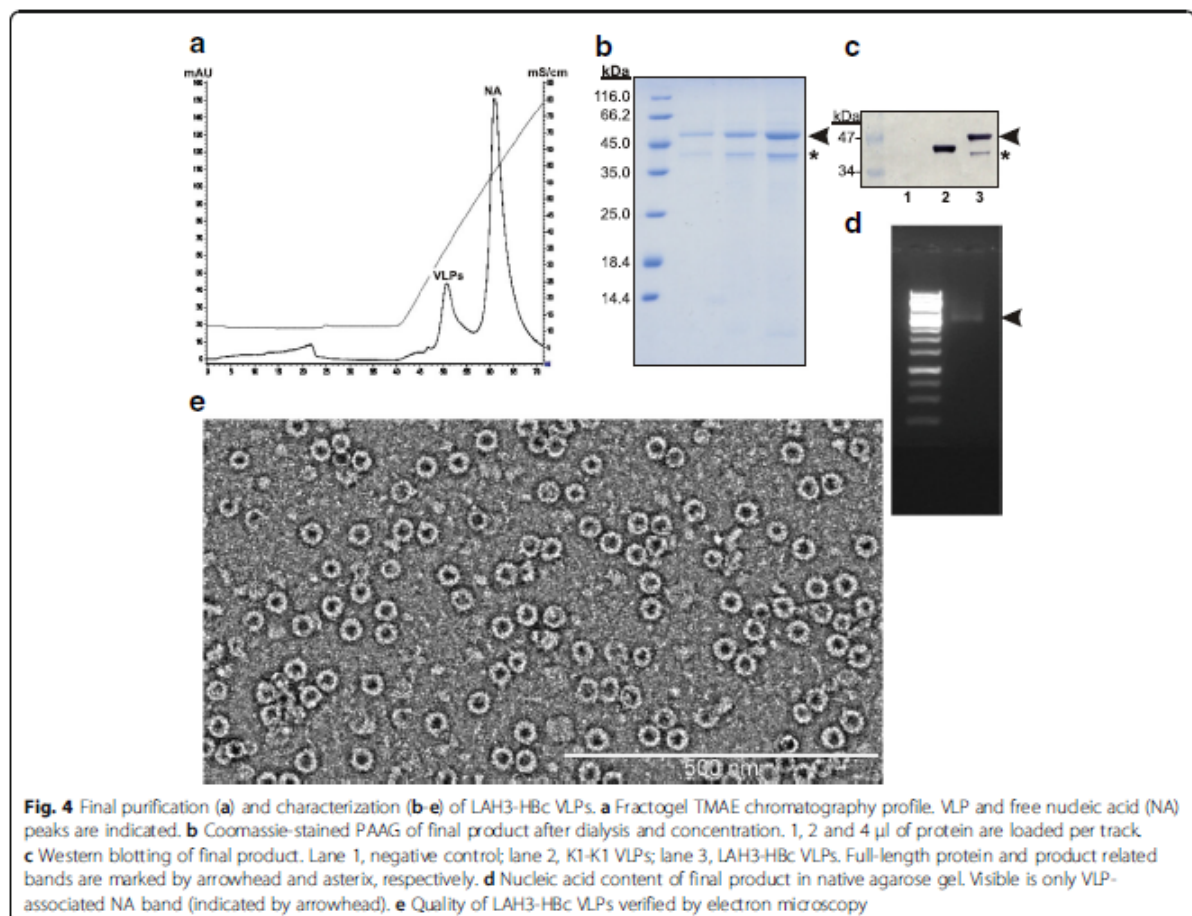


integrated expression units ensured high-level synthesis of the soluble target protein and was easily purified from yeast cells as correctly formed HbC VLPs (Fig. 1b-c).

Our early attempts to incorporate a highly hydrophobic LAH domain from influenza HA stalk into the MIR of monomeric HbC gene in *E. coli* resulted in insoluble products (data not shown). This is in line with previous observations [19] and indicated that specific approaches like tandem core technology might be necessary to improve solubility and achieve formation of VLPs in incorporating LAH. Since very promising results were obtained with the hetero-tandem HbC based K1-K1 construct, we inserted the LAH-encoding sequence into the MIR of the truncated HbC gene (Core 1) while the MIR of the full-length HbC (Core 2) remained unchanged (Fig. 2a-b). In order to exploit "endotoxin-free" cells with the potential for further industrial scale-up possibilities we transferred the chimeric tandem core gene into the yeast *P. pastoris* vector system resulting in LAH3-HbC construct.

Expression of LAH3-HbC construct in yeast

Recently, a number of novel influenza monoclonal antibodies have been identified against the stalk domain of the HA relatively conserved across most HA subtypes. These antibodies are able to broadly neutralize a wide spectrum of influenza virus strains and subtypes [20]. The LAH domain is a small alpha-helical portion of the stalk domain which contains a well-characterised neutralizing epitope for mAb 12D1 [21]. However, when out of structural context LAH does not generate neutralizing antibodies. Nevertheless, several studies from different research groups suggest that the LAH domain is a promising vaccine component. The current hypothesis for the mechanism of action involves non-neutralising antibody mediated cellular immune processes such as antibody dependent cellular cytotoxicity and complement dependent cytotoxicity [22] which are difficult to measure in mice. The synthetic LAH peptide from H3N2 virus coupled to carrier protein keyhole limpet hemocyanin induced in mice not only strong protection

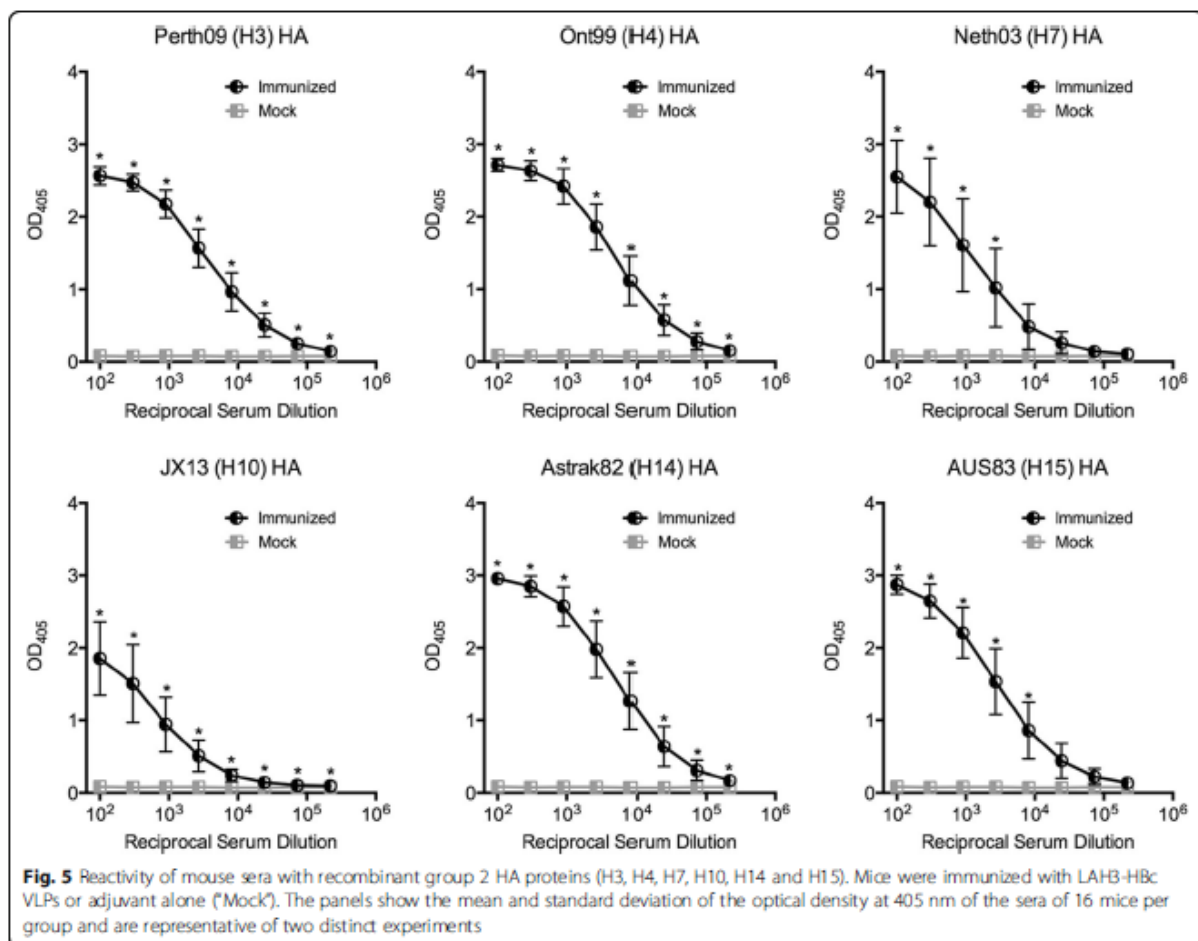


against homologous virus but also partial protection against distinct virus strains [23]. Similarly, the LAH region of H7N9 influenza virus was inserted into the Hbc gene and the resulting chimeric Hbc-LAH VLPs induced strong protection against homologous and heterologous virus strains in mice [24]. The latter study, however, required a complex renaturation procedure extracting chimeric protein from insoluble aggregates in *E. coli*, a process that would be costly and difficult to scale-up for industrial manufacturing. In addition, this approach is also compromised by the presence of bacterial endotoxins.

To avoid these problems we aimed to produce LAH3-Hbc VLPs in yeast cells. Yeast *P. pastoris* is well-adapted for large-scale fermentation and is a useful system for the expression of milligram-to-gram quantities of proteins for both basic laboratory research and industrial manufacture [25, 26]. Clones with multiply integrated expression cassettes were obtained in order to ensure maximal synthesis of the target protein in line with

previous reports [27, 28]. Here, the clone with 50 ± 2 integrated expression units was selected for further experiments (see Additional file 1).

Fermentation conditions were established to maximise product yield in the soluble fraction, as determined by Hbc-specific Western blots and its assembly into a VLPs, as determined by electron microscopy. It should be noted that several induction strategies were evaluated, including the standard methanol induction method for Mut^S strains. We observed that for the K1-K1 construct, the methanol only induction method yielded the most VLP material, yet when this same method was used for the LAH3-Hbc construct, little or no product was observed (data not shown). The different constructs did not appear to effect biomass as both seemed to grow well. We therefore sought to examine different induction methods, including various flowrates and glycerol:methanol ratios in the induction feed. Eventually we discovered that the 60:40 ratio of 50% glycerol:methanol over 48 h of induction provided the best yield for

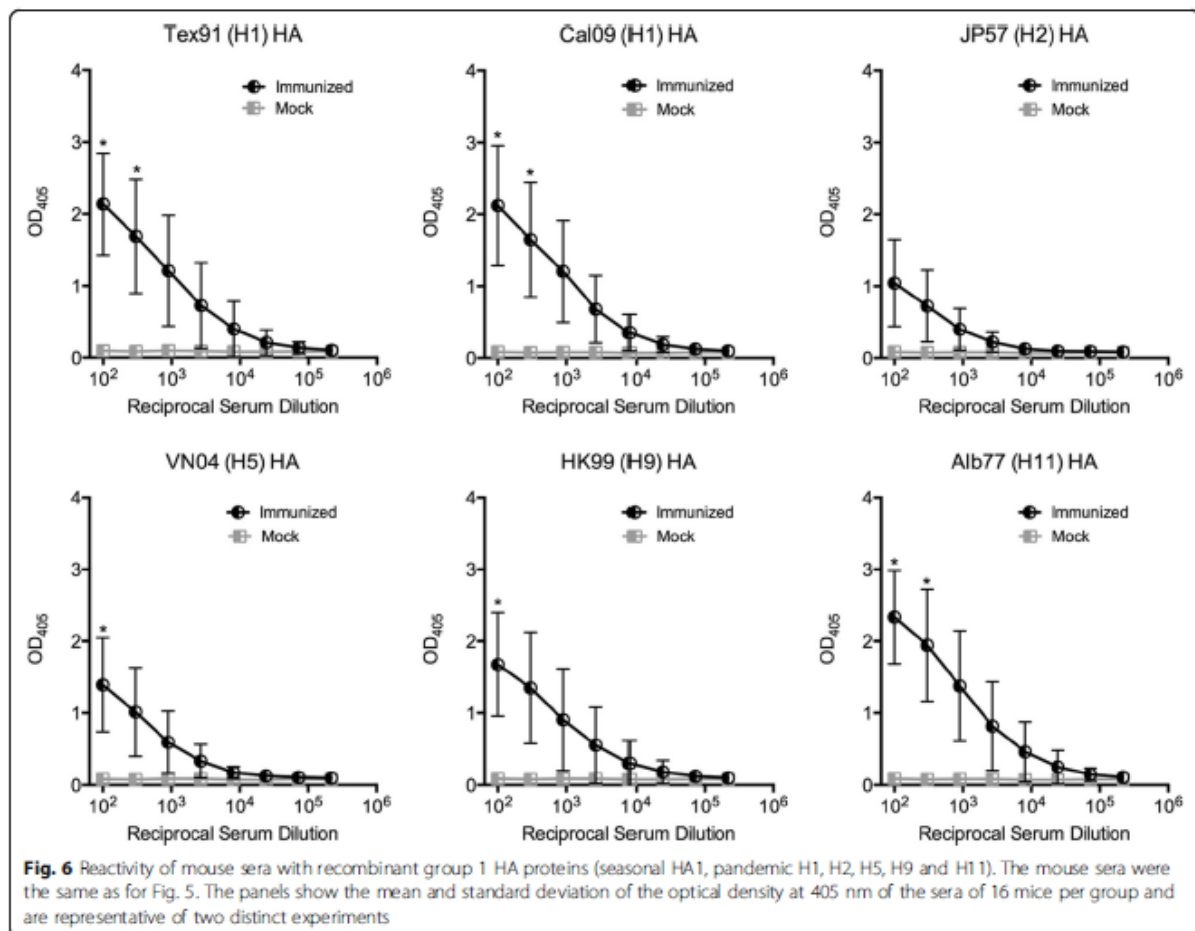


LAH3-HBc. Based on the off-gas data (not shown), in all cases the cells seemed metabolically active and grew well, however product expression was construct dependent – possibly indicating that the complexity and self-assembly of different VLP constructs are not intrinsically linked to cell metabolism during fermentation. Wet cell weight at the end of fermentation reached 178 g/L. The overall fermentation process is presented schematically in Fig. 2c.

Purification and characterization of chimeric LAH3-HBc VLPs

Efficient and selective concentration of the protein of interest from crude cell lysates is often a critical step determining overall success of the whole purification process. For HBc VLPs, ammonium sulfate precipitation has been used with good results ([17] and references herein). However, in this particular case it resulted in co-precipitation of the VLPs with other host cell proteins which were difficult to remove in the subsequent purification steps (data not shown). In contrast, addition of

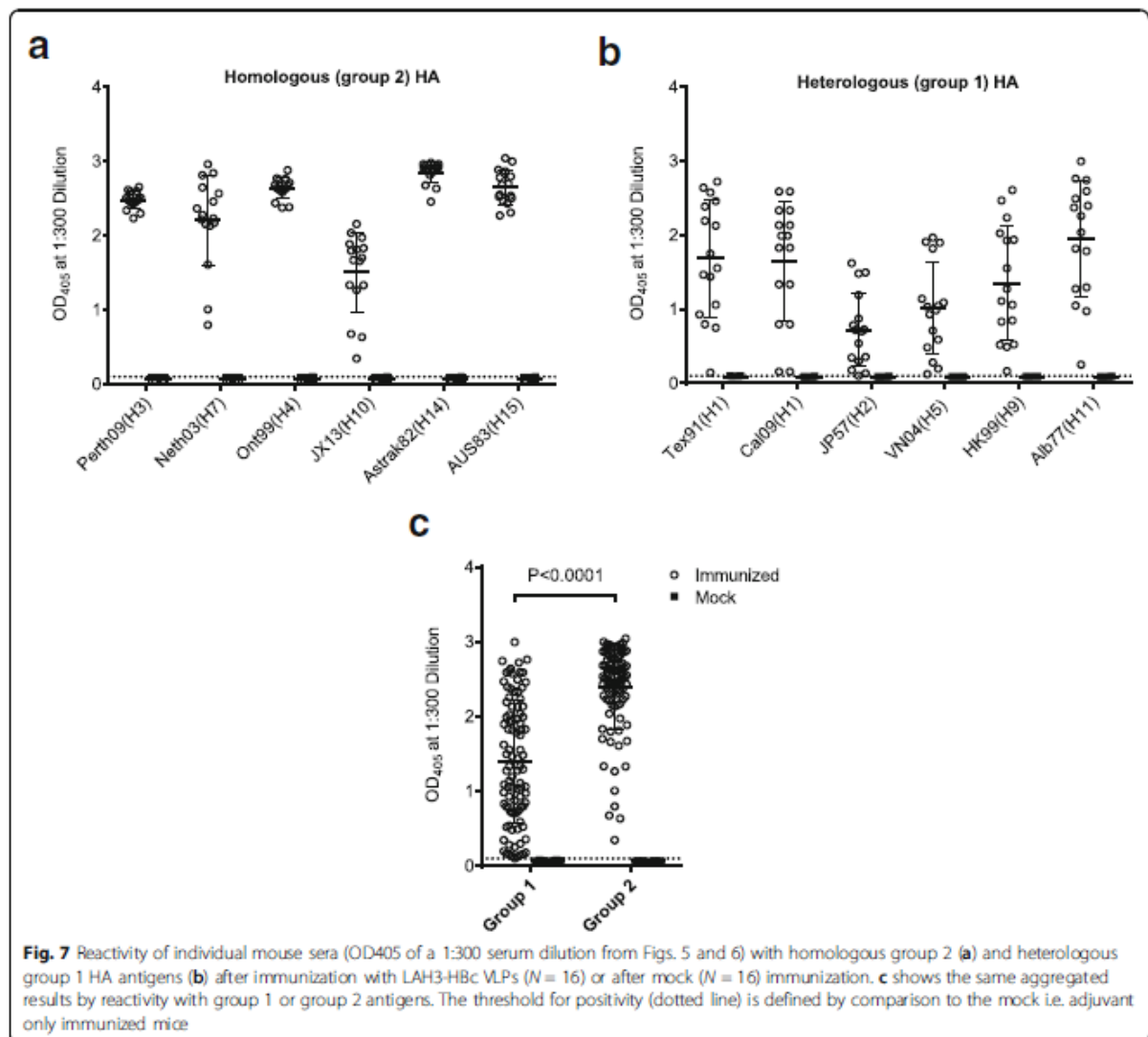
PEG led to selective enrichment of the target protein with a calculated MW of 48.2 kDa from cell supernatant (Fig. 3a). Since the LAH domain is highly hydrophobic, addition of urea was necessary to complete solubilization of the PEG precipitate and reduce aggregation caused by hydrophobic interactions. Next, the protein mixture was loaded onto a size-exclusion chromatography (SEC) column containing Sepharose 4 FF, a matrix developed for industrial processing of large molecules and virus particles at high flow rates and moderate pressures. We did not exceed the bed height of 25 cm in line with manufacturer's recommendations. A typical chromatography profile is shown in Fig. 3b. The aggregate peak appears first and this also contains a minor proportion of the target protein. The peak fractions are cloudy, contain a large amount of contaminating proteins and are not useful for the further purification of LAH3-HBc VLPs (data not shown). The next part of the profile is the so called "flat" region which theoretically corresponds to migration of VLP-size proteins. Indeed, SDS-PAGE analysis revealed the presence of LAH3-HBc sized protein in



these fractions (Fig. 3a) while electron microscopy confirmed the presence of correctly formed VLPs (Fig. 3c). However, the major component of these fractions comprised misassembled but soluble protein material.

For the second stage of the purification we aimed to maximally reduce the content of (i) contaminating proteins, (ii) misassembled LAH3-HBc aggregates and (iii) VLP non-associated nucleic acid. Ideally, this should be achieved by a single chromatography step. Our attempts to use either Sephacryl S1000 SEC, or differential precipitation of fractions by ammonium sulfate/PEG generally failed due to low yield and/or poor reproducibility (data not shown). We then subjected the protein solution to several anion exchangers as a relatively cheap, robust material capable of withstanding harsh cleaning-in-place conditions. The strong anion exchanger Sepharose

Q HP matrix ensured good separation of nucleic acid but led to disassembly of VLPs (data not shown). Experiments were continued with Fractogel DEAE and TMAE matrices representing weak and strong anion exchangers, respectively. Both of them resulted in significant enrichment of correctly folded VLPs in column-eluted material, however, only the TMAE matrix ensured nearly complete separation of VLPs from VLP-free nucleic acid (Fig. 4a). After dialysis and concentration the final product was analyzed for its purity, nucleic acid content and VLP quality (Fig. 4b-e). The final product reached at least 90% of homogeneity but appeared as two bands in PAAG (Fig. 4b). However, both bands reacted in Western blotting with anti-HBc antibody (Fig. 4c) indicating that the lower one is not a contaminant but a product related band. Since this protein was



not removed by SEC we assume it is incorporated into the VLPs.

After the first SEC column, the total protein content of VLP region was calculated as ~4 mg per 5 g of wet cells. These fractions, however, contained a mixture of proteins with an indeterminate percentage of correctly folded VLPs. In contrast, after elution from the anion exchange column more than 80% of material was in the form of VLPs but the yield in terms of total protein was decreased to ~0.5 mg. This result is in line with the assumption that correctly assembled VLPs comprise about 10% of total protein after SEC separation. These data were reproduced with consistency in at least three independent purification processes.

To summarize, in conditions described a final yield of LAH3-HBc VLPs could be estimated as 17–18 mg/L. For comparison, outcome of K1-K1 VLPs is typically ~0.8 mg per 1 g of cells, with its biomass after fermentation 260–270 g/L, which gives final yield 208–216 mg/L. Therefore incorporation of LAH domain decreases outcome of VLPs by more than the order of magnitude. This is still acceptable for industrial manufacturing, although further optimisation may increase the outcome and lower the process cost.

Induction of broadly reactive antibodies by immunization

To elicit antibodies against the influenza virus, BALB/c mice were immunized 3 times with chimeric LAH3-HBc VLPs at two weeks intervals. 10 days after the third immunization all immunized animals showed high titers of antibodies against the homologous group 2 HA proteins, including H3, H4, H7, H10, H14, and H15, while the mock group showed no reactivity with the antisera. Only H10 gave a weaker reaction (Fig. 5). In addition, the VLP-induced antisera cross-reacted significantly with the heterologous group 1 HA proteins, including H1, H2, H5, H9, and H11, but the reactivity was significantly weaker ($P < 0,0001$) than with group 2 HA (Figs. 6 and 7). The lowest reactivity was with H2 and H5 antigens. Fig. 7 shows that all mice reacted at a serum dilution of 1:300 with all group 2 HA species. Those with the lowest reactivity to the group 2 HA antigen were also the same one or two mice which had consistently low levels of reactivity with group 1 HA. Thus chimeric LAH3-HBc VLPs induced broadly reactive anti-influenza serum against both group 1 and 2 HA proteins. While all animals reacted with the “empty” K1-K1 HBc VLPs, none of them showed any reactivity ($OD < 0,1$) with the irrelevant antigens (EBV, CMV, Toxoplasma, see Additional file 2).

Conclusion

We have demonstrated that the tandem core technology is a useful tool for incorporation of “difficult” sequences like the hydrophobic LAH domain into HBc VLPs while

cloning into the classical, unmodified monomeric HBc gene results in insoluble products. The chimeric LAH3-HBc VLPs were successfully produced in a bioreactor using yeast *P. pastoris* expression system. The relatively low production yield was partially compensated by an efficient purification protocol of the chimeric VLPs. The LAH3-HBc VLPs induced broadly reactive antibodies against both group 1 and 2 HA proteins, the hallmark of a universal vaccine against influenza A viruses.

Additional files

Additional file 1: Determination of copy number for integrated expression units in selected *P. pastoris* clones. Description of the methodology used for quantification of copy number for expression cassettes integrated in selected *P. pastoris* clones. The method is based on real time PCR amplification of zeocin gene. (DOCX 186 kb)

Additional file 2: Serum IgG reactivity against the “empty” K1-K1 HBc VLPs and against irrelevant antigens (Cytomegalovirus antigen, purified EBV capsid protein, Toxoplasma gondii antigen). Reactivity of mouse sera with carrier HBc-derived VLPs (positive control) in comparison with irrelevant antigens (negative control) demonstrating specificity of ELISA method used. (PPTX 91 kb)

Abbreviations

HA: Hemagglutinin; HBc: Hepatitis B virus core protein; LAH: Long alpha helix; MIR: Major immunodominant region; OD: Optical density; PAAG: Polyacrylamide gel; SEC: size exclusion chromatography; VLPs: Virus-like particles

Acknowledgements

We wish to thank Oluwapelumi Adeyemi (University of Leeds) for preparing Fig. 2b.

Funding

This study was accomplished in the frames of the FP7 project “Development of a universal influenza vaccine based on tandem core technology” (FLUTCORE). The project has received funding from the European Union’s Seventh Framework Programme for research, technological development and demonstration under grant agreement N° 602,437.

Availability of data and materials

The datasets supporting the conclusions of this article are available from the corresponding author on reasonable request.

Authors’ contributions

WMR acquired the funding and designed the whole study. BB, OO, TM, MPO and AKr participated in high cell density fermentations. AKa, IA, JB, AR, VC, AKi and TK designed and carried out protein purification experiments and analyzed data. I-NL, SF and CPM designed and performed mouse experiments and ELISA analysis. VO carried out electron microscopy. AKa collected the data and wrote the manuscript. NJS, DJR and KT participated in data interpretation. CPM and WMR revised and enhanced the paper. All authors reviewed and approved the final manuscript.

Ethics approval and consent to participate

All mouse experiments were performed in accordance with protocols approved by the Animal Welfare Structure of the Minister of Agriculture, Viticulture and the Consumer Protection of the Grand Duchy of Luxembourg (Ref. LNSI-2014-02).

Consent for publication

Not applicable.

Competing interests

The authors declare that they have no competing interests.

Publisher's Note

Springer Nature remains neutral with regard to jurisdictional claims in published maps and institutional affiliations.

Author details

¹Latvian Biomedical Research and Study Centre, Ratsupites 1, Riga LV-1067, Latvia. ²Department of Infection and Immunity, Luxembourg Institute of Health, 29, rue Henri Koch, L-4354 Esch-sur-Alzette, Luxembourg. ³Qur Limited, 2 Royal College Street, London NW1 0NH, UK. ⁴Department of Biochemical Engineering, University College London, Gower Street, London WC1E 6BT, UK. ⁵3P Biopharmaceuticals SL, Calle Mocholi 2 Poligono Mocholi, Noain, 31110 Navarra, Spain. ⁶Faculty of Biological Sciences, University of Leeds, Leeds LS2 9JT, UK. ⁷Institute for Liver and Digestive Health, Division of Medicine, University College London, Royal Free Campus, NW3 2PF, London, UK. ⁸Faculty of Biology, Department of Molecular Biology, Jelgavas 1, Riga LV-1004, Latvia.

Received: 28 April 2017 Accepted: 31 October 2017

Published online: 10 November 2017

References

- Kolpe A, Schepens B, Fiers W, Saelens X. M2-based influenza vaccines: recent advances and clinical potential. *Expert Rev Vaccines*. 2017;16(2):123–36.
- Carrat F, Flahault A. Influenza vaccine: the challenge of antigenic drift. *Vaccine*. 2007;25(39–40):6852–62.
- Berlanda Scorza F, Tsvetnitsky V, Donnelly JJ. Universal influenza vaccines: shifting to better vaccines. *Vaccine*. 2016;34(26):2926–33.
- Zhang H, Wang L, Compans RW, Wang BZ. Universal influenza vaccines, a dream to be realized soon. *Viruses*. 2014;6(5):1974–91.
- Pushko P, Pumpens P, Grens E. Development of virus-like particle technology from small highly symmetric to large complex virus-like particle structures. *Intervirology*. 2013;56(3):141–65.
- Neiryck S, Deroo T, Saelens X, Vanlandschoot P, Jou WM, Fiers W. A universal influenza A vaccine based on the extracellular domain of the M2 protein. *Nat Med*. 1999;5(10):1157–63.
- Ionescu RM, Przysiecki CT, Liang X, Garsky VM, Fan J, Wang B, Troutman R, Rippeon Y, Flanagan E, Shiver J, et al. Pharmaceutical and immunological evaluation of human papillomavirus viruslike particle as an antigen carrier. *J Pharm Sci*. 2006;95(1):70–9.
- De Filette M, Min Jou W, Birkett A, Lyons K, Schultz B, Tonkyro A, Resch S, Fiers W. Universal influenza A vaccine: optimization of M2-based constructs. *Virology*. 2005;337(1):149–61.
- Bessa J, Schmitz N, Hinton HJ, Schwarz K, Jegerlehner A, Bachmann MF. Efficient induction of mucosal and systemic immune responses by virus-like particles administered intranasally: implications for vaccine design. *Eur J Immunol*. 2008;38(1):114–26.
- Peyret H, Gehin A, Thuenemann EC, Blond D, El Turabi A, Beales L, Clarke D, Gilbert RJ, Fry EE, Stuart DL, et al. Tandem fusion of hepatitis B core antigen allows assembly of virus-like particles in bacteria and plants with enhanced capacity to accommodate foreign proteins. *PLoS One*. 2015;10(4):e0120751.
- Yan D, Wei YQ, Guo HC, Sun SQ. The application of virus-like particles as vaccines and biological vehicles. *Appl Microbiol Biotechnol*. 2015;99(24):10415–32.
- Lee EJ, Lee NK, Kim IS. Bioengineered protein-based nanocage for drug delivery. *Adv Drug Deliv Rev*. 2016;106(Pt A):157–71.
- Pumpens P, Grens E. The true story and advantages of the famous hepatitis B virus core particles: outlook 2016. *Mol Biol (Mosk)*. 2016;50(4):558–76.
- Walker A, Skamel C, Nassal M. SplitCore: an exceptionally versatile viral nanoparticle for native whole protein display regardless of 3D structure. *Sci Rep*. 2011;1:5.
- Bokhina EA, Kuprianov VV, Stepanova IA, Tsybalova LM, Kiselev OI, Ravin NV, Skryabin KG. A molecular assembly system for presentation of antigens on the surface of HBc virus-like particles. *Virology*. 2013;435(2):299–300.
- Holmes K, Shepherd DA, Ashcroft AE, Whelan M, Rowlands DJ, Stonehouse NJ. Assembly pathway of hepatitis B Core virus-like particles from genetically fused dimers. *J Biol Chem*. 2015;290(26):16238–45.
- Freivalds J, Dislers A, Ose V, Pumpens P, Tars K, Kazaks A. Highly efficient production of phosphorylated hepatitis B core particles in yeast *Pichia Pastoris*. *Protein Expr Purif*. 2011;75(2):218–24.
- Jegerlehner A, Zabel F, Langer A, Dietmeier K, Jennings GT, Saudan P, Bachmann MF. Bacterially produced recombinant influenza vaccines based on virus-like particles. *PLoS One*. 2013;8(11):e78947.
- Chen S, Zheng D, Li C, Zhang W, Xu W, Liu X, Fang F, Chen Z. Protection against multiple subtypes of influenza viruses by virus-like particle vaccines based on a hemagglutinin conserved epitope. *Biomed Res Int*. 2015;2015:901817.
- Krammer F, Palese P, Steel J. Advances in universal influenza virus vaccine design and antibody mediated therapies based on conserved regions of the hemagglutinin. *Curr Top Microbiol Immunol*. 2015;386:301–21.
- Wang TT, Tan GS, Hai R, Pica N, Petersen E, Moran TM, Palese P. Broadly protective monoclonal antibodies against H3 influenza viruses following sequential immunization with different hemagglutinins. *PLoS Pathog*. 2010;6(2):e1000796.
- Dilillo DJ, Tan GS, Palese P, Ravetch JV. Broadly neutralizing hemagglutinin stalk-specific antibodies require FcγR interactions for protection against influenza virus in vivo. *Nat Med*. 2014;20(2):143–51.
- Wang TT, Tan GS, Hai R, Pica N, Ngai L, Böert DC, Wilson IA, Garcia-Sastre A, Moran TM, Palese P. Vaccination with a synthetic peptide from the influenza virus hemagglutinin provides protection against distinct viral subtypes. *Proc Natl Acad Sci U S A*. 2010;107(44):18979–84.
- Zheng D, Chen S, Qu D, Chen J, Wang F, Zhang R, Chen Z. Influenza H7N9 LAH-HBc virus-like particle vaccine with adjuvant protects mice against homologous and heterologous influenza viruses. *Vaccine*. 2016;34(51):6464–71.
- Macaulay-Patrick S, Fazenda ML, McNeil B, Harvey LM. Heterologous protein production using the *Pichia Pastoris* expression system. *Yeast*. 2005;22(4):249–70.
- Ahmad M, Hirz M, Pichler H, Schwab H. Protein expression in *Pichia Pastoris*: recent achievements and perspectives for heterologous protein production. *Appl Microbiol Biotechnol*. 2014;98(12):5301–17.
- Mansur M, Cabello C, Hernandez L, Pais J, Varas L, Valdes J, Terrero Y, Hidalgo A, Plana L, Besada V, et al. Multiple gene copy number enhances insulin precursor secretion in the yeast *Pichia Pastoris*. *Biotechnol Lett*. 2005;27(5):339–45.
- Norden K, Agemark M, Danielson JA, Alexandersson E, Kjellbom P, Johanson U. Increasing gene dosage greatly enhances recombinant expression of aquaporins in *Pichia Pastoris*. *BMC Biotechnol*. 2011;11:47.

Submit your next manuscript to BioMed Central and we will help you at every step:

- We accept pre-submission inquiries
- Our selector tool helps you to find the most relevant journal
- We provide round the clock customer support
- Convenient online submission
- Thorough peer review
- Inclusion in PubMed and all major indexing services
- Maximum visibility for your research

Submit your manuscript at
www.biomedcentral.com/submit



3.2 Structure and applications of novel influenza HA tri-stalk protein for evaluation of HA stem-specific immunity

Highlights:

- A fast and efficient 3-step chromatography method was developed for purification of the tri-stalk protein, yielding at least 90% target protein homogeneity with the outcome of 5 mg target protein per g of wet cells. Matching the fold of the corresponding portion of a full-length post-fusion HA, the tri-stalk protein adapted an extended six-helix bundle structure, formed by a trimer of hairpins, as confirmed by its crystal structure.
- LAH1-PP7 fusion protein was produced and purified; it did not assemble into VLPs, but formed soluble aggregates. Sera from the LAH1-PP7 fusion protein vaccinated mice was used to set up the ELISA conditions to detect the HA stalk-specific antibody levels in mice and human sera.
- 70% of the sera from people with occupational contact to swine pre-2009 pandemic exhibited a positive reaction against the tri-stalk while stalk-reactive antibodies were detected in only 42% of the sera from non-exposed people.
- The pre-pandemic sera from the swine-workers exhibited neutralizing activity against the pandemic H1N1 virus, and there was a strong correlation between the neutralizing antibody titers and the tri-stalk specific antibody titers.

RESEARCH ARTICLE

Structure and applications of novel influenza HA tri-stalk protein for evaluation of HA stem-specific immunity

I-Na Lu¹✉, Anna Kirsteina²✉, Sophie Farinelle¹, Stéphanie Willieme¹, Kaspars Tars^{2,3}, Claude P. Muller^{1,4}, Andris Kazaks^{2*}

1 Department of Infection and Immunity, Luxembourg Institute of Health, Esch-sur-Alzette, Luxembourg, **2** Latvian Biomedical Research and Study Centre, Riga, Latvia, **3** Department of Molecular Biology, Faculty of Biology, Riga, Latvia, **4** Laboratoire National de Santé, Dudelange, Luxembourg

✉ These authors contributed equally to this work.

* andris@biomed.lu.lv



OPEN ACCESS

Citation: Lu I-N, Kirsteina A, Farinelle S, Willieme S, Tars K, Muller CP, et al. (2018) Structure and applications of novel influenza HA tri-stalk protein for evaluation of HA stem-specific immunity. PLoS ONE 13(9): e0204776. <https://doi.org/10.1371/journal.pone.0204776>

Editor: Florian Krammer, Icahn School of Medicine at Mount Sinai, UNITED STATES

Received: June 29, 2018

Accepted: September 13, 2018

Published: September 27, 2018

Copyright: ©2018 Lu et al. This is an open access article distributed under the terms of the [Creative Commons Attribution License](https://creativecommons.org/licenses/by/4.0/), which permits unrestricted use, distribution, and reproduction in any medium, provided the original author and source are credited.

Data Availability Statement: Coordinates and structure factors are deposited in the Protein Data Bank with accession code 6GOL. All other relevant data are within the paper.

Funding: The research leading to these results has received funding from the European Union Seventh Framework Programme for research, technological development and demonstration under grant agreement 602437 (all authors) and from European Regional Development Fund project 1.1.1.1/16/A/054 (AKI, KT and AKa). The funders

Abstract

Long alpha helix (LAH) from influenza virus hemagglutinin (HA) stem or stalk domain is one of the most conserved influenza virus antigens. Expression of N-terminally extended LAH in *E. coli* leads to assembly of α -h elical homotrimer which is structurally nearly identical to the corresponding region of post-fusion form of native HA. This novel tri-stalk protein was able to differentiate between group 1 and 2 influenza in ELISA with virus-infected mice sera. It was also successfully applied for enzyme-linked immunospot assay to estimate the number of HA stem-reactive antibody (Ab)-secreting cells in mice. An in-house indirect ELISA was developed using a HA tri-stalk protein as a coating antigen for evaluation of HA stem-specific Ab levels in human sera collected in Luxembourg from 211 persons with occupational exposure to swine before the pandemic H1N1/09 virus had spread to Western Europe. Our results show that 70% of these pre-pandemic sera are positive for HA stem-specific Abs. In addition, levels of HA stem-specific Abs have positive correlation with the corresponding IgG titers and neutralizing activities against pandemic H1N1/09 virus.

Introduction

With the annual epidemics causing 3 to 5 million cases of severe illness and up to 650 000 deaths per year human influenza virus remains a significant health and economic burden worldwide (WHO 2018: [http://www.who.int/en/news-room/fact-sheets/detail/influenza-\(seasonal\)](http://www.who.int/en/news-room/fact-sheets/detail/influenza-(seasonal))) [1]. Apart from the seasonal epidemics which are caused by antigenic drift of influenza viruses, the introduction of novel virus variants from the zoonotic pool via antigenic shift can result in viruses capable of initiating human pandemics [2]. In the past hundred years, four influenza pandemics have spread in the human population [3], the deadliest of them being the 1918 influenza pandemic when the mortality reached up to 50 million cases [4]. Some avian influenza strains, such as H5N1, H7N9 and H6N1, represent a risk that if they become transmissible among humans new pandemic influenza strains will emerge inducing

had no role in study design, data collection and analysis, decision to publish, or preparation of the manuscript.

Competing interests: The authors have declared that no competing interests exist.

even more devastating effects to the public health [5–7]. Rapid diagnostics can speed up the treatment decreasing the spreading of the influenza virus and is one of the key components of pandemic preparedness.

Influenza virus hemagglutinin (HA) is the major surface antigen of the virion and the primary target of virus neutralizing antibodies (Abs) [8]. HA is a homotrimeric surface glycoprotein, with each monomer consisting of two disulfide-linked subunits (HA1, HA2), resulting from the proteolytic cleavage products of a single HA precursor protein. The HA1 chain forms a membrane-distal globular head and a part of the membrane-proximal stem region. The HA2 chain represents the major component of the stem region [9]. The head of HA mediates receptor binding while the membrane-anchored stem is the main part of membrane fusion machinery [10]. Neutralizing Ab responses are mainly targeted to the immunodominant head domain of HA [11]. However, because of the high genetic plasticity of the head region epitopes [12] Ab responses are strain-specific and lack broad cross-reactivity with different HA subtypes [11]. In contrast, sequence and structure of the subdominant HA stem are much more conserved across different influenza subtypes and broadly neutralizing Abs against this domain are considered promising therapeutic tools against various influenza virus strains [8], [13]. Indeed, there are some Abs known that cross-react with HA stem from all influenza A subtypes [14] or even with HA stem from both influenza A and B viruses [15].

One of the most conservative HA stem regions is a 55 amino acid (aa) long alpha helix (LAH) which is currently under intensive investigation as a potential universal influenza virus antigen [16–17]. Recently, we demonstrated that the LAH, as well as its N-terminally extended variant (72 aa), incorporated into hepatitis B virus core (HBc) particles is highly immunogenic in mice [18–19]. Expression of the extended LAH antigen in *Escherichia coli* resulted in efficient synthesis of a soluble product. We purified and crystallized the protein and determined its three-dimensional structure, revealing formation of an α -helical trimer (referred to as tri-stalk protein) highly similar to the corresponding region of native HA in its post-fusion form.

We have developed an in-house indirect ELISA using the HA tri-stalk protein as immobilized antigen to evaluate HA stem-specific Ab levels in mice and human sera. In addition, tri-stalk protein was successfully used in an enzyme-linked immunospot (ELISPOT) assay to estimate numbers of HA stem-reactive Ab-secreting cells in mice. To extend the previous study [20] and examine the level of pre-existing Abs in this population, our in-house ELISA was used to test human sera pool collected from people with direct occupational contacts to swine before the pandemic H1N1/09 virus had spread to Western Europe. Our results show that 70% of these pre-pandemic sera are positive for group 1 HA stem-specific Abs. In addition, the levels of HA stem-specific Abs have positive correlation with the corresponding IgG titers and neutralizing activities against pandemic H1N1/09 virus. Taken together, we have demonstrated that the novel HA tri-stalk protein is a useful tool for evaluation of HA stem-specific immunity in both mice and humans.

Materials and methods

HA tri-stalk protein

The tri-stalk protein encoding HA amino acids 403–474 of the pandemic strain A/Luxembourg/43/2009(H1N1) was PCR-amplified and cloned in the pETDuet-1 vector (*Novagen*) using *NcoI* and *BspTI* restriction sites. The construct was expressed in *Escherichia coli* BL21 (DE3) cells using a standard protocol (https://assets.thermofisher.com/TFS-Assets/LSG/manuals/oneshotbl21_man.pdf). Briefly, cells were cultivated in 2×TY medium in Erlenmeyer flasks under continuous shaking (200 rpm) at +37°C. When optical density $OD_{A540} = 0.6–0.8$

was reached IPTG was added to a final concentration of 0.1 mM. After another 3 h, the cells were collected by low-speed centrifugation and stored at -20°C until use.

For purification of the antigen, the cells were disrupted in lysis buffer A containing 20 mM Tris HCl, pH 8.0, and 100 mM NaCl (6 mL of buffer per 1 g of cells) by sonication. The soluble fraction was isolated by centrifugation ($18,000 \times g$, 30 min). The supernatant was subjected to thermal treatment for 30 min at 55°C and centrifuged again. The soluble fraction was applied to a weak anion exchange HiPrep 16/10 DEAE FF column in buffer A. Bound protein was linearly eluted (4 mL/min) with buffer B (20 mM Tris HCl, pH 8.0, 1 M NaCl) in 3 column volumes (CVs) until concentration of 0.6 M NaCl was reached. Selected fractions were pooled, diluted twice with 20 mM Tris HCl, pH 8.0, and applied onto a strong anion exchange column MonoQ 5/50 GL in buffer A (1 mL/min). Column-bound proteins were linearly eluted with buffer B in 10 CVs until concentration of 0.5 M NaCl was reached. Finally, protein was subjected to size exclusion chromatography on a Superdex 200 10/300 GL column in 20 mM Tris HCl, pH 8.0, 200 mM NaCl at 0.5 mL/min. All runs were performed at room temperature and monitored using the ÄKTA FPLC chromatography system (Amersham Biosciences). Purified HA tri-stalk protein was aliquoted and stored at -20°C until use.

Crystallization and structure determination

Prior to crystallization, purified HA tri-stalk protein was concentrated to 10 mg/mL in 20 mM Tris HCl, pH 8.0, 200 mM NaCl, using Amicon 10 kDa MWCO filter (Millipore), and crystallized by mixing with equal volume of precipitant solution (1 μL each) using the sitting-drop vapor-diffusion technique. The HA tri-stalk crystals used for data collection were obtained at 2.0 M ammonium sulfate and 0.1 M Bis-Tris, pH 5.5. For data collection, the crystals were flash-frozen in liquid nitrogen, after brief soaking in a cryoprotectant containing reservoir liquor and 30% glycerol. Datasets were collected at MAX-lab beamline I911-3 (Lund University, Sweden).

The diffraction images were integrated with MOSFLM [21], and scaled using SCALA [22] from the CCP4i program suite [23]. The crystal structure of HA tri-stalk protein was solved by molecular replacement with PHASER [24], using the corresponding fragment of structure of influenza HA at the pH of membrane fusion as the search model [25]. Initially the model was generated in BUCCANEER [26]. The structure was manually adjusted and validated using the COOT software program [27] and refinement was carried out in REFMAC [28]. The HA tri-stalk 3D structure was visualized in PyMOL (The PyMol Molecular Graphics System, Version 1.8 Schrödinger, LLC). SSM-superimposition was carried out in COOT. Statistics for data collection and structure refinement are presented in Table 1. Coordinates and structure factors are deposited in the Protein Data Bank with accession code 6GOL.

Mouse infection and immunization

Female BALB/c mice were purchased from Harlan Laboratories, Inc., the Netherlands. All mice experiments were performed in accordance with protocols approved by the Animal Welfare Structure of Luxembourg Institute of Health and by the Minister of Agriculture, Viticulture and the Consumer Protection of the Grand Duchy of Luxembourg (Ref. LNSI-2014-02). All experiments with live influenza virus were performed in a biosafety level 3 (BSL-3) containment facility, and mice were kept in positive-pressured isocage system.

For virus infection, 10-week-old BALB/c mice ($n = 8$ mice/group) were infected intranasally with a sublethal dose (8×10^4 half maximal tissue culture infectious dose; TCID₅₀) of pandemic H1N1 influenza strain A/Luxembourg/46/2009 (pH1N1), A/Texas/36/91 seasonal H1N1 (sH1N1), A/Puerto Rico/8/34 H1N1 (PR8), A/Lux/01/2005 seasonal H3N2 (sH3N2), A/

Table 1. Data collection and refinement statistics.

Data collection and scaling	
Beamline	1911-3
Wavelength (Å)	1.00000
Space group	P6 ₃
Unit cell parameters (Å)	a = b = 41.80, c = 90.12
Resolution (Å)	23.12–1.7 (1.79–1.7)
Observations	36458
Unique reflections	9803 (1439)
Completeness (%)	99.7 (100)
I/σ _I	10 (1.8)
R _{merge}	0.063 (0.664)
Multiplicity	3.7 (3.7)
Refinement statistics	
R _{work}	0.17771 (0.322)
R _{free}	0.21914 (0.320)
Average B-value (Å ²)	36.711
Wilson B-value (Å ²)	22.7
Protein atoms	538
Waters	57
RMSD from ideal geometry	
Bond length (Å)	0.024
Bond angles (°)	2.009
Ramachandran outliers	
Residues in favored regions (%)	100

<https://doi.org/10.1371/journal.pone.0204776.t001>

Aishi/68 H3N2 (X-31), or B/Lee/40 virus in 50 µL phosphate-buffered saline (PBS), after anesthesia with isoflurane. We evaluated and weighed the mice every day at 10:00 AM for 14 days following sub-lethal infection, and no adverse or unexpected events were observed.

For immunization of mice, LAH domain-encoding sequence from pH1N1/09 strain was genetically fused to the N-terminus of bacteriophage PP7 coat protein gene separated by a short GSG-encoding linker, designated as LAH-PP7. This fusion gene was cloned and expressed as described for HA tri-stalk construct. The cells were disrupted in lysis buffer A by sonication and centrifuged at 18,000 × g for 30 min. Insoluble fraction was washed twice with lysis buffer and sonication repeated with the addition of 0.25 M urea in buffer A. After centrifugation, the soluble fraction containing LAH-PP7 fusion protein was loaded onto a Superdex 200 10/300 GL column in buffer A and target protein fractions were collected.

8-week-old female BALB/c mice (n = 8 mice/group) were vaccinated three times with 2-week interval intraperitoneally with 200 µL of 30 µg LAH-PP7 fusion protein, tri-stalk protein or PBS in aluminium hydroxide gel adjuvant (Brenntag Biosector, Denmark). One week after the final boost, mice were killed by intraperitoneal injection of 200 mg/kg of sodium pentobarbital. Blood and spleens were collected for HA tri-stalk protein based ELISA and ELI-SPOT assay, respectively.

Enzyme linked immunosorbent assay (ELISA)

The indirect ELISA conditions were optimized by checkerboard titration using serial dilutions of HA tri-stalk protein tested against serial dilutions of positive and negative sera. Briefly, the HA tri-stalk protein was coated overnight at 4°C to 384-well microtiter plates (Greiner Bio-

One GmbH, Austria) using concentrations of 0.156, 0.313, 0.625, 1.25, 2.5, 5.0 and 10.0 $\mu\text{g}/\text{mL}$. After washing, free binding sites were saturated at room temperature with 1% BSA in Tris buffer. After 2 h, plates were washed again and diluted mouse (starting with 100-fold dilutions) or human sera (starting with 300-fold dilutions) were added and incubated for 90 min at room temperature. Binding was assessed by alkaline phosphatase-conjugated goat anti-human IgG (1/1000 dilution, Southern Biotech, Birmingham, AL) and 4-nitrophenyl phosphate disodium salt hexahydrate (Phosphatase substrate, Sigma-Aldrich, Germany). Absorbance was measured at 405 nm (SpectraMax Plus 384 Microplate reader), after 60 min of incubation at 37°C. Sera from naïve mice and low-titer sera from young children served as negative controls.

3.5 $\mu\text{g}/\text{mL}$ purified recombinant HA protein from A/Texas/36/1991 (HA H1/91) and A/California/4/2009 (HA H1/09, both purchased from Sino Biological Inc.) were coated respectively to the plates following the above ELISA protocol. Positive and negative control sera were used on all plates for normalization between plates.

Influenza-specific IgG response in mice immunized with LAH-PP7 was measured by indirect ELISA using the following purified recombinant group 1 and group 2 HA antigens: A/California/4/2009 (Cal09; H1), A/Japan/305/57 (JP57; H2), A/Perth/16/2009 (Perth09; H3), A/Swine/Ontario/01911-1/99 (Onta99; H4), A/Vietnam/1203/04 (VN04; H5), A/Netherlands/219/2003 (Neth03; H7), A/Hong Kong/1073/99 (HK99; H9), A/Jiangxi-Donghu/346/2013 (JX13; H10), A/mallard/Alberta/294/1977 (Alb77; H11), A/mallard/Astrakhan/263/1982 (Astrak82; H14), A/duck/AUS/341/1983 (AUS83; H15) and A/black-headed gull/Sweden/5/99 (SW99; H16), all purchased from Sino Biological Inc.

Enzyme-linked immunospot (ELISPOT)

The numbers of Ab-secreting cells under stimulation by HA tri-stalk protein were counted using commercial mouse IgG1 and IgG2a single-color ELISPOT assay kits (Cellular Technology Limited, Cleveland, OH) as per the manufacturer's instructions. Freshly isolated splenocytes from mock or LAH-PP7 immunized mice were pre-stimulated for 4 days at 37°C in a 7% CO₂ incubator, the cells were then transferred to capture Ab-coated polyvinylidene fluoride (PVDF) 96-well plates (5×10^5 cells/well). Following incubation for 20–24 h at 37°C in a 5% CO₂ incubator, the cell suspensions were removed. All wells were washed twice with PBS and twice with 0.05% Tween-PBS, anti-murine IgG1 or IgG2a detection solution was added, and the plates were incubated for 2 h at room temperature. After 3 washes with 0.05% Tween-PBS, tertiary solution (Streptavidin-alkaline phosphatase conjugate) was added at 80 μL per well for 1 h at room temperature. Following four more washes, 80 μL of blue developer solution (Substrate mix) was added for 15–20 min at room temperature in the dark to yield colored spots. Finally, the reaction was stopped by thoroughly rinsing with tap water. The plates were air-dried and stored in the dark until analysis. The number of spots was counted using the ImageQuant software (Molecular Dynamics, Sunnyvale, CA). The average number of spot-forming cells was adjusted to 1×10^6 splenocytes.

Donors and serum samples

Swine workers (SW) are defined in this study as persons whose professions involve direct contact with swine. 211 SW, including pig farmers, slaughterhouse workers and veterinarians, aged 18 to 94 years, were recruited to donate serum samples prior to the outbreak of pandemic H1N1/09 as described before [20]. Pre-pandemic sera from 71 non-swine workers (non-SW) were also collected as control. Informed consent was gathered from all participants enrolled. The study was approved by the National Ethical Committee for Research in Humans of the Grand Duchy of Luxembourg.

Microneutralization assay

Heat inactivated (30 min at 56°C) and receptor destroying enzyme (RDE, purchased from DENKA SEIKEN UK Ltd, Coventry, UK) treated sera were tested by microneutralization assay against influenza A/Luxembourg/43/2009 (H1N1/09) virus according to the World Health Organization (WHO) protocol (Serological Diagnosis of Influenza by Microneutralization Assay. WHO 2010). Equal volumes of serum and virus diluted to 2×10^3 median tissue culture infective doses (TCID₅₀) per milliliter were incubated for 1 h at 37°C. The mixture was added to a confluent layer of Madin-Darby canine kidney (MDCK) cells in 96-well tissue culture plates (1.5×10^4 cells/well) and incubated for 20 h. After fixation with ice-cold 80% acetone in PBS for 15 min, anti-influenza A NP mouse monoclonal Ab (1:1000 dilution) was added to the monolayers for 1 h. Virus-infected cells were detected using an alkaline phosphatase conjugated with anti-mouse second step Ab. The optical density value of half-maximal effective dose (EC50) was then determined by the following equation: $[(\text{average OD}_{405} \text{ of virus control wells}) - (\text{average OD}_{405} \text{ of cell control wells})]/2$. The reciprocal serum dilution corresponding to EC50 is the 50% neutralizing Ab titer for the serum sample.

Statistical analysis

GraphPad Prism software was used for statistical evaluation of data. One-way ANOVA followed by Holm's test was applied for statistical analysis (* $p < 0.01$, *** $p < 0.0001$, **** $p < 0.00001$). Spearman correlation test was employed to determine correlations.

Results

Purification of HA tri-stalk protein

Our long-term research goal is exposition of the LAH region on virus-like particles (VLPs) in its native trimeric conformation. To assess structural and immunological properties of different LAH derivatives a number of constructs containing the LAH region have been compared for expression and solubility in *E. coli*. These peptides had the same C-terminus but differed by their N-terminal extensions. The stem peptide encoding HA amino acids 403–474 was the longest fragment (Mw = 8.5 kDa) which was efficiently produced in a soluble form and was selected for downstream applications as HA tri-stalk protein. For purification, we developed a fast and efficient method involving a combination of three chromatography steps: a weak anion-exchange, a strong anion-exchange and size-exclusion columns (Fig 1A–1C). Standard expression conditions generated high-levels of soluble tri-stalk protein (Fig 1D, lane 1). To simplify the purification procedure, the soluble protein mixture was subjected to thermal treatment at 55°C. As expected, a lot of contaminating proteins precipitated under these conditions while the majority of target protein remained in solution (Fig 1D, lane 2). Next, the protein solution was loaded on a weak anion exchange DEAE column. While the majority of contaminants passed through the column the tri-stalk protein was efficiently bound and eluted with ~200 mM salt (Fig 1A and 1D, lanes 3–4). The solution was then loaded on a strong anion exchanger MonoQ which further improved the purity of the tri-stalk protein (Fig 1B and 1D, lanes 5–6). Finally, protein was subjected to size-exclusion chromatography where two major peaks were observed (Fig 1C). Both peaks contained predominantly target protein, but only the first peak corresponded to the trimer size (Mw = 25.6 kDa) according to its elution volume, while the second peak seemed to contain non-assembled product and was discarded. The final product had at least 90% purity (Fig 1D, lanes 7–8) and was further used for structural and diagnostic studies.

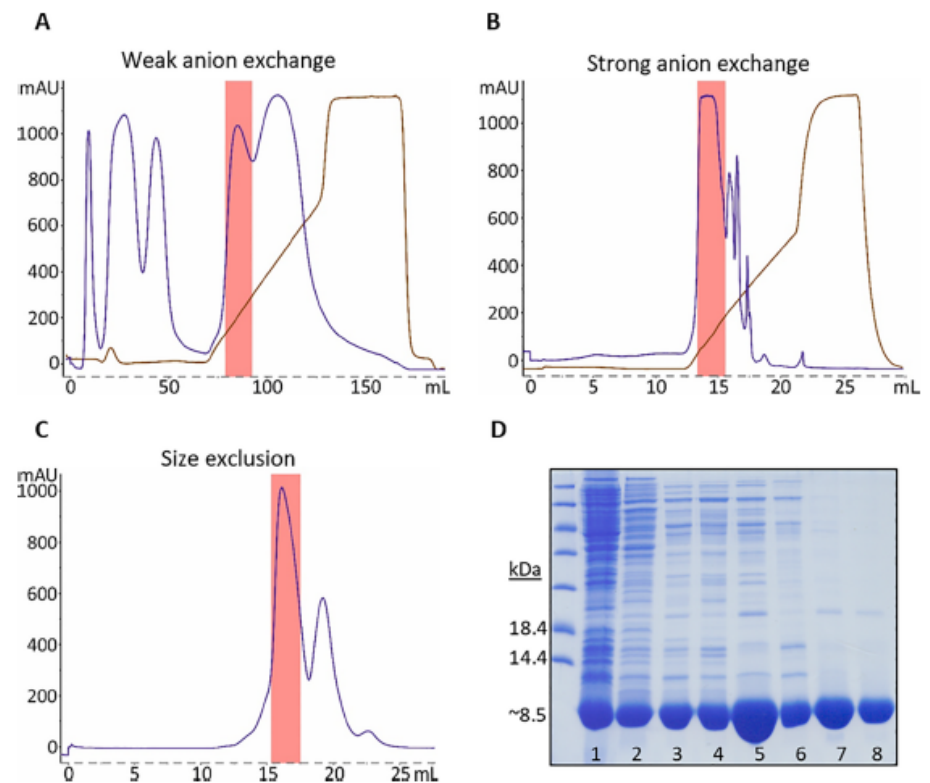


Fig 1. Purification of HA tri-stalk protein. Chromatography profiles of protein fractionation on DEAE FF (A), MonoQ (B) and Superdex (C) columns. Blue lines represent protein peaks while brown lines correspond to salt gradient. HA tri-stalk containing fractions are marked by red squares. (D) Coomassie-stained PAAG illustrating individual purification steps: 1 and 2, supernatant before and after thermal treatment, respectively; 3–4, DEAE column fractions; 5–6, MonoQ column fractions; 7–8, Superdex column fractions.

<https://doi.org/10.1371/journal.pone.0204776.g001>

HA tri-stalk protein structure

The crystal structure of HA tri-stalk protein was solved to 1.7 Å resolution using molecular replacement technique. The space group was $P6_3$ and the HA tri-stalk protein was found to be located on the crystallographic 3-fold axis. Therefore, the crystallographic asymmetric unit contained one protein molecule. The final model included a single protein chain with 65 residues and 57 water molecules. The first 3 N-terminal and 3 C-terminal residues were not included in the final model due to poor electron density.

The structure revealed that HA tri-stalk is an elongated trimer with the length of approximately 63 Å (Fig 2A and 2B). Each monomer consists of a long α -helix at the N-terminus, shorter antiparallel α -helix at the C-terminus, and a small flexible loop region on the surface of the protein connecting both helices. The end of the N-terminus extends away from the rest of the protein. The central long α -helices form a tripartite coiled coil with the short α -helices packing along them and forming a 6-helix bundle-like structure. The protein clearly matched the structure of the corresponding stem fragment of the native HA at its low pH-induced post-fusion conformation [25]. However, it displayed some minor deviations from the wild-type

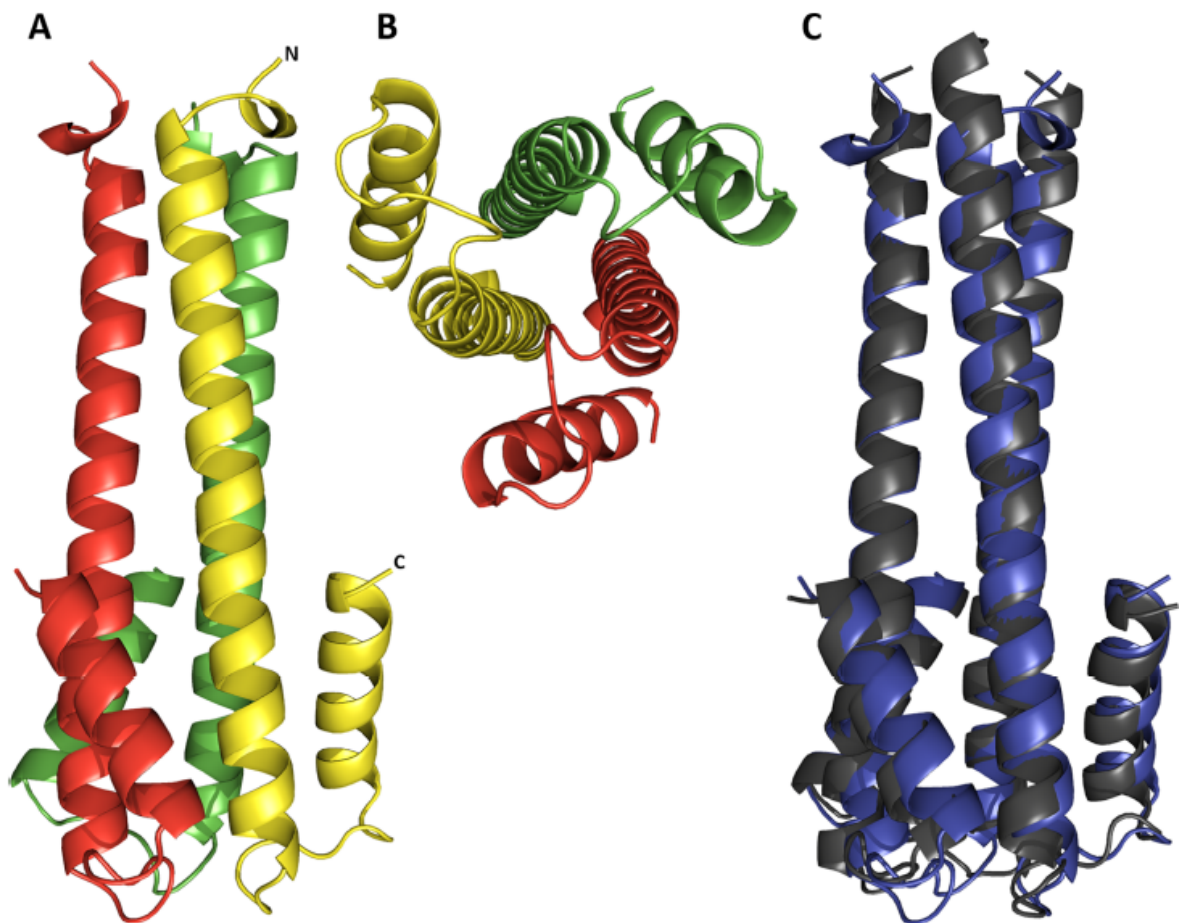


Fig 2. The structure of HA tri-stalk at pH 5.5. Side (A) and top (B) view on tri-stalk protein. Individual monomers are colored in red, green and yellow. (C) Structural alignment of HA tri-stalk protein (blue) with the corresponding stem fragment of native post-fusion HA (grey) (PDB code 1HTM, residues 63 to 127). Only matching sequence length is shown for clarity.

<https://doi.org/10.1371/journal.pone.0204776.g002>

HA in the loop region and at the termini of the helices with C α atom root-mean-square deviations (RMSDs) of about 0.94 Å (60 residues of one monomer were aligned) (Fig 2C).

HA tri-stalk reactive Abs in influenza virus infected mice

In order to set up the optimal condition using HA tri-stalk protein as a coating antigen in indirect ELISA for the detection of seroreactivity to HA stem, the checkerboard titration method was conducted using sera from mice immunized with LAH-PP7 fusion protein (see [Materials and methods](#)) as positive samples and naïve mouse sera as negative controls. Optimal signal to noise (S/N) ratio was found with 1.25 µg/mL coated HA tri-stalk protein and serum dilution of 1:2700 (S/N ratio = 36, Fig 3A). The LAH-PP7 construct was originally designed to expose LAH peptide on the surface of bacteriophage PP7 shells in a form of natural trimer. Although

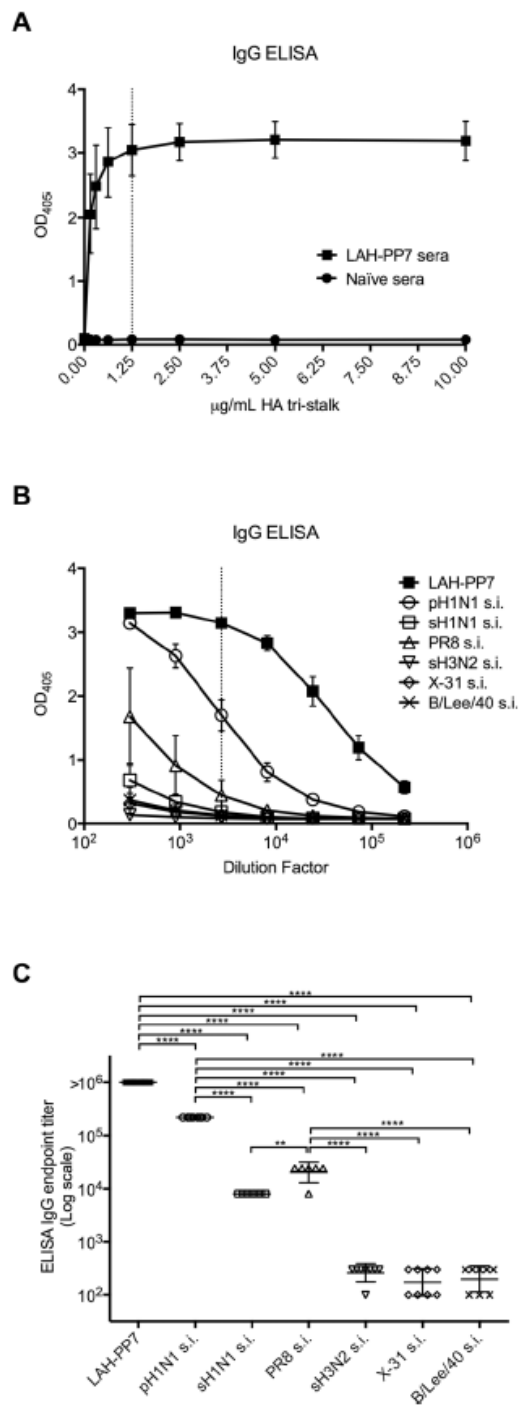


Fig 3. HA tri-stalk specific seroreactivity in mice. (A) Serial dilutions of HA tri-stalk protein (0.15625, 0.3125, 0.625, 1.25, 2.5, 5.0 and 10.0 µg/mL) tested against 1:2700 dilution of sera from LAH-PP7 vaccinated mice or naive mice. (B) Total IgG ELISA was used to determine the HA tri-stalk specific seroreactivity induced by vaccination with LAH-PP7 or by sublethal infection (s.i.) of A/Luxembourg/46/2009 pandemic H1N1 (pH1N1), A/Texas/36/91 seasonal H1N1 (sH1N1), A/Puerto Rico/8/34 H1N1 (PR8), A/Lux/01/2005 seasonal H3N2 (sH3N2), A/Aishi/68 H3N2 (X-31), or B/Lee/40 virus. Total HA tri-stalk specific IgG titers were assayed in sera after the third immunization with LAH-PP7 or after 2 weeks post sublethal virus infection. (C) Comparison of HA tri-stalk specific IgG endpoint titers (n = 8 mice/group; **p<0.001, ***p<0.00001).

<https://doi.org/10.1371/journal.pone.0204776.g003>

we failed to detect the formation of VLPs, expression of this chimeric construct resulted in formation of soluble protein aggregates (S1 Fig) capable to induce strong seroconversion to both group 1 and group 2 HA antigens in mice (S2 Fig), which makes LAH-PP7 fusion protein particularly suitable to assess HA stem-specific Ab responses in mice.

These ELISA conditions were then used to determine the HA tri-stalk specific total IgG titer in sera (3-fold dilutions from 1:300, to 1:218700) from mice vaccinated with LAH-PP7 or sublethally infected (s.i.) by pH1N1, sH1N1, PR8, sH3N2, X-31, or B/Lee/40 virus (Fig 3B). As expected, vaccination with LAH-PP7 induced significantly higher level of HA tri-stalk specific total IgG comparing to sublethal infection by viruses of all the tested strains (Fig 3B and 3C). Nevertheless, mice s.i. by group 1 viruses pH1N1 or PR8 showed significantly higher levels of HA tri-stalk specific IgG than the animals s.i. by the other viruses (Fig 3C). Mice s.i. by strains with group 2 (sH3N2 and X-31) or B/Lee/40 virus exhibited no seroreactivity with HA tri-stalk protein (Fig 3C).

HA tri-stalk reactive Ab-secreting cells in mouse splenocytes after vaccination

To evaluate HA tri-stalk specific Ab-secreting B cells induced by vaccination, BALB/c mice were immunized 3 times i.p. with LAH-PP7 fusion protein that induced high levels of humoral immunity against LAH domain of HA stem as described above. Two weeks after the last immunization, the splenocytes were stimulated *ex vivo* with HA tri-stalk protein. HA tri-stalk reactive Ab-secreting cells were enumerated by ELISPOT assay (Fig 4A). Visually distinct populations of IgG1- and IgG2a- secreting B cells were detected after HA tri-stalk protein stimulation in the vaccinated but not in the mock mice. Although in LAH-PP7 vaccinated mice the IgG1-secreting cells formed larger immunospots than the IgG2a-secreting cells (Fig 4B), there was no significant difference in absolute numbers between both isotype subclasses (Fig 4C). The vaccinated mice showed significantly (up to 10 times) higher numbers of both IgG1- and IgG2a-secreting cells after HA tri-stalk immunization than the mock mice (Fig 4C). This further supports the value of HA tri-stalk protein for monitoring vaccine-induced memory B cell responses against the stem domain.

Pre-pandemic HA tri-stalk specific Abs in SW

The newly developed indirect ELISA using the purified HA tri-stalk protein as a coating antigen was further applied to examine human seroreactivity to HA stem (as described in the Materials and methods). The mean OD of the negative sera was found 0.2115, +/- 0.1251 (SD), and the cut-off point of 0.5868 was calculated as the mean of the negative control sera plus three SD. Sera with an OD >0.5868 were classified as seropositive. A total of 147 of 211 (70%) pre-pandemic SW sera were considered positive for HA stem-specific Abs, whereas only 30 of 71 (42%) pre-pandemic sera from non-SW showed positive for HA stem-specific Abs (S3 Fig). Interestingly, there was a strong correlation between HA stem-specific IgG titer and HA H1/09 IgG titer in these pre-pandemic sera (Fig 5A).

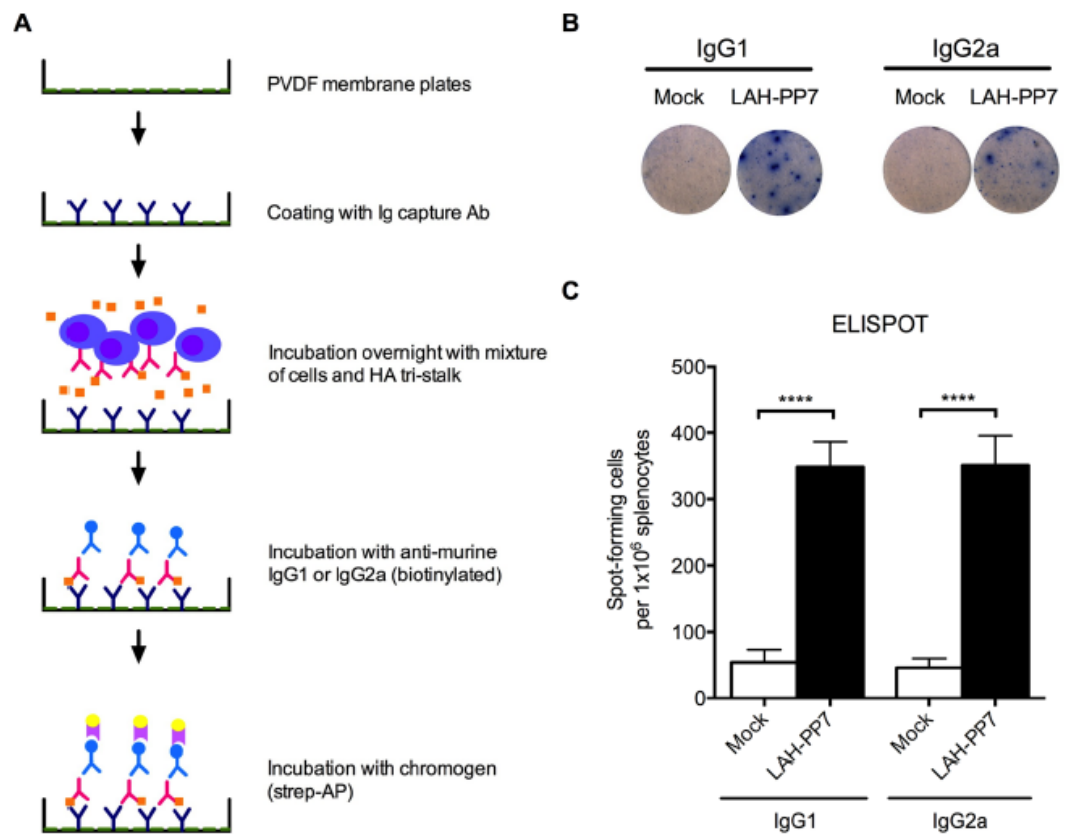


Fig 4. Detection of HA tri-stalk specific memory B cells. (A) ELISPOT assay workflow. (B) Representative pictures of spot-forming IgG1- or IgG2a-secreting cells in mice injected with PBS (mock) or LAH-PP7 fusion protein. (C) Comparison of total IgG1- and IgG2a-secreting B cells under stimulation by HA tri-stalk protein in the spleen of mice from mock and LAH-PP7 vaccinated groups ($n = 8$ mice/group; [29], **** $p < 0.00001$).

<https://doi.org/10.1371/journal.pone.0204776.g004>

We observed a stronger correlation between HA tri-stalk specific IgG titer and HA H1/09 IgG titer (Fig 5A, Spearman $r = 0.4999$, $p < 10^{-4}$). These results indicate that already before the pandemic (H1N1) 2009 virus had spread to Western Europe, substantial levels of cross-reactive Abs against HA stem and HA H1/09 could be detected in humans with professional contact to swine.

Furthermore, we tested the SW for neutralizing Abs against influenza A/Luxembourg/43/2009 (H1N1/09) virus. Significant correlations were observed between H1N1/09 neutralizing titers with HA H1/09 IgG titer (Fig 5B, Spearman $r = 0.2538$, $p = 0.0002$) as well as with HA stem-specific IgG titer (Fig 5C, Spearman $r = 0.1601$, $p = 0.0209$). Whereas, IgG levels to HA of a pre-existing seasonal H1N1 virus, A/Texas/36/1991, showed no correlation with H1N1/09 neutralizing titers (Fig 5D, Spearman $r = 0.1128$, $p = 0.1066$). These observations in SW indicate that pre-pandemic Ab levels to HA tri-stalk protein also translated into neutralizing activities against H1N1/09 virus.

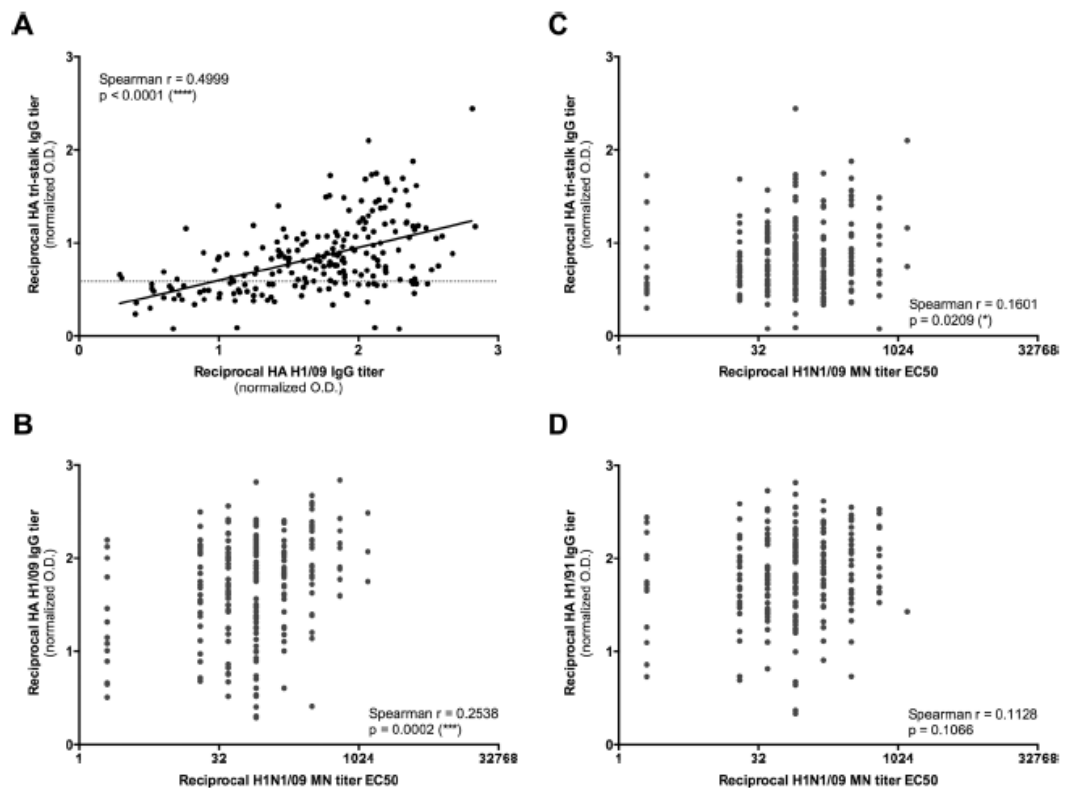


Fig 5. HA tri-stalk specific Abs and neutralizing Abs against pandemic H1N1/09 virus in human. (A) Correlations between HA tri-stalk specific Abs and HA H1/09 specific Abs. Sera with an OD >0.5868 (dotted line) were classified as seropositive to HA tri-stalk. (B) Correlations between H1N1/09 microneutralization Abs and Abs to HA H1/09. (C) Correlations between H1N1/09 microneutralization Abs and HA tri-stalk specific Abs. (D) Correlations between H1N1/09 microneutralization Abs and Abs to HA H1/91 (A/Texas/36/1991).

<https://doi.org/10.1371/journal.pone.0204776.g005>

Discussion

In this study, we have focused on the structure and applications of a novel HA tri-stalk protein comprising LAH region which has attracted much attention as a potential universal influenza vaccine component [16–19]. *E. coli* expressed tri-stalk protein can be purified to near homogeneity using a convenient three-step chromatography method. Structural data revealed that tri-stalk protein folding closely matches the native HA post-fusion conformation. This is in line with a previous study where HA2 polypeptide 38–175 was also *E. coli* expressed in post-fusion form [30]. Our tri-stalk protein is significantly shorter and corresponds to HA2 amino acids 59–130. In contrast to polypeptide 38–175 being able to resist incubation at 68 °C some portion of tri-stalk protein was found unassembled already after heating at 55 °C indicating that the lack of internal cysteines negatively affects its thermostability (Fig 1C). Nevertheless, the outcome of assembled tri-stalk protein using our purification method is estimated at about 5 mg/g of wet cells which makes it attractive for downstream immunogenicity and antigenicity studies and co-crystallization for structural and immunological analysis.

Since the discovery of broadly neutralizing Abs against HA stem [8] a number of attempts have been performed to construct universal stem-based influenza vaccines. One direction of

investigations is targeted to design the trimeric mini-stem constructs being able to bind conformational Abs and protect mice from lethal influenza virus challenge [31–32]. The constructs described are notably longer than tri-stalk protein and contain either intermolecular disulfide bridge, or trimerization (foldon) motif to stabilize the structure. At this stage, our aim was not to outperform these proteins in terms of protection, but to produce an alternative variant in a cost-effective way to be applied in several immune assays for evaluating the future universal vaccine-induced response. While tri-stalk protein is only 72 aa long, it is promising candidate for exposition on the surface of VLPs which is a highly powerful platform for vaccine construction. Incorporation of the LAH within the major immunodominant loop of the hepatitis B core protein allows formation of chimeric VLPs [17–19], however, anchoring of both LAH ends prevents folding of native trimeric conformation. Nevertheless, this strategy led to strong seroconversion to both HA group antigens in mice [18] while immunization with tri-stalk protein alone generated Abs only against homologous group HA antigen (S4 Fig). Ideally, both approaches should be combined to obtain possible synergistic effect. Genetic fusion of LAH-encoding sequence with N- or C-termini of a carrier protein gene would theoretically allow such assembly. Among large variety of carriers coat proteins of small RNA phages organized in simple $T = 3$ symmetry particles offer an attractive scaffold for exposition of trimeric proteins in their native form, since N- and C- terminal ends of the phage coat protein are arranged closely around quasi-threefold axis of $T = 3$ particle. Although we failed to expose LAH peptide on the surface of PP7 VLPs (S1 Fig), it could be speculated that this chimeric protein at least partially assembles in trimeric structures capable to elicit potent immune responses (S2 Fig). This assembly is, however, hard to prove due to irregularity of LAH-VLP aggregates (S1 Fig).

Although HA stem is closely packed to the viral membrane and therefore partly covered by the head domain, the majority of conserved region is accessible to anti-stem Abs [33]. However, immune responses post-infection and post-vaccination are mainly targeted to the immunodominant HA head region [11]. Accordingly, it is well established that anti-stem Abs are normally not found in individuals vaccinated with seasonal inactivated influenza virus vaccines whereas low levels of these Abs are induced by natural virus infection in humans as well as in mice [34]. In contrast, infection of individuals with 2009 pandemic H1N1 virus induced high levels of stem-reactive Ab responses [35]. Cross-reactive immunity derived from anti-stem-specific Abs also tends to increase upon exposure to antigenically diverse influenza viruses [36], [8]. Swine play a particular role in cross-species transmission of diverse influenza viruses because they are susceptible to both avian and human influenza viruses and can act as “mixing vessel” for reassortment of viral gene segments [37]. Previous study showed that, before the outbreak of the pandemic H1N1 2009, persons with professional contact with swine obtained higher serological cross-reactivity with various influenza viruses, including pandemic H1N1 2009 virus, European avian-like subtype H1N1 SIV, and 2007–2008 seasonal influenza subtype H1N1 virus [20]. We therefore hypothesize that these SW harbor pre-existing cross-immunity against various influenza strains, possibly mediated by Ab targeting to conserved viral epitopes, like the HA stem. Indeed, using tri-stalk protein based ELISA to determine the binding of the cross-reactive Abs in these pre-pandemic sera, the results show that Abs targeting the tri-stalk epitope significantly correlate with the Abs specific to the novel antigen, HA H1/09. In addition, tri-stalk specific Abs also have a positive correlation with the neutralizing activities against the pandemic H1N1 2009 virus.

Conclusion

Altogether, our results demonstrate that the novel HA tri-stalk protein, which comprises of the HA LAH region, can be applied in various immunological assays to determine HA stem-

specific humoral responses in both clinical and animal samples. The conserved feature of LAH domain makes the HA tri-stalk protein a promising tool for evaluation of pre-existing or cross-reactive immunity to a newly emerged influenza viruses.

Supporting information

S1 Fig. Purification of LAH-PP7 fusion protein. (A) Coomassie-stained PAAG illustrating individual purification steps. Lane 1, summary expression; lane 2, supernatant; lane 3, urea extract loaded onto Superdex column; lane 4, peak protein fraction from Superdex column. (B) Size-exclusion chromatography profile and (C) Electron microscopy indicating aggregation of target protein. (PDF)

S2 Fig. The cross-reactivity of mouse sera. (A) Reactivity with group 1 HA proteins (H1, H2, H5, H9, H11 and H16). (B) Reactivity with group 2 HA proteins (H3, H4, H7, H10, H14 and H15). Mice were immunized with LAH-PP7 fusion protein or adjuvant alone (mock). The panels show the mean and standard deviation of the optical density at 405 nm of the sera from 10 mice per group. (PDF)

S3 Fig. Comparison of HA tri-stalk ELISA results between SW and non-SW. HA tri-stalk specific seroreactivities were evaluated in pre-pandemic sera from 211 SW and 71 non-SW. (TIFF)

S4 Fig. Comparison of Ab responses after vaccination of LAH-HBc VLPs [18] and tri-stalk protein. (TIFF)

S5 Fig. Full wwPDB X-ray structure validation report. (PDF)

S6 Fig. The ARRIVE guidelines checklist. (DOCX)

Author Contributions

Conceptualization: Kaspars Tars, Claude P. Muller, Andris Kazaks.

Data curation: I-Na Lu, Anna Kirsteina, Sophie Farinelle, Stéphanie Willieme.

Investigation: I-Na Lu, Anna Kirsteina, Andris Kazaks.

Methodology: Sophie Farinelle, Stéphanie Willieme.

Supervision: Claude P. Muller, Andris Kazaks.

Validation: Kaspars Tars.

Writing – original draft: I-Na Lu, Anna Kirsteina, Andris Kazaks.

Writing – review & editing: Kaspars Tars, Claude P. Muller, Andris Kazaks.

References

1. Preaud E, Durand L, Macabeo B, Farkas N, Sloesen B, Palache A, et al. Annual public health and economic benefits of seasonal influenza vaccination: a European estimate. *BMC Public Health*. 2014; 14:813. <https://doi.org/10.1186/1471-2458-14-813> PMID: 25103091

2. Paules C, Subbarao K. Influenza. *Lancet*. 2017; 390(10095):697–708. [https://doi.org/10.1016/S0140-6736\(17\)30129-0](https://doi.org/10.1016/S0140-6736(17)30129-0) PMID: 28302313
3. de Vries RD, Herfst S, Richard M. Avian Influenza A Virus Pandemic Preparedness and Vaccine Development. *Vaccines (Basel)*. 2018; 6(3). <https://doi.org/10.3390/vaccines6030046> PMID: 30044370
4. Johnson NP, Mueller J. Updating the accounts: global mortality of the 1918–1920 “Spanish” influenza pandemic. *Bull Hist Med*. 2002; 76(1):105–15. PMID: 11875246.
5. Yuen KY, Chan PK, Peiris M, Tsang DN, Que TL, Shorridge KF, et al. Clinical features and rapid viral diagnosis of human disease associated with avian influenza A H5N1 virus. *Lancet*. 1998; 351(9101):467–71. PMID: 9482437.
6. Gao R, Cao B, Hu Y, Feng Z, Wang D, Hu W, et al. Human infection with a novel avian-origin influenza A (H7N9) virus. *N Engl J Med*. 2013; 368(20):1888–97. <https://doi.org/10.1056/NEJMoa1304459> PMID: 23577628
7. Wei SH, Yang JR, Wu HS, Chang MC, Lin JS, Lin CY, et al. Human infection with avian influenza A H6N1 virus: an epidemiological analysis. *Lancet Respir Med*. 2013; 1(10):771–8. [https://doi.org/10.1016/S2213-2600\(13\)70221-2](https://doi.org/10.1016/S2213-2600(13)70221-2) PMID: 24461756
8. Krammer F, Palese P. Influenza virus hemagglutinin stalk-based antibodies and vaccines. *Curr Opin Virol*. 2013; 3(5):521–30. <https://doi.org/10.1016/j.coviro.2013.07.007> PMID: 23978327
9. Wilson IA, Skehel JJ, Wiley DC. Structure of the haemagglutinin membrane glycoprotein of influenza virus at 3 Å resolution. *Nature*. 1981; 289(5796):366–73. PMID: 7464906.
10. Xu R, Wilson IA. Structural characterization of an early fusion intermediate of influenza virus hemagglutinin. *J Virol*. 2011; 85(10):5172–82. <https://doi.org/10.1128/JVI.02430-10> PMID: 21367895
11. Ellebedy AH, Ahmed R. Re-engaging cross-reactive memory B cells: the influenza puzzle. *Front Immunol*. 2012; 3:53. <https://doi.org/10.3389/fimmu.2012.00053> PMID: 22566934
12. Heaton NS, Sachs D, Chen CJ, Hai R, Palese P. Genome-wide mutagenesis of influenza virus reveals unique plasticity of the hemagglutinin and NS1 proteins. *Proc Natl Acad Sci U S A*. 2013; 110(50):20248–53. <https://doi.org/10.1073/pnas.1320524110> PMID: 24277853
13. Neu KE, Henry Dunand CJ, Wilson PC. Heads, stalks and everything else: how can antibodies eradicate influenza as a human disease? *Curr Opin Immunol*. 2016; 42:48–55. <https://doi.org/10.1016/j.coi.2016.05.012> PMID: 27268395
14. Kallewaard NL, Corti D, Collins PJ, Neu U, McAuliffe JM, Benjamin E, et al. Structure and Function Analysis of an Antibody Recognizing All Influenza A Subtypes. *Cell*. 2016; 166(3):596–608. <https://doi.org/10.1016/j.cell.2016.05.073> PMID: 27453466
15. Dreyfus C, Laursen NS, Kwaks T, Zuijdgeest D, Khayat R, Ekiert DC, et al. Highly conserved protective epitopes on influenza B viruses. *Science*. 2012; 337(6100):1343–8. <https://doi.org/10.1126/science.1222908> PMID: 22878502
16. Wang TT, Tan GS, Hai R, Pica N, Ngai L, Ekiert DC, et al. Vaccination with a synthetic peptide from the influenza virus hemagglutinin provides protection against distinct viral subtypes. *Proc Natl Acad Sci U S A*. 2010; 107(44):18979–84. <https://doi.org/10.1073/pnas.1013387107> PMID: 20956293
17. Chen S, Zheng D, Li C, Zhang W, Xu W, Liu X, et al. Protection against multiple subtypes of influenza viruses by virus-like particle vaccines based on a hemagglutinin conserved epitope. *Biomed Res Int*. 2015; 2015:901817. <https://doi.org/10.1155/2015/901817> PMID: 25767809
18. Kazaks A, Lu IN, Farinelle S, Ramirez A, Crescente V, Blaha B, et al. Production and purification of chimeric HBc virus-like particles carrying influenza virus LAH domain as vaccine candidates. *BMC Biotechnol*. 2017; 17(1):79. <https://doi.org/10.1186/s12896-017-0396-8> PMID: 29126399
19. Ramirez A, Morris S, Maucourant S, D’Ascanio I, Crescente V, Lu IN, et al. A virus-like particle vaccine candidate for influenza A virus based on multiple conserved antigens presented on hepatitis B tandem core particles. *Vaccine*. 2018; 36(6):873–80. <https://doi.org/10.1016/j.vaccine.2017.12.053> PMID: 29306508
20. Gerloff NA, Kremer JR, Charpentier E, Sausy A, Olinger CM, Weicherding P, et al. Swine influenza virus antibodies in humans, western Europe, 2009. *Emerg Infect Dis*. 2011; 17(3):403–11. <https://doi.org/10.3201/eid1703.100851> PMID: 21392430
21. Battye TG, Kontogiannis L, Johnson O, Powell HR, Leslie AG. iMOSFLM: a new graphical interface for diffraction-image processing with MOSFLM. *Acta Crystallogr D Biol Crystallogr*. 2011; 67(Pt 4):271–81. <https://doi.org/10.1107/S0907444910048675> PMID: 21460445
22. Scaling Evans P. and assessment of data quality. *Acta Crystallogr D Biol Crystallogr*. 2006; 62(Pt 1):72–82.
23. Potterton E, Briggs P, Turkenburg M, Dodson E. A graphical user interface to the CCP4 program suite. *Acta Crystallogr D Biol Crystallogr*. 2003; 59(Pt 7):1131–7. PMID: 12832755.

24. McCoy AJ, Grosse-Kunstleve RW, Storoni LC, Read RJ. Likelihood-enhanced fast translation functions. *Acta Crystallogr D Biol Crystallogr*. 2005; 61(Pt 4):458–64. <https://doi.org/10.1107/S0907444905001617> PMID: 15805601
25. Bullough PA, Hughson FM, Skehel JJ, Wiley DC. Structure of influenza haemagglutinin at the pH of membrane fusion. *Nature*. 1994; 371(6492):37–43. <https://doi.org/10.1038/371037a0> PMID: 8072525
26. Cowtan K. The Buccaneer software for automated model building. 1. Tracing protein chains. *Acta Crystallogr D Biol Crystallogr*. 2006; 62(Pt 9):1002–11. <https://doi.org/10.1107/S0907444906022116> PMID: 16929101
27. Emsley P, Cowtan K. Coot: model-building tools for molecular graphics. *Acta Crystallogr D Biol Crystallogr*. 2004; 60(Pt 12 Pt 1):2126–32. <https://doi.org/10.1107/S0907444904019158> PMID: 15572765
28. Murshudov GN, Skubak P, Lebedev AA, Pannu NS, Steiner RA, Nicholls RA, et al. REFMAC5 for the refinement of macromolecular crystal structures. *Acta Crystallogr D Biol Crystallogr*. 2011; 67(Pt 4):355–67. <https://doi.org/10.1107/S0907444911001314> PMID: 21460454
29. Sasaki S, Sullivan M, Narvaez CF, Holmes TH, Furman D, Zheng NY, et al. Limited efficacy of inactivated influenza vaccine in elderly individuals is associated with decreased production of vaccine-specific antibodies. *J Clin Invest*. 2011; 121(8):3109–19. <https://doi.org/10.1172/JCI57834> PMID: 21785218
30. Chen J, Wharton SA, Weissenhom W, Calder LJ, Hughson FM, Skehel JJ, et al. A soluble domain of the membrane-anchoring chain of influenza virus hemagglutinin (HA2) folds in *Escherichia coli* into the low-pH-induced conformation. *Proc Natl Acad Sci U S A*. 1995; 92(26):12205–9. PMID: 8618870
31. Valkenburg SA, Mallajosyula VV, Li OT, Chin AW, Carnell G, Temperton N, et al. Stalking influenza by vaccination with pre-fusion headless HA mini-stem. *Sci Rep*. 2016; 6:22666. <https://doi.org/10.1038/srep22666> PMID: 26947245
32. Impagliazzo A, Milder F, Kuipers H, Wagner MV, Zhu X, Hoffman RM, et al. A stable trimeric influenza hemagglutinin stem as a broadly protective immunogen. *Science*. 2015; 349(6254):1301–6. <https://doi.org/10.1126/science.aac7263> PMID: 26303961
33. Harris AK, Meyerson JR, Matsuoka Y, Kuybeda O, Moran A, Bliss D, et al. Structure and accessibility of HA trimers on intact 2009 H1N1 pandemic influenza virus to stem region-specific neutralizing antibodies. *Proc Natl Acad Sci U S A*. 2013; 110(12):4592–7. <https://doi.org/10.1073/pnas.1214913110> PMID: 23460696
34. Margine I, Hai R, Albrecht RA, Obermoser G, Harrod AC, Banchereau J, et al. H3N2 influenza virus infection induces broadly reactive hemagglutinin stalk antibodies in humans and mice. *J Virol*. 2013; 87(8):4728–37. <https://doi.org/10.1128/JVI.03509-12> PMID: 23408625
35. Pica N, Hai R, Krammer F, Wang TT, Maamary J, Eggink D, et al. Hemagglutinin stalk antibodies elicited by the 2009 pandemic influenza virus as a mechanism for the extinction of seasonal H1N1 viruses. *Proc Natl Acad Sci U S A*. 2012; 109(7):2573–8. <https://doi.org/10.1073/pnas.1200039109> PMID: 22308500
36. Miller MS, Gardner TJ, Krammer F, Aguado LC, Tortorella D, Basler CF, et al. Neutralizing antibodies against previously encountered influenza virus strains increase over time: a longitudinal analysis. *Sci Transl Med*. 2013; 5(198):198ra07. <https://doi.org/10.1126/scitranslmed.3006637> PMID: 23946196
37. Shortridge KF, Webster RG, Butterfield WK, Campbell CH. Persistence of Hong Kong influenza virus variants in pigs. *Science*. 1977; 196(4297):1454–5. PMID: 867041.



3.3 Construction and Immunogenicity of a Novel Multivalent Vaccine Prototype Based on Conserved Influenza Virus Antigens

Highlights:

- Genetic fusion and modular functionalization techniques were applied to yield chimeric AP VLPs displaying HA tri-stalk or 3M2e, or presenting both conserved influenza antigens on a single particle.
- Chimeric VLPs displaying the tri-stalk antigen induced broad and robust antibody responses against a variety of group 1 rHAs (homologous cH6/1 and heterologous pre-2009 H1, H2, H5, H6, H8, H9, and H11 HA proteins), as well as cross-reacted with several group 2 rHAs (H3, H4, and H10 HAs).
- Chimeric AP-M2e and AP-M2e/tri-stalk particles were able to protect mice against lethal unmatched H1N1 and heterologous H3N2 virus challenge, with minimal disease symptoms. The AP/tri-stalk VLPs and a free tri-stalk antigen conferred only partial protection against the H1N1 challenge and no protection against the H3N2 virus infection.
- Both AP-M2e and AP-M2e/tri-stalk VLPs fully protected mice against lethal rgH5N1 challenge via the immune sera from vaccinated mice.
- Only the particles displaying both conserved antigens could protect mice against high-dose lethal homologous H1N1 challenge in mice, with no significant disease symptoms observed.
- Both the tri-stalk and 3M2e mediated protection was mainly afforded by the ADCC mechanisms, but the 3M2e antigen was able to induce 3M2e-specific cytotoxic T-cell responses.

Article

Construction and Immunogenicity of a Novel Multivalent Vaccine Prototype Based on Conserved Influenza Virus Antigens

Anna Kirsteina¹, Inara Akopjana¹, Janis Bogans¹, Ilva Lieknina¹, Juris Jansons¹, Dace Skrastina¹, Tatjana Kazaka¹, Kaspars Tars¹, Irina Isakova-Sivak² , Daria Mezhenskaya² , Tatiana Kotomina², Victoria Matyushenko², Larisa Rudenko² and Andris Kazaks^{1,*}

¹ Latvian Biomedical Research and Study Centre, LV-1067 Riga, Latvia; anna.kirsteina@biomed.lu.lv (A.K.); inara@biomed.lu.lv (I.A.); janis@biomed.lu.lv (J.B.); ilva@biomed.lu.lv (I.L.); jansons@biomed.lu.lv (J.J.); daceskr@biomed.lu.lv (D.S.); tatyana@biomed.lu.lv (T.K.); kaspars@biomed.lu.lv (K.T.)

² Department of Virology, Institute of Experimental Medicine, Saint Petersburg 197376, Russia; isakova.sivak@iemspb.ru (I.I.-S.); dasmez@iemspb.ru (D.M.); kotomina@iemspb.ru (T.K.); matyushenko@iemspb.ru (V.M.); rudenko.lg@iemspb.ru (L.R.)

* Correspondence: andris@biomed.lu.lv

Received: 30 March 2020; Accepted: 21 April 2020; Published: 24 April 2020



Abstract: Influenza, an acute, highly contagious respiratory disease, remains a significant threat to public health. More effective vaccination strategies aimed at inducing broad cross-protection not only against seasonal influenza variants, but also zoonotic and emerging pandemic influenza strains are urgently needed. A number of conserved protein targets to elicit such cross-protective immunity have been under investigation, with long alpha-helix (LAH) from hemagglutinin stalk and ectodomain of matrix protein 2 ion channel (M2e) being the most studied ones. Recently, we have reported the three-dimensional structure and some practical applications of LAH expressed in *Escherichia coli* system (referred to as tri-stalk protein). In the present study, we investigated the immunogenicity and efficacy of a panel of broadly protective influenza vaccine prototypes based on both influenza tri-stalk and triple M2e (3M2e) antigens integrated into phage AP205 virus-like particles (VLPs). While VLPs containing the 3M2e alone induced protection against standard homologous and heterologous virus challenge in mice, only the combination of both conserved influenza antigens into a single VLP fully protected mice from a high-dose homologous H1N1 influenza infection. We propose that a combination of genetic fusion and chemical coupling techniques to expose two different foreign influenza antigens on a single particle is a perspective approach for generation of a broadly-effective vaccine candidate that could protect against the constantly emerging influenza virus strains.

Keywords: influenza; conserved antigens; hemagglutinin stalk; M2e protein; virus-like particles; protection; vaccines

1. Introduction

Influenza, an acute, highly contagious respiratory disease, remains a significant threat to public health. The co-circulating influenza A (subtypes H1N1 and H3N2) and B (lineages Victoria and Yamagata) viruses cause seasonal epidemics, which affect a major part of the global population causing high morbidity and up to 645,832 influenza-associated deaths annually [1,2]. Consequently, seasonal influenza viruses are responsible for a significant economic burden on the health care systems and society [3,4].

Although influenza is considered to be a vaccine-preventable disease, the effectiveness of seasonal influenza vaccines varies greatly across the risk groups and seasons, on average between 19–60% [5,6]. Currently licensed vaccines induce a strain-specific antibody response, hence vaccine effectiveness is significantly compromised by the persistent antigenic changes of influenza viruses [7,8]. Continuous antibody-mediated immune pressure and the lack of a proof-reading function for RNA polymerase errors result in accumulation of point mutations in the hemagglutinin (HA) and neuraminidase genes and in constant emergence of mutant variants affecting immune recognition. This process, characteristic to both influenza A and B viruses, is known as antigenic drift and it has the potential to cause local outbreaks and seasonal epidemics [7–10]. Moreover, sporadic reassortment of segmented influenza A virus genomes in a double-infected host cell can result in an antigenic shift, which can lead to a global pandemic by producing an unpredicted virus strain to which the immunologically naive human population is particularly susceptible. Interspecies transmissions of influenza A viruses from animal reservoirs have resulted in four pandemics since the beginning of the 20th century; the Spanish influenza pandemic in 1918 is considered to be the most lethal in history, with a mortality rate of over 50 million cases [11,12].

Annual immunization with updated seasonal vaccine formulations is recommended [1], but prediction mismatches between the vaccine strains and circulating viruses can dramatically decrease the vaccine effectiveness [5–8,13]. Furthermore, the components of commercially available influenza vaccines are mainly obtained by propagating viruses in embryonated chicken eggs which is a complex, time-consuming, and expensive process with limitations for highly pathogenic avian-borne influenza virus vaccine preparations [14,15]. The capability to manufacture large amounts of strain-specific vaccine doses in the event of a sudden influenza pandemic is limited, which means that during the months of vaccine preparation, testing and distribution, society can be particularly vulnerable to the newly emerged virus strain [11,14,15]. The persistent threat of highly pathogenic poultry influenza viruses (H5Nx) and other zoonotic influenza strains (H6N1, H7N9, H10N8) overcoming the species barrier and adapting to mammalian hosts highlights a continuous pandemic risk [16–19]. Currently, numerous strategies to improve the effectiveness of seasonal influenza vaccines, like the use of new adjuvants, increased doses, or different vaccination strategies, are under investigation [11]. However, many of these approaches could not provide broad and durable protection from influenza virus drift and shift variants.

All these challenges indicate the need for more effective vaccination strategies aimed at inducing broad cross-protection not only against seasonal influenza variants but also zoonotic and emerging pandemic influenza strains. A number of conserved protein targets to elicit such cross-protective immunity have been under investigation for almost two decades, with long alpha-helix (LAH) from HA stalk and ectodomain of matrix protein 2 ion channel (M2e) being the most studied ones [20–29]. Due to the close packing to the viral envelope, these conserved antigens are immunosubdominant and natural influenza infections and current vaccination regimens elicit little or no antibody responses [20,25,30]. Yet, various strategies to elicit more potent immune responses have been developed. Antigen presentation on the surface of virus-like particles (VLPs) stands out as one of the most efficient techniques to enhance the exposure of such weak immunogens to the host immune system by displaying the antigens of choice in a symmetric, highly organized structure with a large number of repetitions [31].

However, despite the highly conserved nature, vaccines based solely on one conserved influenza antigen most often cannot provide complete protection against highly divergent heterosubtypic virus infections [21–25]. Furthermore, although M2e vaccine prototypes have shown promising effects in animal models, the results do not always translate well to human studies, with high-dose associated adverse reactions, rapidly decreasing antibody titers or narrow cell-mediated immunity [25]. Vaccine candidates including several conserved epitopes might confer broader and longer-lasting protection against influenza virus infections. In the present study, we investigated the immunogenicity and efficacy of a panel of broadly protective influenza vaccine prototypes based on influenza HA stalk and M2e antigens integrated into bacteriophage AP205 coat protein (CP) VLPs expressed in *Escherichia coli*

system. As the termini of AP205 CP are surface exposed, it is particularly tolerant to N- and C-terminal fusions. In addition, due to the interdimer disulfide bonds, AP205 CPVLPs are very stable, making them a particularly suitable platform for carrying foreign antigens [32]. The merging of genetic fusion and chemical coupling techniques to expose two different foreign influenza antigens on a single particle without compromising the trimeric conformation of the stalk protein is a perspective approach for a broadly-effective vaccine candidate that could protect against the constantly emerging influenza virus strains. Similar VLP vaccine candidates have employed a linear LAH epitope [24,29,33]; however, such strategy does not embrace the immunological advantages of conformational epitopes [34].

2. Materials and Methods

2.1. Antigen Expression and Purification

HA tri-stalk: Production and purification of soluble H1N1 A/Luxembourg/43/2009 subtype HA tri-stalk protein were accomplished using previously reported methods [35].

3M2e protein: The gene of a 3M2e protein, corresponding to a triplet 24 aa sequence of the M2e, derived from H1N1, H5N1 and H1N9 subtypes [29] (Table S1), was synthesized and supplied by BioCat GmbH (Heidelberg, Germany), cloned in a pET24a(+) vector. The construct was originally designed for chemical coupling purposes and contained a 6His-Tag sequence along with the TEV protease cleavage site at the N-terminus and a cysteine separated by a rigid EAAAK linker at the C-terminus. The construct was expressed in *E. coli* BL21 (DE3) cells according to the manufacturer's recommendations. For purification, cells were disrupted in lysis buffer (20 mM Tris-HCl (pH 8.0) and 300 mM NaCl) by sonication. Supernatant was passed through a 1 mL HisTrap™ FF crude column (GE Healthcare, Uppsala, Sweden) in lysis buffer containing 10 mM imidazole. Bound protein was eluted with a linear gradient of 0.5 M imidazole in lysis buffer. For the final polishing, the protein was passed through the Superdex 200 10/300 GL column (GE Healthcare, Uppsala, Sweden) in 20 mM Tris-HCl (pH 8.0) and 200 mM NaCl.

AP205 and AP-M2e VLPs: The gene encoding wild-type AP205 CP [32] was introduced into the pETDuet-1 expression vector (Novagen, Merck KGaA, Darmstadt, Germany). The 72 aa sequence encoding the 3M2e protein was genetically fused to the C-terminus of AP205 CP; the final construct was designated as AP-M2e. AP205 and AP-M2e VLPs were produced in *E. coli* BL21 (DE3) cells. The cells were lysed by sonication in buffer A (20 mM Tris-HCl (pH 8.0) and 100 mM NaCl). To the supernatant, ammonium sulphate was added to 40% saturation following incubation for 1 h at +4 °C. The precipitate was dissolved in a minimal volume of 20 mM Tris-HCl (pH 8.0), and subjected to thermal treatment (30 min at +55 °C) following cooling down to the RT and centrifugation. For purification of AP205 VLPs, supernatant was passed through a size-exclusion Sepharose 4 FF matrix (GE Healthcare, Uppsala, Sweden) in buffer A. Selected fractions were loaded on an anion-exchange Fractogel TMAE (M) matrix (Merck KGaA, Darmstadt, Germany) in buffer A. Bound protein was eluted with a linear salt gradient of buffer B (20 mM Tris-HCl (pH 8.0) and 1 M NaCl). Ammonium sulphate was added to the selected fractions to the concentration of 1.5 M. For final purification, a hydrophobic-interaction Fractogel Propyl (S) matrix (Merck KGaA, Darmstadt, Germany), equilibrated with 50 mM NaHPO₄ (pH 7.3) and 1.5 mM ammonium sulphate buffer, was used. Bound protein was linearly eluted with 25 mM NaHPO₄ (pH 7.3) buffer. For purification of chimeric AP-M2e VLPs, soluble fraction was passed through a size-exclusion Sepharose 4 FF matrix in buffer A. Selected fractions were loaded on an anion-exchange Fractogel DEAE (M) matrix (Merck KGaA, Darmstadt, Germany) equilibrated with buffer A. Bound protein was eluted with a linear salt gradient of buffer B.

Purified proteins were aliquoted and stored at −20 °C. Protein purity was assessed by SDS/PAGE.

2.2. Chemical Coupling of HA Tri-Stalk Protein to VLPs via SATA Reagent

To introduce a sulfhydryl group into tri-stalk protein, SATA reagent was added according to the manufacturer's protocol (Thermo Scientific, Rockford, IL, USA). Briefly, tri-stalk protein was combined

with a 3.3-fold molar excess of SATA in DMSO and incubated for 30 min at room temperature (RT). Unreacted SATA was removed using Zeba™ Spin desalting column (Thermo Scientific, Rockford, IL, USA). Free sulfhydryl groups were generated by mixing the protein solution with 1/10 volume of deacetylation solution (0.5 M hydroxylamine, 25 mM EDTA in PBS, pH 7.2–7.5) and incubating for 2 h at RT. Hydroxylamine was removed by desalting. The sulfhydryl-modified tri-stalk was promptly used for chemical coupling to AP205 or AP-M2e VLPs. First, VLPs were mixed with a 10-fold excess of SMPH crosslinker (Thermo Scientific, Rockford, IL, USA) in DMSO and incubated for 30 min at RT. Residual crosslinker was removed by desalting. Subsequently, the amine-modified VLPs were combined with a 3-fold excess of sulfhydryl-modified tri-stalk protein and incubated for 30 min at RT; part of the unreacted tri-stalk protein was removed using Amicon-Ultra 4, 100K (Merck-Millipore, Cork, Ireland). Coupling efficiency was determined by SDS/PAGE. Single use aliquots of the conjugated proteins were stored at $-20\text{ }^{\circ}\text{C}$.

2.3. Viruses and Recombinant Full-Length HA Proteins

Influenza viruses used in the experiments were PR8 (wild-type H1N1 A/Puerto Rico/8/1934 virus, Institute of Experimental Medicine, Saint Petersburg, Russia), Cal/09 (a mouse-adapted H1N1 A/California/7/2009 virus, Smorodintsev Research Institute of Influenza, Saint Petersburg, Russia), H3N2 (a mouse-adapted PR8-based reassortant H3N2 A/Philippines/2/1982 (X-79) virus, ISMMS, New York, USA), and rgH5N1 (a mouse-adapted PR8-based reassortant virus with HA and NA genes from H5N1 A/Viet Nam/1203/2004 virus, CDC, Atlanta, GA, USA). For ICS analyses, H1N1 A/California/7/2009 virus was purified by ultracentrifugation in a sucrose gradient. The viruses were propagated in eggs for 2 days at $+37\text{ }^{\circ}\text{C}$ and stored in single-use aliquots at $-70\text{ }^{\circ}\text{C}$. All experiments with viruses were performed in a BSL2 conditions.

Recombinant full-length HA proteins used in this study, kindly provided by Professor F. Krammer (ISMMS, New York, USA), are listed as follows: cH6/1 (head domain from H6N1 A/mallard/Sweden/81/2002 virus and stalk domain from Cal/09 virus), H1 (H1N1 A/Solomon islands/03/2006), H2 (H2N2 A/Japan/305/1957), H3 (H3N2 A/Wyoming/3/2003), H4 (H4N6 A/red knot/Delaware/541/1988), H5 (H5N1 A/Indonesia/5/2005), H6 (H6N4 A/mallard/Sweden/81/2002), H7 (H7N9 A/Shanghai/1/2013), H8 (H8N4 A/mallard/Sweden/24/2002), H9 (H9N2 A/guinea fowl/Hong Kong/WF10/1999), H10 (H10N8 A/Jiangxi-Donghu/346/2013), and H11 (H11N9 A/shoveler/Netherlands/18/1999). All proteins were stored at $-70\text{ }^{\circ}\text{C}$.

2.4. Animals

Eight- to ten-week-old female BALB/c and C57BL/6J mice were purchased from the laboratory breeding nursery of the Russian Academy of Sciences “Stolbovaya” (Moscow region, Russia). Mice were anesthetized for all intranasal procedures, retro-orbital bleeding and retro-orbital injections with isoflurane. The handling of animals was performed in accordance with the “Manual for laboratory animals and alternative models in biomedical research” (2010). The study design was approved by the Local Institutional Ethical Committee (ethical approval number 1/19 dated 08 February 2019).

2.5. Vaccination and Challenge

Direct protection: BALB/c mice were immunized intraperitoneally with three doses of each vaccine antigen at a dose of $25\text{ }\mu\text{g}$ of protein per mouse, two weeks apart (the number of animal is indicated in Figure 1). The proteins were diluted to 0.25 mg/mL in PBS and $100\text{ }\mu\text{L}$ of antigen were combined with $100\text{ }\mu\text{L}$ of Alum adjuvant (AlumVax Hydroxide 2% ready-to-use suspension, OZ Biosciences, Marseille, France). The control group received sterile PBS with adjuvant. Two weeks after the last immunization mice were bled via retro-orbital sinus to obtain serum samples. At day 45, mice were challenged intranasally with $50\text{ }\mu\text{L}$ of $3 \times \text{LD}_{50}$ of either PR8 or H3N2 virus, or $30 \times \text{LD}_{50}$ of Cal/09 virus. Weight loss and survival of the challenged mice were monitored daily for 14 days post-infection. Survival was defined as a 25% weight loss for PR8 and H3N2 viruses and 30% for the Cal/09 virus.

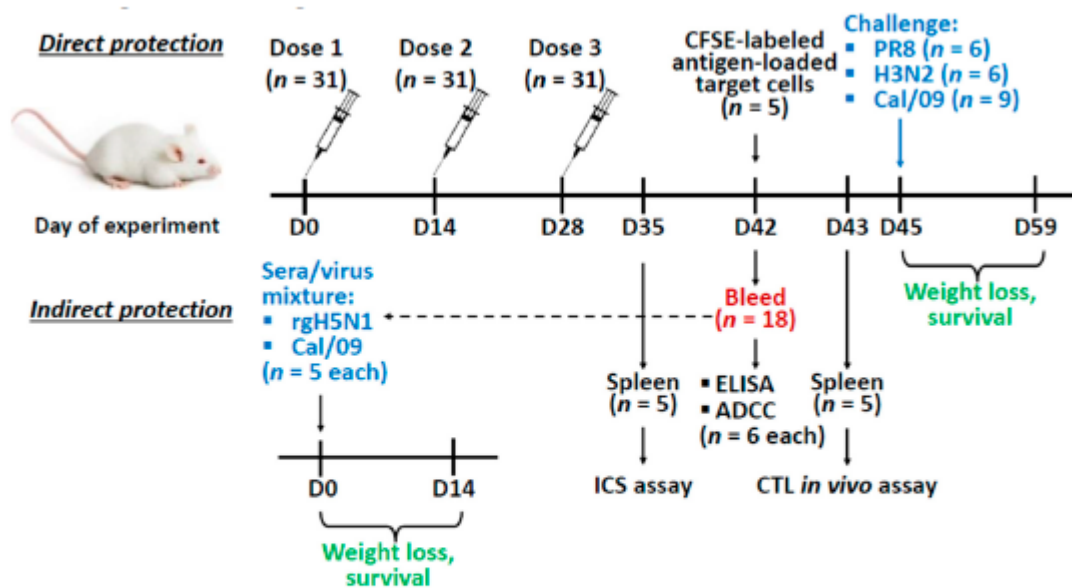


Figure 1. Overview of the mice study design. Mice were immunized with the recombinant vaccine prototypes three times with a two-week interval. Two weeks after the last immunization mice were bled to assess antibody titers and antibody-dependent cellular cytotoxicity (ADCC) ($n = 6$ for each), and to test the indirect protection of immune sera. For the *in vivo* indirect protection experiment, naïve mice were inoculated with 1:1 sera/virus mixture ($3 \times LD_{50}$ of rgH5N1 or Cal/09 ($n = 5$ for each)) and monitored daily for weight loss and survival for 14 days. In addition, on day 35 and 43 spleens ($n = 5$) were collected for the intracellular cytokine staining (ICS) assay or cytotoxic T-lymphocyte (CTL) *in vivo* assay respectively. On day 45 immunized mice were infected with a lethal dose of challenge virus ($3 \times LD_{50}$ of either PR8 or H3N2 ($n = 6$ for each), or $30 \times LD_{50}$ Cal/09 virus ($n = 9$)) and monitored daily for weight loss and survival for 14 days.

Passive transfer: An *in vivo* indirect protection assay was carried out as described previously [36]. Briefly, sera from immunized or naïve mice obtained during the direct protection experiment were mixed with PBS at a 1:1 ratio and heat-inactivated at 56°C for 1 h. Then the sera were mixed 1:1 with rgH5N1 or Cal/09 virus, to reach the dose $3 \times LD_{50}$ and incubated at RT for 30 min. Naïve BALB/c mice were infected intranasally with a mixture of virus and sera at a volume of $50 \mu\text{L}$ and monitored for their survival rates and weight loss for 14 days post-infection (Figure 1). Survival was defined as a 25% weight loss for the rgH5N1 virus and 30% for the Cal/09 virus.

2.6. Enzyme Linked Immunosorbent Assay (ELISA)

For ELISA, EIA/RIA 96-Well microtitration plates (Corning Life Sciences, Tewksbury, MA, USA) were coated with $50 \mu\text{L}$ of the recombinant proteins at a concentration of $2 \mu\text{g}/\text{mL}$ overnight at $+4^\circ\text{C}$. Plates were washed with 0.05% Tween 20 in PBS (PBST) and blocked with $50 \mu\text{L}$ of 1% bovine serum albumin (BSA) in PBS for 30 min at $+37^\circ\text{C}$. Three-fold dilutions of sera were prepared starting from 1:100 (for IgG and IgG1) or 1:10 (for IgG2a) and added to the coated wells ($50 \mu\text{L}/\text{well}$). The plates were incubated for 1 h at $+37^\circ\text{C}$ and washed four times with PBST. Bound IgG, IgG1, and IgG2a antibodies were detected with $50 \mu\text{L}$ of horseradish peroxidase (HRPO) conjugated goat anti-mouse IgG (Sigma-Aldrich, Saint Louis, MO, USA) or primary rabbit anti-mouse IgG1 and IgG2a antibodies (Abcam, Cambridge, UK) respectively, followed by the addition of secondary HRPO conjugated goat anti-rabbit IgG (Sigma-Aldrich, Saint Louis, MO, USA) for IgG1 and IgG2a antibody detection. Plates were incubated with primary antibody or the conjugates for 30 min at $+37^\circ\text{C}$ and washed four times with PBST. The detection of antibody binding was performed with 3,3', 5,5'-tetramethylbenzidine substrate (1-Step Ultra TMB-ELISA Substrate Solution, Thermo Scientific, Rockford, IL, USA). The endpoint serum IgG antibody titers were determined as the last serum dilution with OD_{450} value exceeding at least twice the mean OD values of the control wells

(all the components except mouse sera). For negative specimens, the titers were assigned a value of 1:50 (for IgG and IgG1) or 1:5 (for IgG2a) for group comparison purposes. The log₁₀-transformed antibody titers were used for statistical analyses.

2.7. Antibody-Dependent Cellular Cytotoxicity (ADCC) Assay

The functional activity of the induced antibody was assessed by ADCC assay, performed by measuring the levels of NK-cell degranulation activity. MDCK cells were used as target cells expressing viral antigens since it is known that HA and M2 proteins are expressed abundantly on the surface of influenza virus infected cells [37]. MDCK cell monolayers, seeded in 96-well plates (tissue culture plate 96-well flat, Sarstedt, Nümbrecht, Germany) the day before, were infected with Cal/09 virus at a multiplicity of infection (MOI) 3. Two h after inoculation, conditional medium was removed and 15 µL of serum samples were added in duplicates to the wells, followed by incubation at +37 °C in a 5% CO₂ atmosphere for 15 min. Then, 135 µL of CR-0 (2.5 mL 1 M HEPES, 5 mL Glutamax (Gibco), 5 mL antibiotic-antimycotic (Gibco), 17 µL β-mercaptoethanol, RPMI-1640 (Gibco) up to 500 mL) with 1×10^6 murine splenocytes collected from naïve C57BL/6J mice were added to each sample and incubated overnight. After 16–18 h, supernatants were collected from the plate and stained with ZombieAqua fixable viability dye, anti-CD3, anti-CD49b, anti-CD45.2, anti-CD107a antibody-conjugates for 20 min in a cool dark place (Table 1). Samples were then washed twice with 200 µL of PBS. Plates were stored in a cool dark place prior to flow cytometric analysis. At least 100,000 events were measured using a Navios flow cytometer (Beckman Coulter, Brea, CA, USA). Data were analysed using FlowJo software (TriStar Inc., El Segundo, CA, USA). Gating strategy is shown in Supplementary (Figure S1).

Table 1. A mixture of antibody-conjugates (Biolegend, San Diego, CA, USA) used for ADCC.

Mixture Component	Antibody	Dye	Cat.no	µL per Sample
1	Anti-CD3	FITC	121420	0.25
2	Anti-CD49b	PE	108907	0.25
3	Anti-CD45.2	Pacific Blue	109820	0.25
4	Anti-CD107a or Iso anti-CD107a	APC-Cy7 APC-Cy7	104435 400524	0.25 or 0.25
5	ZombieAqua	BV-510	123102	0.3
6	PBS	-	-	98.7

APC: allophycocyanin; PE: phycoerythrin; BV: brilliant violet; FITC: fluorescein isothiocyanate.

2.8. Intracellular Cytokine Staining (ICS)

T-cell-mediated immune responses were analyzed by ICS to gamma-interferon (IFN γ) and tumor necrosis factor alpha (TNF α). Murine splenocytes were isolated one week after the third immunization and red blood cells were lysed by ammonium-chloride potassium lysis buffer (ACK Lysing Buffer, Thermo Scientific, Rockford, IL, USA). For in vitro stimulation, 1×10^6 cells were incubated with either purified antigens (tri-stalk and 3M2e) at 1 µg/well or sucrose-gradient purified Cal/09 virus at an MOI of 1.0 EID₅₀/cell for one h in 100 µL of CR-0, in 96-well microtitration U-bottom well plates (Sarstedt, Nümbrecht, Germany). Then, 50 µL of CR-30 (CR-0 with 30% FBS) was added, to the final FBS concentration of 10%. After 16–18 h, 50 µL of GolgiPlug solution (Becton Dickinson, Franklin Lakes, NJ, USA)—alone or with PMA (Phorbol myristate acetate as positive control)—were added at 1:250 dilution and the mixture was incubated for another five h. Samples were stained with ZombieAqua fixable viability dye, anti-CD4, anti-CD8, anti-CD44, anti-CD62L antibody-conjugates for 20 min in a cool dark place (Table 2).

Table 2. A mixture of antibody-conjugates (Biolegend, San Diego, CA, USA) used for T-cell staining.

Mixture Component	Antibody	Dye	Cat.no	µL per Sample
1	Anti-CD4	PC5.5	100540	0.25
2	Anti-CD8	APC-Cy7	100714	0.25
3	Anti-CD44	PE	103008	0.25
4	Anti-CD62L	BV-421	104435	0.25
5	ZombieAqua	BV-510	123102	0.3
6	Staining buffer	-	-	98.7

PC5.5: PerCP/Cyanine.5; APC: allophycocyanin; PE: phycoerythrin; BV: brilliant violet.

Samples were then washed twice with 200 µL of staining buffer (0.8 g BSA, 4 mL 5% NaN₃, PBS up to 400 mL). ICS was performed with Cytotfix/Cytoperm kit (Becton Dickinson, Franklin Lakes, NJ, USA) according to the manufacturer's instructions followed by staining samples with anti-IFN γ , and anti-TNF α antibody-conjugates for 20 min in a cool dark place (Table 3).

Table 3. A mixture of anti-IFN γ , and anti-TNF α antibody-conjugates (Biolegend, San Diego, CA, USA).

Mixture Component	Antibody	Dye	Cat.no	µL per Sample
1	Anti-IFN- γ	FITC	505806	0.4
2	Anti-TNF- α	APC	506314	0.4
3	Isotype TNF- α	APC	400418	or 0.4
4	Wash buffer	-	-	49.2

IFN γ : interferon gamma; TNF α : tumor necrosis factor alpha; APC: allophycocyanin; FITC: fluorescein isothiocyanate.

Then, samples were washed twice with 200 µL of wash buffer (Cytotfix/Cytoperm kit). Samples were fixed in 1% paraformaldehyde and stored in a cool dark place prior to flow cytometric analysis. At least 100,000 events were measured using a Navios flow cytometer (Beckman Coulter, Brea, CA, USA). Data were analyzed using FlowJo software (TriStar Inc., El Segundo, CA, USA). Gating strategy is shown in Supplementary (Figure S2). The percentage of virus/antigen-specific T-cells was calculated by subtracting the negative control from the cytokine-positive T-cells.

2.9. The Cytotoxic T-Lymphocyte (CTL) In Vivo Assay

An in vivo cytotoxicity assay was performed as described by Durward et al. [38] with modifications. Briefly, target cells were prepared from splenocytes of naïve BALB/c mice (1×10^8 splenocytes in 10 mL complete DMEM supplemented with 10% FBS) and loaded with either 200 µg of protein (tri-stalk or 3M2e) or an equal volume of PBS for one h at +37 °C, with occasional mixing. Next, cells were washed with PBS and stained with different concentrations of carboxyfluorescein succinimidyl ester (CFSE) in PBS (60, 15 or 3.75 mM CFSE for 3M2e, tri-stalk and PBS control, respectively). Cells were then washed, resuspended in Hanks solution, and mixed in equal amounts to the final concentration of 1×10^8 cells/mL. Ten million prefiltered target cells were administered in 100 µL to anaesthetized BALB/c mice by retro-orbital injection. After 16–18 h, mice were sacrificed; splenocytes were harvested and assessed by flow cytometry. Gating strategy is shown in Supplementary (Figure S3). The ratio of peptide-loaded to control target cells was calculated as a normalized measure of protein-specific cytotoxicity between immunization groups. The ratio in placebo group samples (PBS) was assumed as survival at basal protein-specific cytotoxicity.

2.10. Statistical Analyses

Data were analyzed with the GraphPad Prism 6.0 software (GraphPad Software Inc., La Jolla, CA, USA). Statistical significance of immunogenicity outcomes (the log₁₀-transformed antibody titers,

ADCC levels, virus/peptide-specific T-cell levels, or the *in vivo* killing activity of CTLs) and protection outcomes (AUC of weight loss values) were determined by one-way ANOVA followed by a Tukey's multiple comparison test (for comparing ELISA endpoint titer values). Differences in the survival rates after challenge were analyzed by a log-rank Mantel–Cox test.

3. Results

3.1. Antigen Design

In this study, to generate and test different broadly protective influenza vaccine candidates, HA tri-stalk and a triple M2e protein (3M2e) were integrated into an AP205 VLP platform, alone or in combination, creating five different broadly protective influenza vaccine prototypes (Figure 2).

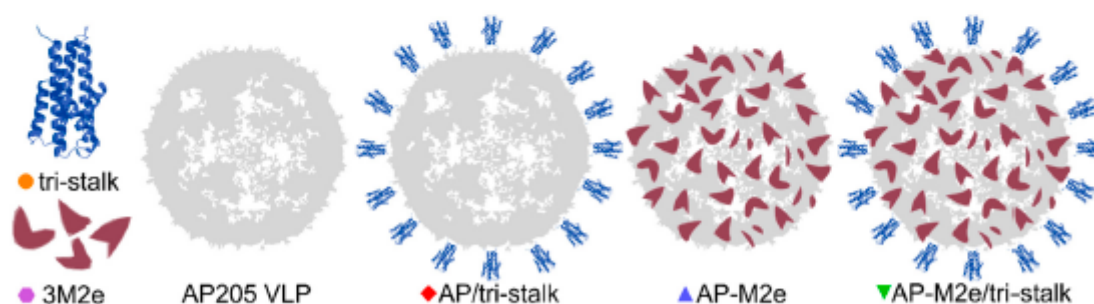


Figure 2. Schematics of the recombinant protein design. We produced three soluble antigens: an N-terminally extended long alpha-helix of H1 hemagglutinin (tri-stalk), a triple M2e peptide (3M2e), and a wild-type bacteriophage AP205 coat protein that self-assembles into virus-like particles (VLPs). The genes of 3M2e and AP205 coat protein (CP) were genetically fused and expressed as a single protein, yielding in stable chimeric particles (AP-M2e), and the tri-stalk protein was coupled to the surface of AP205 VLPs (AP/tri-stalk) or AP-M2e VLPs (AP-M2e/tri-stalk).

Since aa 10–24 of M2e peptide vary between influenza virus subtypes, combining the M2e from different subtypes can increase the vaccine-induced cross-protection [25]. Therefore, a 3M2e protein, corresponding to three variants of the conserved M2e peptide, was expressed in *E. coli* and purified until near homogeneity (Figure 3A, Table S1). The 3M2e sequence was derived from the M2e of the highly pathogenic H5N1 virus, as well as H1N1 and H11N9 subtypes to cover a wider range of influenza viruses. Noteworthy, two of the M2e fragments comprising the 3M2e protein share high sequence similarity with the M2e from H3N2 viruses. In parallel, sequence of the 3M2e was genetically fused to the C-terminus of AP205 CP yielding in expression of stable chimeric AP-M2e particles. Phage AP205 VLPs and AP-M2e VLPs were expressed in *E. coli* and purified as described in Materials and Methods section (Figure 3B).

An N-terminally extended LAH of H1 HA stalk (referred to as tri-stalk protein) was expressed and purified using a three-step chromatography method as described in our previous study (Figure 3B) [35]. Produced in *E. coli*, it forms an α -helical trimer highly similar to the corresponding region of native HA in its post-fusion form. It has been shown previously that the monomeric LAH is highly immunogenic in mice when incorporated into hepatitis B virus core particles [29,33]. Moreover, post-fusion LAH-specific antibodies have been shown to elicit a durable cross-protective immunity independent of virus neutralization activity [34]. HA tri-stalk protein was chemically coupled to the surface of purified AP205 or AP-M2e VLPs (Figure 3C,D). This was done by chemical crosslinking via the SMPH linker between the VLPs and SATA-modified tri-stalk protein. Due to the crosslinking of subunits, derivatization of VLPs shows the typical VLP ladder with monomeric and multimeric subunits. Although some aggregation was observed, the chimeric particles were stable upon freezing at $-20\text{ }^{\circ}\text{C}$ and subsequent thawing as confirmed by SDS/PAGE and electron microscopy (Figure 3E).

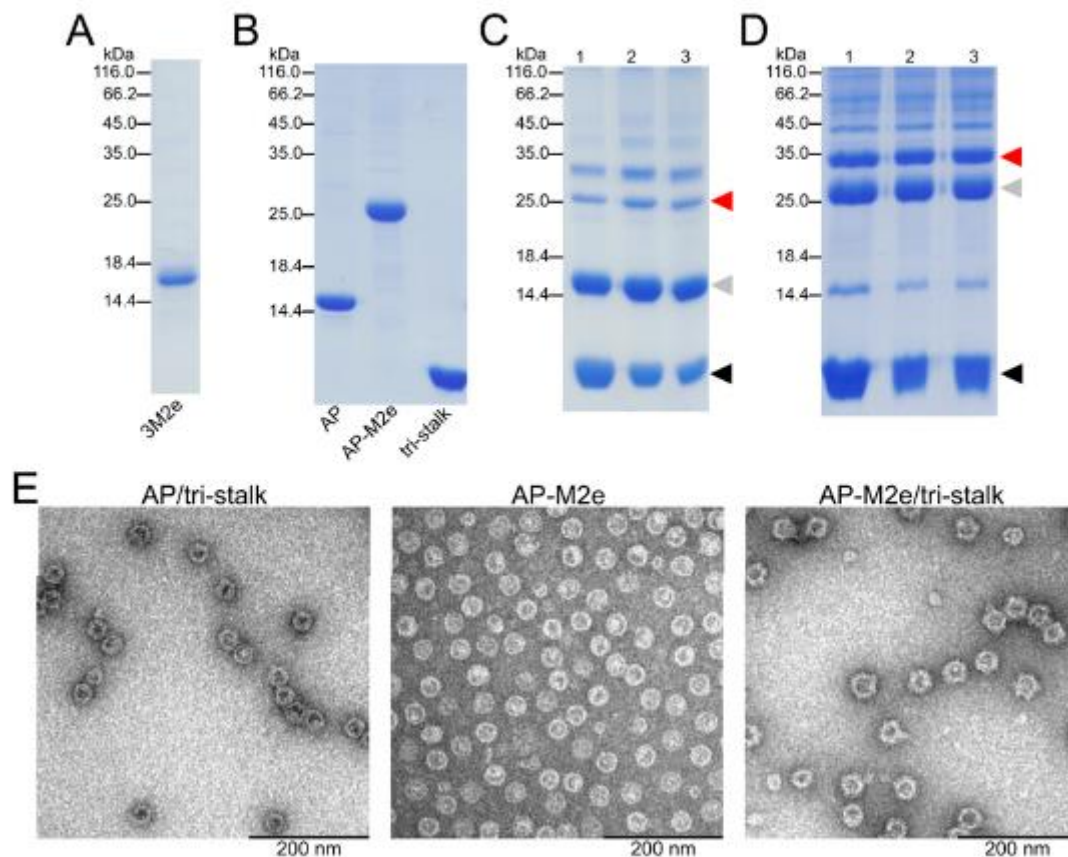


Figure 3. Characterization of recombinant protein constructs produced in *E. coli*. The purity of recombinant proteins—(A) 3M2e, (B) AP205, AP-M2e, and tri-stalk—was analyzed in SDS/PAGE under reducing conditions. Hemagglutinin (HA) tri-stalk protein was then coupled to the surface of (C) AP205 VLPs and (D) AP-M2e VLPs and subsequently analysed in SDS/PAGE under reducing conditions: lane 1—immediately after coupling; lane 2—after Amicon Ultra 4 filtration; lane 3—after freeze-thawing. Red arrow refers to the coupling zone, grey arrow—coat protein monomer, black arrow—tri-stalk protein. Coupling bands indicate a successful reaction. (E) Electron microscopy images of chimeric particles after freeze-thawing.

3.2. Immunization with Chimeric VLPs Generates Broadly Cross-Reactive Antibodies to Heterosubtypic Influenza A Hemagglutinins

Female BALB/c mice were intraperitoneally immunized with one of the four protein antigens (tri-stalk, AP/tri-stalk, AP-M2e, AP-M2e/tri-stalk) combined with Alum adjuvant in a prime-boost schedule with two-week intervals between the three immunizations; the control group received PBS with Alum adjuvant. Two weeks after the last immunization mice ($n = 6$) were bled and sera were analyzed for their reactivity to different influenza antigens by ELISA.

All vaccine prototypes induced high levels of homologous serum IgG antibody against the tri-stalk and 3M2e antigens (Figure 4A,B). Significant differences in the amount of tri-stalk binding antibody were observed, with chimeric VLPs exposing tri-stalk inducing higher antibody levels than the tri-stalk protein alone. Both VLP vaccines induced comparable levels of tri-stalk targeted antibody since both constructs carry identical viral antigen on the same delivery vehicle. However, coupling of the tri-stalk antigen to the AP-M2e VLPs slightly reduced the reactivity of antisera with anti-M2e antibodies. Furthermore, we examined the IgG1/IgG2a subclass profile of the induced serum antibody. The tri-stalk antigen predominantly elicited homologous antibody of the IgG1 subclass, suggesting the induction of Th2-biased immune responses (Figure 4C). Yet, coupling of the tri-stalk to either

AP205 VLPs or AP-M2e VLPs significantly increased the proportion of the tri-stalk-reactive IgG2a antibody. Since the IgG1 levels between these three vaccine groups were comparable, the differences in the total IgG antibody were driven mainly by the IgG2a subclass. Similarly, although the majority of M2e-binding antibodies were of IgG1 subclass, some levels of M2e-reactive IgG2a antibody were also detected (Figure 4D). For the 3M2e antigen, the differences in the immunogenicity between the two M2e-containing vaccines were driven by the IgG1 subclass antibody, further suggesting that the induction of IgG2a antibody is dependent on the VLP vehicle, rather than the antigen itself.

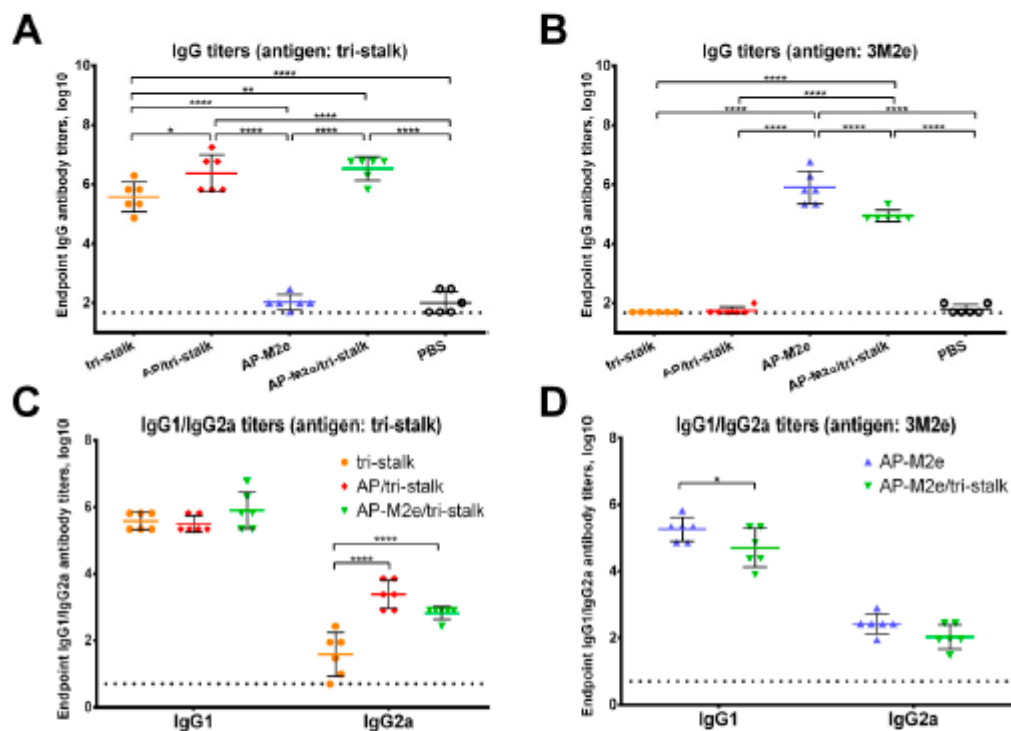


Figure 4. Immunogenicity of the recombinant vaccine candidates included in the study. Serum IgG antibodies from BALB/c mice ($n = 6$) immunized with vaccine candidates were tested by ELISA for their binding activity against the proteins included in the vaccine candidates: (A) IgG antibody binding to the tri-stalk protein; (B) IgG antibody binding to the 3M2e protein; (C) IgG1/IgG2a subclasses binding to the tri-stalk protein; (D) IgG1/IgG2a subclasses binding to the 3M2e protein. The dotted line indicates the limit of antibody detection; error bars represent mean \pm SD. Statistical analysis was performed using one-way ANOVA (A–B) or two-way ANOVA (C–D) followed by a Tukey’s multiple comparison test (* $p < 0.05$; ** $p < 0.01$; *** $p < 0.001$; **** $p < 0.0001$).

Furthermore, we assessed the reactivity of the serum IgG antibody with a panel of full-length recombinant group 1 and 2 HA proteins (Figures 5 and 6). As the AP-M2e vaccination group had no HA-targeted antibody, sera from this group were not included in the cross-reactivity analysis. Chimeric cH6/1 HA contained an irrelevant head domain from avian H6N1 virus and a stalk originated from Cal/09 virus, perfectly matching the sequence of the tri-stalk protein. High levels of homologous cH6/1-binding antibody were observed in the AP/tri-stalk and AP-M2e/tri-stalk vaccination groups, with lower levels identified in the group vaccinated with tri-stalk protein alone (Figure 5A). Similarly, both chimeric VLPs elicited broad antibody responses against other heterosubtypic group 1 HA proteins (pre-2009 H1, H2, H5, H6, H8, H9, and H11) whereas antisera from the tri-stalk vaccine group had weak cross-reactivity (Figure 5B–H), showing that proper presentation of the viral antigen on the VLP platform can significantly improve the cross-reactive potential of the induced antibody. In addition, AP/tri-stalk induced antisera cross-reacted substantially with group 2 H3, H4, and H10 HAs, but not against the H7 HA protein (Figure 6). Some group 2 cross-reactivity was observed in

the AP-M2e/tri-stalk vaccination group as well, however, it was lower than in the AP/tri-stalk group, suggesting that the addition of the 3M2e antigen to the AP/tri-stalk vaccine could reduce cross-reactivity of HA-binding antibody.

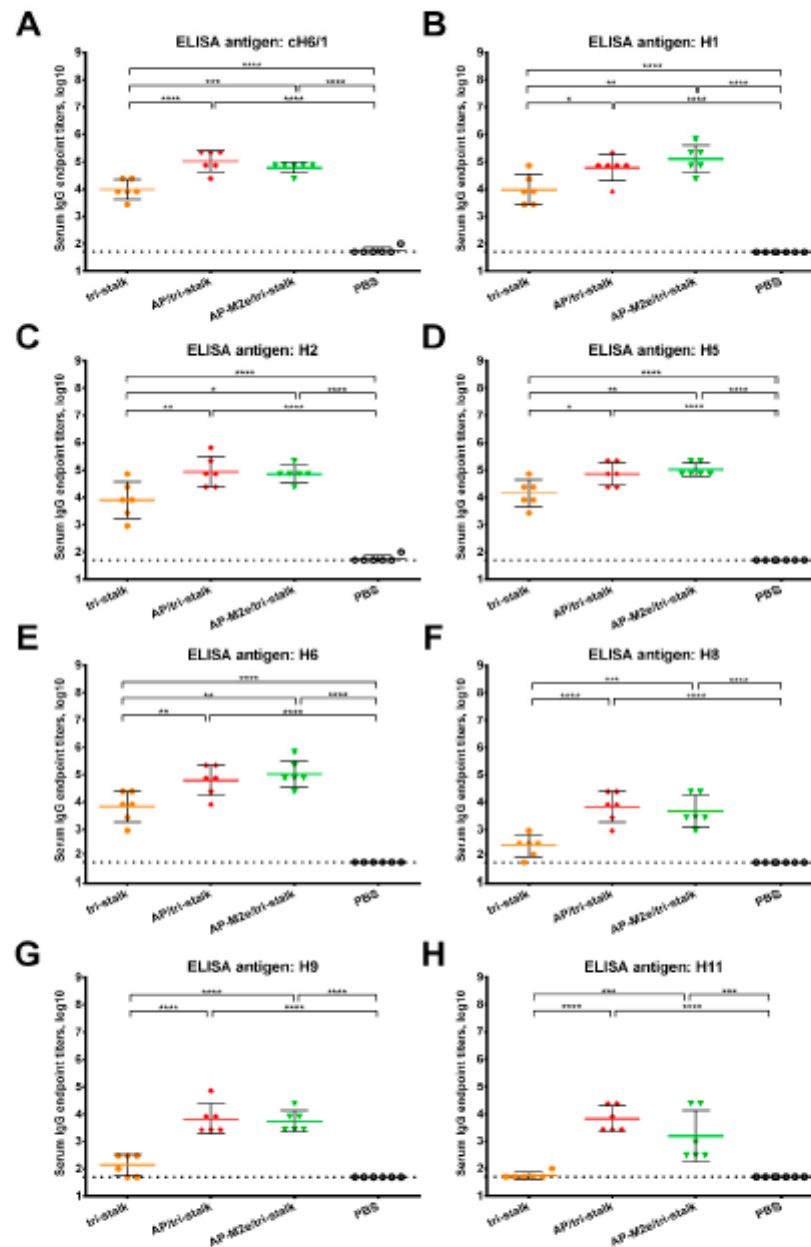


Figure 5. Cross-reactivity of the recombinant vaccine candidates against group 1 hemagglutinins. Breadth of the antibody response elicited by the immunization of BALB/c mice ($n = 6$) with the vaccine prototypes was determined by ELISA against a panel of full-length recombinant HA proteins: (A) cH6/1—head domain from H6N1 A/mallard/Sweden/81/2002 virus and stalk domain from H1N1 A/California/04/2009 virus; (B) H1N1 A/Solomon islands/03/2006; (C) H2N2 A/Japan/305/1957; (D) H5N1 A/Indonesia/5/2005; (E) H6N4 A/mallard/Sweden/81/2002; (F) H8N4 A/mallard/Sweden/24/2002; (G) H9N2 A/guinea fowl/Hong Kong/WF10/1999; (H) H11N9 A/shoveler/Netherlands/18/1999. The dotted line indicates the limit of antibody detection; error bars represent mean \pm SD. Statistical analysis was performed using one-way ANOVA followed by a Tukey's multiple comparison test (* $p < 0.05$; ** $p < 0.01$; *** $p < 0.001$; **** $p < 0.0001$).

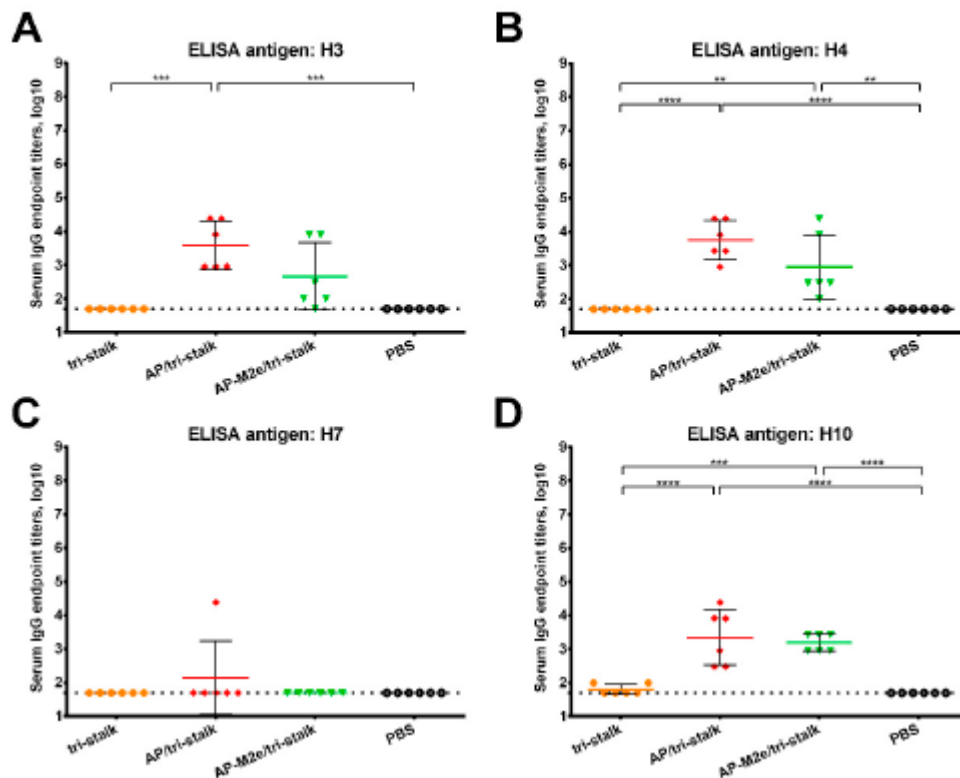


Figure 6. Cross-reactivity of the recombinant vaccine candidates against group 2 hemagglutinins. Breadth of the antibody response elicited by the immunization of BALB/c mice ($n = 6$) with the vaccine prototypes was determined by ELISA against a panel of full-length recombinant HA proteins: (A) H3N2 A/Wyoming/3/2003; (B) H4N6 A/red knot/Delaware/541/1988; (C) H7N9 A/Shanghai/1/2013; (D) H10N8 A/Jiangxi-Donghu/346/2013. The dotted line indicates the limit of antibody detection; error bars represent mean \pm SD. Statistical analysis was performed using one-way ANOVA followed by a Tukey's multiple comparison test (** $p < 0.01$; *** $p < 0.001$; **** $p < 0.0001$).

3.3. Chimeric 3M2e Exposing VLPs Afford Full Protection Against Heterologous and Heterosubtypic Influenza Challenge

To test the cross-protective efficacy of the recombinant protein vaccine candidates, groups of 6 BALB/c mice, immunized with the indicated immunogens, were challenged with lethal doses of heterologous and heterosubtypic influenza viruses (Figure 7). The antibody responses induced by AP-M2e and AP-M2e/tri-stalk immunizations fully protected mice against a lethal unmatched PR8 virus challenge (Figure 7A). Mice from these two groups displayed minimal signs of disease, measured as weight loss, and completely recovered from the infection. Tri-stalk protein and AP/tri-stalk VLPs provided partial 66.7% protection against PR8 virus challenge, although these vaccination groups experienced significant weight loss. Furthermore, while HA stalk-based vaccine prototypes often elicit incomplete cross-group protection, limited to the sequence similarity between the immunization antigen and challenge virus [21–24], all AP-M2e and AP-M2e/tri-stalk vaccinated animals were completely protected from the group 2 H3N2 virus challenge. The weight loss during the challenge phase did not exceed 10% (Figure 7B). In contrast to the PR8 challenge, immunization with the tri-stalk protein and AP/tri-stalk vaccine candidates did not protect mice against death and weight loss caused by the heterosubtypic H3N2 virus, suggesting that the M2e-targeted antibody were the main contributors to the cross-protection.

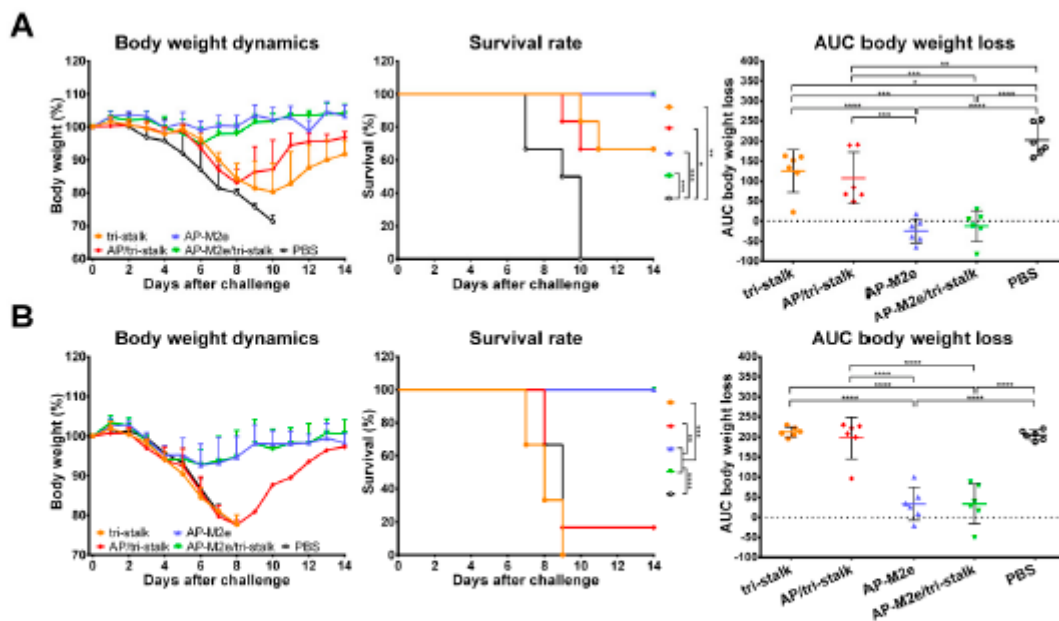


Figure 7. Protective immunity induced in mice immunized with recombinant vaccine candidates. BALB/c mice were vaccinated with Alum-adjuvanted recombinant proteins or placebo group samples (PBS) at days 0, 14, and 28. 17 days after the final vaccination mice were challenged with $3 \times LD_{50}$ of (A) H1N1 A/Puerto Rico/8/1934 virus ($n = 6$) or with (B) H3N2 A/Philippines/2/1982 (X-79) virus ($n = 6$) and monitored for body weight loss (left) and survival (middle) for 14 days. Right panel shows analysis of body weight loss by measuring the area under the curve (AUC, relative to 100% value) for each mouse. For mice that died or were humanely euthanized a 75% value was assigned to all subsequent days for the purpose of statistical analysis. Error bars represent mean \pm SD. The survival rates were analyzed by Mantel–Cox test, and the AUC values were compared using one-way ANOVA followed by a Tukey’s multiple comparison test (* $p < 0.05$; ** $p < 0.01$; *** $p < 0.001$; **** $p < 0.0001$).

3.4. Antibodies Elicited by Chimeric VLPs Protect Mice Against rgH5N1 Viral Challenge in a Passive Serum Transfer Challenge Experiment

We also performed an *in vivo* passive transfer experiment. Immune sera, collected as described above, was mixed with $3 \times LD_{50}$ of rgH5N1 challenge virus and intranasally administered to groups of 6 naïve BALB/c mice. Sera from AP-M2e and AP-M2e/tri-stalk immunized mice possessed a strong cross-protective activity against heterosubtypic lethal rgH5N1 virus showing a 100% survival rate and no significant weight loss (Figure 8). AP/tri-stalk immune sera conferred partial protection against the rgH5N1 virus challenge, and mice from this group exhibited significantly decreased weight loss as compared to the negative control group. In contrast, sera from the tri-stalk immunized mice were not cross-protective, suggesting that the VLP delivery of the tri-stalk protein can significantly improve the breadth of antibody reactivity. Similar to the direct protection experiment, these data demonstrate that the M2e-based vaccines provide full protection against the rgH5N1 challenge, whereas the tri-stalk antigen can only partially protect mice against this virus.

3.5. Chimeric AP-M2e/Tri-Stalk VLPs Confer Robust Protection Against a High Dose of Homologous H1N1 A/California/7/2009 Influenza Challenge

We conducted an additional challenge experiment with a high dose of homologous Ca/09 virus. For the direct protection study, groups of 9 BALB/c mice were vaccinated as described above, with an additional vaccination group immunized with an Alum-adjuvanted 3M2e protein. All vaccine constructs were very immunogenic, as showed by ELISA, with serum IgG antibody raised to the

corresponding antigen present in each vaccine candidate, affirming the data obtained in at the previous experiments and confirming that the immunizations were successful (Figure S4).

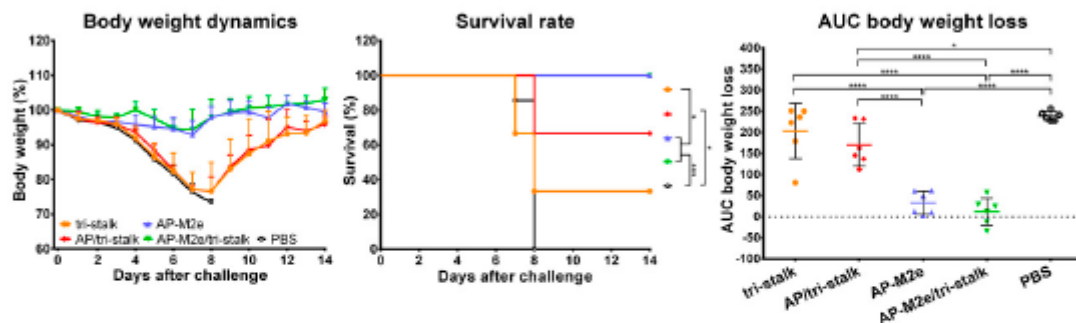


Figure 8. Indirect protection of immune sera. Naïve BALB/c mice ($n = 6$) were inoculated with a mixture of immune sera and $3 \times LD_{50}$ rgH5N1 A/Viet Nam/1203/2004 virus and monitored for average weight changes (left) and survival (middle) for 14 days post-challenge. Right panel shows analysis of body weight loss by measuring the area under the curve (AUC, relative to 100% value) for each mouse. For mice that died or were humanely euthanized a 75% value was assigned to all subsequent days for the purpose of statistical analysis. Error bars represent mean \pm SD. The survival rates were analyzed by Mantel–Cox test, and the AUC values were compared using one-way ANOVA followed by a Tukey’s multiple comparison test (* $p < 0.05$; *** $p < 0.001$; **** $p < 0.0001$).

Vaccinated mice were challenged with $30 \times LD_{50}$ of the Cal/09 virus. Antibody responses induced by all five vaccine candidates delayed the infection and significantly improved the survival rates of mice after infection (Figure 9A). However, the tri-stalk protein, AP/tri-stalk, AP-M2e, and 3M2e vaccine prototypes did not protect animals from a significant weight loss, and only 11.1–55.6% of mice survived the infection. In contrast, an impressive 100% survival was achieved in the AP-M2e/tri-stalk group, with no significant weight loss observed. Noteworthy, the AP-M2e/tri-stalk vaccine afforded significantly better protection against this challenge than the AP-M2e vaccine.

For the indirect protection study, immune sera from the vaccinated mice were combined with $3 \times LD_{50}$ of the Cal/09 virus and groups of 5 BALB/c mice were inoculated as described above. Only the sera from AP/tri-stalk and AP-M2e/tri-stalk immunized mice possessed a strong protective activity against the homologous Cal/09 virus (Figure 9B). In addition, the AP-M2e/tri-stalk immune sera significantly enhanced survival rates as compared to the tri-stalk and AP/tri-stalk groups, and it was the only vaccine candidate to protect animals against significant weight loss. These data suggest that the tri-stalk targeted antibodies are critical for the protection against a homologous influenza virus infection, and the antibodies targeted to M2e play a supporting role.

3.6. Protection Induced by Recombinant Vaccine Prototypes is Mediated by Fc-Receptor Dependent Effector Mechanisms

Levels of ADCC were measured by determining degranulation activity of mouse NK-cells under the influence of the immune sera. NK-cells recognize viral antigens on the surfaces of virus-infected cells and directly induce their clearance [39]. MDCK cells expressing Cal/09 viral proteins were used as target cells capturing virus-specific antibodies from immune sera. The NK-cell degranulation induced by the Fc-domains of the captured antibody was assessed by flow cytometric analysis. All five vaccine prototypes induced significant degranulation by NK-cells (Figure 10), however, more distinct ADCC activity was seen for the AP/tri-stalk and AP-M2e/tri-stalk immune sera. Although the difference between the AP-M2e and AP-M2e/tri-stalk groups was not significant by the ANOVA test, a direct comparison of these groups using a non-parametric Mann–Whitney U test revealed a strong significance ($p = 0.0087$), suggesting that the tri-stalk targeted antibodies possess stronger ADCC activity than the M2e-targeted antibody.

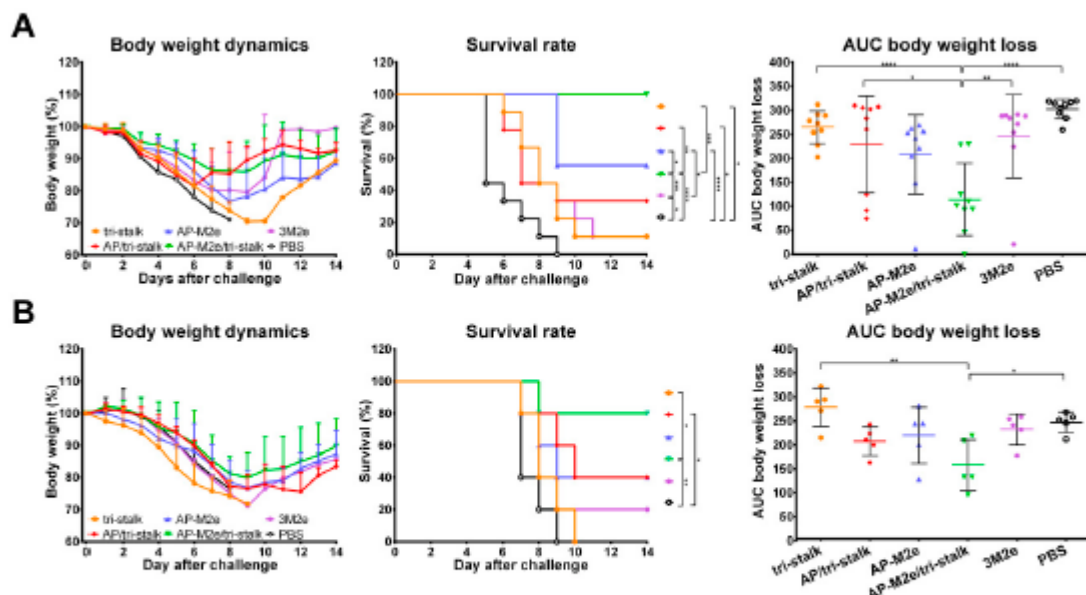


Figure 9. Immune protection conferred against lethal H1N1 A/California/7/2009 influenza virus challenge. (A) BALB/c mice were vaccinated with Alum-adjuvanted recombinant proteins or PBS at days 0, 14, and 28. 17 days after the final vaccination mice ($n = 9$) were challenged with $30 \times LD_{50}$ of Cal/09 virus and monitored for 14 days post-challenge. (B) Naïve BALB/c mice ($n = 5$) were inoculated with a mixture of immune sera and $3 \times LD_{50}$ Cal/09 virus and monitored for 14 days post-challenge. Left panel shows dynamics of body weight change; middle panel shows survival rates; right panel shows analysis of average body weight loss by measuring the area under the curve (AUC, relative to 100% value) for each mouse. For mice that died or were humanely euthanized a 75% value was assigned to all subsequent days for the purpose of statistical analysis. Error bars represent mean \pm SD. The survival rates were analyzed by Mantel–Cox test, and the AUC values were compared using one-way ANOVA followed by a Tukey’s multiple comparison test (* $p < 0.05$; ** $p < 0.01$; *** $p < 0.001$; **** $p < 0.0001$).

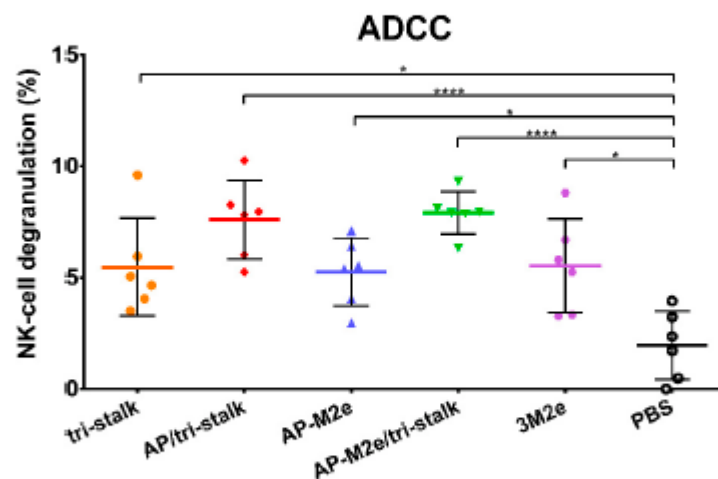


Figure 10. Antibody-dependent cellular cytotoxicity (ADCC) of the immune sera. Serum samples of BALB/c mice ($n = 6$) immunized with the recombinant vaccine candidates were assessed in duplicates for their ability to induce NK-cell degranulation measured by flow cytometry. Error bars represent mean \pm SD. The NK-cell degranulation values were compared using one-way ANOVA followed by a Tukey’s multiple comparison test (* $p < 0.05$; **** $p < 0.0001$).

3.7. M2e Containing Vaccines Induce T-Cell Mediated Immune Responses

The levels of virus/protein-specific CD4⁺/CD8⁺ T-cells were assessed by ICS assay. A week after the last immunization, spleens were isolated from immunized BALB/c mice (*n* = 5). Splenocytes were stimulated with one of the antigens (whole Cal/09 virus, tri-stalk, 3M2e) in vitro. Neither vaccine candidate could induce significant levels of CD8⁺ T-cell responses to any of the antigens (Figure 11, right panel). There were no significant increases in the population of Cal/09 and tri-stalk specific CD4⁺ T-cell levels after immunizations (Figure 11, left panel). However, vaccination with 3M2e and AP-M2e significantly increased the population of M2e-specific TNF α -secreting CD4⁺ T-cells (Figure 11C). Interestingly, chemical attachment of the tri-stalk protein to AP-M2e VLPs led to the decrease of the M2e-specific TNF α -secreting CD4⁺ T-cells (Figure 11C). Analysis of effector memory CD4⁺ T-cell subsets (CD44⁺CD62L⁻) led to similar findings: only M2e-containing vaccines could induce significant levels of the M2e-specific CD4 T-cells (Figure 11E).

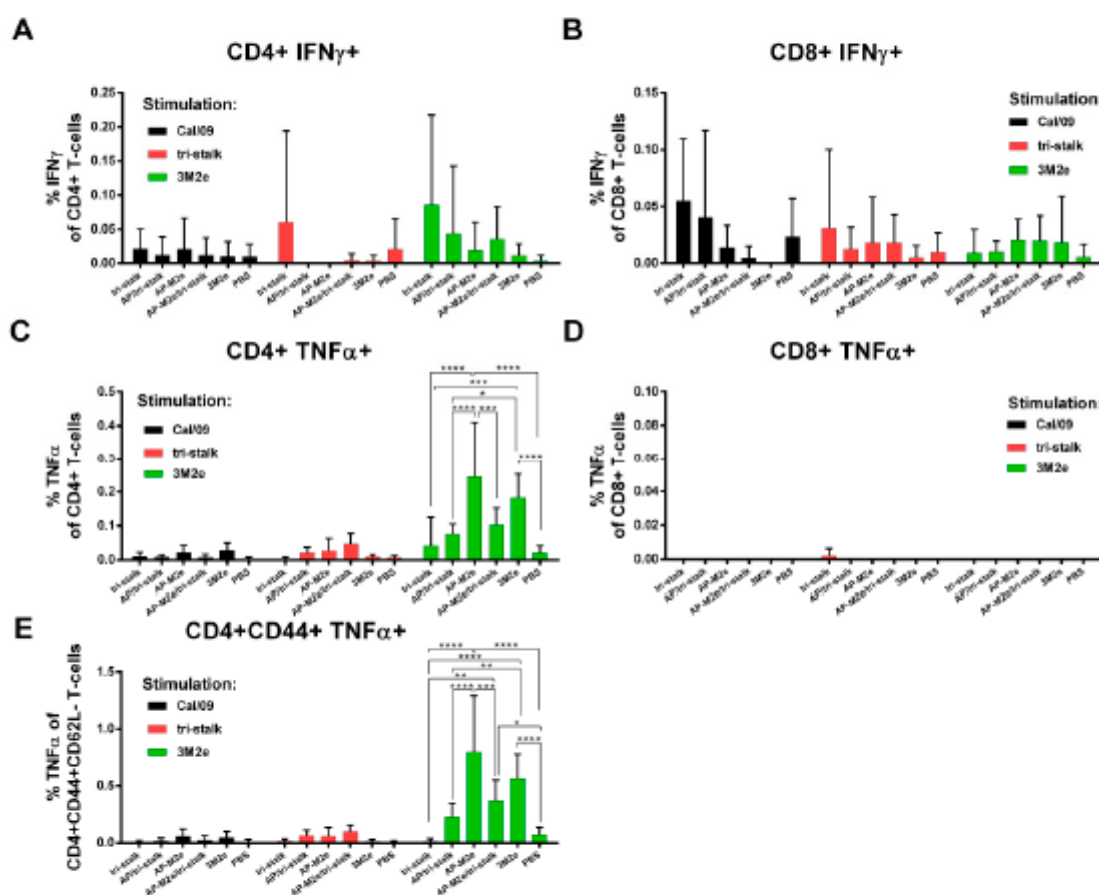


Figure 11. T-cell responses of immunized mice. BALB/c mice (*n* = 5) were immunized with recombinant vaccine candidates to measure the levels of virus/protein-specific T-cell responses by intracellular cytokine staining assay: (A) IFN γ -secreting CD4⁺ T-cell responses; (B) TNF α -secreting CD8⁺ T-cell responses; (C) TNF α -secreting CD4⁺ T-cell responses; (D) IFN γ -secreting CD8⁺ T-cell responses; (E) TNF α -secreting effector memory CD4⁺ T-cell subsets (CD44⁺CD62L⁻). Error bars represent mean \pm SD. The T-cell levels were compared using two-way ANOVA followed by a Tukey’s multiple comparison test (* $p < 0.05$; ** $p < 0.01$; *** $p < 0.001$; **** $p < 0.0001$).

The functional activity of cytotoxic T-cells was measured by a CTL in vivo assay. Splenocytes from naïve BALB/c mice were loaded with antigens (tri-stalk, 3M2e) or PBS, differentially labelled with various concentrations of CFSE. This mixture was then administered to BALB/c mice (*n* = 5), immunized

as described previously. On the following day, spleens were collected to count the proportion of tri-stalk or M2e loaded cells to the control cells loaded with PBS. Surprisingly, despite the absence of M2e-specific CD8⁺ T-cells, the immune system of mice vaccinated with M2e-containing vaccine candidates could efficiently recognize and kill the M2e-loaded target cells (Figure 12B). Intriguingly, the 3M2e protein alone induced the highest level of functional cytotoxic T-cells, and the killing activity was significantly higher than in the AP-M2e and AP-M2e/tri-stalk groups. No significant cytotoxic activity against tri-stalk loaded target cells was detected in any group of immunized mice (Figure 12A).

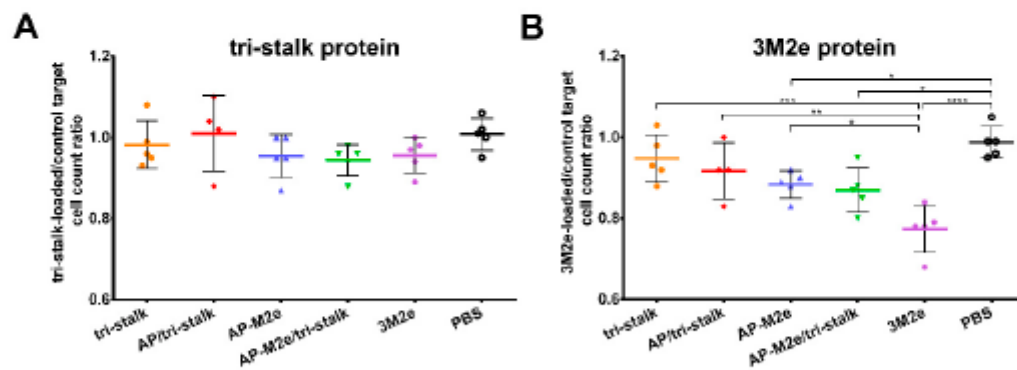


Figure 12. In vivo cytotoxicity of the T-cells in immunized mice. Cytotoxic activity of the induced T-cell immune responses was measured in BALB/c mice ($n = 5$) after immunization with recombinant vaccine candidates: (A) tri-stalk loaded target cells; (B) 3M2e loaded target cells. Error bars represent mean \pm SD. The proportions of protein-loaded to the PBS-loaded target cells between the vaccine groups were compared using one-way ANOVA followed by a Tukey's multiple comparison test (* $p < 0.05$; ** $p < 0.01$; *** $p < 0.001$; **** $p < 0.0001$).

4. Discussion

Evolutionarily conserved influenza antigens could potentially provide broad-spectrum protection against highly variable influenza virus subtypes, while significantly reducing the time and costs of vaccine production. Furthermore, recombinant vaccines help to avoid potentially harmful influenza viruses grown in embryonated eggs or cell cultures and therefore attract significant research interest. Here we evaluated the antigenicity and protective potential of recombinant influenza vaccine prototypes, generated by combining the methods of genetic fusion and covalent coupling to present the otherwise poor immunogens HA tri-stalk and 3M2e on the surface of AP205 VLPs.

The sequence and structure of the HA stalk are relatively conserved [20,40], highlighting HA stalk as a prospective component for a broadly protective influenza vaccine. However, with a few exceptions [41–43], a great part of the stalk-specific antibodies have a group-specific binding profile, dependent on the structural divergence between group 1 and group 2 HAs [44–47]. Comparison of aa sequences of N-terminally extended LAH fragment of HA proteins used in this study revealed that the observed differences in cross-reactivity of the tri-stalk induced antibody also correlate with the conservation difference between the immunization antigen and HA proteins (Figures 5 and 6, Table S2). The HA stalk-targeted antibodies were cross-reactive and could efficiently recognize HA proteins from heterologous group 1 influenza viruses; notably, cross-reactivity with group 2 antigens was also observed in the AP/tri-stalk vaccination group, and to some extent—in the AP-M2e/tri-stalk vaccination group. In general, higher sequence identity was associated with increased cross-reactivity, with H7 LAH protein being the most distant from the tri stalk fragment, thus demonstrating the lowest cross-reactivity of the induced antibody. The delivery of the tri-stalk antigen using the AP205 VLP platform significantly improved the cross-reactivity of the HA-based antibody. Accordingly, the assessment of IgG antibody subclasses revealed that our vaccine candidates predominantly elicited the IgG1 antibodies, while the delivery of the virus antigens by the AP205 VLPs promoted switching

to the IgG2a subclass. Mouse IgG subclasses play different roles in the antiviral immunity and their biological activities are dependent on the binding affinities to the activating and inhibitory Fc gamma receptors (FcγRs), with IgG1 subclass considered less protective than the IgG2 subclass [48–50]. The vehicle-based shifting to IgG2a subclass might be linked to the VLP-packed RNA as removal of bacteriophage VLP RNA has been shown to result in a shift of the induced IgG isotypes from IgG2a/c to IgG1 [51]. However, even prevailing induction of IgG1 subclass of post-fusion LAH-specific antibodies can provide significant protection against lethal heterologous virus infection [34].

Consequently, the tri-stalk antigen was capable to confer partial protection against lethal heterologous PR8 virus infection, with which the tri-stalk shares a high sequence similarity (Table S3). Consistent with previous reports [21–24], the protective immunity induced by the tri-stalk protein and AP/tri-stalk vaccines was substantially diminished when challenged with a group 2 virus. Even though the tri-stalk binding antibody had some level of cross-reactivity with the H3 HA protein, they were unable to protect mice against the H3N2 virus challenge, further indicating that the stalk-reactive antibodies afford little cross-protection between group 1 and 2 influenza viruses. Importantly, H3N2 viruses show the highest degree of antigenic drift when compared to other seasonal influenza viruses, posing the greatest risk of unmatched seasonal vaccine formulations and therefore the lowest seasonal vaccine effectiveness [7,8].

Although many researchers highlight the necessity to create a multi-component vaccine including epitopes from both group 1 and group 2 viruses to achieve a complete cross-protection against type A influenza [22–24], here we bypass the issue of insufficient cross-protective efficacy by incorporating both an H1 derived tri-stalk and a conserved 3M2e protein in a single recombinant immunogen. Even though our M2e-based vaccine candidates predominantly induced antibodies of IgG1 subclass, M2e-specific IgG1 antibodies have been shown to result in significant protection against divergent influenza viruses, probably because the high level of IgG1 antibodies could compensate their low affinity to activated FcγRs [52]. Likewise, in this study, the addition of the 3M2e antigen to the AP/tri-stalk antigen increased the cross-protective efficiency of the chimeric VLPs to an impressive 100% when challenged with heterosubtypic group 1 and group 2 viruses. Unlike observed in previous studies [26,27], challenged AP-M2e/tri-stalk vaccinated mice did not experience significant disease symptoms. However, it should be noted that the H3N2 virus carries internal genes from the PR8 virus (including the M2e peptide) (Table S3), therefore the M2e-targeted antibody had a comparable protective effect in both challenge groups. Similar protection results have recently been achieved by a 5xM2e VLP antigen, produced in the baculovirus expression system [28]; yet, our approach allows for a cheaper and more efficient high-yield antigen production, an important hallmark for a broadly protective influenza vaccine, accessible to the general public. Even though in this study we used the *E. coli* expression system, characterized by the presence of bacterial endotoxins, our extensive experience with yeast expression systems could easily help to overcome this problem in the future [33,53,54].

An *in vivo* passive transfer-challenge experiment demonstrated that the induced cross-protection is mainly antibody-mediated but acts by different modes. The tri-stalk targeted antibodies elicited by the AP/tri-stalk immunization were able to partially protect mice against lethal heterosubtypic rgH5N1 virus challenge, whereas sera from the tri-stalk immunized mice failed to protect animals. The M2e-specific antibodies were even more effective, resulting in full protection against the clinical manifestations of the infection. In this study, only the levels of IgG antibody binding were studied as a measure of immunogenicity and cross-reactivity of the vaccine, without testing their neutralizing capacity, as we did not expect high levels of virus-neutralizing antibody. Although some anti-stalk antibodies can directly neutralize the influenza virus [41–43], antibodies against M2e do not possess virus-neutralizing activity [25,55]. Yet, a great part of the stalk and M2e specific antibodies confer Fc-receptor dependent protection mediated by the effector mechanisms such as ADCC [20,25,48,55]. Here, the ADCC assay demonstrated that the tri-stalk induced protection is mostly dependent on the antibody effector functions, thus preserving the protective potential in serum transfer experiments. In contrast, the M2e-based protection is mediated both by the antibody Fc-receptor effector mechanisms

and by some T-cell based activity, which has been shown to correlate with better vaccine-induced protection in the elderly and to confer a durable protective efficiency [56,57]. Also, it was previously demonstrated that the CD4⁺ T-cells can possess a cytolytic function on influenza-infected cells in mice, other than their classical helper role [58,59]. It remains to be investigated whether the M2e-specific CD4⁺ T-cells possess direct cytotoxic activity, or if there are other immune cells with cytotoxic potential which are induced by the M2e-based vaccine candidates. Additional challenge experiment with a high dose of homologous H1N1 influenza virus emphasized the important role of tri-stalk targeted antibody as in this experiment the tri-stalk antibodies were the main mediators of protection. Although M2e-binding antibodies were also involved in mediating the protection, a passive serum transfer experiment showed that they were not sufficient to defend mice against the infection. It is therefore not surprising that the best protective effect could be achieved when these conserved antigens were combined in single vaccine preparation.

The study has several limitations. First, the performance of the vaccine candidates was assessed only by measuring immune responses and monitoring weight loss and survival upon a lethal influenza virus challenge. Assessment of virus replication in the mouse respiratory tract could provide additional evidence for the ability of the induced antibody and T-cells to clear the virus but would require a much larger number of mice for this study. Nevertheless, for the vaccines that do not induce neutralizing antibodies the assessment of vaccine efficacy only by a clinical endpoint is widely accepted [60–62]. Finally, the immunogenicity of the constructed VLPs was evaluated only in the presence of an adjuvant, yet there are multiple confirmations that VLPs contribute to robust and durable IgG responses themselves due to their highly repetitive and particulate properties [63].

5. Conclusions

The combination of multiple conserved influenza antigens into a multivalent single-component AP-M2e/tri-stalk vaccine protected mice from high dose homologous influenza challenge and induced robust heterosubtypic immunity. Since persistent vaccine-induced immunity is a highly desirable feature of a broadly protective influenza vaccine, it should be noted that both the post-fusion LAH- and M2e-based vaccines are known to elicit long-lasting antibody responses [34,55]. Therefore, the long-term immune responses induced by the AP-M2e/tri-stalk vaccine candidate could be the subject of our future research. The vaccine candidates can be further improved by changing their formulation for intranasal delivery since intranasal administration of VLPs with relevant mucosal adjuvants has been shown to induce strong and durable cross-protective immunity [64,65]. Taken together, these data suggest that the AP-M2e/tri-stalk vaccine prototype might provide broad protection against seasonal and emergent influenza strains, thus replacing the current vaccination strategies.

Supplementary Materials: The following are available online at <http://www.mdpi.com/2076-393X/8/2/197/s1>, Figure S1: Gating strategy for NK-cell degranulation assay (antibody-dependent cellular cytotoxicity, ADCC), Figure S2: Gating strategy for intracellular cytokine staining (ICS) assay, Figure S3: Gating strategy in flow cytometry analysis of target cells for CTL in vivo assay, Figure S4: Immunogenicity of the recombinant vaccine candidates included in the study, Table S1: Amino acid sequences of the M2e fragments comprising the 3M2e protein used in this study, Table S2: Comparison of amino acid sequences of N-terminally extended long alpha-helix fragment of various influenza A HA proteins used in this study, Table S3: Sequence conservation between the vaccination antigens and the corresponding protein fragments of influenza A challenge viruses used in this study.

Author Contributions: Conceptualization, A.K. (Andris Kazaks), K.T.; methodology, A.K. (Anna Kirsteina), J.B., J.J., I.L.-S., V.M., D.M.; software, A.K. (Anna Kirsteina), I.L.-S.; validation, A.K. (Anna Kirsteina), I.L.-S.; formal analysis, A.K. (Andris Kazaks), K.T.; investigation, A.K. (Andris Kazaks), A.K. (Anna Kirsteina), I.A., J.B., I.L., J.J., D.S., T.K. (Tatjana Kazaka), I.L.-S., D.M., T.K. (Tatiana Kotomina), V.M.; data curation, A.K. (Anna Kirsteina); writing—Original draft preparation, A.K. (Anna Kirsteina); writing—Review and editing, A.K. (Andris Kazaks), I.L.-S.; supervision, A.K. (Andris Kazaks), K.T.; project administration, A.K. (Andris Kazaks), L.R.; funding acquisition, A.K. (Andris Kazaks). All authors have read and agreed to the published version of the manuscript.

Funding: This study was funded by European Regional Development Fund project 1.1.1.1/16/A/054.

Conflicts of Interest: The authors declare no conflict of interest.

References

1. WHO. Influenza (Seasonal). Available online: [https://www.who.int/en/news-room/fact-sheets/detail/influenza-\(seasonal\)](https://www.who.int/en/news-room/fact-sheets/detail/influenza-(seasonal)) (accessed on 6 March 2020).
2. Iuliano, A.D.; Roguski, K.M.; Chang, H.H.; Muscatello, D.J.; Palekar, R.; Tempia, S.; Cohen, C.; Gran, J.M.; Scharzter, D.; Cowling, B.J.; et al. Estimates of global seasonal influenza-associated respiratory mortality: A modelling study. *Lancet* **2018**, *391*, 1285–1300. [CrossRef]
3. Putri, W.C.W.S.; Muscatello, D.J.; Stockwell, M.S.; Newall, A.T. Economic burden of seasonal influenza in the United States. *Vaccine* **2018**, *36*, 3960–3966. [CrossRef]
4. Preaud, E.; Durand, L.; Macabeo, B.; Farkas, N.; Sloesen, B.; Palache, A.; Shupo, F.; Samson, S.I.; Vaccines Europe Influenza Working Group. Annual public health and economic benefits of seasonal influenza vaccination: A European estimate. *BMC Public Health* **2014**, *14*, 813. [CrossRef] [PubMed]
5. CDC. CDC Seasonal Flu Vaccine Effectiveness Studies. Available online: <https://www.cdc.gov/flu/vaccines-work/effectiveness-studies.htm> (accessed on 6 March 2020).
6. ECDC. Influenza Vaccine Effectiveness. Available online: <https://www.ecdc.europa.eu/en/seasonal-influenza/prevention-and-control/vaccine-effectiveness> (accessed on 6 March 2020).
7. Belongia, E.A.; Simpson, M.D.; King, J.P.; Sundaram, M.E.; Kelley, N.S.; Osterholm, M.T.; McLean, H.Q. Variable influenza vaccine effectiveness by subtype: A systematic review and meta-analysis of test-negative design studies. *Lancet Infect. Dis.* **2016**, *16*, 942–951. [CrossRef]
8. Bedford, T.; Riley, S.; Barr, I.G.; Broor, S.; Chadha, M.; Cox, N.J.; Daniels, R.S.; Gunasekaran, C.P.; Hurt, A.C.; Kelso, A.; et al. Global circulation patterns of seasonal influenza viruses vary with antigenic drift. *Nature* **2015**, *523*, 217–220. [CrossRef] [PubMed]
9. Heaton, N.S.; Sachs, D.; Chen, C.-J.; Hai, R.; Palese, P. Genome-wide mutagenesis of influenza virus reveals unique plasticity of the hemagglutinin and NS1 proteins. *Proc. Natl. Acad. Sci. USA* **2013**, *110*, 20248–20253. [CrossRef]
10. Wong, K.K.Y.; Rockman, S.; Ong, C.; Bull, R.; Stelzer-Braid, S.; Rawlinson, W. Comparison of influenza virus replication fidelity in vitro using selection pressure with monoclonal antibodies. *J. Med. Virol.* **2013**, *85*, 1090–1094. [CrossRef]
11. Auladell, M.; Jia, X.; Hensen, L.; Chua, B.; Fox, A.; Nguyen, T.H.O.; Doherty, P.C.; Kedzierska, K. Recalling the Future: Immunological Memory Toward Unpredictable Influenza Viruses. *Front. Immunol.* **2019**, *10*, 1400. [CrossRef]
12. Tscherne, D.M.; García-Sastre, A. Virulence determinants of pandemic influenza viruses. *J. Clin. Investig.* **2011**, *121*, 6–13. [CrossRef]
13. Luksza, M.; Lässig, M. A predictive fitness model for influenza. *Nature* **2014**, *507*, 57–61. [CrossRef]
14. Hannoun, C. The evolving history of influenza viruses and influenza vaccines. *Expert Rev. Vaccines* **2013**, *12*, 1085–1094. [CrossRef] [PubMed]
15. Baz, M.; Luke, C.J.; Cheng, X.; Jin, H.; Subbarao, K. H5N1 vaccines in humans. *Virus Res.* **2013**, *178*, 78–98. [CrossRef]
16. Nuñez, I.A.; Ross, T.M. A review of H5Nx avian influenza viruses. *Ther. Adv. Vaccines Immunother.* **2019**, *7*, 2515135518821625. [CrossRef] [PubMed]
17. Wei, S.-H.; Yang, J.-R.; Wu, H.-S.; Chang, M.-C.; Lin, J.-S.; Lin, C.-Y.; Liu, Y.-L.; Lo, Y.-C.; Yang, C.-H.; Chuang, J.-H.; et al. Human infection with avian influenza A H6N1 virus: An epidemiological analysis. *Lancet Respir. Med.* **2013**, *1*, 771–778. [CrossRef]
18. Gao, R.; Cao, B.; Hu, Y.; Feng, Z.; Wang, D.; Hu, W.; Chen, J.; Jie, Z.; Qiu, H.; Xu, K.; et al. Human infection with a novel avian-origin influenza A (H7N9) virus. *N. Engl. J. Med.* **2013**, *368*, 1888–1897. [CrossRef] [PubMed]
19. Chen, H.; Yuan, H.; Gao, R.; Zhang, J.; Wang, D.; Xiong, Y.; Fan, G.; Yang, F.; Li, X.; Zhou, J.; et al. Clinical and epidemiological characteristics of a fatal case of avian influenza A H10N8 virus infection: A descriptive study. *Lancet* **2014**, *383*, 714–721. [CrossRef]
20. Nachbagauer, R.; Krammer, F. Universal influenza virus vaccines and therapeutic antibodies. *Clin. Microbiol. Infect.* **2017**, *23*, 222–228. [CrossRef]
21. Valkenburg, S.A.; Mallajosyula, V.V.A.; Li, O.T.W.; Chin, A.W.H.; Carnell, G.; Temperton, N.; Varadarajan, R.; Poon, L.L.M. Stalking influenza by vaccination with pre-fusion headless HA mini-stem. *Sci. Rep.* **2016**, *6*, 22666. [CrossRef]
22. Krammer, F.; Pica, N.; Hai, R.; Margine, I.; Palese, P. Chimeric hemagglutinin influenza virus vaccine constructs elicit broadly protective stalk-specific antibodies. *J. Virol.* **2013**, *87*, 6542–6550. [CrossRef]

23. Zheng, D.; Chen, S.; Qu, D.; Chen, J.; Wang, F.; Zhang, R.; Chen, Z. Influenza H7N9 LAH-HBc virus-like particle vaccine with adjuvant protects mice against homologous and heterologous influenza viruses. *Vaccine* **2016**, *34*, 6464–6471. [[CrossRef](#)]
24. Chen, S.; Zheng, D.; Li, C.; Zhang, W.; Xu, W.; Liu, X.; Fang, F.; Chen, Z. Protection against multiple subtypes of influenza viruses by virus-like particle vaccines based on a hemagglutinin conserved epitope. *BioMed Res. Int.* **2015**, *2015*, 901817. [[CrossRef](#)] [[PubMed](#)]
25. Kolpe, A.; Schepens, B.; Fiers, W.; Saelens, X. M2-based influenza vaccines: Recent advances and clinical potential. *Expert Rev. Vaccines* **2017**, *16*, 123–136. [[CrossRef](#)] [[PubMed](#)]
26. De Filette, M.; Min Jou, W.; Birkett, A.; Lyons, K.; Schultz, B.; Tonkyro, A.; Resch, S.; Fiers, W. Universal influenza A vaccine: Optimization of M2-based constructs. *Virology* **2005**, *337*, 149–161. [[CrossRef](#)] [[PubMed](#)]
27. Sui, Z.; Chen, Q.; Wu, R.; Zhang, H.; Zheng, M.; Wang, H.; Chen, Z. Cross-protection against influenza virus infection by intranasal administration of M2-based vaccine with chitosan as an adjuvant. *Arch. Virol.* **2010**, *155*, 535–544. [[CrossRef](#)] [[PubMed](#)]
28. Lee, Y.-T.; Ko, E.-J.; Lee, Y.; Kim, K.-H.; Kim, M.-C.; Lee, Y.-N.; Kang, S.-M. Intranasal vaccination with M2e5x virus-like particles induces humoral and cellular immune responses conferring cross-protection against heterosubtypic influenza viruses. *PLoS ONE* **2018**, *13*, e0190868. [[CrossRef](#)] [[PubMed](#)]
29. Ramirez, A.; Morris, S.; Maucourant, S.; D'Ascanio, I.; Crescente, V.; Lu, L.-N.; Farinelle, S.; Muller, C.P.; Whelan, M.; Rosenberg, W. A virus-like particle vaccine candidate for influenza A virus based on multiple conserved antigens presented on hepatitis B tandem core particles. *Vaccine* **2018**, *36*, 873–880. [[CrossRef](#)]
30. Ellebedy, A.H.; Ahmed, R. Re-engaging cross-reactive memory B cells: The influenza puzzle. *Front. Immunol.* **2012**, *3*, 53. [[CrossRef](#)]
31. Pushko, P.; Pumpens, P.; Grens, E. Development of virus-like particle technology from small highly symmetric to large complex virus-like particle structures. *Intervirology* **2013**, *56*, 141–165. [[CrossRef](#)]
32. Shishovs, M.; Rumnieks, J.; Diebold, C.; Jaudzems, K.; Andreas, L.B.; Stanek, J.; Kazaks, A.; Kotelovica, S.; Akopjana, I.; Pintacuda, G.; et al. Structure of AP205 Coat Protein Reveals Circular Permutation in ssRNA Bacteriophages. *J. Mol. Biol.* **2016**, *428*, 4267–4279. [[CrossRef](#)]
33. Kazaks, A.; Lu, L.-N.; Farinelle, S.; Ramirez, A.; Crescente, V.; Blaha, B.; Ogonah, O.; Mukhopadhyay, T.; de Obanos, M.P.; Krimer, A.; et al. Production and purification of chimeric HBc virus-like particles carrying influenza virus LAH domain as vaccine candidates. *BMC Biotechnol.* **2017**, *17*, 79. [[CrossRef](#)]
34. Adachi, Y.; Tonouchi, K.; Nithichanon, A.; Kuraoka, M.; Watanabe, A.; Shinnakasu, R.; Asanuma, H.; Aina, A.; Ohmi, Y.; Yamamoto, T.; et al. Exposure of an occluded hemagglutinin epitope drives selection of a class of cross-protective influenza antibodies. *Nat. Commun.* **2019**, *10*, 3883. [[CrossRef](#)] [[PubMed](#)]
35. Lu, L.-N.; Kirsteina, A.; Farinelle, S.; Willieme, S.; Tars, K.; Muller, C.P.; Kazaks, A. Structure and applications of novel influenza HA tri-stalk protein for evaluation of HA stem-specific immunity. *PLoS ONE* **2018**, *13*, e0204776. [[CrossRef](#)] [[PubMed](#)]
36. Lee, Y.-N.; Lee, Y.-T.; Kim, M.-C.; Hwang, H.S.; Lee, J.S.; Kim, K.-H.; Kang, S.-M. Fc receptor is not required for inducing antibodies but plays a critical role in conferring protection after influenza M2 vaccination. *Immunology* **2014**, *143*, 300–309. [[CrossRef](#)] [[PubMed](#)]
37. Leser, G.P.; Lamb, R.A. Influenza virus assembly and budding in raft-derived microdomains: A quantitative analysis of the surface distribution of HA, NA and M2 proteins. *Virology* **2005**, *342*, 215–227. [[CrossRef](#)] [[PubMed](#)]
38. Durward, M.; Harms, J.; Splitter, G. Antigen specific killing assay using CFSE labeled target cells. *J. Vis. Exp.* **2010**, *45*, e2250. [[CrossRef](#)]
39. Jegaskanda, S.; Weinfurter, J.T.; Friedrich, T.C.; Kent, S.J. Antibody-dependent cellular cytotoxicity is associated with control of pandemic H1N1 influenza virus infection of macaques. *J. Virol.* **2013**, *87*, 5512–5522. [[CrossRef](#)]
40. Krystal, M.; Elliott, R.M.; Benz, E.W.; Young, J.F.; Palese, P. Evolution of influenza A and B viruses: Conservation of structural features in the hemagglutinin genes. *Proc. Natl. Acad. Sci. USA* **1982**, *79*, 4800–4804. [[CrossRef](#)]
41. Corti, D.; Voss, J.; Gamblin, S.J.; Codoni, G.; Macagno, A.; Jarrossay, D.; Vachieri, S.G.; Pinna, D.; Minola, A.; Vanzetta, F.; et al. A neutralizing antibody selected from plasma cells that binds to group 1 and group 2 influenza A hemagglutinins. *Science* **2011**, *333*, 850–856. [[CrossRef](#)]
42. Nakamura, G.; Chai, N.; Park, S.; Chiang, N.; Lin, Z.; Chiu, H.; Fong, R.; Yan, D.; Kim, J.; Zhang, J.; et al. An in vivo human-plasmablast enrichment technique allows rapid identification of therapeutic influenza A antibodies. *Cell Host Microbe* **2013**, *14*, 93–103. [[CrossRef](#)]

43. Dreyfus, C.; Laursen, N.S.; Kwaks, T.; Zuijdgheest, D.; Khayat, R.; Ekiert, D.C.; Lee, J.H.; Metlagel, Z.; Bujny, M.V.; Jongeneelen, M.; et al. Highly conserved protective epitopes on influenza B viruses. *Science* **2012**, *337*, 1343–1348. [[CrossRef](#)]
44. Throsby, M.; van den Brink, E.; Jongeneelen, M.; Poon, L.L.M.; Alard, P.; Cornelissen, L.; Bakker, A.; Cox, F.; van Deventer, E.; Guan, Y.; et al. Heterosubtypic neutralizing monoclonal antibodies cross-protective against H5N1 and H1N1 recovered from human IgM+ memory B cells. *PLoS ONE* **2008**, *3*, e3942. [[CrossRef](#)]
45. Tan, G.S.; Krammer, F.; Eggink, D.; Kongchanagul, A.; Moran, T.M.; Palese, P. A pan-H1 anti-hemagglutinin monoclonal antibody with potent broad-spectrum efficacy in vivo. *J. Virol.* **2012**, *86*, 6179–6188. [[CrossRef](#)]
46. Henry Dunand, C.J.; Leon, P.E.; Huang, M.; Choi, A.; Chromikova, V.; Ho, I.Y.; Tan, G.S.; Cruz, J.; Hirsh, A.; Zheng, N.-Y.; et al. Both Neutralizing and Non-Neutralizing Human H7N9 Influenza Vaccine-Induced Monoclonal Antibodies Confer Protection. *Cell Host Microbe* **2016**, *19*, 800–813. [[CrossRef](#)]
47. Ekiert, D.C.; Friesen, R.H.E.; Bhabha, G.; Kwaks, T.; Jongeneelen, M.; Yu, W.; Ophorst, C.; Cox, F.; Korse, H.J.W.M.; Brandenburg, B.; et al. A highly conserved neutralizing epitope on group 2 influenza A viruses. *Science* **2011**, *333*, 843–850. [[CrossRef](#)]
48. DiLillo, D.J.; Tan, G.S.; Palese, P.; Ravetch, J.V. Broadly neutralizing hemagglutinin stalk-specific antibodies require FcγR interactions for protection against influenza virus in vivo. *Nat. Med.* **2014**, *20*, 143–151. [[CrossRef](#)] [[PubMed](#)]
49. Nimmerjahn, F.; Ravetch, J.V. Divergent immunoglobulin g subclass activity through selective Fc receptor binding. *Science* **2005**, *310*, 1510–1512. [[CrossRef](#)] [[PubMed](#)]
50. Nimmerjahn, F.; Ravetch, J.V. Fcγ receptors: Old friends and new family members. *Immunity* **2006**, *24*, 19–28. [[CrossRef](#)] [[PubMed](#)]
51. Schmitz, N.; Beerli, R.R.; Bauer, M.; Jegerlehner, A.; Dietmeier, K.; Maudrich, M.; Pumpens, P.; Saudan, P.; Bachmann, M.F. Universal vaccine against influenza virus: Linking TLR signaling to anti-viral protection. *Eur. J. Immunol.* **2012**, *42*, 863–869. [[CrossRef](#)] [[PubMed](#)]
52. Stepanova, L.A.; Kotlyarov, R.Y.; Kovaleva, A.A.; Potapchuk, M.V.; Korotkov, A.V.; Sergeeva, M.V.; Kasianenko, M.A.; Kuprianov, V.V.; Ravin, N.V.; Tsybalova, L.M.; et al. Protection against multiple influenza A virus strains induced by candidate recombinant vaccine based on heterologous M2e peptides linked to flagellin. *PLoS ONE* **2015**, *10*, e0119520. [[CrossRef](#)]
53. Leitans, J.; Kazaks, A.; Balode, A.; Ivanova, J.; Zalubovskis, R.; Supuran, C.T.; Tars, K. Efficient Expression and Crystallization System of Cancer-Associated Carbonic Anhydrase Isoform IX. *J. Med. Chem.* **2015**, *58*, 9004–9009. [[CrossRef](#)]
54. Freivalds, J.; Kotelovica, S.; Voronkova, T.; Ose, V.; Tars, K.; Kazaks, A. Yeast-expressed bacteriophage-like particles for the packaging of nanomaterials. *Mol. Biotechnol.* **2014**, *56*, 102–110. [[CrossRef](#)] [[PubMed](#)]
55. Mezhenkaya, D.; Isakova-Sivak, I.; Rudenko, L. M2e-based universal influenza vaccines: A historical overview and new approaches to development. *J. Biomed. Sci.* **2019**, *26*, 76. [[CrossRef](#)] [[PubMed](#)]
56. McElhaney, J.E.; Xie, D.; Hager, W.D.; Barry, M.B.; Wang, Y.; Kleppinger, A.; Ewen, C.; Kane, K.P.; Bleackley, R.C. T cell responses are better correlates of vaccine protection in the elderly. *J. Immunol.* **2006**, *176*, 6333–6339. [[CrossRef](#)] [[PubMed](#)]
57. Eliasson, D.G.; Omokanye, A.; Schön, K.; Wenzel, U.A.; Bernasconi, V.; Bemark, M.; Kolpe, A.; El Bakkouri, K.; Ysenbaert, T.; Deng, L.; et al. M2e-tetramer-specific memory CD4 T cells are broadly protective against influenza infection. *Mucosal Immunol.* **2018**, *11*, 273–289. [[CrossRef](#)] [[PubMed](#)]
58. Brown, D.M.; Dilzer, A.M.; Meents, D.L.; Swain, S.L. CD4 T cell-mediated protection from lethal influenza: Perforin and antibody-mediated mechanisms give a one-two punch. *J. Immunol.* **2006**, *177*, 2888–2898. [[CrossRef](#)]
59. Schotsaert, M.; Ibañez, L.I.; Fiers, W.; Saelens, X. Controlling influenza by cytotoxic T-cells: Calling for help from destroyers. *J. Biomed. Biotechnol.* **2010**, *2010*, 863985. [[CrossRef](#)]
60. Rowell, J.; Lo, C.-Y.; Price, G.E.; Misplon, J.A.; Crim, R.L.; Jayanti, P.; Beeler, J.; Epstein, S.L. The effect of respiratory viruses on immunogenicity and protection induced by a candidate universal influenza vaccine in mice. *PLoS ONE* **2019**, *14*, e0215321. [[CrossRef](#)]
61. Herrera-Rodriguez, J.; Meijerhof, T.; Niesters, H.G.; Stjernholm, G.; Hovden, A.-O.; Sørensen, B.; Ökvist, M.; Sommerfelt, M.A.; Huckriede, A. A novel peptide-based vaccine candidate with protective efficacy against influenza A in a mouse model. *Virology* **2018**, *515*, 21–28. [[CrossRef](#)]

62. Asthagiri Arunkumar, G.; McMahon, M.; Pavot, V.; Aramouni, M.; Ioannou, A.; Lambe, T.; Gilbert, S.; Krammer, F. Vaccination with viral vectors expressing NP, M1 and chimeric hemagglutinin induces broad protection against influenza virus challenge in mice. *Vaccine* **2019**, *37*, 5567–5577. [[CrossRef](#)]
63. Kang, S.-M.; Kim, M.-C.; Compans, R.W. Virus-like particles as universal influenza vaccines. *Expert Rev. Vaccines* **2012**, *11*, 995–1007. [[CrossRef](#)]
64. Schwartzman, L.M.; Cathcart, A.L.; Pujanauski, L.M.; Qi, L.; Kash, J.C.; Taubenberger, J.K. An Intranasal Virus-Like Particle Vaccine Broadly Protects Mice from Multiple Subtypes of Influenza A Virus. *mBio* **2015**, *6*, e01044. [[CrossRef](#)] [[PubMed](#)]
65. Bessa, J.; Schmitz, N.; Hinton, H.J.; Schwarz, K.; Jegerlehner, A.; Bachmann, M.F. Efficient induction of mucosal and systemic immune responses by virus-like particles administered intranasally: Implications for vaccine design. *Eur. J. Immunol.* **2008**, *38*, 114–126. [[CrossRef](#)] [[PubMed](#)]



© 2020 by the authors. Licensee MDPI, Basel, Switzerland. This article is an open access article distributed under the terms and conditions of the Creative Commons Attribution (CC BY) license (<http://creativecommons.org/licenses/by/4.0/>).

3.4 Structural Analysis of an Antigen Chemically Coupled on Virus-Like Particles in Vaccine Formulation

Highlights:

- The crystal structure of LAH trimer showed that each LAH monomer adapts a hairpin-structure, consisting of two antiparallel α -helices, and they form a six-helix bundle of 3 monomers. This structure was used as a reference and to assist assigning resonance of the MAS-NMR data.
- Uniformly (U)- ^{13}C -, ^{15}N -labeled free LAH antigen was analyzed via the conventional MAS-NMR. The results indicated the presence of two antiparallel α -helices for each LAH monomer, almost identical to those in the crystal structure when superimposed.
- MAS-NMR allowed to obtain structural information from heterologous Q β -LAH particles with a sensitivity boost from proton detection and high-field dynamic nuclear polarization, even despite the target antigen dilution. The VLP-display of the LAH antigen did not change its structural identity, and LAH retained its trimeric helix-bundle structure in the vaccine formulation. The differences were mainly limited to the less-structured regions near the polypeptide termini and around the loop connecting both helices of the LAH monomer hairpin.



How to cite:

International Edition: doi.org/10.1002/anie.202013189

German Edition: doi.org/10.1002/ange.202013189

Structural Analysis of an Antigen Chemically Coupled on Virus-Like Particles in Vaccine Formulation

Kristaps Jaudzems,* Anna Kirsteina, Tobias Schubeis, Gilles Casano, Olivier Ouari, Janis Bogans, Andris Kazaks, Kaspars Tars, Anne Lesage,* and Guido Pintacuda*

Abstract: Structure determination of adjuvant-coupled antigens is essential for rational vaccine development but has so far been hampered by the relatively low antigen content in vaccine formulations and by their heterogeneous composition. Here we show that magic-angle spinning (MAS) solid-state NMR can be used to assess the structure of the influenza virus hemagglutinin stalk long alpha helix antigen, both in its free, unformulated form and once chemically coupled to the surface of large virus-like particles (VLPs). The sensitivity boost provided by high-field dynamic nuclear polarization (DNP) and proton detection at fast MAS rates allows to overcome the penalty associated with the antigen dilution. Comparison of the MAS NMR fingerprints between the free and VLP-coupled forms of the antigen provides structural evidence of the conservation of its native fold upon bioconjugation. This work demonstrates that high-sensitivity MAS NMR is ripe to play a major role in vaccine design, formulation studies, and manufacturing process development.

Virus-like particles (VLPs) are empty, non-infectious shells of viruses, which are extensively used in pharmaceutical industry as potent vaccine adjuvants.^[1,2] In these applications, the surface of VLPs is typically decorated with antigens from various infectious agents^[3–5] or with haptens^[6] increasing by one or two orders of magnitude the antibody titers, and significantly enhancing T-cell and innate immune response.^[7] A relevant immune response can however only be provoked if antigens retain their native 3D structure once immobilized on

VLPs. The design of efficient vaccines relies therefore on the possibility to characterize the structure of the intermediate and final products during the genetic fusion or bioconjugation steps which are conventionally used to couple protein antigens to the surface of VLPs. Genetic fusion is technically simpler, but it often leads to insoluble or assembly-deficient products, so chemical ligation to free cysteines or lysines is usually the method of choice.^[8,9] This protocol yields however assemblies that are too heterogeneous to be studied by either X-ray crystallography or cryo-EM, and that are too large in size to be investigated by solution NMR.

In this context, magic-angle spinning (MAS) solid-state NMR spectroscopy appears particularly adapted, as this technique can provide structure information in supramolecular biological assemblies independently from their molecular size and the long-range order in the sample formulation.^[10,11] A pioneering study in this direction has indeed demonstrated the possibility to characterize a pilot model of protein antigen adsorbed on aluminum hydroxide.^[12] The main challenge for MAS NMR structural analysis of surface-coupled antigens is however greatly reduced NMR signal intensity associated with the small relative mass ratio of the antigen compared to the VLP. This problem adds to the difficulties in obtaining tens-of-milligrams labeled sample amounts needed by conventional MAS NMR approaches and to potential heterogeneity introduced by the chemical coupling. These limitations clearly prevent the widespread use of MAS NMR in vaccine research.

Two recent developments in MAS NMR, namely dynamic nuclear polarization (DNP)^[13] and ¹H-detection at increased magic-angle spinning (MAS) frequencies,^[14,15] address the sensitivity problem, reducing the amount of sample and the acquisition times needed for a structural analysis. In the context of vaccine research, proton-detected solid-state NMR spectroscopy under 100 kHz MAS frequency has recently allowed the structural determination of 2.5 MDa VLP with sub-milligrams sample quantities.^[16] In parallel, DNP-enhanced MAS NMR has been successfully applied to reveal multiple conformations of lipid-anchored peptides^[17] as well as the adsorption mode of antigens onto aluminum-based adjuvants.^[18]

Here we take advantage of both approaches to perform the structural analysis of the influenza virus hemagglutinin (HA) stalk long alpha helix (LAH) antigen coupled to the surface of a VLP. We first use conventional MAS NMR to determine the 3D structure of the free antigen in microcrystalline form. We then exploit the sensitivity boost provided by proton detection and high-field DNP to assess the integrity of the antigen structure after the attachment

[*] Prof. K. Jaudzems
 Latvian Institute of Organic Synthesis
 Aizkraukles 21, Riga LV-1006 (Latvia)
 E-mail: kristaps.jaudzems@osi.lv

A. Kirsteina, J. Bogans, Dr. A. Kazaks, Prof. K. Tars
 Latvian Biomedical Research and Study Centre
 Ratsupites 1 k1, Riga LV-1067 (Latvia)

Dr. T. Schubeis, Dr. A. Lesage, Dr. G. Pintacuda
 Centre de RMN à Très Hauts Champs de Lyon—UMR 5082 (CNRS,
 ENS Lyon, UCB Lyon 1)
 Université de Lyon
 69100 Villeurbanne (France)
 E-mail: anne.lesage@ens-lyon.fr
 guido.pintacuda@ens-lyon.fr

Dr. G. Casano, Dr. O. Ouari
 Institut de Chimie Radicalaire
 AixMarseille Université
 13013 Marseille (France)

Supporting information and the ORCID identification number(s) of the author(s) of this article can be found under:
<https://doi.org/10.1002/anie.202013189>.

onto the VLP surface, as well as to identify the structurally divergent regions. To our best knowledge, this work represents the first example of an atomic level structural analysis of a VLP-coupled protein.

The HA stalk LAH is one of the most conservative influenza virus antigens and is being investigated as a potential universal influenza vaccine component.^[19] The immunogenic form of the protein is an α -helical trimer resembling the corresponding region of native HA in its post-fusion form.^[20] We studied a short, N-terminally truncated version of the LAH antigen comprising HA residues 418–474. A high-resolution (1.34 Å) crystal structure of the LAH trimer was determined as a reference and to assist resonance assignment of MAS NMR spectra (Figure S1).

To increase antibody titers and obtain a stronger T-cell response, the antigen was coupled to VLPs of ssRNA bacteriophage Q β (Figure 1), which have been used previously in vaccine development.^[6,21,22] Uniformly (U)- ^{13}C , ^{15}N -labeled LAH antigen (HA residues 418–474) was produced by expression in *Escherichia coli* and purified as described in the Supporting Information. The free form of the protein was precipitated using saturated ammonium sulfate. The coupling of labeled LAH antigen to unlabeled Q β VLPs was performed via SATA–maleimide conjugation chemistry (Figure S2) and the resulting product was sedimented by ultracentrifugation.^[23,24]

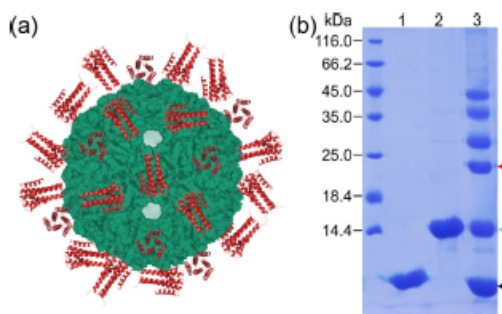


Figure 1. a) Structural model of LAH antigen coupled to the surface of Q β VLP. b) SDS-PAGE analysis of the coupling reaction: lanes 1 and 2—HA stalk LAH and Q β coat proteins before coupling; lane 3—after coupling. Red arrow refers to the coupling zone, gray arrow—coat protein monomer, black arrow—HA stalk LAH protein. Coupling bands indicate a successful reaction.

We started our study with the ^{13}C and ^{15}N chemical shift assignment of free LAH antigen by recording ^{13}C -detected experiments at moderate MAS frequencies (12.5–20 kHz in a 3.2 mm rotor) on a U - ^{13}C , ^{15}N -labeled sample. An excellent spectral quality was observed in the 2D RFDR^[25] and DARR^[26] spectra (Figure S3), where isolated resonances displayed line widths of approximately 0.7 ppm. The backbone and side chain assignment was completed for residues 5–58, except for L30, L46, L54, K55 using 3D NCOCX, NCACX, CONCA, and CANCO spectra (Figure S4). Figure 2 a,b shows the assigned 2D NCO and NCA spectra.

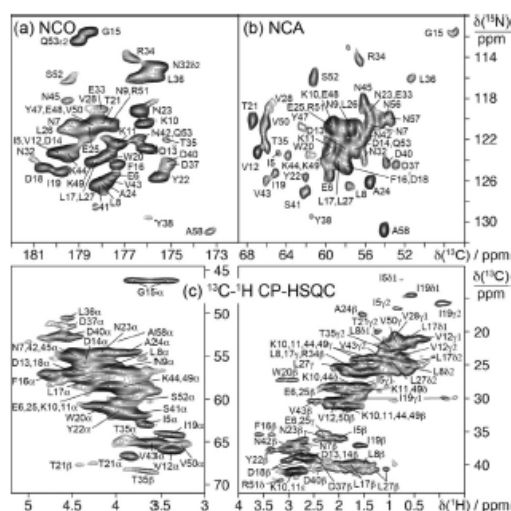


Figure 2. Chemical shift assignment of free LAH antigen. a,b) Assigned NCO and NCA spectra of U - ^{13}C , ^{15}N -labeled LAH antigen at 800 MHz with 17 kHz MAS. c) Assigned ^1H -detected 2D ^{13}C , ^1H CP-HSQC spectra of U - ^{13}C , ^{15}N -labeled free LAH antigen at 1 GHz with 105 kHz MAS.

Further, to obtain the ^1H chemical shift assignments we recorded experiments to correlate the ^{15}N and ^{13}C chemical shifts to those of their bound ^1H nuclei. To this end, we repacked the sample of free LAH antigen in a 0.7 mm rotor and acquired 3D (H)NCAH, (H)CBCAH, (H)COCAH, and (H)CCH spectra^[27] with 105 kHz MAS. Analysis of these spectra allowed assignment of the resonances of most H α nuclei as well as of side chain protons (Figure 2c, Figure S5).

To determine the secondary structure elements, deviations of our assigned $^{13}\text{C}\alpha,\beta$ chemical shifts from random-coil values were analyzed (Figure 3a). This procedure predicted two helices with locations almost identical to those in the crystal structure, except that the helix 2 appeared to be shorter near the C-terminus by two residues. Further, to verify the same relative positioning of the two helices, we calculated the expected intramolecular interresidual H–H contacts <5 Å from the crystal structure and checked their manifestation in the 2D C(HH)C and N(HH)C spectra (Figure 3 b,c). A total of 689 (out of 1334) contacts were confirmed in this way including 297 sequential, 314 medium-range (2–4 residues apart) and 78 long-range (5 and more residues apart) contacts, which indicates a good fit between the MAS NMR data and the crystal structure.

Finally, we calculated the 3D structure of the LAH trimer subunit using CYANA^[28] with the confirmed H–H contacts as upper-limit distance restraints of 5 Å and backbone torsion angle (ψ , ϕ) restraints derived from chemical shifts using TALOS.^[29] Notably, because cross peaks observed from a U - ^{13}C , ^{15}N -labeled sample can arise from both intramolecular and intermolecular contacts the quaternary structure could not be determined based on these data. Although the

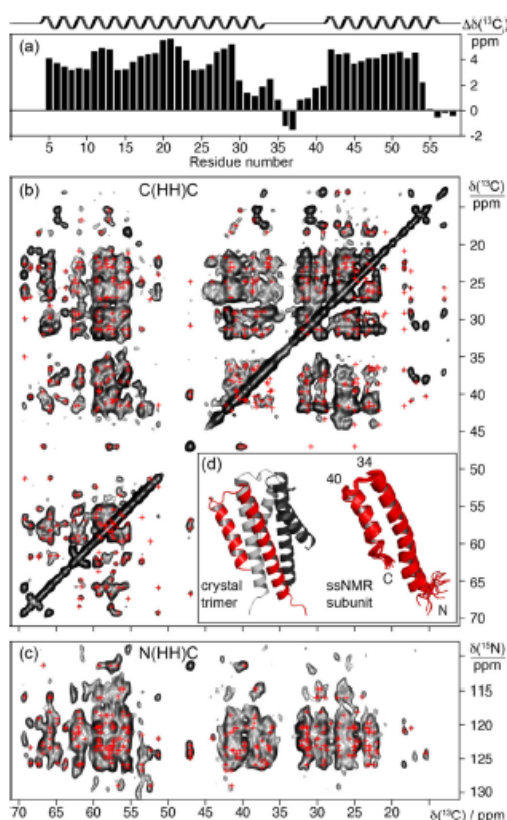


Figure 3. Secondary and tertiary structure of free LAH antigen. a) ^{13}C α and ^{13}C β chemical shift deviations from random-coil values in LAH antigen. $\Delta\delta(^{13}\text{C})$ values above 1 are indicative of helices, while values below -1 indicate β -strand or extended structure. The $\Delta\delta(^{13}\text{C})$ value for each residue i was determined as an average over three residues. Locations of helices in the crystal structure of LAH trimer are indicated above the plot. b,c) Expansion of 2D C(HH)C and N(HH)C spectra of $\text{U-}^{13}\text{C}$, ^{15}N -labeled LAH antigen at 800 MHz with 20 kHz MAS. Confirmed interresidual H-H proximities < 5 Å expected based on the crystal structure of LAH trimer are indicated with a red cross. d) MAS NMR structure of LAH trimer subunit and comparison with the crystal structure.

intermolecular contacts were ignored, our calculation converged to a single structure. The obtained structure is well defined, except for the first four and the last four residues, and agrees well with the crystal trimer subunit yielding a backbone heavy-atom RMSD of 0.89 Å, when superimposed (Figure 3 d).

Once coupled to VLP, we estimate that the LAH antigen occupies no more than approximately 10% of the sample volume (see Figure S2). In order to overcome the associated sensitivity drop, and to allow a structural comparison of the free and VLP-coupled LAH antigen in reasonable experi-

mental times, DNP-enhanced and proton-detected MAS NMR were employed.

DNP-enhanced NMR was applied at 800 MHz with 40 kHz MAS in a 1.3 mm rotor and under cryogenic temperatures. The sample was doped with the polarizing agent M-TinyPol,^[30] which allows to combine the advantages of high magnetic fields and fast MAS^[31] with large sensitivity enhancements. Under these conditions, a sensitivity enhancement of about 40 was notably observed for the resonances of the VLP-coupled dilute LAH antigen (Figure S6), which enables the acquisition of sensitive 2D carbon-carbon fingerprints in 38 hours. Figure 4a-c shows expansions of the overlaid 2D ^{13}C , ^{13}C dipolar correlation spectra of free and VLP-coupled LAH antigen acquired using DNP-NMR.

In parallel, 2D ^1H -detected CP-HSQC experiments (with a theoretical sensitivity gain by a factor of approx. 8 with respect to direct ^{13}C acquisition) were recorded at 1 GHz and at ambient temperature, in 1 hour. Experiments were carried out at intermediate spinning speeds (60 kHz) and rotor size

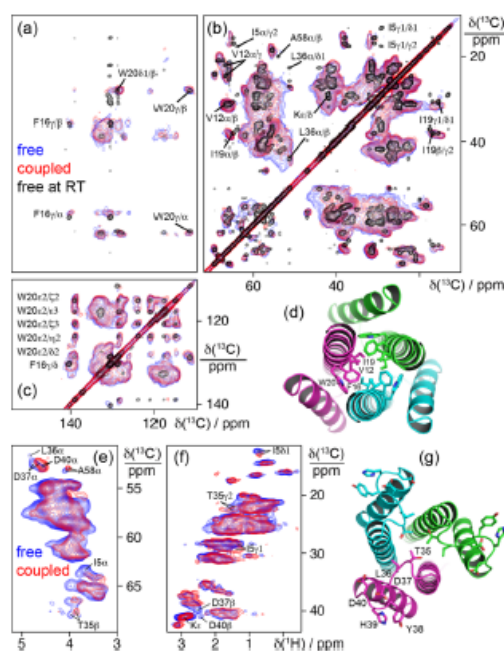


Figure 4. Comparison of free and VLP-coupled LAH antigen. a-c) Overlays of different spectral regions from DNP-enhanced 2D DARR spectra of $\text{U-}^{13}\text{C}$, ^{15}N -labeled free (blue) and VLP-coupled (red) LAH antigen at 800 MHz and 115 K with 40 kHz MAS with the room temperature 2D DARR spectrum of free LAH antigen (black) at 800 MHz with 20 kHz MAS. d) Crystal structure of LAH antigen showing the side chains of V12, F16, I19, and W20 that make up the hydrophobic core of the trimer. e,f) Overlays of $\text{H}\alpha$ - $\text{C}\alpha$ and side chain regions from ^1H -detected 2D ^{13}C , ^1H CP-HSQC spectra of $\text{U-}^{13}\text{C}$, ^{15}N -labeled free (blue) and VLP-coupled (red) LAH antigen at 1 GHz with 60 kHz MAS. g) Crystal structure of LAH trimer showing the side chains of residues T35-D40 in the loop between helices 1 and 2.

(1.3 mm) which represents in our hands the best compromise between absolute sensitivity and resolution. Despite the lower expected sensitivity gain, the ^1H -detected experiments allow monitoring the ^1H NMR resonances that are more sensitive to small structural and environmental changes given the peripheral location of proton nuclei in proteins. Figure 4 e–f shows expansions of the overlaid 2D $^{13}\text{C},^1\text{H}$ dipolar correlation spectra of the two forms. DNP-enhanced 2D $^{15}\text{N},^{13}\text{C}$ and ^1H -detected 2D $^{15}\text{N},^1\text{H}$ dipolar correlations were also recorded but were not sufficiently resolved for site-specific analysis (Figure S7). With respect to the DNP spectra, we note that sample freezing induces a substantial line broadening (cf. the room temperature spectrum of the free form superimposed in black) and causes the disappearance of several signals corresponding to the most dynamically disordered segments that are frozen out in different conformations under DNP conditions. This is the case for the first assigned N-terminal residue I5 and the C-terminal A58 (visible in INEPT spectrum, see Figure S6c) as well as part of cross-peaks from L36 located in the loop between helix 1 and 2, all of which are expected to exhibit significant mobility at ambient temperature.

The DNP-enhanced and proton-detected NMR fingerprints report on the 3D structural identity at atomic level of LAH trimer before and after chemical coupling to the VLP surface. In particular, the two pairs of spectra are virtually identical both in regions containing isolated peaks and also in the most crowded areas where the intensity distribution is unchanged. Notably, several well-resolved cross-peaks from residues V12, F16, I19, and W20 forming the hydrophobic core of the trimer (Figure 4d) feature a perfect overlap between the two forms in the DNP-enhanced NMR spectra, confirming that the trimeric fold of LAH antigen is preserved in its VLP-coupled form. Although the chemical coupling involved modification of the amino group of lysines, no indication of heterogeneity (e.g. peak doubling of H ϵ /C ϵ correlations) could be seen in the spectra. At the same time a small number of signals are either shifted or lose intensity upon coupling in the proton-detected CP-HSQC spectra. These signals correspond to the dynamical regions of the antigen, which are invisible under DNP at cryogenic temperature, and include peaks from the first assigned N-terminal residue I5 and the C-terminal A58 as well as from residues T35, L36, D37, and D40 located in the loop between helix 1 and 2. This likely reports on variations due to different aggregation states. For example, intermolecular contacts in the microcrystalline preparation are abrogated upon coupling to the VLP, as in the X-ray structure trimers pack with the loops against each other. The possibility to spot such interactions is a particular strength of the method as they may affect the availability of the antigen with an overall impact on the efficiency of the vaccine formulation.

In summary, MAS NMR spectroscopy was used to investigate the structure of the HA stalk LAH antigen both in free form and coupled to the surface of a VLP. Notably, the sensitivity and resolution afforded by high-field DNP-enhanced and ^1H -detected MAS NMR were sufficient for an atomic-level structural screening of the antigen with the extreme dilution imposed by the fusion with the large VLP

carrier. The results revealed a high structural similarity of the free and coupled forms, with noticeable differences being limited to the less well-structured regions near the N and C termini and in the inter-helix loop confirming the preservation of the trimeric helix bundle of the LAH antigen in the vaccine formulation.

The MAS NMR methodology described herein is expected to be valuable beyond applications in vaccine development, since the characterization of biomolecules upon chemical coupling is a common problem in many biotechnology problems. Some examples include covalent linking of enzymes to antibodies, protein labeling, and exposure of “addresses” on the surface of protein nanocontainers. We expect that MAS NMR with high sensitivity will be able to contribute to the structure determination of the different components after bioconjugation in these many different areas.

Acknowledgements

We acknowledge funding from Egide (Osmosis project no. 39719WH), State Education and Development Agency of Latvia (Osmoze project no. LV-FR/2018/2) and ERDF project 1.1.1./16/A/054 “Diagnostic and immunoprotective potential of influenza virus hemagglutinin stalk peptide: generation of novel vaccine prototypes”. The work was additionally funded by the European Research Council (ERC-2015-CoG GA 648974 to GP), and access to high-field NMR was cofunded by the CNRS (IR-RMN FR3050) and by the EC (project iNext GA 653706). Financial support from Equipex contracts ANR-10-EQPX-47-01 and ANR-15-CE29-0022-01 is gratefully acknowledged.

Conflict of interest

The authors declare no conflict of interest.

Keywords: antigen structure · dynamic nuclear polarization · solid-state NMR spectroscopy · vaccine development · virus-like particle

- [1] M. F. Bachmann, G. T. Jennings, *Nat. Rev. Immunol.* **2010**, *10*, 787–796.
- [2] M. F. Bachmann, U. H. Rohrer, T. M. Kündig, K. Bürki, H. Hengartner, R. M. Zinkernagel, *Science* **1993**, *262*, 1448–1451.
- [3] A. Kirsteina, I. Akopjana, J. Bogans, I. Lieknina, J. Jansons, D. Skrastina, T. Kazaka, K. Tars, I. Isakova-Sivak, D. Mezhenkaya, T. Kotomina, V. Matyushenko, L. Rudenko, A. Kazaks, *Vaccines (Basel)* **2020**, *8*, 197.
- [4] A. L. Marcinkiewicz, I. Lieknina, S. Kotelovica, X. Yang, P. Kraicz, U. Pal, Y.-P. Lin, K. Tars, *Front. Immunol.* **2018**, *9*, 181.
- [5] M. F. Bachmann, A. Zeltins, G. Kalnins, I. Balke, N. Fischer, A. Rostaher, K. Tars, C. Favrot, *J. Allergy Clin. Immunol.* **2018**, *142*, 279–281.
- [6] J. Cornuz, S. Zwahlen, W. F. Jungi, J. Osterwalder, K. Klingler, G. van Melle, Y. Bangala, I. Guessous, P. Müller, J. Willers, P. Maurer, M. F. Bachmann, T. Cerny, *PLoS One* **2008**, *3*, e2547.

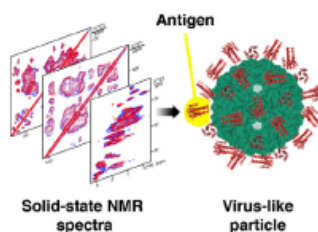
Communications



Solid-State NMR Spectroscopy

K. Jaudzems,* A. Kirsteina, T. Schubeis,
G. Casano, O. Ouari, J. Bogans,
A. Kazaks, K. Tars, A. Lesage,*
G. Pintacuda* ———— ■■■—■■■

Structural Analysis of an Antigen
Chemically Coupled on Virus-Like
Particles in Vaccine Formulation



The sensitivity boost provided by dynamic nuclear polarization and proton detection with fast magic-angle spinning renders solid-state NMR spectroscopy capable of structural analysis in heterogeneous vaccine formulations with dilute adjuvant-coupled antigens. This methodology is demonstrated on the influenza virus hemagglutinin stalk long alpha helix antigen after coupling to virus-like particles.

4. DISCUSSION

Whilst vaccination is the key to prevent influenza occurrence and mortality, antigenic drift reduces the protection afforded by pre-existing antibodies. Thus, along with the time-consuming and labor-intensive vaccine manufacturing, it has become the major challenge of seasonal IV production (Belongia et al., 2016; Gouma et al., 2020). Lately, scientific efforts have been focused on the development of a broadly protective IV that could induce diverse immunity against antigenically non-matching and emerging viral strains. Vaccines based on the evolutionarily conserved influenza antigens, such as the M2e peptide or HA stalk, show much promise as components of such broadly effective vaccine, with a potential of decreased vaccine production timeline and reduced costs (Appendix 1). A variety of broadly reactive HA stalk-specific antibodies have been identified, emphasizing its potential to afford broadly protective immunity (Wu & Wilson, 2018). Due to the immunodominance of the HA head domain, stalk-specific antibodies are generally less potent than the head-specific antibodies (Krammer, 2015; Zost et al., 2019). In order to elicit effective stalk-specific antibody levels, the vaccine should be rationally designed to expose the stalk domain to the immune system. Here, we analyzed several influenza virus HA stalk antigens in their free or VLP-displayed form for their potency to induce cross-reactive antibody responses and to protect against various influenza virus infections in mice.

The long alpha helix (LAH) from influenza HA stalk is one of the most conserved regions of this domain and it contains a great proportion of the epitopes targeted by broadly-reactive antibodies; yet, there is a notable group-specific sequence and structure divergence between different HA stalks (Joyce et al., 2016; Russell et al., 2004; T. T. Wang et al., 2010). In this thesis, we screened several constructs encoding the LAH fragment from influenza A/H1N1 or A/H3N2 viruses for their production yields and solubility. These constructs had overlapping C-termini and N-terminus of varying length. We chose two stalk antigens for downstream immunogenicity and protection studies – the LAH protein and an N-terminally extended LAH protein, referred to as tri-stalk. Our first attempts to induce stalk-reactive immunity were based on a vaccine prototype including a linear LAH epitope from the A/H3N2 virus stalk (LAH3 for short). Conformational epitopes usually have functional advantages over linear epitopes (Adachi et al., 2019; Dreyfus et al., 2013; Ekiert et al., 2009; Kallewaard et al., 2016). Here, though, the LAH3 gene was anchored at both ends preventing the folding in its native trimeric conformation. Application of genetic fusion technique to express chimeric VLPs is considered relatively easy due to the simple target gene construction as well as expression of a single fusion

protein (Chackerian, 2007). However, HA stalk is considered a problematic protein for VLP display via genetic fusion due to its hydrophobic nature, often producing inclusion bodies and requiring complex renaturation procedures (S. Chen et al., 2015; Zheng et al., 2016). Unsurprisingly, our experiments confirmed that insertion of the influenza LAH3 encoding gene into the surface exposed MIR of an HBc monomer gene yields an insoluble product.

Alternatively, the tandem core idea is based on assembly-competent HBc dimers that tolerate relatively large foreign inserts in one of the surface displayed MIR spikes (Peyret et al., 2015). We applied this technology to develop a chimeric LAH3-HBc construct that was successfully expressed in a *P. pastoris* fermentation system as soluble and assembled particles. Target proteins expressed in *P. pastoris* cells are not contaminated with bacterial endotoxins and this system is suitable for scale-up (Ahmad et al., 2014; Mamat et al., 2015). We ensured to follow the requirements for fermentation and purification scale-up to match industrial settings, which is often problematic for complex expression and purification procedures. However, in the forthcoming studies we switched the recombinant protein production to the *E. coli* expression system, as it offers more flexibility than the yeast fermentation in a bioreactor. Yet, the experience of our lab regarding the yeast expression systems should allow for rapid transfer from bacterial to yeast expression if necessary (Freivalds et al., 2014; Leitans et al., 2015). Both of these microbial platforms offer rapid high-yield cost-effective protein expression, which is particularly relevant to promptly provide a vaccine to combat seasonal influenza outbreaks and for better pandemic preparedness (Huang et al., 2017; H. J. Kim & Kim, 2017).

Although the chimeric tandem core particles displayed the LAH antigen in its linear form, they induced potent antibody responses against a variety of group 2 rHAs in mice, highlighting the key role of VLP shells in immune response enhancement. However, cross-reactive antibody responses against heterosubtypic group 1 rHAs were notably weaker than for the homologous proteins, probably owing to the linear epitope. In addition, immune responses afforded by linear stalk epitopes do not retrain the infection and therefore are associated with notable manifestations of disease symptoms (Ramirez et al., 2018; Zheng et al., 2016). As the LAH3-HBc strategy did not embrace the immunological benefits of conformational epitopes, in the subsequent studies, we attempted to display the stalk antigen in its native trimer conformation (Adachi et al., 2019). Furthermore, in the vaccine context, there is a concern that immunity against the carrier protein can diminish the immune response to its displayed foreign epitopes (McCluskie et al., 2016). Many people have pre-existing antibodies to the HBc antigen

due to vaccination or previous infection; therefore, we chose to employ bacteriophage-derived coat protein shells for our following experiments (Nelson et al., 2016).

In the next publication of this thesis, we aimed to target conformational epitopes of the HA tri-stalk and LAH antigens from A/H1N1 influenza virus to assess the diagnostic potential of the stalk-antigen. Assuring the presence of structural epitopes can have a fundamental role in induction of potent immune responses (Krammer, 2015). The crystal structure of the tri-stalk protein was therefore determined, showing a trimeric structure that almost identically matched the corresponding fragment of the full-length post-fusion HA (Bullough et al., 1994). Despite the structural conservation, in mice this protein induced only group-specific antibody responses. Previously, it has been reported that the low-pH state of HA stalk does not contain the relevant epitopes for cross-reactive antibody binding (Krammer, 2015). However, it is now known that the post-fusion stalk is also a target of cross-group specific antibody (Adachi et al., 2019). Therefore, in the context of this publication, it was probably the small size of the free tri-stalk that prevented induction of cross-reactive antibody responses, and the addition of adjuvants or a carrier platform was necessary to induce stronger immune reactions (Bachmann & Jennings, 2010). However, at this stage, our goal was to employ the tri-stalk antigen as a tool to evaluate the stalk-specific immunity. In this regard, the tri-stalk protein is an attractive antigen for downstream applications in immunological assays and vaccine research, as it is possible to easily obtain mg amounts of purified protein per each g of expression cells. The simplicity of purification should allow for a rapid scale-up if necessary.

Since the particle-displayed monomeric LAH3 induced cross-reactive yet weak antibody responses, we aimed to develop VLPs that would present the LAH antigen in its native trimeric conformation. Similar to other small RNA phages, the coat proteins of the PP7 bacteriophage are organized in a T=3 symmetry (Tars et al., 2000). Both termini of the coat protein are surface exposed, and the distance between the N-termini are, in theory, similar to the distance between the N-termini of stalk monomers. Accordingly, we assumed it would be possible to produce an assembly-competent PP7 shell that would present the HA stalk in its native trimeric conformation. However, the chimeric LAH1-PP7 proteins were produced as soluble aggregates with no way of efficiently ascertaining the formation of any trimeric LAH structures due to the irregularity of the product. Notably, although only results with the LAH1-PP7 fusion protein were featured in the publication, we screened various small RNA phages for their ability to display the stalk antigen in its trimeric conformation. We altered the coat protein C- and N-termini for target sequence insertions and tested rigid and flexible linkers of varying lengths. However, all our attempts were unsuccessful, yielding either insoluble products or

un-assembled fusion proteins. Since then, many of these phage shells have been confirmed as potent carriers for small foreign epitopes, suggesting that particle display of the stalk trimer by approach proposed in this thesis might not be possible (Liekniņa et al., 2020). Notwithstanding the lack of particle formation, LAH1-PP7 fusion protein was capable to elicit antibody responses to group 1 and group 2 rHAs in mice. Both IgG1 and IgG2a antibody subclasses prevailed equally. In mice, the IgG2a isotype is known to exhibit the best ratio of activating-to-inhibitory Fc-receptor binding and therefore to possess the strongest effector functions. Hence, the IgG2a antibody are generally considered to be the most potent IgG subclass to aid in the clearance of viral infections (DiLillo et al., 2014; Nimmerjahn & Ravetch, 2005; Schmitz et al., 2012). However, the less potent antibodies of IgG1 isotype are also able to limit viral infections and are therefore protective (Adachi et al., 2019). In general, stimulation of both IgG1 and IgG2 subclasses would be preferable for the development of potent IV (Huber et al., 2006).

Natural virus infection has shown to elicit relatively poor levels of stalk-specific antibody, which coincides with our findings with sub-lethal influenza challenge in mice (Margine et al., 2013; Zost et al., 2019). However, sequential exposure to antigenically diverse influenza viruses and infection with novel influenza subtypes tends to stimulate antibody responses directed against the stalk (Krammer et al., 2013; Nachbagauer et al., 2015, 2021; Pica et al., 2012). On the other hand, occupational contact to livestock, especially swine and poultry, has been reported as a predisposing factor to increase the antibody cross-reactivity with a variety of influenza viruses (Gerloff et al., 2011; Nelli et al., 2010; Y. Wan & Jeffrey, 2014). Hence, we proposed that the cross-immunity observed in swine-workers might be at least partially mediated by the anti-stalk antibody. The tri-stalk protein was used as the target antigen to assess the stalk-reactive immunity in the pre-pandemic sera of swine-workers. Indeed, the swine-worker sera exhibited boosted anti-stalk and H1 (A/California/4/2009) HA-specific antibody levels even before the pandemic virus had spread to Western Europe and they positively correlated with neutralizing activity against the pandemic A/H1N1 influenza virus. Our results therefore suggest that the cross-reactivity of the swine-worker sera observed in previous studies is likely the outcome of stalk-based immunity (Gerloff et al., 2011). Altogether, these observations support the potential role of the HA tri-stalk protein for evaluating HA stalk-specific immune responses in clinical and animal samples.

Up to this point, our studies suggested that both retaining the natural tertiary structure and particle display are of essential matter to induce broadly reactive immunity via the stalk antigen. Hence, the failed antigen display by genetic fusion encouraged us to apply the chemical coupling approach to yield chimeric particles. Since there are reports on particle decoration via

the modular functionalization approach with diverse conformational epitopes, it should be possible to preserve the natural trimeric structure of the stalk domain while increasing its immunogenicity via chemical coupling to VLPs (Low et al., 2014; Röhn et al., 2006). The separate production and purification of the platform and display antigens can be seen both as an advantage and disadvantage. It adds an extra step in the manufacturing; yet, both antigens can be produced in their optimal expression systems, and the VLP platform can be stockpiled in advance. Thus, in the following experiments, we expressed and purified the HA stalk antigens and VLP platforms in a modular fashion, and then covalently coupled them *in vitro* via the SATA-maleimide conjugation chemistry.

Our previous results prompted us to develop IV candidate based on the particle-displayed HA tri-stalk protein to be tested in mice. However, most stalk-specific antibodies are known to recognize viruses from the same subtype or group (Ekiert et al., 2009, 2011; Friesen et al., 2014; Kashyap et al., 2008; Okuno et al., 1993; Sui et al., 2009). We therefore hypothesized that incorporation of several conserved influenza antigens in the vaccine composition might diversify the mechanisms of the immune responses and broaden the potential cross-immunity. In this regard, we combined the genetic and chemical functionalization techniques to yield chimeric AP205 particles displaying both the tri-stalk protein and a 3M2e antigen, or either of them. While the tri-stalk alone could elicit only group-specific antibody responses, which was also observed in our previous study, particle-display enhanced its ability to elicit cross-reactive antibodies (Lu et al., 2018). The potency of the induced antibody responses correlated with the conservation degree between the tri-stalk and target antigen, with more distant rHAs eliciting lower antibody responses. Hence, cross-reactivity of this vaccine candidate could be greatly improved with addition of a group 2 stalk antigen. In our study, the majority of antibody elicited by the stalk and M2e proteins were of IgG1 subclass, but particle delivery increased the proportion of IgG2a antibody, probably, owing to the encapsulated nucleic acid (Schmitz et al., 2012).

The challenge experiments allowed us to evaluate the potency of induced antibody to protect against lethal influenza virus infections and confirmed our hypothesis that the inclusion of multiple conserved antigens in a vaccine increases its efficacy. The tri-stalk antigen afforded substantial, yet partial, protection only against group 1 viruses. Although the AP-M2e particles were protective in the challenge experiments with heterologous and heterosubtypic A/H1N1 PR8, A/H3N2 and A/H5N1 viruses, they could not confer protection against a high-dose lethal infection with A/H1N1 Cal/09 virus. Confirming our assumption, only the multimeric particles displaying both the tri-stalk and 3M2e antigens afforded strong protection against the high-dose

challenge. Although the tri-stalk displaying particles were less protective in this lethal challenge than we anticipated, the high-dose challenge emphasized the role of tri-stalk induced protective immunity.

The protective effect of both the tri-stalk and 3M2e was afforded mainly by antibody responses, as confirmed by serum-transfer experiments. The post-fusion HA stalk and M2e antigens are known to confer infection-permissive immunity, meaning that the induced antibodies are generally non-sterilizing (Adachi et al., 2019; El Bakkouri et al., 2011; Fu et al., 2009). Hence, their induced protection is largely attributed to antibody effector functions which, in turn, are associated with broader immune responses (DiLillo et al., 2014, 2014, 2016; El Bakkouri et al., 2011; Kolpe et al., 2017; Y.-N. Lee et al., 2014; Nimmerjahn & Ravetch, 2005; Srivastava et al., 2013). Consistent with the above, the stalk-induced protection in this thesis was predominantly mediated by effector mechanisms, but the 3M2e antigen induced both effector activity and some CD4⁺ T-cells responses. Cell-mediated immune responses are linked with better protective immunity in older adults and associated with long-term protection in mice (Eliasson et al., 2018; McElhaney et al., 2006). Likewise, the stalk- and M2e-directed antibodies are associated with longevity, which could potentially alleviate the problem of plummeting immune responses of conventional IV (Adachi et al., 2019; Schotsaert et al., 2016; Young et al., 2018). The long-term protection, however, was not assessed in this thesis and should be a subject of our future studies. The infection-permissive immunity can be viewed as a disadvantage as individuals might still become infected. On the other hand, the limited viral replication that occurs can induce additional immune mechanisms (e.g. HA-specific antibody responses and CD8⁺ T-cells), enhancing subsequent heterosubtypic protection, and is less likely to produce virus escape mutants (Bodewes et al., 2010; Choi et al., 2020; Kirkpatrick et al., 2018; Y.-N. Lee et al., 2016). Notably, even though the protection afforded by the multivalent VLPs was non-sterilizing, only minor clinical symptoms were observed, highlighting the strength of these immune responses in the suppression of virus replication. There are, however, open questions regarding virus shedding and virus clearance in vaccinated virus-infected animals that should be addressed in our forthcoming studies.

Nevertheless, up to this point, we had no information about the structural characteristics of the surface-displayed stalk antigen. Covalent binding can disrupt the conformation of the display antigen that can reduce vaccine effectiveness (Brune & Howarth, 2018; Kumru et al., 2014). Thus, information about the structural preservation is critical to design a vaccine with the optimal immunogenicity. Yet, although the coupling can be confirmed by SDS/PAGE and the particle integrity – by electron microscopy, it is challenging to assess the structural features

of the display antigen. The VLP decoration via the SATA reagent occurs randomly, yielding heterogeneous particles. The uneven decoration makes it difficult to analyze these particles by X-ray crystallography or cryogenic electron microscopy, and they are too large to be characterized by solution nuclear magnetic resonance (NMR) (Brune & Howarth, 2018; Demers et al., 2018). In this respect, the magic-angle spinning (MAS) solid-state NMR spectroscopy technique has lately proven to be a suitable tool in the studies of large and complex protein assemblies (Cerofolini et al., 2019; Demers et al., 2018; Mandala & Hong, 2019). Therefore, in the remaining publication of this thesis, we aimed to analyze the structure of free and VLP-displayed LAH1 antigen by MAS NMR.

The superimposition of HA LAH1 trimer structures, determined by the X-ray crystallography and the conventional MAS NMR with free, uniformly ^{13}C - and ^{15}N -labeled antigen, revealed matching structures. The above methods, however, were not applicable to analyze the structure of labeled LAH antigen in a VLP-bound state. The VLP-displayed LAH most likely occupies as little as 1/10 of the sample volume, but a small amount of protein bound to the particle is associated with an NMR signal sensitivity drop. Furthermore, the conventional MAS NMR requires large amounts of the labeled protein material, which is difficult to acquire in the lab-scale chimeric vaccine context (Demers et al., 2018; Mandala & Hong, 2019). Nevertheless, these limitations can be overcome as the sensitivity of MAS NMR has increased with recent advances in the high-field dynamic nuclear polarization (DNP) and high-resolution proton detection (Andreas et al., 2015; Jaudzems et al., 2019; Mandala & Hong, 2019). Complementary application of these technologies allowed us to determine the structure of VLP-coupled LAH antigen – the covalent immobilization did not disrupt the structural integrity of the LAH protein and it preserved its trimeric folding state. In addition, we acquired structural information about the dynamic regions of the antigen, which are typically difficult to analyze. This is particularly relevant in the vaccine research context as any conformational changes can disturb antibody-binding epitopes and reduce the potency of the vaccine to elicit relevant antibodies. To our knowledge, we are the first to report an atomic-level structure of a VLP-displayed antigen; yet, these findings suggest that hereafter MAS NMR might become a widespread tool for applications in vaccine development and other fields.

Our results herein indicate that broadening the mechanisms of the immune responses can also induce more potent and cross-protective immunity against distinct influenza viruses. However, this thesis is intended as a proof-of-concept study, not as a final vaccine. Further vaccine development could benefit from incorporation of additional conserved viral components to enhance vaccine potency, such as group 2 HA tri-stalk, pre-fusion stalk, or

fivefold tandem repeat epitopes of the M2e antigen (M.-C. Kim et al., 2013; Y.-N. Lee et al., 2016; Valkenburg et al., 2016). Other vaccine delivery routes should also be considered, as mucosal administration with relevant adjuvants has been shown to increase IV efficacy (Calzas & Chevalier, 2019). However, the recombinant production of our vaccine candidate in a microbial system as well as its ability to provide heterosubtypic protection help to overcome several of the conventional vaccine limitations. Thus, the multivalent vaccine candidate presented in this thesis has the potential to limit the spread of seasonal and emerging influenza viruses and replace the current vaccination strategies.

5. CONCLUSIONS

1. The HA tri-stalk and LAH proteins in their free form adopt a trimeric fold that corresponds to the post-fusion conformation of full-length HA.
2. The native trimeric fold of the HA LAH is preserved upon chemical coupling to the VLP surface.
3. The high sensitivity MAS NMR is a particularly useful tool for structure characterization of antigens in heterogeneous and large biomolecule assemblies that cannot be produced in large quantities.
4. The cross-reactivity of pre-pandemic sera of swine-workers is likely at least partially mediated by the anti-stalk antibody.
5. While the tri-stalk trimer is highly immunogenic in its free form, VLP display significantly increases its ability to induce cross-reactive antibody responses.
6. The conservation degree between the HA stalk and target virus HA is a correlate of the potency of the induced antibody responses.
7. Vaccination with free or VLP-displayed tri-stalk is not sufficient to provide complete protection against lethal influenza challenge in mice, therefore, it is likely to serve as one of the several components of a broadly reactive influenza vaccine.
8. Combination of tri-stalk and a triple M2e antigen presented on a single particle induces robust and heterosubtypic protective immunity in mice.

6. THESIS

1. VLP-display of weak influenza immunogens can beneficially affect antibody cross-reactivity with heterologous influenza viruses.
2. The tri-stalk protein has a high potential to be used as a tool for evaluation of HA stalk-specific immunity in clinical and animal samples.
3. Combination of genetic and chimeric functionalization techniques to display multiple antigens on a single virus-like particle is a perspective approach to generate multivalent vaccine candidates.
4. Targeting multiple conserved influenza antigens can broaden the induced immune mechanisms and confer more potent cross-protection.

7. PUBLICATIONS

I. Kazaks A., Lu I. N., Farinelle S., Ramirez A., Crescente V., Blaha B., Ogonah O., Mukhopadhyay T., de Obanos M. P., Krimer A., Akopjana I., Bogans J., Ose V., **Kirsteina A.**, Kazaka T., Stonehouse N. J., Rowlands D. J., Muller C. P., Tars K., & Rosenberg W. M. (2017). Production and Purification of Chimeric HBc Virus-like Particles Carrying Influenza Virus LAH Domain As Vaccine Candidates. *BMC biotechnology*, 17(1), 79. <https://doi.org/10.1186/s12896-017-0396-8>

II. Lu I. N.[#], **Kirsteina A.**[#], Farinelle S., Willieme S., Tars K., Muller C. P., & Kazaks A. (2018). Structure and Applications of Novel Influenza HA Tri-stalk Protein for Evaluation of HA Stem-specific Immunity. *PloS one*, 13(9), e0204776. <https://doi.org/10.1371/journal.pone.0204776>

[#]Contributed equally

III. **Kirsteina A.**, Akopjana I., Bogans J., Lieknina I., Jansons J., Skrastina D., Kazaka, T., Tars K., Isakova-Sivak I., Mezhenskaya D., Kotomina T., Matyushenko V., Rudenko L., & Kazaks A. (2020). Construction and Immunogenicity of a Novel Multivalent Vaccine Prototype Based on Conserved Influenza Virus Antigens. *Vaccines*, 8(2), 197. <https://doi.org/10.3390/vaccines8020197>

IV. Jaudzems K., **Kirsteina A.**, Schubeis T., Casano G., Ouari O., Bogans J., Kazaks A., Tars K., Lesage A., & Pintacuda G. (2021). Structural Analysis of an Antigen Chemically Coupled on Virus-Like Particles in Vaccine Formulation. *Angewandte Chemie (International ed. in English)*, 60(23), 12847–12851. <https://doi.org/10.1002/anie.202013189>

8. APPROBATION OF THE RESEARCH

1. **Kirsteina A.**, Akopjana I., Bogans J., Lieknina I., Jansons J., Skrastina D., Kazaka K., Tars K., Isakova-Sivak I., Mezhenskaya D., Kotomina T., Matyushenko V., Rudenko L., Kazaks A. Construction and immunogenicity of a novel multivalent vaccine prototype based on conserved influenza virus antigens. 14th Vaccine Congress. Poster presentation. Online event, 2020.
2. **Kirsteina A.**, Akopjana I., Bogans J., Kazaka T., Tars K., Kazaks A. Construction of a novel multivalent vaccine based on conserved influenza virus antigens. 13th Vaccine Congress. Poster presentation. 2019, Bangkok, Thailand.
3. **Kirsteina A.**, Akopjana I., Bogans J., Kazaka T., Kazaks A. Construction of a novel multivalent influenza vaccine based on conserved influenza antigens. 1st Latvian Biochemical Society FEBS3+ conference. Oral presentation. 2019, Riga, Latvia.
4. **Kirsteina A.**, Akopjana I., Bogans J., Kazaka T., Tars K., Kazaks A. Structure of trimeric influenza hemagglutinin stalk fragment and its exposition on the surface of virus like particles. Virus-Like Particle & Nano-Particle Vaccines conference. Poster presentation. 2018, Bern, Switzerland.
5. **Kirsteina A.**, Akopjana I., Kazaka T., Tars K., Kazaks A. Incorporation of universal influenza virus antigens into virus-like particles. 76th International Scientific Conference of the University of Latvia, Molecular Biology Section. Oral presentation. 2018, Riga, Latvia.
6. **Kirsteina A.**, Lu I. N., Farinelle S., Akopjana I., Kazaka T., Muller C. P., Tars K., Kazaks A. Construction of virus-like particles carrying homotrimeric LAH domain from hemagglutinin stalk as potential influenza vaccine candidates. Virus-Like Particle & Nano-Particle Vaccines conference. Poster presentation. 2017, Singapore.
7. **Kirsteina A.**, Lu I., Farinelle S., Muller C. P., Tars K., Kazaks A. Expression, purification and immunological properties of influenza virus hemagglutinin peptides. 75th International Scientific Conference of the University of Latvia, Molecular Biology Section. Oral presentation. 2017, Riga, Latvia.

9. ACKNOWLEDGEMENTS AND FUNDING

The research was supported by the EU Seventh Framework Programme for research (No. 602,437), ERDF grant (No. 1.1.1.1/16/A/054), Egide (Osmosis project No. 39719WH), State Education and Development Agency of Latvia (Osmosis project No. LV-FR/2018/2), European Research Council (ERC-2015-CoG GA 648974 to GP), CNRS (IR-RMN FR3050), EC (project iNext GA 653706), and Equipex contracts (ANR-10-EQPX-47-01; ANR-15-CE29-0022-01).

My deepest gratitude goes to my supervisor, Dr. biol. Andris Kazāks, whose patience, guidance, and continuous support have motivated me during my research and helped to bring my work to a higher level. I kindly thank all my colleagues from the BMC Structural Biology group for the motivating environment and advice. Many thanks to Ināra Akopjana for never refusing to help and willingness to answer my countless questions through the years. I am thankful to professor Kaspars Tārs for guiding me through the determination of protein crystal structures and to Jānis Leitāns, who helped me to deposit these structures in the PDB. I acknowledge all the people who contributed to data acquisition, especially, Jānis Bogāns for support with protein purification and Juris Jansons for help with electron microscopy, as well as my co-authors, particularly, I-Na Lu, Irina Isakova-Sivak, and Kristaps Jaudzems, for making this project possible.

I would also like to thank the Foundation of the University of Latvia for the financial support with a scholarship during my PhD studies.

Special thanks to Elīna and Elviss for helping to keep me sane in the long lab hours, to my friends Zane and Anna for our joint struggles with the PhD studies, and to my partner Ansis for believing in me when I myself could not.

REFERENCES

- Acosta, E., Hallman, S. A., Dillon, L. Y., Ouellette, N., Bourbeau, R., Herring, D. A., Inwood, K., Earn, D. J. D., Madrenas, J., Miller, M. S., & Gagnon, A. (2019). Determinants of Influenza Mortality Trends: Age-Period-Cohort Analysis of Influenza Mortality in the United States, 1959-2016. *Demography*, *56*(5), 1723–1746. <https://doi.org/10.1007/s13524-019-00809-y>
- Adachi, Y., Tonouchi, K., Nithichanon, A., Kuraoka, M., Watanabe, A., Shinnakasu, R., Asanuma, H., Aina, A., Ohmi, Y., Yamamoto, T., Ishii, K. J., Hasegawa, H., Takeyama, H., Lertmemongkolchai, G., Kurosaki, T., Ato, M., Kelsoe, G., & Takahashi, Y. (2019). Exposure of an occluded hemagglutinin epitope drives selection of a class of cross-protective influenza antibodies. *Nature Communications*, *10*(1), 3883. <https://doi.org/10.1038/s41467-019-11821-6>
- Ahmad, M., Hirz, M., Pichler, H., & Schwab, H. (2014). Protein expression in *Pichia pastoris*: Recent achievements and perspectives for heterologous protein production. *Applied Microbiology and Biotechnology*, *98*(12), 5301–5317. <https://doi.org/10.1007/s00253-014-5732-5>
- Ahsan, F., Rivas, I. P., Khan, M. A., & Torres Suarez, A. I. (2002). Targeting to macrophages: Role of physicochemical properties of particulate carriers--liposomes and microspheres--on the phagocytosis by macrophages. *Journal of Controlled Release: Official Journal of the Controlled Release Society*, *79*(1–3), 29–40. [https://doi.org/10.1016/s0168-3659\(01\)00549-1](https://doi.org/10.1016/s0168-3659(01)00549-1)
- Alvarez, P., Zylberman, V., Ghersi, G., Boado, L., Palacios, C., Goldbaum, F., & Mattion, N. (2013). Tandem repeats of the extracellular domain of Matrix 2 influenza protein exposed in *Brucella lumazine synthase* decameric carrier molecule induce protection in mice. *Vaccine*, *31*(5), 806–812. <https://doi.org/10.1016/j.vaccine.2012.11.072>
- Andersson, A.-M. C., Håkansson, K. O., Jensen, B. A. H., Christensen, D., Andersen, P., Thomsen, A. R., & Christensen, J. P. (2012). Increased immunogenicity and protective efficacy of influenza M2e fused to a tetramerizing protein. *PLoS One*, *7*(10), e46395. <https://doi.org/10.1371/journal.pone.0046395>
- Andreas, L. B., Le Marchand, T., Jaudzems, K., & Pintacuda, G. (2015). High-resolution proton-detected NMR of proteins at very fast MAS. *Journal of Magnetic Resonance (San Diego, Calif.: 1997)*, *253*, 36–49. <https://doi.org/10.1016/j.jmr.2015.01.003>
- Arranz, R., Coloma, R., Chichón, F. J., Conesa, J. J., Carrascosa, J. L., Valpuesta, J. M., Ortín, J., & Martín-Benito, J. (2012). The structure of native influenza virion ribonucleoproteins. *Science (New York, N.Y.)*, *338*(6114), 1634–1637. <https://doi.org/10.1126/science.1228172>
- Asha, K., & Kumar, B. (2019). Emerging Influenza D Virus Threat: What We Know so Far! *Journal of Clinical Medicine*, *8*(2), E192. <https://doi.org/10.3390/jcm8020192>
- Atcheson, E., Hill, A. V. S., & Reyes-Sandoval, A. (2021). A VLP for validation of the *Plasmodium falciparum* circumsporozoite protein junctional epitope for vaccine development. *NPJ Vaccines*, *6*(1), 46. <https://doi.org/10.1038/s41541-021-00302-x>
- Austyn, J. M. (2016). Dendritic Cells in the Immune System-History, Lineages, Tissues, Tolerance, and Immunity. *Microbiology Spectrum*, *4*(6). <https://doi.org/10.1128/microbiolspec.MCHD-0046-2016>
- Bachmann, M. F., & Jennings, G. T. (2010). Vaccine delivery: A matter of size, geometry, kinetics and molecular patterns. *Nature Reviews. Immunology*, *10*(11), 787–796. <https://doi.org/10.1038/nri2868>
- Bachmann, M. F., & Zinkernagel, R. M. (1997). Neutralizing antiviral B cell responses. *Annual Review of Immunology*, *15*, 235–270. <https://doi.org/10.1146/annurev.immunol.15.1.235>
- Bahar, M. W., Porta, C., Fox, H., Macadam, A. J., Fry, E. E., & Stuart, D. I. (2021). Mammalian expression of virus-like particles as a proof of principle for next generation polio vaccines. *NPJ Vaccines*, *6*(1), 5. <https://doi.org/10.1038/s41541-020-00267-3>
- Balke, I., & Zeltins, A. (2020). Recent Advances in the Use of Plant Virus-Like Particles as Vaccines. *Viruses*, *12*(3), E270. <https://doi.org/10.3390/v12030270>
- Bangaru, S., Lang, S., Schotsaert, M., Vandervan, H. A., Zhu, X., Kose, N., Bombardi, R., Finn, J. A., Kent, S. J., Gilchuk, P., Gilchuk, I., Turner, H. L., García-Sastre, A., Li, S., Ward, A. B., Wilson, I. A., & Crowe, J. E. (2019). A Site of Vulnerability on the Influenza Virus Hemagglutinin Head Domain Trimer Interface. *Cell*, *177*(5), 1136–1152.e18. <https://doi.org/10.1016/j.cell.2019.04.011>
- Barr, I. G., Donis, R. O., Katz, J. M., McCauley, J. W., Odagiri, T., Trusheim, H., Tsai, T. F., & Wentworth, D. E. (2018). Cell culture-derived influenza vaccines in the severe 2017-2018 epidemic season: A step towards improved influenza vaccine effectiveness. *NPJ Vaccines*, *3*, 44. <https://doi.org/10.1038/s41541-018-0079-z>
- Barrington, R. A., Pozdnyakova, O., Zafari, M. R., Benjamin, C. D., & Carroll, M. C. (2002). B lymphocyte memory: Role of stromal cell complement and FcγRIIB receptors. *The Journal of Experimental Medicine*, *196*(9), 1189–1199. <https://doi.org/10.1084/jem.20021110>

- Basnak, G., Morton, V. L., Rolfsson, O., Stonehouse, N. J., Ashcroft, A. E., & Stockley, P. G. (2010). Viral genomic single-stranded RNA directs the pathway toward a T=3 capsid. *Journal of Molecular Biology*, 395(5), 924–936. <https://doi.org/10.1016/j.jmb.2009.11.018>
- Batista, F. D., & Harwood, N. E. (2009). The who, how and where of antigen presentation to B cells. *Nature Reviews. Immunology*, 9(1), 15–27. <https://doi.org/10.1038/nri2454>
- Battye, T. G. G., Kontogiannis, L., Johnson, O., Powell, H. R., & Leslie, A. G. W. (2011). iMOSFLM: A new graphical interface for diffraction-image processing with MOSFLM. *Acta Crystallographica. Section D, Biological Crystallography*, 67(Pt 4), 271–281. <https://doi.org/10.1107/S0907444910048675>
- Baudin, F., Bach, C., Cusack, S., & Ruigrok, R. W. (1994). Structure of influenza virus RNP. I. Influenza virus nucleoprotein melts secondary structure in panhandle RNA and exposes the bases to the solvent. *The EMBO Journal*, 13(13), 3158–3165.
- Beale, R., Wise, H., Stuart, A., Ravenhill, B. J., Digard, P., & Randow, F. (2014). A LC3-interacting motif in the influenza A virus M2 protein is required to subvert autophagy and maintain virion stability. *Cell Host & Microbe*, 15(2), 239–247. <https://doi.org/10.1016/j.chom.2014.01.006>
- Bedford, T., Riley, S., Barr, I. G., Broor, S., Chadha, M., Cox, N. J., Daniels, R. S., Gunasekaran, C. P., Hurt, A. C., Kelso, A., Klimov, A., Lewis, N. S., Li, X., McCauley, J. W., Odagiri, T., Potdar, V., Rambaut, A., Shu, Y., Skepner, E., ... Russell, C. A. (2015). Global circulation patterns of seasonal influenza viruses vary with antigenic drift. *Nature*, 523(7559), 217–220. <https://doi.org/10.1038/nature14460>
- Belongia, E. A., Simpson, M. D., King, J. P., Sundaram, M. E., Kelley, N. S., Osterholm, M. T., & McLean, H. Q. (2016). Variable influenza vaccine effectiveness by subtype: A systematic review and meta-analysis of test-negative design studies. *The Lancet. Infectious Diseases*, 16(8), 942–951. [https://doi.org/10.1016/S1473-3099\(16\)00129-8](https://doi.org/10.1016/S1473-3099(16)00129-8)
- Belshe, R. B. (2010). The need for quadrivalent vaccine against seasonal influenza. *Vaccine*, 28 Suppl 4, D45-53. <https://doi.org/10.1016/j.vaccine.2010.08.028>
- Benton, D. J., Gamblin, S. J., Rosenthal, P. B., & Skehel, J. J. (2020). Structural transitions in influenza haemagglutinin at membrane fusion pH. *Nature*, 583(7814), 150–153. <https://doi.org/10.1038/s41586-020-2333-6>
- Bernstein, D. I., Guptill, J., Naficy, A., Nachbagauer, R., Berlanda-Scorza, F., Feser, J., Wilson, P. C., Solórzano, A., Van der Wielen, M., Walter, E. B., Albrecht, R. A., Buschle, K. N., Chen, Y.-Q., Claey, C., Dickey, M., Dugan, H. L., Ermler, M. E., Freeman, D., Gao, M., ... Krammer, F. (2020). Immunogenicity of chimeric haemagglutinin-based, universal influenza virus vaccine candidates: Interim results of a randomised, placebo-controlled, phase 1 clinical trial. *The Lancet. Infectious Diseases*, 20(1), 80–91. [https://doi.org/10.1016/S1473-3099\(19\)30393-7](https://doi.org/10.1016/S1473-3099(19)30393-7)
- Billaud, J.-N., Peterson, D., Barr, M., Chen, A., Sallberg, M., Garduno, F., Goldstein, P., McDowell, W., Hughes, J., Jones, J., & Milich, D. (2005). Combinatorial approach to hepadnavirus-like particle vaccine design. *Journal of Virology*, 79(21), 13656–13666. <https://doi.org/10.1128/JVI.79.21.13656-13666.2005>
- Black, R. A., Rota, P. A., Gorodkova, N., Klenk, H. D., & Kendal, A. P. (1993). Antibody response to the M2 protein of influenza A virus expressed in insect cells. *The Journal of General Virology*, 74 (Pt 1), 143–146. <https://doi.org/10.1099/0022-1317-74-1-143>
- Bodewes, R., Kreijtz, J. H. C. M., Hillaire, M. L. B., Geelhoed-Mieras, M. M., Fouchier, R. A. M., Osterhaus, A. D. M. E., & Rimmelzwaan, G. F. (2010). Vaccination with whole inactivated virus vaccine affects the induction of heterosubtypic immunity against influenza virus A/H5N1 and immunodominance of virus-specific CD8+ T-cell responses in mice. *The Journal of General Virology*, 91(Pt 7), 1743–1753. <https://doi.org/10.1099/vir.0.020784-0>
- Boivin, S., Cusack, S., Ruigrok, R. W. H., & Hart, D. J. (2010). Influenza A virus polymerase: Structural insights into replication and host adaptation mechanisms. *The Journal of Biological Chemistry*, 285(37), 28411–28417. <https://doi.org/10.1074/jbc.R110.117531>
- Bommakanti, G., Lu, X., Citron, M. P., Najjar, T. A., Heidecker, G. J., ter Meulen, J., Varadarajan, R., & Liang, X. (2012). Design of Escherichia coli-expressed stalk domain immunogens of H1N1 hemagglutinin that protect mice from lethal challenge. *Journal of Virology*, 86(24), 13434–13444. <https://doi.org/10.1128/JVI.01429-12>
- Bottazzi, B., Doni, A., Garlanda, C., & Mantovani, A. (2010). An integrated view of humoral innate immunity: Pentraxins as a paradigm. *Annual Review of Immunology*, 28, 157–183. <https://doi.org/10.1146/annurev-immunol-030409-101305>
- Braakman, I., Hoover-Litty, H., Wagner, K. R., & Helenius, A. (1991). Folding of influenza hemagglutinin in the endoplasmic reticulum. *The Journal of Cell Biology*, 114(3), 401–411. <https://doi.org/10.1083/jcb.114.3.401>
- Brandenburg, B., Koudstaal, W., Goudsmit, J., Klaren, V., Tang, C., Bujny, M. V., Korse, H. J. W. M., Kwaks, T., Otterstrom, J. J., Juraszek, J., van Oijen, A. M., Vogels, R., & Friesen, R. H. E. (2013). Mechanisms of hemagglutinin targeted influenza virus neutralization. *PloS One*, 8(12), e80034. <https://doi.org/10.1371/journal.pone.0080034>

- Bresee, J., Fitzner, J., Campbell, H., Cohen, C., Cozza, V., Jara, J., Krishnan, A., Lee, V., & WHO Working Group on the Burden of Influenza Disease. (2018). Progress and Remaining Gaps in Estimating the Global Disease Burden of Influenza. *Emerging Infectious Diseases*, 24(7), 1173–1177. <https://doi.org/10.3201/eid2407.171270>
- Broadbent, A. J., & Subbarao, K. (2011). Influenza virus vaccines: Lessons from the 2009 H1N1 pandemic. *Current Opinion in Virology*, 1(4), 254–262. <https://doi.org/10.1016/j.coviro.2011.08.002>
- Brune, K. D., & Howarth, M. (2018). New Routes and Opportunities for Modular Construction of Particulate Vaccines: Stick, Click, and Glue. *Frontiers in Immunology*, 9, 1432. <https://doi.org/10.3389/fimmu.2018.01432>
- Brune, K. D., Leneghan, D. B., Brian, I. J., Ishizuka, A. S., Bachmann, M. F., Draper, S. J., Biswas, S., & Howarth, M. (2016). Plug-and-Display: Decoration of Virus-Like Particles via isopeptide bonds for modular immunization. *Scientific Reports*, 6, 19234. <https://doi.org/10.1038/srep19234>
- Bullough, P. A., Hughson, F. M., Skehel, J. J., & Wiley, D. C. (1994). Structure of influenza haemagglutinin at the pH of membrane fusion. *Nature*, 371(6492), 37–43. <https://doi.org/10.1038/371037a0>
- Bundy, B. C., & Swartz, J. R. (2011). Efficient disulfide bond formation in virus-like particles. *Journal of Biotechnology*, 154(4), 230–239. <https://doi.org/10.1016/j.jbiotec.2011.04.011>
- Caini, S., Huang, Q. S., Ciblak, M. A., Kuszniarz, G., Owen, R., Wangchuk, S., Henriques, C. M. P., Njouom, R., Fasce, R. A., Yu, H., Feng, L., Zambon, M., Clara, A. W., Kosasih, H., Puzelli, S., Kadjo, H. A., Emukule, G., Heraud, J.-M., Ang, L. W., ... Global Influenza B Study. (2015). Epidemiological and virological characteristics of influenza B: Results of the Global Influenza B Study. *Influenza and Other Respiratory Viruses*, 9 Suppl 1, 3–12. <https://doi.org/10.1111/irv.12319>
- Calzas, C., & Chevalier, C. (2019). Innovative Mucosal Vaccine Formulations Against Influenza A Virus Infections. *Frontiers in Immunology*, 10, 1605. <https://doi.org/10.3389/fimmu.2019.01605>
- Carr, C. M., Chaudhry, C., & Kim, P. S. (1997). Influenza hemagglutinin is spring-loaded by a metastable native conformation. *Proceedings of the National Academy of Sciences of the United States of America*, 94(26), 14306–14313. <https://doi.org/10.1073/pnas.94.26.14306>
- Carrico, Z. M., Farkas, M. E., Zhou, Y., Hsiao, S. C., Marks, J. D., Chokhawala, H., Clark, D. S., & Francis, M. B. (2012). N-Terminal labeling of filamentous phage to create cancer marker imaging agents. *ACS Nano*, 6(8), 6675–6680. <https://doi.org/10.1021/nn301134z>
- Carroll, M. C., & Isenman, D. E. (2012). Regulation of humoral immunity by complement. *Immunity*, 37(2), 199–207. <https://doi.org/10.1016/j.immuni.2012.08.002>
- Carter, C., Houser, K. V., Yamshchikov, G. V., Bellamy, A. R., May, J., Enama, M. E., Sarwar, U., Larkin, B., Bailer, R. T., Koup, R., Chen, G. L., Patel, S. M., Winokur, P., Belshe, R., Dekker, C. L., Graham, B. S., Ledgerwood, J. E., & VRC 703 study team. (2019). Safety and immunogenicity of investigational seasonal influenza hemagglutinin DNA vaccine followed by trivalent inactivated vaccine administered intradermally or intramuscularly in healthy adults: An open-label randomized phase 1 clinical trial. *PLoS One*, 14(9), e0222178. <https://doi.org/10.1371/journal.pone.0222178>
- Caton, A. J., Brownlee, G. G., Yewdell, J. W., & Gerhard, W. (1982). The antigenic structure of the influenza virus A/PR/8/34 hemagglutinin (H1 subtype). *Cell*, 31(2 Pt 1), 417–427. [https://doi.org/10.1016/0092-8674\(82\)90135-0](https://doi.org/10.1016/0092-8674(82)90135-0)
- CDC. (2019). *Influenza Historic Timeline | Pandemic Influenza (Flu) | CDC*. <https://www.cdc.gov/flu/pandemic-resources/pandemic-timeline-1930-and-beyond.htm>
- CDC. (2021a). *CDC Seasonal Flu Vaccine Effectiveness Studies | CDC*. <https://www.cdc.gov/flu/vaccines-work/effectiveness-studies.htm>
- CDC. (2021b). *Leading Causes of Death*. <https://www.cdc.gov/nchs/fastats/leading-causes-of-death.htm>
- Cerofolini, L., Giuntini, S., Ravera, E., Luchinat, C., Berti, F., & Fragai, M. (2019). Structural characterization of a protein adsorbed on aluminum hydroxide adjuvant in vaccine formulation. *NPJ Vaccines*, 4, 20. <https://doi.org/10.1038/s41541-019-0115-7>
- Chackerian, B. (2007). Virus-like particles: Flexible platforms for vaccine development. *Expert Review of Vaccines*, 6(3), 381–390. <https://doi.org/10.1586/14760584.6.3.381>
- Chackerian, B., Rangel, M., Hunter, Z., & Peabody, D. S. (2006). Virus and virus-like particle-based immunogens for Alzheimer's disease induce antibody responses against amyloid-beta without concomitant T cell responses. *Vaccine*, 24(37–39), 6321–6331. <https://doi.org/10.1016/j.vaccine.2006.05.059>
- Chen, B. J., Leser, G. P., Jackson, D., & Lamb, R. A. (2008). The influenza virus M2 protein cytoplasmic tail interacts with the M1 protein and influences virus assembly at the site of virus budding. *Journal of Virology*, 82(20), 10059–10070. <https://doi.org/10.1128/JVI.01184-08>
- Chen, J., Skehel, J. J., & Wiley, D. C. (1999). N- and C-terminal residues combine in the fusion-pH influenza hemagglutinin HA(2) subunit to form an N cap that terminates the triple-stranded coiled coil. *Proceedings of the National Academy of Sciences of the United States of America*, 96(16), 8967–8972. <https://doi.org/10.1073/pnas.96.16.8967>
- Chen, J., Wharton, S. A., Weissenhorn, W., Calder, L. J., Hughson, F. M., Skehel, J. J., & Wiley, D. C. (1995). A soluble domain of the membrane-anchoring chain of influenza virus hemagglutinin (HA2) folds in Escherichia

- coli into the low-pH-induced conformation. *Proceedings of the National Academy of Sciences of the United States of America*, 92(26), 12205–12209. <https://doi.org/10.1073/pnas.92.26.12205>
- Chen, J.-R., Liu, Y.-M., Tseng, Y.-C., & Ma, C. (2020). Better influenza vaccines: An industry perspective. *Journal of Biomedical Science*, 27(1), 33. <https://doi.org/10.1186/s12929-020-0626-6>
- Chen, S., Zheng, D., Li, C., Zhang, W., Xu, W., Liu, X., Fang, F., & Chen, Z. (2015). Protection against multiple subtypes of influenza viruses by virus-like particle vaccines based on a hemagglutinin conserved epitope. *BioMed Research International*, 2015, 901817. <https://doi.org/10.1155/2015/901817>
- Chen, W., Calvo, P. A., Malide, D., Gibbs, J., Schubert, U., Bacik, I., Basta, S., O'Neill, R., Schickli, J., Palese, P., Henklein, P., Bennink, J. R., & Yewdell, J. W. (2001). A novel influenza A virus mitochondrial protein that induces cell death. *Nature Medicine*, 7(12), 1306–1312. <https://doi.org/10.1038/nm1201-1306>
- Choi, A., Ibañez, L. I., Strohmeier, S., Krammer, F., García-Sastre, A., & Schotsaert, M. (2020). Non-sterilizing, Infection-Permissive Vaccination With Inactivated Influenza Virus Vaccine Reshapes Subsequent Virus Infection-Induced Protective Heterosubtypic Immunity From Cellular to Humoral Cross-Reactive Immune Responses. *Frontiers in Immunology*, 11, 1166. <https://doi.org/10.3389/fimmu.2020.01166>
- Chothe, S. K., Bhushan, G., Nissly, R. H., Yeh, Y.-T., Brown, J., Turner, G., Fisher, J., Sewall, B. J., Reeder, D. M., Terrones, M., Jayarao, B. M., & Kuchipudi, S. V. (2017). Avian and human influenza virus compatible sialic acid receptors in little brown bats. *Scientific Reports*, 7(1), 660. <https://doi.org/10.1038/s41598-017-00793-6>
- Clark, T. W., Pareek, M., Hoschler, K., Dillon, H., Nicholson, K. G., Groth, N., & Stephenson, I. (2009). Trial of 2009 influenza A (H1N1) monovalent MF59-adjuvanted vaccine. *The New England Journal of Medicine*, 361(25), 2424–2435. <https://doi.org/10.1056/NEJMoa0907650>
- Clifford, M., Twigg, J., & Upton, C. (2009). Evidence for a novel gene associated with human influenza A viruses. *Virology Journal*, 6, 198. <https://doi.org/10.1186/1743-422X-6-198>
- Cohen, M., Zhang, X.-Q., Senaati, H. P., Chen, H.-W., Varki, N. M., Schooley, R. T., & Gagneux, P. (2013). Influenza A penetrates host mucus by cleaving sialic acids with neuraminidase. *Virology Journal*, 10, 321. <https://doi.org/10.1186/1743-422X-10-321>
- Coleman, B. L., Fadel, S. A., Fitzpatrick, T., & Thomas, S.-M. (2018). Risk factors for serious outcomes associated with influenza illness in high- versus low- and middle-income countries: Systematic literature review and meta-analysis. *Influenza and Other Respiratory Viruses*, 12(1), 22–29. <https://doi.org/10.1111/irv.12504>
- Colman, P. M., Varghese, J. N., & Laver, W. G. (1983). Structure of the catalytic and antigenic sites in influenza virus neuraminidase. *Nature*, 303(5912), 41–44. <https://doi.org/10.1038/303041a0>
- Copeland, C. S., Doms, R. W., Bolzau, E. M., Webster, R. G., & Helenius, A. (1986). Assembly of influenza hemagglutinin trimers and its role in intracellular transport. *The Journal of Cell Biology*, 103(4), 1179–1191. <https://doi.org/10.1083/jcb.103.4.1179>
- Corti, D., Suguitan, A. L., Pinna, D., Silacci, C., Fernandez-Rodriguez, B. M., Vanzetta, F., Santos, C., Luke, C. J., Torres-Velez, F. J., Temperton, N. J., Weiss, R. A., Sallusto, F., Subbarao, K., & Lanzavecchia, A. (2010). Heterosubtypic neutralizing antibodies are produced by individuals immunized with a seasonal influenza vaccine. *The Journal of Clinical Investigation*, 120(5), 1663–1673. <https://doi.org/10.1172/JCI41902>
- Corti, D., Voss, J., Gamblin, S. J., Codoni, G., Macagno, A., Jarrossay, D., Vachieri, S. G., Pinna, D., Minola, A., Vanzetta, F., Silacci, C., Fernandez-Rodriguez, B. M., Agatic, G., Bianchi, S., Giacchetto-Sasselli, I., Calder, L., Sallusto, F., Collins, P., Haire, L. F., ... Lanzavecchia, A. (2011). A neutralizing antibody selected from plasma cells that binds to group 1 and group 2 influenza A hemagglutinins. *Science (New York, N.Y.)*, 333(6044), 850–856. <https://doi.org/10.1126/science.1205669>
- Cowtan, K. (2006). The Buccaneer software for automated model building. 1. Tracing protein chains. *Acta Crystallographica. Section D, Biological Crystallography*, 62(Pt 9), 1002–1011. <https://doi.org/10.1107/S0907444906022116>
- Cox, M. M. J., Izikson, R., Post, P., & Dunkle, L. (2015). Safety, efficacy, and immunogenicity of Flublok in the prevention of seasonal influenza in adults. *Therapeutic Advances in Vaccines*, 3(4), 97–108. <https://doi.org/10.1177/2051013615595595>
- Cross, K. J., Langley, W. A., Russell, R. J., Skehel, J. J., & Steinhauer, D. A. (2009). Composition and functions of the influenza fusion peptide. *Protein and Peptide Letters*, 16(7), 766–778. <https://doi.org/10.2174/092986609788681715>
- Crowe, S. R., Miller, S. C., & Woodland, D. L. (2006). Identification of protective and non-protective T cell epitopes in influenza. *Vaccine*, 24(4), 452–456. <https://doi.org/10.1016/j.vaccine.2005.07.090>
- Cummings, J. F., Guerrero, M. L., Moon, J. E., Waterman, P., Nielsen, R. K., Jefferson, S., Gross, F. L., Hancock, K., Katz, J. M., Yusibov, V., & Fraunhofer USA Center for Molecular Biotechnology Study Group. (2014). Safety and immunogenicity of a plant-produced recombinant monomer hemagglutinin-based influenza vaccine derived from influenza A (H1N1)pdm09 virus: A Phase 1 dose-escalation study in healthy adults. *Vaccine*, 32(19), 2251–2259. <https://doi.org/10.1016/j.vaccine.2013.10.017>
- Curcio, M. J., Lutz, S., & Lesage, P. (2015). The Ty1 LTR-retrotransposon of budding yeast, *Saccharomyces cerevisiae*. *Microbiology Spectrum*, 3(2), 1–35. <https://doi.org/10.1128/microbiolspec.MDNA3-0053-2014>

- Dandagi, G. L., & Byahatti, S. M. (2011). An insight into the swine-influenza A (H1N1) virus infection in humans. *Lung India: Official Organ of Indian Chest Society*, 28(1), 34–38. <https://doi.org/10.4103/0970-2113.76299>
- Daniels, R. S., Downie, J. C., Hay, A. J., Knossow, M., Skehel, J. J., Wang, M. L., & Wiley, D. C. (1985). Fusion mutants of the influenza virus hemagglutinin glycoprotein. *Cell*, 40(2), 431–439. [https://doi.org/10.1016/0092-8674\(85\)90157-6](https://doi.org/10.1016/0092-8674(85)90157-6)
- De Filette, M., Martens, W., Roose, K., Deroo, T., Vervalle, F., Bentahir, M., Vandekerckhove, J., Fiers, W., & Saelens, X. (2008). An influenza A vaccine based on tetrameric ectodomain of matrix protein 2. *The Journal of Biological Chemistry*, 283(17), 11382–11387. <https://doi.org/10.1074/jbc.M800650200>
- Demers, J.-P., Fricke, P., Shi, C., Chevelkov, V., & Lange, A. (2018). Structure determination of supra-molecular assemblies by solid-state NMR: Practical considerations. *Progress in Nuclear Magnetic Resonance Spectroscopy*, 109, 51–78. <https://doi.org/10.1016/j.pnmrs.2018.06.002>
- Di Lella, S., Herrmann, A., & Mair, C. M. (2016). Modulation of the pH Stability of Influenza Virus Hemagglutinin: A Host Cell Adaptation Strategy. *Biophysical Journal*, 110(11), 2293–2301. <https://doi.org/10.1016/j.bpj.2016.04.035>
- DiazGranados, C. A., Dunning, A. J., Kimmel, M., Kirby, D., Treanor, J., Collins, A., Pollak, R., Christoff, J., Earl, J., Landolfi, V., Martin, E., Gurunathan, S., Nathan, R., Greenberg, D. P., Tornieporth, N. G., Decker, M. D., & Talbot, H. K. (2014). Efficacy of high-dose versus standard-dose influenza vaccine in older adults. *The New England Journal of Medicine*, 371(7), 635–645. <https://doi.org/10.1056/NEJMoa1315727>
- DiLillo, D. J., Palese, P., Wilson, P. C., & Ravetch, J. V. (2016). Broadly neutralizing anti-influenza antibodies require Fc receptor engagement for in vivo protection. *The Journal of Clinical Investigation*, 126(2), 605–610. <https://doi.org/10.1172/JCI84428>
- DiLillo, D. J., Tan, G. S., Palese, P., & Ravetch, J. V. (2014). Broadly neutralizing hemagglutinin stalk-specific antibodies require FcγR interactions for protection against influenza virus in vivo. *Nature Medicine*, 20(2), 143–151. <https://doi.org/10.1038/nm.3443>
- Dintzis, R. Z., Vogelstein, B., & Dintzis, H. M. (1982). Specific cellular stimulation in the primary immune response: Experimental test of a quantized model. *Proceedings of the National Academy of Sciences of the United States of America*, 79(3), 884–888. <https://doi.org/10.1073/pnas.79.3.884>
- Dou, D., Revol, R., Östbye, H., Wang, H., & Daniels, R. (2018). Influenza A Virus Cell Entry, Replication, Virion Assembly and Movement. *Frontiers in Immunology*, 9, 1581. <https://doi.org/10.3389/fimmu.2018.01581>
- Downey, J., Pernet, E., Coulombe, F., & Divangahi, M. (2018). Dissecting host cell death programs in the pathogenesis of influenza. *Microbes and Infection*, 20(9–10), 560–569. <https://doi.org/10.1016/j.micinf.2018.03.005>
- Dreyfus, C., Ekiert, D. C., & Wilson, I. A. (2013). Structure of a classical broadly neutralizing stem antibody in complex with a pandemic H2 influenza virus hemagglutinin. *Journal of Virology*, 87(12), 7149–7154. <https://doi.org/10.1128/JVI.02975-12>
- Dreyfus, C., Laursen, N. S., Kwaks, T., Zuijdgheest, D., Khayat, R., Ekiert, D. C., Lee, J. H., Metlagel, Z., Bujny, M. V., Jongeneelen, M., van der Vlugt, R., Lamrani, M., Korse, H. J. W. M., Geelen, E., Sahin, Ö., Sieuwerts, M., Brakenhoff, J. P. J., Vogels, R., Li, O. T. W., ... Friesen, R. H. E. (2012). Highly conserved protective epitopes on influenza B viruses. *Science (New York, N.Y.)*, 337(6100), 1343–1348. <https://doi.org/10.1126/science.1222908>
- Duwe, S. (2017). Influenza viruses—Antiviral therapy and resistance. *GMS Infectious Diseases*, 5, Doc04. <https://doi.org/10.3205/id000030>
- Dynavax. (2011). *Dynavax Reports New Phase 1a and Phase 1b Data for Universal Flu Vaccine Candidate | Dynavax Technologies Corporation*. <https://investors.dynavax.com/news-releases/news-release-details/dynavax-reports-new-phase-1a-and-phase-1b-data-universal-flu>
- Eggink, D., Goff, P. H., & Palese, P. (2014). Guiding the immune response against influenza virus hemagglutinin toward the conserved stalk domain by hyperglycosylation of the globular head domain. *Journal of Virology*, 88(1), 699–704. <https://doi.org/10.1128/JVI.02608-13>
- Eichelberger, M. C., & Wan, H. (2015). Influenza neuraminidase as a vaccine antigen. *Current Topics in Microbiology and Immunology*, 386, 275–299. https://doi.org/10.1007/82_2014_398
- Ekiert, D. C., Bhabha, G., Elsliger, M.-A., Friesen, R. H. E., Jongeneelen, M., Throsby, M., Goudsmit, J., & Wilson, I. A. (2009). Antibody recognition of a highly conserved influenza virus epitope. *Science (New York, N.Y.)*, 324(5924), 246–251. <https://doi.org/10.1126/science.1171491>
- Ekiert, D. C., Friesen, R. H. E., Bhabha, G., Kwaks, T., Jongeneelen, M., Yu, W., Ophorst, C., Cox, F., Korse, H. J. W. M., Brandenburg, B., Vogels, R., Brakenhoff, J. P. J., Kompier, R., Koldijk, M. H., Cornelissen, L. A. H. M., Poon, L. L. M., Peiris, M., Koudstaal, W., Wilson, I. A., & Goudsmit, J. (2011). A highly conserved neutralizing epitope on group 2 influenza A viruses. *Science (New York, N.Y.)*, 333(6044), 843–850. <https://doi.org/10.1126/science.1204839>
- Ekiert, D. C., Kashyap, A. K., Steel, J., Rubrum, A., Bhabha, G., Khayat, R., Lee, J. H., Dillon, M. A., O’Neil, R. E., Faynboym, A. M., Horowitz, M., Horowitz, L., Ward, A. B., Palese, P., Webby, R., Lerner, R. A., Bhatt, R.

- R., & Wilson, I. A. (2012). Cross-neutralization of influenza A viruses mediated by a single antibody loop. *Nature*, 489(7417), 526–532. <https://doi.org/10.1038/nature11414>
- El Bakkouri, K., Descamps, F., De Filette, M., Smet, A., Festjens, E., Birkett, A., Van Rooijen, N., Verbeek, S., Fiers, W., & Saelens, X. (2011). Universal vaccine based on ectodomain of matrix protein 2 of influenza A: Fc receptors and alveolar macrophages mediate protection. *Journal of Immunology (Baltimore, Md.: 1950)*, 186(2), 1022–1031. <https://doi.org/10.4049/jimmunol.0902147>
- Eliasson, D. G., El Bakkouri, K., Schön, K., Ramne, A., Festjens, E., Löwenadler, B., Fiers, W., Saelens, X., & Lycke, N. (2008). CTA1-M2e-DD: A novel mucosal adjuvant targeted influenza vaccine. *Vaccine*, 26(9), 1243–1252. <https://doi.org/10.1016/j.vaccine.2007.12.027>
- Eliasson, D. G., Omokanye, A., Schön, K., Wenzel, U. A., Bernasconi, V., Bemark, M., Kolpe, A., El Bakkouri, K., Ysenbaert, T., Deng, L., Fiers, W., Saelens, X., & Lycke, N. (2018). M2e-tetramer-specific memory CD4 T cells are broadly protective against influenza infection. *Mucosal Immunology*, 11(1), 273–289. <https://doi.org/10.1038/mi.2017.14>
- Ellebedy, A. H., & Ahmed, R. (2012). Re-engaging cross-reactive memory B cells: The influenza puzzle. *Frontiers in Immunology*, 3, 53. <https://doi.org/10.3389/fimmu.2012.00053>
- Emsley, P., Lohkamp, B., Scott, W. G., & Cowtan, K. (2010). Features and development of Coot. *Acta Crystallographica. Section D, Biological Crystallography*, 66(Pt 4), 486–501. <https://doi.org/10.1107/S0907444910007493>
- Epstein, S. L., Kong, W., Mispion, J. A., Lo, C.-Y., Tumpey, T. M., Xu, L., & Nabel, G. J. (2005). Protection against multiple influenza A subtypes by vaccination with highly conserved nucleoprotein. *Vaccine*, 23(46–47), 5404–5410. <https://doi.org/10.1016/j.vaccine.2005.04.047>
- Evans, P. (2006). Scaling and assessment of data quality. *Acta Crystallographica. Section D, Biological Crystallography*, 62(Pt 1), 72–82. <https://doi.org/10.1107/S0907444905036693>
- Fan, J., Liang, X., Horton, M. S., Perry, H. C., Citron, M. P., Heidecker, G. J., Fu, T.-M., Joyce, J., Przysiecki, C. T., Keller, P. M., Garsky, V. M., Ionescu, R., Rippeon, Y., Shi, L., Chastain, M. A., Condra, J. H., Davies, M.-E., Liao, J., Emini, E. A., & Shiver, J. W. (2004). Preclinical study of influenza virus A M2 peptide conjugate vaccines in mice, ferrets, and rhesus monkeys. *Vaccine*, 22(23–24), 2993–3003. <https://doi.org/10.1016/j.vaccine.2004.02.021>
- Feldman, R. A., Fuhr, R., Smolenov, I., Mick Ribeiro, A., Panther, L., Watson, M., Senn, J. J., Smith, M., Almarsson, Örn, Pujar, H. S., Laska, M. E., Thompson, J., Zaks, T., & Ciaramella, G. (2019). mRNA vaccines against H10N8 and H7N9 influenza viruses of pandemic potential are immunogenic and well tolerated in healthy adults in phase 1 randomized clinical trials. *Vaccine*, 37(25), 3326–3334. <https://doi.org/10.1016/j.vaccine.2019.04.074>
- Fiebiger, E., Meraner, P., Weber, E., Fang, I. F., Stingl, G., Ploegh, H., & Maurer, D. (2001). Cytokines regulate proteolysis in major histocompatibility complex class II-dependent antigen presentation by dendritic cells. *The Journal of Experimental Medicine*, 193(8), 881–892. <https://doi.org/10.1084/jem.193.8.881>
- Fifis, T., Gamvrellis, A., Crimeen-Irwin, B., Pietersz, G. A., Li, J., Mottram, P. L., McKenzie, I. F. C., & Plebanski, M. (2004). Size-dependent immunogenicity: Therapeutic and protective properties of nano-vaccines against tumors. *Journal of Immunology (Baltimore, Md.: 1950)*, 173(5), 3148–3154. <https://doi.org/10.4049/jimmunol.173.5.3148>
- Freivalds, J., Kotelovica, S., Voronkova, T., Ose, V., Tars, K., & Kazaks, A. (2014). Yeast-expressed bacteriophage-like particles for the packaging of nanomaterials. *Molecular Biotechnology*, 56(2), 102–110. <https://doi.org/10.1007/s12033-013-9686-0>
- Friesen, R. H. E., Lee, P. S., Stoop, E. J. M., Hoffman, R. M. B., Ekiert, D. C., Bhabha, G., Yu, W., Juraszek, J., Koudstaal, W., Jongeneelen, M., Korse, H. J. W. M., Ophorst, C., Brinkman-van der Linden, E. C. M., Throsby, M., Kwakkenbos, M. J., Bakker, A. Q., Beaumont, T., Spits, H., Kwaks, T., ... Wilson, I. A. (2014). A common solution to group 2 influenza virus neutralization. *Proceedings of the National Academy of Sciences of the United States of America*, 111(1), 445–450. <https://doi.org/10.1073/pnas.1319058110>
- Fu, T.-M., Freed, D. C., Horton, M. S., Fan, J., Citron, M. P., Joyce, J. G., Garsky, V. M., Casimiro, D. R., Zhao, Q., Shiver, J. W., & Liang, X. (2009). Characterizations of four monoclonal antibodies against M2 protein ectodomain of influenza A virus. *Virology*, 385(1), 218–226. <https://doi.org/10.1016/j.virol.2008.11.035>
- Fukuyama, S., & Kawaoka, Y. (2011). The pathogenesis of influenza virus infections: The contributions of virus and host factors. *Current Opinion in Immunology*, 23(4), 481–486. <https://doi.org/10.1016/j.coi.2011.07.016>
- Furuta, Y., Gowen, B. B., Takahashi, K., Shiraki, K., Smee, D. F., & Barnard, D. L. (2013). Favipiravir (T-705), a novel viral RNA polymerase inhibitor. *Antiviral Research*, 100(2), 446–454. <https://doi.org/10.1016/j.antiviral.2013.09.015>
- Gallagher, J. R., Torian, U., McCraw, D. M., & Harris, A. K. (2017). Structural studies of influenza virus RNPs by electron microscopy indicate molecular contortions within NP supra-structures. *Journal of Structural Biology*, 197(3), 294–307. <https://doi.org/10.1016/j.jsb.2016.12.007>
- Gamblin, S. J., Haire, L. F., Russell, R. J., Stevens, D. J., Xiao, B., Ha, Y., Vasisht, N., Steinhauer, D. A., Daniels, R. S., Elliot, A., Wiley, D. C., & Skehel, J. J. (2004). The structure and receptor binding properties of the

- 1918 influenza hemagglutinin. *Science (New York, N.Y.)*, 303(5665), 1838–1842. <https://doi.org/10.1126/science.1093155>
- Gamblin, S. J., & Skehel, J. J. (2010). Influenza hemagglutinin and neuraminidase membrane glycoproteins. *The Journal of Biological Chemistry*, 285(37), 28403–28409. <https://doi.org/10.1074/jbc.R110.129809>
- Gannagé, M., Dormann, D., Albrecht, R., Dengjel, J., Torossi, T., Rämmer, P. C., Lee, M., Strowig, T., Arrey, F., Conenello, G., Pypaert, M., Andersen, J., García-Sastre, A., & Münz, C. (2009). Matrix protein 2 of influenza A virus blocks autophagosome fusion with lysosomes. *Cell Host & Microbe*, 6(4), 367–380. <https://doi.org/10.1016/j.chom.2009.09.005>
- Gao, J., Gui, M., & Xiang, Y. (2020). Structural intermediates in the low pH-induced transition of influenza hemagglutinin. *PLoS Pathogens*, 16(11), e1009062. <https://doi.org/10.1371/journal.ppat.1009062>
- Gao, X., Wang, W., Li, Y., Zhang, S., Duan, Y., Xing, L., Zhao, Z., Zhang, P., Li, Z., Li, R., Wang, X., & Yang, P. (2013). Enhanced Influenza VLP vaccines comprising matrix-2 ectodomain and nucleoprotein epitopes protects mice from lethal challenge. *Antiviral Research*, 98(1), 4–11. <https://doi.org/10.1016/j.antiviral.2013.01.010>
- Garcia, N. K., Guttman, M., Ebner, J. L., & Lee, K. K. (2015). Dynamic changes during acid-induced activation of influenza hemagglutinin. *Structure (London, England: 1993)*, 23(4), 665–676. <https://doi.org/10.1016/j.str.2015.02.006>
- Gerdil, C. (2003). The annual production cycle for influenza vaccine. *Vaccine*, 21(16), 1776–1779. [https://doi.org/10.1016/s0264-410x\(03\)00071-9](https://doi.org/10.1016/s0264-410x(03)00071-9)
- Gerloff, N. A., Kremer, J. R., Charpentier, E., Sausy, A., Olinger, C. M., Weicherding, P., Schuh, J., Van Reeth, K., & Muller, C. P. (2011). Swine influenza virus antibodies in humans, western Europe, 2009. *Emerging Infectious Diseases*, 17(3), 403–411. <https://doi.org/10.3201/eid1703.100851>
- Gething, M. J., McCammon, K., & Sambrook, J. (1986). Expression of wild-type and mutant forms of influenza hemagglutinin: The role of folding in intracellular transport. *Cell*, 46(6), 939–950. [https://doi.org/10.1016/0092-8674\(86\)90076-0](https://doi.org/10.1016/0092-8674(86)90076-0)
- Getie-Kebtie, M., Sultana, I., Eichelberger, M., & Alterman, M. (2013). Label-free mass spectrometry-based quantification of hemagglutinin and neuraminidase in influenza virus preparations and vaccines. *Influenza and Other Respiratory Viruses*, 7(4), 521–530. <https://doi.org/10.1111/irv.12001>
- Giles, M. L., Krishnaswamy, S., & Wallace, E. M. (2018). Maternal immunisation: What have been the gains? Where are the gaps? What does the future hold? *F1000Research*, 7, F1000 Faculty Rev-1733. <https://doi.org/10.12688/f1000research.15475.1>
- Gomes, A. C., Mohsen, M., & Bachmann, M. F. (2017). Harnessing Nanoparticles for Immunomodulation and Vaccines. *Vaccines*, 5(1), E6. <https://doi.org/10.3390/vaccines5010006>
- Gopal, R., & Schneemann, A. (2018). Production and Application of Insect Virus-Based VLPs. *Methods in Molecular Biology (Clifton, N.J.)*, 1776, 125–141. https://doi.org/10.1007/978-1-4939-7808-3_8
- Gouma, S., Anderson, E. M., & Hensley, S. E. (2020). Challenges of Making Effective Influenza Vaccines. *Annual Review of Virology*, 7(1), 495–512. <https://doi.org/10.1146/annurev-virology-010320-044746>
- Gubareva, L. V., Trujillo, A. A., Okomo-Adhiambo, M., Mishin, V. P., Deyde, V. M., Sleeman, K., Nguyen, H. T., Sheu, T. G., Garten, R. J., Shaw, M. W., Fry, A. M., & Klimov, A. I. (2010). Comprehensive assessment of 2009 pandemic influenza A (H1N1) virus drug susceptibility in vitro. *Antiviral Therapy*, 15(8), 1151–1159. <https://doi.org/10.3851/IMP1678>
- Hale, B. G., Randall, R. E., Ortín, J., & Jackson, D. (2008). The multifunctional NS1 protein of influenza A viruses. *The Journal of General Virology*, 89(Pt 10), 2359–2376. <https://doi.org/10.1099/vir.0.2008/004606-0>
- Harfoot, R., & Webby, R. J. (2017). H5 influenza, a global update. *Journal of Microbiology (Seoul, Korea)*, 55(3), 196–203. <https://doi.org/10.1007/s12275-017-7062-7>
- Harris, A., Cardone, G., Winkler, D. C., Heymann, J. B., Brecher, M., White, J. M., & Steven, A. C. (2006). Influenza virus pleiomorphy characterized by cryoelectron tomography. *Proceedings of the National Academy of Sciences of the United States of America*, 103(50), 19123–19127. <https://doi.org/10.1073/pnas.0607614103>
- Harris, A. K., Meyerson, J. R., Matsuoka, Y., Kuybeda, O., Moran, A., Bliss, D., Das, S. R., Yewdell, J. W., Sapiro, G., Subbarao, K., & Subramaniam, S. (2013). Structure and accessibility of HA trimers on intact 2009 H1N1 pandemic influenza virus to stem region-specific neutralizing antibodies. *Proceedings of the National Academy of Sciences of the United States of America*, 110(12), 4592–4597. <https://doi.org/10.1073/pnas.1214913110>
- Hashemi, H., Pouyanfard, S., Bandehpour, M., Noroozbabaei, Z., Kazemi, B., Saelens, X., & Mokhtari-Azad, T. (2012). Immunisation with M2e-displaying T7 bacteriophage nanoparticles protects against influenza A virus challenge. *PLoS One*, 7(9), e45765. <https://doi.org/10.1371/journal.pone.0045765>
- Hause, B. M., Ducatez, M., Collin, E. A., Ran, Z., Liu, R., Sheng, Z., Armien, A., Kaplan, B., Chakravarty, S., Hoppe, A. D., Webby, R. J., Simonson, R. R., & Li, F. (2013). Isolation of a novel swine influenza virus from Oklahoma in 2011 which is distantly related to human influenza C viruses. *PLoS Pathogens*, 9(2), e1003176. <https://doi.org/10.1371/journal.ppat.1003176>
- Hua, Z., & Hou, B. (2013). TLR signaling in B-cell development and activation. *Cellular & Molecular Immunology*, 10(2), 103–106. <https://doi.org/10.1038/cmi.2012.61>

- Huang, X., Wang, X., Zhang, J., Xia, N., & Zhao, Q. (2017). Escherichia coli-derived virus-like particles in vaccine development. *NPJ Vaccines*, 2, 3. <https://doi.org/10.1038/s41541-017-0006-8>
- Huber, V. C., McKeon, R. M., Brackin, M. N., Miller, L. A., Keating, R., Brown, S. A., Makarova, N., Perez, D. R., Macdonald, G. H., & McCullers, J. A. (2006). Distinct contributions of vaccine-induced immunoglobulin G1 (IgG1) and IgG2a antibodies to protective immunity against influenza. *Clinical and Vaccine Immunology: CVI*, 13(9), 981–990. <https://doi.org/10.1128/CVI.00156-06>
- ICTV. (2020). *Taxonomy, International Committee on Taxonomy of Viruses*. <https://talk.ictvonline.org/taxonomy/>
- Impagliazzo, A., Milder, F., Kuipers, H., Wagner, M. V., Zhu, X., Hoffman, R. M. B., van Meersbergen, R., Huizingh, J., Wannings, P., Verspuij, J., de Man, M., Ding, Z., Apetri, A., Kükreker, B., Sneekes-Vriese, E., Tomkiewicz, D., Laursen, N. S., Lee, P. S., Zakrzewska, A., ... Radošević, K. (2015). A stable trimeric influenza hemagglutinin stem as a broadly protective immunogen. *Science (New York, N.Y.)*, 349(6254), 1301–1306. <https://doi.org/10.1126/science.aac7263>
- Ionescu, R. M., Przysiecki, C. T., Liang, X., Garsky, V. M., Fan, J., Wang, B., Troutman, R., Rippeon, Y., Flanagan, E., Shiver, J., & Shi, L. (2006). Pharmaceutical and immunological evaluation of human papillomavirus viruslike particle as an antigen carrier. *Journal of Pharmaceutical Sciences*, 95(1), 70–79. <https://doi.org/10.1002/jps.20493>
- Ip, D. K. M., Lau, L. L. H., Chan, K.-H., Fang, V. J., Leung, G. M., Peiris, M. J. S., & Cowling, B. J. (2016). The Dynamic Relationship Between Clinical Symptomatology and Viral Shedding in Naturally Acquired Seasonal and Pandemic Influenza Virus Infections. *Clinical Infectious Diseases: An Official Publication of the Infectious Diseases Society of America*, 62(4), 431–437. <https://doi.org/10.1093/cid/civ909>
- Ito, T., Gorman, O. T., Kawaoka, Y., Bean, W. J., & Webster, R. G. (1991). Evolutionary analysis of the influenza A virus M gene with comparison of the M1 and M2 proteins. *Journal of Virology*, 65(10), 5491–5498. <https://doi.org/10.1128/JVI.65.10.5491-5498.1991>
- Iuliano, A. D., Roguski, K. M., Chang, H. H., Muscatello, D. J., Palekar, R., Tempia, S., Cohen, C., Gran, J. M., Schanzer, D., Cowling, B. J., Wu, P., Kyncl, J., Ang, L. W., Park, M., Redlberger-Fritz, M., Yu, H., Espenhain, L., Krishnan, A., Emukule, G., ... Global Seasonal Influenza-associated Mortality Collaborator Network. (2018). Estimates of global seasonal influenza-associated respiratory mortality: A modelling study. *Lancet (London, England)*, 391(10127), 1285–1300. [https://doi.org/10.1016/S0140-6736\(17\)33293-2](https://doi.org/10.1016/S0140-6736(17)33293-2)
- Jagger, B. W., Wise, H. M., Kash, J. C., Walters, K.-A., Wills, N. M., Xiao, Y.-L., Dunfee, R. L., Schwartzman, L. M., Ozinsky, A., Bell, G. L., Dalton, R. M., Lo, A., Efstathiou, S., Atkins, J. F., Firth, A. E., Taubenberger, J. K., & Digard, P. (2012). An overlapping protein-coding region in influenza A virus segment 3 modulates the host response. *Science (New York, N.Y.)*, 337(6091), 199–204. <https://doi.org/10.1126/science.1222213>
- Jaudzems, K., Polenova, T., Pintacuda, G., Oschkinat, H., & Lesage, A. (2019). DNP NMR of biomolecular assemblies. *Journal of Structural Biology*, 206(1), 90–98. <https://doi.org/10.1016/j.jsb.2018.09.011>
- Jegaskanda, S., Reading, P. C., & Kent, S. J. (2014). Influenza-specific antibody-dependent cellular cytotoxicity: Toward a universal influenza vaccine. *Journal of Immunology (Baltimore, Md.: 1950)*, 193(2), 469–475. <https://doi.org/10.4049/jimmunol.1400432>
- Jegerlehner, A., Schmitz, N., Storni, T., & Bachmann, M. F. (2004). Influenza A vaccine based on the extracellular domain of M2: Weak protection mediated via antibody-dependent NK cell activity. *Journal of Immunology (Baltimore, Md.: 1950)*, 172(9), 5598–5605. <https://doi.org/10.4049/jimmunol.172.9.5598>
- Jegerlehner, A., Storni, T., Lipowsky, G., Schmid, M., Pumpens, P., & Bachmann, M. F. (2002). Regulation of IgG antibody responses by epitope density and CD21-mediated costimulation. *European Journal of Immunology*, 32(11), 3305–3314. [https://doi.org/10.1002/1521-4141\(200211\)32:11<3305::AID-IMMU3305>3.0.CO;2-J](https://doi.org/10.1002/1521-4141(200211)32:11<3305::AID-IMMU3305>3.0.CO;2-J)
- Jegerlehner, A., Zabel, F., Langer, A., Dietmeier, K., Jennings, G. T., Saudan, P., & Bachmann, M. F. (2013). Bacterially produced recombinant influenza vaccines based on virus-like particles. *PLoS One*, 8(11), e78947. <https://doi.org/10.1371/journal.pone.0078947>
- Jennings, G. T., & Bachmann, M. F. (2008). The coming of age of virus-like particle vaccines. *Biological Chemistry*, 389(5), 521–536. <https://doi.org/10.1515/bc.2008.064>
- Jennings, L., Huang, Q. S., Barr, I., Lee, P.-I., Kim, W. J., Buchy, P., Sanicas, M., Mungall, B. A., & Chen, J. (2018). Literature review of the epidemiology of influenza B disease in 15 countries in the Asia-Pacific region. *Influenza and Other Respiratory Viruses*, 12(3), 383–411. <https://doi.org/10.1111/irv.12522>
- Jeong, H., & Seong, B. L. (2017). Exploiting virus-like particles as innovative vaccines against emerging viral infections. *Journal of Microbiology (Seoul, Korea)*, 55(3), 220–230. <https://doi.org/10.1007/s12275-017-7058-3>
- Jia, R., Guo, J. H., & Fan, M. W. (2012). The effect of antigen size on the immunogenicity of antigen presenting cell targeted DNA vaccine. *International Immunopharmacology*, 12(1), 21–25. <https://doi.org/10.1016/j.intimp.2011.08.016>
- Jones, N. (2020). How COVID-19 is changing the cold and flu season. *Nature*, 588(7838), 388–390. <https://doi.org/10.1038/d41586-020-03519-3>
- Joyce, M. G., Wheatley, A. K., Thomas, P. V., Chuang, G.-Y., Soto, C., Bailer, R. T., Druz, A., Georgiev, I. S., Gillespie, R. A., Kanekiyo, M., Kong, W.-P., Leung, K., Narpala, S. N., Prabhakaran, M. S., Yang, E. S., Zhang,

- B., Zhang, Y., Asokan, M., Boyington, J. C., ... McDermott, A. B. (2016). Vaccine-Induced Antibodies that Neutralize Group 1 and Group 2 Influenza A Viruses. *Cell*, *166*(3), 609–623. <https://doi.org/10.1016/j.cell.2016.06.043>
- Kallewaard, N. L., Corti, D., Collins, P. J., Neu, U., McAuliffe, J. M., Benjamin, E., Wachter-Rosati, L., Palmer-Hill, F. J., Yuan, A. Q., Walker, P. A., Vorlaender, M. K., Bianchi, S., Guarino, B., De Marco, A., Vanzetta, F., Agatic, G., Foglierini, M., Pinna, D., Fernandez-Rodriguez, B., ... Skehel, J. J. (2016). Structure and Function Analysis of an Antibody Recognizing All Influenza A Subtypes. *Cell*, *166*(3), 596–608. <https://doi.org/10.1016/j.cell.2016.05.073>
- Kaminski, D. A., & Lee, F. E.-H. (2011). Antibodies against conserved antigens provide opportunities for reform in influenza vaccine design. *Frontiers in Immunology*, *2*, 76. <https://doi.org/10.3389/fimmu.2011.00076>
- Kashyap, A. K., Steel, J., Oner, A. F., Dillon, M. A., Swale, R. E., Wall, K. M., Perry, K. J., Faynboym, A., Ilhan, M., Horowitz, M., Horowitz, L., Palese, P., Bhatt, R. R., & Lerner, R. A. (2008). Combinatorial antibody libraries from survivors of the Turkish H5N1 avian influenza outbreak reveal virus neutralization strategies. *Proceedings of the National Academy of Sciences of the United States of America*, *105*(16), 5986–5991. <https://doi.org/10.1073/pnas.0801367105>
- Kashyap, A. K., Steel, J., Rubrum, A., Estelles, A., Briante, R., Ilyushina, N. A., Xu, L., Swale, R. E., Faynboym, A. M., Foreman, P. K., Horowitz, M., Horowitz, L., Webby, R., Palese, P., Lerner, R. A., & Bhatt, R. R. (2010). Protection from the 2009 H1N1 pandemic influenza by an antibody from combinatorial survivor-based libraries. *PLoS Pathogens*, *6*(7), e1000990. <https://doi.org/10.1371/journal.ppat.1000990>
- Kawano, J., Onta, T., Kida, H., & Yanagawa, R. (1978). Distribution of antibodies in animals against influenza B and C viruses. *The Japanese Journal of Veterinary Research*, *26*(3–4), 74–80.
- Killingly, B., & Nguyen-Van-Tam, J. (2013). Routes of influenza transmission. *Influenza and Other Respiratory Viruses*, *7* Suppl 2, 42–51. <https://doi.org/10.1111/irv.12080>
- Kim, H. J., & Kim, H.-J. (2017). Yeast as an expression system for producing virus-like particles: What factors do we need to consider? *Letters in Applied Microbiology*, *64*(2), 111–123. <https://doi.org/10.1111/lam.12695>
- Kim, M.-C., Lee, Y.-N., Ko, E.-J., Lee, J. S., Kwon, Y.-M., Hwang, H. S., Song, J.-M., Song, B.-M., Lee, Y.-J., Choi, J.-G., Kang, H.-M., Quan, F.-S., Compans, R. W., & Kang, S.-M. (2014). Supplementation of influenza split vaccines with conserved M2 ectodomains overcomes strain specificity and provides long-term cross protection. *Molecular Therapy: The Journal of the American Society of Gene Therapy*, *22*(7), 1364–1374. <https://doi.org/10.1038/mt.2014.33>
- Kim, M.-C., Song, J.-M., O, E., Kwon, Y.-M., Lee, Y.-J., Compans, R. W., & Kang, S.-M. (2013). Virus-like particles containing multiple M2 extracellular domains confer improved cross-protection against various subtypes of influenza virus. *Molecular Therapy: The Journal of the American Society of Gene Therapy*, *21*(2), 485–492. <https://doi.org/10.1038/mt.2012.246>
- Kim, P., Jang, Y. H., Kwon, S. B., Lee, C. M., Han, G., & Seong, B. L. (2018). Glycosylation of Hemagglutinin and Neuraminidase of Influenza A Virus as Signature for Ecological Spillover and Adaptation among Influenza Reservoirs. *Viruses*, *10*(4), E183. <https://doi.org/10.3390/v10040183>
- Kirkpatrick, E., Qiu, X., Wilson, P. C., Bahl, J., & Krammer, F. (2018). The influenza virus hemagglutinin head evolves faster than the stalk domain. *Scientific Reports*, *8*(1), 10432. <https://doi.org/10.1038/s41598-018-28706-1>
- Klimek, L., Wicht-Langhammer, S., von Bernus, L., Thorn, C., Cazan, D., Pfaar, O., & Hörmann, K. (2017). [Anaphylactic reactions to vaccines: Chicken egg allergy and the influenza H1N1 vaccination]. *HNO*, *65*(10), 834–839. <https://doi.org/10.1007/s00106-017-0363-7>
- Kochs, G., García-Sastre, A., & Martínez-Sobrido, L. (2007). Multiple anti-interferon actions of the influenza A virus NS1 protein. *Journal of Virology*, *81*(13), 7011–7021. <https://doi.org/10.1128/JVI.02581-06>
- Koho, T., Ihalainen, T. O., Stark, M., Uusi-Kerttula, H., Wieneke, R., Rahikainen, R., Blazevic, V., Marjomäki, V., Tampé, R., Kulomaa, M. S., & Hytönen, V. P. (2015). His-tagged norovirus-like particles: A versatile platform for cellular delivery and surface display. *European Journal of Pharmaceutics and Biopharmaceutics: Official Journal of Arbeitsgemeinschaft Fur Pharmazeutische Verfahrenstechnik e.V.*, *96*, 22–31. <https://doi.org/10.1016/j.ejpb.2015.07.002>
- Kolpe, A., Schepens, B., Fiers, W., & Saelens, X. (2017). M2-based influenza vaccines: Recent advances and clinical potential. *Expert Review of Vaccines*, *16*(2), 123–136. <https://doi.org/10.1080/14760584.2017.1240041>
- Kolpe, A., Schepens, B., Ye, L., Staeheli, P., & Saelens, X. (2018). Passively transferred M2e-specific monoclonal antibody reduces influenza A virus transmission in mice. *Antiviral Research*, *158*, 244–254. <https://doi.org/10.1016/j.antiviral.2018.08.017>
- Kovalevskiy, O., Nicholls, R. A., Long, F., Carlon, A., & Murshudov, G. N. (2018). Overview of refinement procedures within REFMAC5: Utilizing data from different sources. *Acta Crystallographica. Section D, Structural Biology*, *74*(Pt 3), 215–227. <https://doi.org/10.1107/S2059798318000979>
- Krammer, F. (2015). The Quest for a Universal Flu Vaccine: Headless HA 2.0. *Cell Host & Microbe*, *18*(4), 395–397. <https://doi.org/10.1016/j.chom.2015.10.003>
- Krammer, F. (2016). Novel universal influenza virus vaccine approaches. *Current Opinion in Virology*, *17*, 95–103. <https://doi.org/10.1016/j.coviro.2016.02.002>

- Krammer, F. (2019). The human antibody response to influenza A virus infection and vaccination. *Nature Reviews. Immunology*, 19(6), 383–397. <https://doi.org/10.1038/s41577-019-0143-6>
- Krammer, F., Pica, N., Hai, R., Margine, I., & Palese, P. (2013). Chimeric hemagglutinin influenza virus vaccine constructs elicit broadly protective stalk-specific antibodies. *Journal of Virology*, 87(12), 6542–6550. <https://doi.org/10.1128/JVI.00641-13>
- Krammer, F., Smith, G. J. D., Fouchier, R. A. M., Peiris, M., Kedzierska, K., Doherty, P. C., Palese, P., Shaw, M. L., Treanor, J., Webster, R. G., & García-Sastre, A. (2018). Influenza. *Nature Reviews. Disease Primers*, 4(1), 3. <https://doi.org/10.1038/s41572-018-0002-y>
- Kumru, O. S., Joshi, S. B., Smith, D. E., Middaugh, C. R., Prusik, T., & Volkin, D. B. (2014). Vaccine instability in the cold chain: Mechanisms, analysis and formulation strategies. *Biologicals: Journal of the International Association of Biological Standardization*, 42(5), 237–259. <https://doi.org/10.1016/j.biologicals.2014.05.007>
- Kuo, R.-L., Zhao, C., Malur, M., & Krug, R. M. (2010). Influenza A virus strains that circulate in humans differ in the ability of their NS1 proteins to block the activation of IRF3 and interferon- β transcription. *Virology*, 408(2), 146–158. <https://doi.org/10.1016/j.virol.2010.09.012>
- Kwon, B., & Hong, M. (2016). The Influenza M2 Ectodomain Regulates the Conformational Equilibria of the Transmembrane Proton Channel: Insights from Solid-State Nuclear Magnetic Resonance. *Biochemistry*, 55(38), 5387–5397. <https://doi.org/10.1021/acs.biochem.6b00727>
- Lakdawala, S. S., Lamirande, E. W., Suguitan, A. L., Wang, W., Santos, C. P., Vogel, L., Matsuoka, Y., Lindsley, W. G., Jin, H., & Subbarao, K. (2011). Eurasian-origin gene segments contribute to the transmissibility, aerosol release, and morphology of the 2009 pandemic H1N1 influenza virus. *PLoS Pathogens*, 7(12), e1002443. <https://doi.org/10.1371/journal.ppat.1002443>
- Lamb, R. A., & Choppin, P. W. (1979). Segment 8 of the influenza virus genome is unique in coding for two polypeptides. *Proceedings of the National Academy of Sciences of the United States of America*, 76(10), 4908–4912. <https://doi.org/10.1073/pnas.76.10.4908>
- Lamb, R. A., Zebedee, S. L., & Richardson, C. D. (1985). Influenza virus M2 protein is an integral membrane protein expressed on the infected-cell surface. *Cell*, 40(3), 627–633. [https://doi.org/10.1016/0092-8674\(85\)90211-9](https://doi.org/10.1016/0092-8674(85)90211-9)
- Lambert, L. C., & Fauci, A. S. (2010). Influenza vaccines for the future. *The New England Journal of Medicine*, 363(21), 2036–2044. <https://doi.org/10.1056/NEJMr1002842>
- Lambert, N. D., Ovsyannikova, I. G., Pankratz, V. S., Jacobson, R. M., & Poland, G. A. (2012). Understanding the immune response to seasonal influenza vaccination in older adults: A systems biology approach. *Expert Review of Vaccines*, 11(8), 985–994. <https://doi.org/10.1586/erv.12.61>
- Landry, N., Ward, B. J., Trépanier, S., Montomoli, E., Dargis, M., Lapini, G., & Vézina, L.-P. (2010). Preclinical and clinical development of plant-made virus-like particle vaccine against avian H5N1 influenza. *PloS One*, 5(12), e15559. <https://doi.org/10.1371/journal.pone.0015559>
- Lang, S., Xie, J., Zhu, X., Wu, N. C., Lerner, R. A., & Wilson, I. A. (2017). Antibody 27F3 Broadly Targets Influenza A Group 1 and 2 Hemagglutinins through a Further Variation in VH1-69 Antibody Orientation on the HA Stem. *Cell Reports*, 20(12), 2935–2943. <https://doi.org/10.1016/j.celrep.2017.08.084>
- Ledgerwood, J. E., Wei, C.-J., Hu, Z., Gordon, I. J., Enama, M. E., Hendel, C. S., McTamney, P. M., Pearce, M. B., Yassine, H. M., Boyington, J. C., Bailer, R., Tumpey, T. M., Koup, R. A., Mascola, J. R., Nabel, G. J., Graham, B. S., & VRC 306 Study Team. (2011). DNA priming and influenza vaccine immunogenicity: Two phase 1 open label randomised clinical trials. *The Lancet. Infectious Diseases*, 11(12), 916–924. [https://doi.org/10.1016/S1473-3099\(11\)70240-7](https://doi.org/10.1016/S1473-3099(11)70240-7)
- Lee, L. Y.-H., Ha, D. L. A., Simmons, C., de Jong, M. D., Chau, N. V. V., Schumacher, R., Peng, Y. C., McMichael, A. J., Farrar, J. J., Smith, G. L., Townsend, A. R. M., Askonas, B. A., Rowland-Jones, S., & Dong, T. (2008). Memory T cells established by seasonal human influenza A infection cross-react with avian influenza A (H5N1) in healthy individuals. *The Journal of Clinical Investigation*, 118(10), 3478–3490. <https://doi.org/10.1172/JCI32460>
- Lee, Y.-N., Lee, Y.-T., Kim, M.-C., Gewirtz, A. T., & Kang, S.-M. (2016). A Novel Vaccination Strategy Mediating the Induction of Lung-Resident Memory CD8 T Cells Confers Heterosubtypic Immunity against Future Pandemic Influenza Virus. *Journal of Immunology (Baltimore, Md.: 1950)*, 196(6), 2637–2645. <https://doi.org/10.4049/jimmunol.1501637>
- Lee, Y.-N., Lee, Y.-T., Kim, M.-C., Hwang, H. S., Lee, J. S., Kim, K.-H., & Kang, S.-M. (2014). Fc receptor is not required for inducing antibodies but plays a critical role in conferring protection after influenza M2 vaccination. *Immunology*, 143(2), 300–309. <https://doi.org/10.1111/imm.12310>
- Leitans, J., Kazaks, A., Balode, A., Ivanova, J., Zalubovskis, R., Supuran, C. T., & Tars, K. (2015). Efficient Expression and Crystallization System of Cancer-Associated Carbonic Anhydrase Isoform IX. *Journal of Medicinal Chemistry*, 58(22), 9004–9009. <https://doi.org/10.1021/acs.jmedchem.5b01343>
- Li, G.-M., Chiu, C., Wrarmert, J., McCausland, M., Andrews, S. F., Zheng, N.-Y., Lee, J.-H., Huang, M., Qu, X., Edupuganti, S., Mulligan, M., Das, S. R., Yewdell, J. W., Mehta, A. K., Wilson, P. C., & Ahmed, R. (2012). Pandemic H1N1 influenza vaccine induces a recall response in humans that favors broadly cross-reactive memory

- B cells. *Proceedings of the National Academy of Sciences of the United States of America*, 109(23), 9047–9052. <https://doi.org/10.1073/pnas.1118979109>
- Li, L., Wong, J. Y., Wu, P., Bond, H. S., Lau, E. H. Y., Sullivan, S. G., & Cowling, B. J. (2018). Heterogeneity in Estimates of the Impact of Influenza on Population Mortality: A Systematic Review. *American Journal of Epidemiology*, 187(2), 378–388. <https://doi.org/10.1093/aje/kwx270>
- Liebowitz, D., Gottlieb, K., Kolhatkar, N. S., Garg, S. J., Asher, J. M., Nazareno, J., Kim, K., McIlwain, D. R., & Tucker, S. N. (2020). Efficacy, immunogenicity, and safety of an oral influenza vaccine: A placebo-controlled and active-controlled phase 2 human challenge study. *The Lancet. Infectious Diseases*, 20(4), 435–444. [https://doi.org/10.1016/S1473-3099\(19\)30584-5](https://doi.org/10.1016/S1473-3099(19)30584-5)
- Liekniņa, I., Černova, D., Rūmnieks, J., & Tārs, K. (2020). Novel ssRNA phage VLP platform for displaying foreign epitopes by genetic fusion. *Vaccine*, 38(38), 6019–6026. <https://doi.org/10.1016/j.vaccine.2020.07.016>
- Liekniņa, I., Kalniņš, G., Akopjana, I., Bogans, J., Šišovs, M., Jansons, J., Rūmnieks, J., & Tārs, K. (2019). Production and characterization of novel ssRNA bacteriophage virus-like particles from metagenomic sequencing data. *Journal of Nanobiotechnology*, 17(1), 61. <https://doi.org/10.1186/s12951-019-0497-8>
- Lillie, P. J., Berthoud, T. K., Powell, T. J., Lambe, T., Mullarkey, C., Spencer, A. J., Hamill, M., Peng, Y., Blais, M.-E., Duncan, C. J. A., Sheehy, S. H., Havelock, T., Faust, S. N., Williams, R. L., Gilbert, A., Oxford, J., Dong, T., Hill, A. V. S., & Gilbert, S. C. (2012). Preliminary assessment of the efficacy of a T-cell-based influenza vaccine, MVA-NP+M1, in humans. *Clinical Infectious Diseases: An Official Publication of the Infectious Diseases Society of America*, 55(1), 19–25. <https://doi.org/10.1093/cid/cis327>
- Lin, S.-C., Liu, W.-C., Jan, J.-T., & Wu, S.-C. (2014). Glycan masking of hemagglutinin for adenovirus vector and recombinant protein immunizations elicits broadly neutralizing antibodies against H5N1 avian influenza viruses. *PLoS One*, 9(3), e92822. <https://doi.org/10.1371/journal.pone.0092822>
- Lindgren, G., Ols, S., Liang, F., Thompson, E. A., Lin, A., Hellgren, F., Bahl, K., John, S., Yuzhakov, O., Hassett, K. J., Brito, L. A., Salter, H., Ciarabella, G., & Loré, K. (2017). Induction of Robust B Cell Responses after Influenza mRNA Vaccination Is Accompanied by Circulating Hemagglutinin-Specific ICOS⁺ PD-1⁺ CXCR3⁺ T Follicular Helper Cells. *Frontiers in Immunology*, 8, 1539. <https://doi.org/10.3389/fimmu.2017.01539>
- Linster, M., van Boheemen, S., de Graaf, M., Schrauwen, E. J. A., Lexmond, P., Mänz, B., Bestebroer, T. M., Baumann, J., van Riel, D., Rimmelzwaan, G. F., Osterhaus, A. D. M. E., Matrosovich, M., Fouchier, R. A. M., & Herfst, S. (2014). Identification, characterization, and natural selection of mutations driving airborne transmission of A/H5N1 virus. *Cell*, 157(2), 329–339. <https://doi.org/10.1016/j.cell.2014.02.040>
- Lo, C.-Y., Wu, Z., Mispion, J. A., Price, G. E., Pappas, C., Kong, W.-P., Tumpey, T. M., & Epstein, S. L. (2008). Comparison of vaccines for induction of heterosubtypic immunity to influenza A virus: Cold-adapted vaccine versus DNA prime-adenovirus boost strategies. *Vaccine*, 26(17), 2062–2072. <https://doi.org/10.1016/j.vaccine.2008.02.047>
- Loo, Y.-M., & Gale, M. (2007). Influenza: Fatal immunity and the 1918 virus. *Nature*, 445(7125), 267–268. <https://doi.org/10.1038/445267a>
- López-Macías, C., Ferat-Osorio, E., Tenorio-Calvo, A., Isibasi, A., Talavera, J., Arteaga-Ruiz, O., Arriaga-Pizano, L., Hickman, S. P., Allende, M., Lenhard, K., Pincus, S., Connolly, K., Raghunandan, R., Smith, G., & Glenn, G. (2011). Safety and immunogenicity of a virus-like particle pandemic influenza A (H1N1) 2009 vaccine in a blinded, randomized, placebo-controlled trial of adults in Mexico. *Vaccine*, 29(44), 7826–7834. <https://doi.org/10.1016/j.vaccine.2011.07.099>
- Lotfi, Z., Golchin, M., Khalili-Yazdi, A., & Khalili, M. (2019). Immunological properties of the SLLTEVET epitope of Influenza A virus in multiple display on filamentous M13 phage. *Comparative Immunology, Microbiology and Infectious Diseases*, 65, 76–80. <https://doi.org/10.1016/j.cimid.2019.05.004>
- Low, J. G. H., Lee, L. S., Ooi, E. E., Ethirajulu, K., Yeo, P., Matter, A., Connolly, J. E., Skibinski, D. A. G., Saudan, P., Bachmann, M., Hanson, B. J., Lu, Q., Maurer-Stroh, S., Lim, S., & Novotny-Diermayr, V. (2014). Safety and immunogenicity of a virus-like particle pandemic influenza A (H1N1) 2009 vaccine: Results from a double-blinded, randomized Phase I clinical trial in healthy Asian volunteers. *Vaccine*, 32(39), 5041–5048. <https://doi.org/10.1016/j.vaccine.2014.07.011>
- Lu, I.-N., Kirsteina, A., Farinelle, S., Willieme, S., Tars, K., Muller, C. P., & Kazaks, A. (2018). Structure and applications of novel influenza HA tri-stalk protein for evaluation of HA stem-specific immunity. *PLoS One*, 13(9), e0204776. <https://doi.org/10.1371/journal.pone.0204776>
- Lua, L. H. L., Connors, N. K., Sainsbury, F., Chuan, Y. P., Wibowo, N., & Middelberg, A. P. J. (2014). Bioengineering virus-like particles as vaccines. *Biotechnology and Bioengineering*, 111(3), 425–440. <https://doi.org/10.1002/bit.25159>
- Ma, Y., Nolte, R. J. M., & Cornelissen, J. J. L. M. (2012a). Virus-based nanocarriers for drug delivery. *Advanced Drug Delivery Reviews*, 64(9), 811–825. <https://doi.org/10.1016/j.addr.2012.01.005>
- Ma, Y., Nolte, R. J. M., & Cornelissen, J. J. L. M. (2012b). Virus-based nanocarriers for drug delivery. *Advanced Drug Delivery Reviews*, 64(9), 811–825. <https://doi.org/10.1016/j.addr.2012.01.005>
- Malakhov, M. P., Aschenbrenner, L. M., Smee, D. F., Wandersee, M. K., Sidwell, R. W., Gubareva, L. V., Mishin, V. P., Hayden, F. G., Kim, D. H., Ing, A., Campbell, E. R., Yu, M., & Fang, F. (2006). Sialidase fusion

- protein as a novel broad-spectrum inhibitor of influenza virus infection. *Antimicrobial Agents and Chemotherapy*, 50(4), 1470–1479. <https://doi.org/10.1128/AAC.50.4.1470-1479.2006>
- Mallajosyula, V. V. A., Citron, M., Ferrara, F., Lu, X., Callahan, C., Heidecker, G. J., Sarma, S. P., Flynn, J. A., Temperton, N. J., Liang, X., & Varadarajan, R. (2014). Influenza hemagglutinin stem-fragment immunogen elicits broadly neutralizing antibodies and confers heterologous protection. *Proceedings of the National Academy of Sciences of the United States of America*, 111(25), E2514–2523. <https://doi.org/10.1073/pnas.1402766111>
- Mamat, U., Wilke, K., Bramhill, D., Schromm, A. B., Lindner, B., Kohl, T. A., Corchero, J. L., Villaverde, A., Schaffer, L., Head, S. R., Souvignier, C., Meredith, T. C., & Woodard, R. W. (2015). Detoxifying *Escherichia coli* for endotoxin-free production of recombinant proteins. *Microbial Cell Factories*, 14, 57. <https://doi.org/10.1186/s12934-015-0241-5>
- Mandala, V. S., & Hong, M. (2019). High-sensitivity protein solid-state NMR spectroscopy. *Current Opinion in Structural Biology*, 58, 183–190. <https://doi.org/10.1016/j.sbi.2019.03.027>
- Manini, I., Trombetta, C. M., Lazzeri, G., Pozzi, T., Rossi, S., & Montomoli, E. (2017). Egg-Independent Influenza Vaccines and Vaccine Candidates. *Vaccines*, 5(3), E18. <https://doi.org/10.3390/vaccines5030018>
- Manolova, V., Flace, A., Bauer, M., Schwarz, K., Saudan, P., & Bachmann, M. F. (2008). Nanoparticles target distinct dendritic cell populations according to their size. *European Journal of Immunology*, 38(5), 1404–1413. <https://doi.org/10.1002/eji.200737984>
- Margine, I., Hai, R., Albrecht, R. A., Obermoser, G., Harrod, A. C., Banchereau, J., Palucka, K., García-Sastre, A., Palese, P., Treanor, J. J., & Krammer, F. (2013). H3N2 influenza virus infection induces broadly reactive hemagglutinin stalk antibodies in humans and mice. *Journal of Virology*, 87(8), 4728–4737. <https://doi.org/10.1128/JVI.03509-12>
- Mazur, I., Anhlan, D., Mitzner, D., Wixler, L., Schubert, U., & Ludwig, S. (2008). The proapoptotic influenza A virus protein PB1-F2 regulates viral polymerase activity by interaction with the PB1 protein. *Cellular Microbiology*, 10(5), 1140–1152. <https://doi.org/10.1111/j.1462-5822.2008.01116.x>
- McCluskie, M. J., Evans, D. M., Zhang, N., Benoit, M., McElhiney, S. P., Unnithan, M., DeMarco, S. C., Clay, B., Huber, C., Deora, A., Thorn, J. M., Stead, D. R., Merson, J. R., & Davis, H. L. (2016). The effect of preexisting anti-carrier immunity on subsequent responses to CRM197 or Qb-VLP conjugate vaccines. *Immunopharmacology and Immunotoxicology*, 38(3), 184–196. <https://doi.org/10.3109/08923973.2016.1165246>
- McCoy, A. J., Grosse-Kunstleve, R. W., Adams, P. D., Winn, M. D., Storoni, L. C., & Read, R. J. (2007). Phaser crystallographic software. *Journal of Applied Crystallography*, 40(4), 658–674. <https://doi.org/10.1107/S0021889807021206>
- McElhaney, J. E., Xie, D., Hager, W. D., Barry, M. B., Wang, Y., Kleppinger, A., Ewen, C., Kane, K. P., & Bleackley, R. C. (2006). T cell responses are better correlates of vaccine protection in the elderly. *Journal of Immunology (Baltimore, Md.: 1950)*, 176(10), 6333–6339. <https://doi.org/10.4049/jimmunol.176.10.6333>
- McLean, K. A., Goldin, S., Nannei, C., Sparrow, E., & Torelli, G. (2016). The 2015 global production capacity of seasonal and pandemic influenza vaccine. *Vaccine*, 34(45), 5410–5413. <https://doi.org/10.1016/j.vaccine.2016.08.019>
- Merckx, J., Wali, R., Schiller, I., Caya, C., Gore, G. C., Chartrand, C., Dendukuri, N., & Papenburg, J. (2017). Diagnostic Accuracy of Novel and Traditional Rapid Tests for Influenza Infection Compared With Reverse Transcriptase Polymerase Chain Reaction: A Systematic Review and Meta-analysis. *Annals of Internal Medicine*, 167(6), 394–409. <https://doi.org/10.7326/M17-0848>
- Mezhenskaya, D., Isakova-Sivak, I., & Rudenko, L. (2019). M2e-based universal influenza vaccines: A historical overview and new approaches to development. *Journal of Biomedical Science*, 26(1), 76. <https://doi.org/10.1186/s12929-019-0572-3>
- Morris, D. E., Cleary, D. W., & Clarke, S. C. (2017). Secondary Bacterial Infections Associated with Influenza Pandemics. *Frontiers in Microbiology*, 8, 1041. <https://doi.org/10.3389/fmicb.2017.01041>
- Mozdzanowska, K., Maiese, K., Furchner, M., & Gerhard, W. (1999). Treatment of influenza virus-infected SCID mice with nonneutralizing antibodies specific for the transmembrane proteins matrix 2 and neuraminidase reduces the pulmonary virus titer but fails to clear the infection. *Virology*, 254(1), 138–146. <https://doi.org/10.1006/viro.1998.9534>
- Munster, V. J., Baas, C., Lexmond, P., Waldenström, J., Wallensten, A., Fransson, T., Rimmelzwaan, G. F., Beyer, W. E. P., Schutten, M., Olsen, B., Osterhaus, A. D. M. E., & Fouchier, R. A. M. (2007). Spatial, temporal, and species variation in prevalence of influenza A viruses in wild migratory birds. *PLoS Pathogens*, 3(5), e61. <https://doi.org/10.1371/journal.ppat.0030061>
- Muramoto, Y., Noda, T., Kawakami, E., Akkina, R., & Kawaoka, Y. (2013). Identification of novel influenza A virus proteins translated from PA mRNA. *Journal of Virology*, 87(5), 2455–2462. <https://doi.org/10.1128/JVI.02656-12>
- Nachbagauer, R., Feser, J., Naficy, A., Bernstein, D. I., Guptill, J., Walter, E. B., Berlanda-Scorza, F., Stadlbauer, D., Wilson, P. C., Aydillo, T., Behzadi, M. A., Bhavsar, D., Bliss, C., Capuano, C., Carreño, J. M., Chromikova, V., Claeys, C., Coughlan, L., Freyn, A. W., ... Krammer, F. (2021). A chimeric hemagglutinin-based

- universal influenza virus vaccine approach induces broad and long-lasting immunity in a randomized, placebo-controlled phase I trial. *Nature Medicine*, 27(1), 106–114. <https://doi.org/10.1038/s41591-020-1118-7>
- Nachbagauer, R., Miller, M. S., Hai, R., Ryder, A. B., Rose, J. K., Palese, P., García-Sastre, A., Krammer, F., & Albrecht, R. A. (2015). Hemagglutinin Stalk Immunity Reduces Influenza Virus Replication and Transmission in Ferrets. *Journal of Virology*, 90(6), 3268–3273. <https://doi.org/10.1128/JVI.02481-15>
- Nair, H., Brooks, W. A., Katz, M., Roca, A., Berkley, J. A., Madhi, S. A., Simmerman, J. M., Gordon, A., Sato, M., Howie, S., Krishnan, A., Ope, M., Lindblade, K. A., Carosone-Link, P., Lucero, M., Ochieng, W., Kamimoto, L., Dueger, E., Bhat, N., ... Campbell, H. (2011). Global burden of respiratory infections due to seasonal influenza in young children: A systematic review and meta-analysis. *Lancet (London, England)*, 378(9807), 1917–1930. [https://doi.org/10.1016/S0140-6736\(11\)61051-9](https://doi.org/10.1016/S0140-6736(11)61051-9)
- Nelli, R. K., Kuchipudi, S. V., White, G. A., Perez, B. B., Dunham, S. P., & Chang, K.-C. (2010). Comparative distribution of human and avian type sialic acid influenza receptors in the pig. *BMC Veterinary Research*, 6, 4. <https://doi.org/10.1186/1746-6148-6-4>
- Nelson, N. P., Easterbrook, P. J., & McMahon, B. J. (2016). Epidemiology of Hepatitis B Virus Infection and Impact of Vaccination on Disease. *Clinics in Liver Disease*, 20(4), 607–628. <https://doi.org/10.1016/j.cld.2016.06.006>
- Neumann, G., & Kawaoka, Y. (2019). Predicting the Next Influenza Pandemics. *The Journal of Infectious Diseases*, 219(Suppl_1), S14–S20. <https://doi.org/10.1093/infdis/jiz040>
- Ng, S., Nachbagauer, R., Balmaseda, A., Stadlbauer, D., Ojeda, S., Patel, M., Rajabhathor, A., Lopez, R., Guglia, A. F., Sanchez, N., Amanat, F., Gresh, L., Kuan, G., Krammer, F., & Gordon, A. (2019). Novel correlates of protection against pandemic H1N1 influenza A virus infection. *Nature Medicine*, 25(6), 962–967. <https://doi.org/10.1038/s41591-019-0463-x>
- Nie, S., Roth, R. B., Stiles, J., Mikhлина, A., Lu, X., Tang, Y.-W., & Babady, N. E. (2014). Evaluation of Alere i Influenza A&B for rapid detection of influenza viruses A and B. *Journal of Clinical Microbiology*, 52(9), 3339–3344. <https://doi.org/10.1128/JCM.01132-14>
- Nimmerjahn, F., & Ravetch, J. V. (2005). Divergent immunoglobulin g subclass activity through selective Fc receptor binding. *Science (New York, N.Y.)*, 310(5753), 1510–1512. <https://doi.org/10.1126/science.1118948>
- Nooraei, S., Bahrulolum, H., Hoseini, Z. S., Katalani, C., Hajzade, A., Easton, A. J., & Ahmadian, G. (2021). Virus-like particles: Preparation, immunogenicity and their roles as nanovaccines and drug nanocarriers. *Journal of Nanobiotechnology*, 19(1), 59. <https://doi.org/10.1186/s12951-021-00806-7>
- Nordén, K., Agemark, M., Danielson, J. Å. H., Alexandersson, E., Kjellbom, P., & Johanson, U. (2011). Increasing gene dosage greatly enhances recombinant expression of aquaporins in *Pichia pastoris*. *BMC Biotechnology*, 11, 47. <https://doi.org/10.1186/1472-6750-11-47>
- Okuno, Y., Isegawa, Y., Sasao, F., & Ueda, S. (1993). A common neutralizing epitope conserved between the hemagglutinins of influenza A virus H1 and H2 strains. *Journal of Virology*, 67(5), 2552–2558. <https://doi.org/10.1128/JVI.67.5.2552-2558.1993>
- Olsen, S. J., Azziz-Baumgartner, E., Budd, A. P., Brammer, L., Sullivan, S., Pineda, R. F., Cohen, C., & Fry, A. M. (2020). Decreased Influenza Activity During the COVID-19 Pandemic—United States, Australia, Chile, and South Africa, 2020. *MMWR. Morbidity and Mortality Weekly Report*, 69(37), 1305–1309. <https://doi.org/10.15585/mmwr.mm6937a6>
- Omoto, S., Speranzini, V., Hashimoto, T., Noshi, T., Yamaguchi, H., Kawai, M., Kawaguchi, K., Uehara, T., Shishido, T., Naito, A., & Cusack, S. (2018). Characterization of influenza virus variants induced by treatment with the endonuclease inhibitor baloxavir marboxil. *Scientific Reports*, 8(1), 9633. <https://doi.org/10.1038/s41598-018-27890-4>
- Osterhaus, A. D., Rimmelzwaan, G. F., Martina, B. E., Bestebroer, T. M., & Fouchier, R. A. (2000). Influenza B virus in seals. *Science (New York, N.Y.)*, 288(5468), 1051–1053. <https://doi.org/10.1126/science.288.5468.1051>
- Owczarek, B., Gerszberg, A., & Hnatuszko-Konka, K. (2019). A Brief Reminder of Systems of Production and Chromatography-Based Recovery of Recombinant Protein Biopharmaceuticals. *BioMed Research International*, 2019, 4216060. <https://doi.org/10.1155/2019/4216060>
- Paget, J., Spreeuwenberg, P., Charu, V., Taylor, R. J., Iuliano, A. D., Bresee, J., Simonsen, L., Viboud, C., & Global Seasonal Influenza-associated Mortality Collaborator Network and GLaMOR Collaborating Teams*. (2019). Global mortality associated with seasonal influenza epidemics: New burden estimates and predictors from the GLaMOR Project. *Journal of Global Health*, 9(2), 020421. <https://doi.org/10.7189/jogh.09.020421>
- Palache, A., Abelin, A., Hollingsworth, R., Cracknell, W., Jacobs, C., Tsai, T., Barbosa, P., & IFPMA Influenza Vaccine Supply (IFPMA IVS) task force. (2017). Survey of distribution of seasonal influenza vaccine doses in 201 countries (2004-2015): The 2003 World Health Assembly resolution on seasonal influenza vaccination coverage and the 2009 influenza pandemic have had very little impact on improving influenza control and pandemic preparedness. *Vaccine*, 35(36), 4681–4686. <https://doi.org/10.1016/j.vaccine.2017.07.053>
- Palma, J., Tokarz-Deptuła, B., Deptuła, J., & Deptuła, W. (2018). Natural antibodies—Facts known and unknown. *Central-European Journal of Immunology*, 43(4), 466–475. <https://doi.org/10.5114/cej.2018.81354>

- Pardi, N., Parkhouse, K., Kirkpatrick, E., McMahon, M., Zost, S. J., Mui, B. L., Tam, Y. K., Karikó, K., Barbosa, C. J., Madden, T. D., Hope, M. J., Krammer, F., Hensley, S. E., & Weissman, D. (2018). Nucleoside-modified mRNA immunization elicits influenza virus hemagglutinin stalk-specific antibodies. *Nature Communications*, 9(1), 3361. <https://doi.org/10.1038/s41467-018-05482-0>
- Park, H. E., Gruenke, J. A., & White, J. M. (2003). Leash in the groove mechanism of membrane fusion. *Nature Structural Biology*, 10(12), 1048–1053. <https://doi.org/10.1038/nsb1012>
- Paterson, D., & Fodor, E. (2012). Emerging roles for the influenza A virus nuclear export protein (NEP). *PLoS Pathogens*, 8(12), e1003019. <https://doi.org/10.1371/journal.ppat.1003019>
- Paules, C. I., Marston, H. D., Eisinger, R. W., Baltimore, D., & Fauci, A. S. (2017). The Pathway to a Universal Influenza Vaccine. *Immunity*, 47(4), 599–603. <https://doi.org/10.1016/j.immuni.2017.09.007>
- Paules, C., & Subbarao, K. (2017). Influenza. *Lancet (London, England)*, 390(10095), 697–708. [https://doi.org/10.1016/S0140-6736\(17\)30129-0](https://doi.org/10.1016/S0140-6736(17)30129-0)
- Peacock, T. H. P., James, J., Sealy, J. E., & Iqbal, M. (2019). A Global Perspective on H9N2 Avian Influenza Virus. *Viruses*, 11(7), E620. <https://doi.org/10.3390/v11070620>
- Pérez Rubio, A., & Eiros, J. M. (2018). Cell culture-derived flu vaccine: Present and future. *Human Vaccines & Immunotherapeutics*, 14(8), 1874–1882. <https://doi.org/10.1080/21645515.2018.1460297>
- Perlmutter, J. D., & Hagan, M. F. (2015). Mechanisms of virus assembly. *Annual Review of Physical Chemistry*, 66, 217–239. <https://doi.org/10.1146/annurev-physchem-040214-121637>
- Peyret, H., Gehin, A., Thuenemann, E. C., Blond, D., El Turabi, A., Beales, L., Clarke, D., Gilbert, R. J. C., Fry, E. E., Stuart, D. I., Holmes, K., Stonehouse, N. J., Whelan, M., Rosenberg, W., Lomonosoff, G. P., & Rowlands, D. J. (2015). Tandem fusion of hepatitis B core antigen allows assembly of virus-like particles in bacteria and plants with enhanced capacity to accommodate foreign proteins. *PLoS One*, 10(4), e0120751. <https://doi.org/10.1371/journal.pone.0120751>
- Pflug, A., Lukarska, M., Resa-Infante, P., Reich, S., & Cusack, S. (2017). Structural insights into RNA synthesis by the influenza virus transcription-replication machine. *Virus Research*, 234, 103–117. <https://doi.org/10.1016/j.virusres.2017.01.013>
- Phan, T. G., Green, J. A., Gray, E. E., Xu, Y., & Cyster, J. G. (2009). Immune complex relay by subcapsular sinus macrophages and noncognate B cells drives antibody affinity maturation. *Nature Immunology*, 10(7), 786–793. <https://doi.org/10.1038/ni.1745>
- Pica, N., Hai, R., Krammer, F., Wang, T. T., Maamary, J., Eggink, D., Tan, G. S., Krause, J. C., Moran, T., Stein, C. R., Banach, D., Wrasmert, J., Belshe, R. B., García-Sastre, A., & Palese, P. (2012). Hemagglutinin stalk antibodies elicited by the 2009 pandemic influenza virus as a mechanism for the extinction of seasonal H1N1 viruses. *Proceedings of the National Academy of Sciences of the United States of America*, 109(7), 2573–2578. <https://doi.org/10.1073/pnas.1200039109>
- Pillet, S., Aubin, É., Trépanier, S., Poulin, J.-F., Yassine-Diab, B., Ter Meulen, J., Ward, B. J., & Landry, N. (2018). Humoral and cell-mediated immune responses to H5N1 plant-made virus-like particle vaccine are differentially impacted by alum and GLA-SE adjuvants in a Phase 2 clinical trial. *NPJ Vaccines*, 3, 3. <https://doi.org/10.1038/s41541-017-0043-3>
- Pillet, S., Couillard, J., Trépanier, S., Poulin, J.-F., Yassine-Diab, B., Guy, B., Ward, B. J., & Landry, N. (2019). Immunogenicity and safety of a quadrivalent plant-derived virus like particle influenza vaccine candidate—Two randomized Phase II clinical trials in 18 to 49 and ≥50 years old adults. *PLoS One*, 14(6), e0216533. <https://doi.org/10.1371/journal.pone.0216533>
- Pinto, L. H., Holsinger, L. J., & Lamb, R. A. (1992). Influenza virus M2 protein has ion channel activity. *Cell*, 69(3), 517–528. [https://doi.org/10.1016/0092-8674\(92\)90452-i](https://doi.org/10.1016/0092-8674(92)90452-i)
- Piroth, L., Cottenet, J., Mariet, A.-S., Bonniaud, P., Blot, M., Tubert-Bitter, P., & Quantin, C. (2021). Comparison of the characteristics, morbidity, and mortality of COVID-19 and seasonal influenza: A nationwide, population-based retrospective cohort study. *The Lancet. Respiratory Medicine*, 9(3), 251–259. [https://doi.org/10.1016/S2213-2600\(20\)30527-0](https://doi.org/10.1016/S2213-2600(20)30527-0)
- Pleguezuelos, O., James, E., Fernandez, A., Lopes, V., Rosas, L. A., Cervantes-Medina, A., Cleath, J., Edwards, K., Neitzey, D., Gu, W., Hunsberger, S., Taubenberger, J. K., Stoloff, G., & Memoli, M. J. (2020). Efficacy of FLU-v, a broad-spectrum influenza vaccine, in a randomized phase IIb human influenza challenge study. *NPJ Vaccines*, 5(1), 22. <https://doi.org/10.1038/s41541-020-0174-9>
- Portela, A., & Digard, P. (2002). The influenza virus nucleoprotein: A multifunctional RNA-binding protein pivotal to virus replication. *The Journal of General Virology*, 83(Pt 4), 723–734. <https://doi.org/10.1099/0022-1317-83-4-723>
- Portnoff, A. D., Patel, N., Massare, M. J., Zhou, H., Tian, J.-H., Zhou, B., Shinde, V., Glenn, G. M., & Smith, G. (2020). Influenza Hemagglutinin Nanoparticle Vaccine Elicits Broadly Neutralizing Antibodies against Structurally Distinct Domains of H3N2 HA. *Vaccines*, 8(1), E99. <https://doi.org/10.3390/vaccines8010099>
- Potter, C. W. (2001). A history of influenza. *Journal of Applied Microbiology*, 91(4), 572–579. <https://doi.org/10.1046/j.1365-2672.2001.01492.x>

- Preaud, E., Durand, L., Macabeo, B., Farkas, N., Sloesen, B., Palache, A., Shupo, F., Samson, S. I., & Vaccines Europe influenza working group. (2014). Annual public health and economic benefits of seasonal influenza vaccination: A European estimate. *BMC Public Health*, *14*, 813. <https://doi.org/10.1186/1471-2458-14-813>
- Price, G. E., Lo, C.-Y., Misplon, J. A., & Epstein, S. L. (2014). Mucosal immunization with a candidate universal influenza vaccine reduces virus transmission in a mouse model. *Journal of Virology*, *88*(11), 6019–6030. <https://doi.org/10.1128/JVI.03101-13>
- Pushko, P., Pumpens, P., & Grens, E. (2013). Development of virus-like particle technology from small highly symmetric to large complex virus-like particle structures. *Intervirology*, *56*(3), 141–165. <https://doi.org/10.1159/000346773>
- Putri, W. C. W. S., Muscatello, D. J., Stockwell, M. S., & Newall, A. T. (2018). Economic burden of seasonal influenza in the United States. *Vaccine*, *36*(27), 3960–3966. <https://doi.org/10.1016/j.vaccine.2018.05.057>
- Qian, C., Liu, X., Xu, Q., Wang, Z., Chen, J., Li, T., Zheng, Q., Yu, H., Gu, Y., Li, S., & Xia, N. (2020). Recent Progress on the Versatility of Virus-Like Particles. *Vaccines*, *8*(1), E139. <https://doi.org/10.3390/vaccines8010139>
- Rajaram, S., Wojcik, R., Moore, C., Ortiz de Lejarazu, R., de Lusignan, S., Montomoli, E., Rossi, A., Pérez-Rubio, A., Trilla, A., Baldo, V., Jandhyala, R., & Kassianos, G. (2020). The impact of candidate influenza virus and egg-based manufacture on vaccine effectiveness: Literature review and expert consensus. *Vaccine*, *38*(38), 6047–6056. <https://doi.org/10.1016/j.vaccine.2020.06.021>
- Rambaut, A., Pybus, O. G., Nelson, M. I., Viboud, C., Taubenberger, J. K., & Holmes, E. C. (2008). The genomic and epidemiological dynamics of human influenza A virus. *Nature*, *453*(7195), 615–619. <https://doi.org/10.1038/nature06945>
- Ramirez, A., Morris, S., Maucourant, S., D’Ascanio, I., Crescente, V., Lu, I.-N., Farinelle, S., Muller, C. P., Whelan, M., & Rosenberg, W. (2018). A virus-like particle vaccine candidate for influenza A virus based on multiple conserved antigens presented on hepatitis B tandem core particles. *Vaccine*, *36*(6), 873–880. <https://doi.org/10.1016/j.vaccine.2017.12.053>
- Ramos, E. L., Mitcham, J. L., Koller, T. D., Bonavia, A., Usner, D. W., Balaratnam, G., Fredlund, P., & Swiderek, K. M. (2015). Efficacy and safety of treatment with an anti-m2e monoclonal antibody in experimental human influenza. *The Journal of Infectious Diseases*, *211*(7), 1038–1044. <https://doi.org/10.1093/infdis/jiu539>
- Ran, Z., Shen, H., Lang, Y., Kolb, E. A., Turan, N., Zhu, L., Ma, J., Bawa, B., Liu, Q., Liu, H., Quast, M., Sexton, G., Krammer, F., Hause, B. M., Christopher-Hennings, J., Nelson, E. A., Richt, J., Li, F., & Ma, W. (2015). Domestic pigs are susceptible to infection with influenza B viruses. *Journal of Virology*, *89*(9), 4818–4826. <https://doi.org/10.1128/JVI.00059-15>
- Raymond, D. D., Stewart, S. M., Lee, J., Ferdman, J., Bajic, G., Do, K. T., Ernandes, M. J., Suphaphiphat, P., Settembre, E. C., Dormitzer, P. R., Del Giudice, G., Finco, O., Kang, T. H., Ippolito, G. C., Georgiou, G., Kepler, T. B., Haynes, B. F., Moody, M. A., Liao, H.-X., ... Harrison, S. C. (2016). Influenza immunization elicits antibodies specific for an egg-adapted vaccine strain. *Nature Medicine*, *22*(12), 1465–1469. <https://doi.org/10.1038/nm.4223>
- Raymond, F. L., Caton, A. J., Cox, N. J., Kendal, A. P., & Brownlee, G. G. (1986). The antigenicity and evolution of influenza H1 haemagglutinin, from 1950-1957 and 1977-1983: Two pathways from one gene. *Virology*, *148*(2), 275–287. [https://doi.org/10.1016/0042-6822\(86\)90325-9](https://doi.org/10.1016/0042-6822(86)90325-9)
- Reddy, S. T., Rehor, A., Schmoekel, H. G., Hubbell, J. A., & Swartz, M. A. (2006). In vivo targeting of dendritic cells in lymph nodes with poly(propylene sulfide) nanoparticles. *Journal of Controlled Release: Official Journal of the Controlled Release Society*, *112*(1), 26–34. <https://doi.org/10.1016/j.jconrel.2006.01.006>
- Röhn, T. A., Jennings, G. T., Hernandez, M., Grest, P., Beck, M., Zou, Y., Kopf, M., & Bachmann, M. F. (2006). Vaccination against IL-17 suppresses autoimmune arthritis and encephalomyelitis. *European Journal of Immunology*, *36*(11), 2857–2867. <https://doi.org/10.1002/eji.200636658>
- Rohr, J. R., Barrett, C. B., Civitello, D. J., Craft, M. E., Delius, B., DeLeo, G. A., Hudson, P. J., Jouanard, N., Nguyen, K. H., Ostfeld, R. S., Remais, J. V., Riveau, G., Sokolow, S. H., & Tilman, D. (2019). Emerging human infectious diseases and the links to global food production. *Nature Sustainability*, *2*(6), 445–456. <https://doi.org/10.1038/s41893-019-0293-3>
- Rossman, J. S., Jing, X., Leser, G. P., & Lamb, R. A. (2010). Influenza virus M2 protein mediates ESCRT-independent membrane scission. *Cell*, *142*(6), 902–913. <https://doi.org/10.1016/j.cell.2010.08.029>
- Rossman, J. S., & Lamb, R. A. (2011). Influenza virus assembly and budding. *Virology*, *411*(2), 229–236. <https://doi.org/10.1016/j.virol.2010.12.003>
- Russell, R. J., Gamblin, S. J., Haire, L. F., Stevens, D. J., Xiao, B., Ha, Y., & Skehel, J. J. (2004). H1 and H7 influenza haemagglutinin structures extend a structural classification of haemagglutinin subtypes. *Virology*, *325*(2), 287–296. <https://doi.org/10.1016/j.virol.2004.04.040>
- Saelens, X. (2019). The Role of Matrix Protein 2 Ectodomain in the Development of Universal Influenza Vaccines. *The Journal of Infectious Diseases*, *219*(Suppl_1), S68–S74. <https://doi.org/10.1093/infdis/jiz003>
- Sakai, T., Nishimura, S. I., Naito, T., & Saito, M. (2017). Influenza A virus hemagglutinin and neuraminidase act as novel motile machinery. *Scientific Reports*, *7*, 45043. <https://doi.org/10.1038/srep45043>

- Sakai-Tagawa, Y., Yamayoshi, S., Kawakami, C., Le, M. Q., Uchida, Y., Saito, T., Nidom, C. A., Humaira, I., Toohey-Kurth, K., Arafa, A.-S., Liu, M.-T., Shu, Y., & Kawaoka, Y. (2017). Reactivity and sensitivity of commercially available influenza rapid diagnostic tests in Japan. *Scientific Reports*, *7*(1), 14483. <https://doi.org/10.1038/s41598-017-14536-0>
- Sandbulte, M. R., Jimenez, G. S., Boon, A. C. M., Smith, L. R., Treanor, J. J., & Webby, R. J. (2007). Cross-reactive neuraminidase antibodies afford partial protection against H5N1 in mice and are present in unexposed humans. *PLoS Medicine*, *4*(2), e59. <https://doi.org/10.1371/journal.pmed.0040059>
- Saunders-Hastings, P. R., & Krewski, D. (2016). Reviewing the History of Pandemic Influenza: Understanding Patterns of Emergence and Transmission. *Pathogens (Basel, Switzerland)*, *5*(4), E66. <https://doi.org/10.3390/pathogens5040066>
- Schmitz, N., Beerli, R. R., Bauer, M., Jegerlehner, A., Dietmeier, K., Maudrich, M., Pumpens, P., Saudan, P., & Bachmann, M. F. (2012). Universal vaccine against influenza virus: Linking TLR signaling to anti-viral protection. *European Journal of Immunology*, *42*(4), 863–869. <https://doi.org/10.1002/eji.201041225>
- Schneemann, A., Speir, J. A., Tan, G. S., Khayat, R., Ekiert, D. C., Matsuoka, Y., & Wilson, I. A. (2012). A virus-like particle that elicits cross-reactive antibodies to the conserved stem of influenza virus hemagglutinin. *Journal of Virology*, *86*(21), 11686–11697. <https://doi.org/10.1128/JVI.01694-12>
- Schnell, J. R., & Chou, J. J. (2008). Structure and mechanism of the M2 proton channel of influenza A virus. *Nature*, *451*(7178), 591–595. <https://doi.org/10.1038/nature06531>
- Schotsaert, M., Ysenbaert, T., Smet, A., Schepens, B., Vanderschaeghe, D., Stegalkina, S., Vogel, T. U., Callewaert, N., Fiers, W., & Saelens, X. (2016). Long-Lasting Cross-Protection Against Influenza A by Neuraminidase and M2e-based immunization strategies. *Scientific Reports*, *6*, 24402. <https://doi.org/10.1038/srep24402>
- Schwarz, B., & Douglas, T. (2015). Development of virus-like particles for diagnostic and prophylactic biomedical applications. *Wiley Interdisciplinary Reviews. Nanomedicine and Nanobiotechnology*, *7*(5), 722–735. <https://doi.org/10.1002/wnan.1336>
- Scotti, N., & Rybicki, E. P. (2013). Virus-like particles produced in plants as potential vaccines. *Expert Review of Vaccines*, *12*(2), 211–224. <https://doi.org/10.1586/erv.12.147>
- Sederdahl, B. K., & Williams, J. V. (2020). Epidemiology and Clinical Characteristics of Influenza C Virus. *Viruses*, *12*(1), E89. <https://doi.org/10.3390/v12010089>
- Seladi-Schulman, J., Steel, J., & Lowen, A. C. (2013). Spherical influenza viruses have a fitness advantage in embryonated eggs, while filament-producing strains are selected in vivo. *Journal of Virology*, *87*(24), 13343–13353. <https://doi.org/10.1128/JVI.02004-13>
- Sellers, S. A., Hagan, R. S., Hayden, F. G., & Fischer, W. A. (2017). The hidden burden of influenza: A review of the extra-pulmonary complications of influenza infection. *Influenza and Other Respiratory Viruses*, *11*(5), 372–393. <https://doi.org/10.1111/irv.12470>
- Selman, M., Dankar, S. K., Forbes, N. E., Jia, J.-J., & Brown, E. G. (2012). Adaptive mutation in influenza A virus non-structural gene is linked to host switching and induces a novel protein by alternative splicing. *Emerging Microbes & Infections*, *1*(11), e42. <https://doi.org/10.1038/emi.2012.38>
- Selzer, L., Su, Z., Pintelie, G. D., Chiu, W., & Kirkegaard, K. (2020). Full-length three-dimensional structure of the influenza A virus M1 protein and its organization into a matrix layer. *PLoS Biology*, *18*(9), e3000827. <https://doi.org/10.1371/journal.pbio.3000827>
- Shah, N. H., & Muir, T. W. (2014). Inteins: Nature's Gift to Protein Chemists. *Chemical Science*, *5*(1), 446–461. <https://doi.org/10.1039/C3SC52951G>
- Shanks, G. D., & Brundage, J. F. (2012). Pathogenic responses among young adults during the 1918 influenza pandemic. *Emerging Infectious Diseases*, *18*(2), 201–207. <https://doi.org/10.3201/eid1802.102042>
- Shinde, V., Fries, L., Wu, Y., Agrawal, S., Cho, I., Thomas, D. N., Spindler, M., Lindner, E., Hahn, T., Plested, J., Flyer, D., Massare, M. J., Zhou, B., Fix, A., Smith, G., & Glenn, G. M. (2018). Improved Titers against Influenza Drift Variants with a Nanoparticle Vaccine. *The New England Journal of Medicine*, *378*(24), 2346–2348. <https://doi.org/10.1056/NEJMc1803554>
- Shirbaghaee, Z., & Bolhassani, A. (2016). Different applications of virus-like particles in biology and medicine: Vaccination and delivery systems. *Biopolymers*, *105*(3), 113–132. <https://doi.org/10.1002/bip.22759>
- Shrestha, S. S., Swerdlow, D. L., Borse, R. H., Prabhu, V. S., Finelli, L., Atkins, C. Y., Owusu-Edusei, K., Bell, B., Mead, P. S., Biggerstaff, M., Brammer, L., Davidson, H., Jernigan, D., Jung, M. A., Kamimoto, L. A., Merlin, T. L., Nowell, M., Redd, S. C., Reed, C., ... Meltzer, M. I. (2011). Estimating the burden of 2009 pandemic influenza A (H1N1) in the United States (April 2009–April 2010). *Clinical Infectious Diseases: An Official Publication of the Infectious Diseases Society of America*, *52* Suppl 1, S75–82. <https://doi.org/10.1093/cid/ciq012>
- Simhadri, V. R., Dimitrova, M., Mariano, J. L., Zenarruabeitia, O., Zhong, W., Ozawa, T., Muraguchi, A., Kishi, H., Eichelberger, M. C., & Borrego, F. (2015). A Human Anti-M2 Antibody Mediates Antibody-Dependent Cell-Mediated Cytotoxicity (ADCC) and Cytokine Secretion by Resting and Cytokine-Preactivated Natural Killer (NK) Cells. *PLoS One*, *10*(4), e0124677. <https://doi.org/10.1371/journal.pone.0124677>

- Simonsen, L., Clarke, M. J., Schonberger, L. B., Arden, N. H., Cox, N. J., & Fukuda, K. (1998). Pandemic versus epidemic influenza mortality: A pattern of changing age distribution. *The Journal of Infectious Diseases*, *178*(1), 53–60. <https://doi.org/10.1086/515616>
- Skowronski, D. M., Janjua, N. Z., De Serres, G., Sabaiduc, S., Eshaghi, A., Dickinson, J. A., Fonseca, K., Winter, A.-L., Gubbay, J. B., Kraiden, M., Petric, M., Charest, H., Bastien, N., Kwindt, T. L., Mahmud, S. M., Van Caesele, P., & Li, Y. (2014). Low 2012-13 influenza vaccine effectiveness associated with mutation in the egg-adapted H3N2 vaccine strain not antigenic drift in circulating viruses. *PloS One*, *9*(3), e92153. <https://doi.org/10.1371/journal.pone.0092153>
- Smith, D. M., Simon, J. K., & Baker, J. R. (2013a). Applications of nanotechnology for immunology. *Nature Reviews. Immunology*, *13*(8), 592–605. <https://doi.org/10.1038/nri3488>
- Smith, D. M., Simon, J. K., & Baker, J. R. (2013b). Applications of nanotechnology for immunology. *Nature Reviews. Immunology*, *13*(8), 592–605. <https://doi.org/10.1038/nri3488>
- Smith, M. T., Hawes, A. K., & Bundy, B. C. (2013). Reengineering viruses and virus-like particles through chemical functionalization strategies. *Current Opinion in Biotechnology*, *24*(4), 620–626. <https://doi.org/10.1016/j.copbio.2013.01.011>
- Smith, W., Andrewes, C. H., & Laidlaw, P. P. (1933). A VIRUS OBTAINED FROM INFLUENZA PATIENTS. *The Lancet*, *222*(5732), 66–68. [https://doi.org/10.1016/S0140-6736\(00\)78541-2](https://doi.org/10.1016/S0140-6736(00)78541-2)
- Smrt, S. T., Draney, A. W., & Lorieau, J. L. (2015). The influenza hemagglutinin fusion domain is an amphipathic helical hairpin that functions by inducing membrane curvature. *The Journal of Biological Chemistry*, *290*(1), 228–238. <https://doi.org/10.1074/jbc.M114.611657>
- Soema, P. C., Kompier, R., Amorij, J.-P., & Kersten, G. F. A. (2015). Current and next generation influenza vaccines: Formulation and production strategies. *European Journal of Pharmaceutics and Biopharmaceutics: Official Journal of Arbeitsgemeinschaft Fur Pharmazeutische Verfahrenstechnik e.V.*, *94*, 251–263. <https://doi.org/10.1016/j.ejpb.2015.05.023>
- Somes, M. P., Turner, R. M., Dwyer, L. J., & Newall, A. T. (2018). Estimating the annual attack rate of seasonal influenza among unvaccinated individuals: A systematic review and meta-analysis. *Vaccine*, *36*(23), 3199–3207. <https://doi.org/10.1016/j.vaccine.2018.04.063>
- Sparrow, E., Wood, J. G., Chadwick, C., Newall, A. T., Torvaldsen, S., Moen, A., & Torelli, G. (2021). Global production capacity of seasonal and pandemic influenza vaccines in 2019. *Vaccine*, *39*(3), 512–520. <https://doi.org/10.1016/j.vaccine.2020.12.018>
- Srivastava, V., Yang, Z., Hung, I. F. N., Xu, J., Zheng, B., & Zhang, M.-Y. (2013). Identification of dominant antibody-dependent cell-mediated cytotoxicity epitopes on the hemagglutinin antigen of pandemic H1N1 influenza virus. *Journal of Virology*, *87*(10), 5831–5840. <https://doi.org/10.1128/JVI.00273-13>
- Staneková, Z., Király, J., Stropkovská, A., Mikušková, T., Mucha, V., Kostolanský, F., & Varečková, E. (2011). Heterosubtypic protective immunity against influenza A virus induced by fusion peptide of the hemagglutinin in comparison to ectodomain of M2 protein. *Acta Virologica*, *55*(1), 61–67. https://doi.org/10.4149/av_2011_01_61
- Steel, J., Lowen, A. C., Wang, T. T., Yondola, M., Gao, Q., Haye, K., García-Sastre, A., & Palese, P. (2010). Influenza virus vaccine based on the conserved hemagglutinin stalk domain. *MBio*, *1*(1), e00018-10. <https://doi.org/10.1128/mBio.00018-10>
- Sui, J., Hwang, W. C., Perez, S., Wei, G., Aird, D., Chen, L., Santelli, E., Stec, B., Cadwell, G., Ali, M., Wan, H., Murakami, A., Yammanuru, A., Han, T., Cox, N. J., Bankston, L. A., Donis, R. O., Liddington, R. C., & Marasco, W. A. (2009). Structural and functional bases for broad-spectrum neutralization of avian and human influenza A viruses. *Nature Structural & Molecular Biology*, *16*(3), 265–273. <https://doi.org/10.1038/nsmb.1566>
- Sutton, T. C. (2018). The Pandemic Threat of Emerging H5 and H7 Avian Influenza Viruses. *Viruses*, *10*(9), E461. <https://doi.org/10.3390/v10090461>
- Syomin, B. V., & Ilyin, Y. V. (2019). Virus-Like Particles as an Instrument of Vaccine Production. *Molecular Biology*, *53*(3), 323–334. <https://doi.org/10.1134/S0026893319030154>
- Tamerius, J. D., Shaman, J., Alonso, W. J., Bloom-Feshbach, K., Uejio, C. K., Comrie, A., & Viboud, C. (2013). Environmental predictors of seasonal influenza epidemics across temperate and tropical climates. *PLoS Pathogens*, *9*(3), e1003194. <https://doi.org/10.1371/journal.ppat.1003194>
- Tang, S., Xuan, B., Ye, X., Huang, Z., & Qian, Z. (2016). A Modular Vaccine Development Platform Based on Sortase-Mediated Site-Specific Tagging of Antigens onto Virus-Like Particles. *Scientific Reports*, *6*, 25741. <https://doi.org/10.1038/srep25741>
- Tao, P., Zhu, J., Mahalingam, M., Batra, H., & Rao, V. B. (2019). Bacteriophage T4 nanoparticles for vaccine delivery against infectious diseases. *Advanced Drug Delivery Reviews*, *145*, 57–72. <https://doi.org/10.1016/j.addr.2018.06.025>
- Tars, K., Fridborg, K., Bundule, M., & Liljas, L. (2000). The three-dimensional structure of bacteriophage PP7 from *Pseudomonas aeruginosa* at 3.7-Å resolution. *Virology*, *272*(2), 331–337. <https://doi.org/10.1006/viro.2000.0373>
- Taubenberger, J. K., & Morens, D. M. (2006). 1918 Influenza: The mother of all pandemics. *Emerging Infectious Diseases*, *12*(1), 15–22. <https://doi.org/10.3201/eid1201.050979>

- Taylor, K. M., Lin, T., Porta, C., Mosser, A. G., Giesing, H. A., Lomonosoff, G. P., & Johnson, J. E. (2000). Influence of three-dimensional structure on the immunogenicity of a peptide expressed on the surface of a plant virus. *Journal of Molecular Recognition: JMR*, *13*(2), 71–82. [https://doi.org/10.1002/\(SICI\)1099-1352\(200003/04\)13:2<71::AID-JMR489>3.0.CO;2-V](https://doi.org/10.1002/(SICI)1099-1352(200003/04)13:2<71::AID-JMR489>3.0.CO;2-V)
- Terajima, M., Babon, J. A. B., Co, M. D. T., & Ennis, F. A. (2013). Cross-reactive human B cell and T cell epitopes between influenza A and B viruses. *Virology Journal*, *10*, 244. <https://doi.org/10.1186/1743-422X-10-244>
- Thermo Scientific. (2021). *Pierce™ SATA (N-succinimidyl S-acetylthioacetate)*. <https://www.thermofisher.com/order/catalog/product/26102>
- Thornburg, N. J., Zhang, H., Bangaru, S., Sapparapu, G., Kose, N., Lampley, R. M., Bombardi, R. G., Yu, Y., Graham, S., Branchizio, A., Yoder, S. M., Rock, M. T., Creech, C. B., Edwards, K. M., Lee, D., Li, S., Wilson, I. A., García-Sastre, A., Albrecht, R. A., & Crowe, J. E. (2016). H7N9 influenza virus neutralizing antibodies that possess few somatic mutations. *The Journal of Clinical Investigation*, *126*(4), 1482–1494. <https://doi.org/10.1172/JCI85317>
- Tompkins, S. M., Zhao, Z.-S., Lo, C.-Y., Mispion, J. A., Liu, T., Ye, Z., Hogan, R. J., Wu, Z., Benton, K. A., Tumpey, T. M., & Epstein, S. L. (2007). Matrix protein 2 vaccination and protection against influenza viruses, including subtype H5N1. *Emerging Infectious Diseases*, *13*(3), 426–435. <https://doi.org/10.3201/eid1303.061125>
- Tong, S., Li, Y., Rivailler, P., Conrardy, C., Castillo, D. A. A., Chen, L.-M., Recuenco, S., Ellison, J. A., Davis, C. T., York, I. A., Turmelle, A. S., Moran, D., Rogers, S., Shi, M., Tao, Y., Weil, M. R., Tang, K., Rowe, L. A., Sammons, S., ... Donis, R. O. (2012). A distinct lineage of influenza A virus from bats. *Proceedings of the National Academy of Sciences of the United States of America*, *109*(11), 4269–4274. <https://doi.org/10.1073/pnas.1116200109>
- Tong, S., Zhu, X., Li, Y., Shi, M., Zhang, J., Bourgeois, M., Yang, H., Chen, X., Recuenco, S., Gomez, J., Chen, L.-M., Johnson, A., Tao, Y., Dreyfus, C., Yu, W., McBride, R., Carney, P. J., Gilbert, A. T., Chang, J., ... Donis, R. O. (2013). New world bats harbor diverse influenza A viruses. *PLoS Pathogens*, *9*(10), e1003657. <https://doi.org/10.1371/journal.ppat.1003657>
- Topham, D. J., Tripp, R. A., & Doherty, P. C. (1997). CD8+ T cells clear influenza virus by perforin or Fas-dependent processes. *Journal of Immunology (Baltimore, Md.: 1950)*, *159*(11), 5197–5200.
- Tsuchiya, E., Sugawara, K., Hongo, S., Matsuzaki, Y., Muraki, Y., Li, Z.-N., & Nakamura, K. (2001). Antigenic structure of the haemagglutinin of human influenza A/H2N2 virus. *The Journal of General Virology*, *82*(Pt 10), 2475–2484. <https://doi.org/10.1099/0022-1317-82-10-2475>
- Tsybalova, L. M., Stepanova, L. A., Kuprianov, V. V., Blokhina, E. A., Potapchuk, M. V., Korotkov, A. V., Gorshkov, A. N., Kasyanenko, M. A., Ravin, N. V., & Kiselev, O. I. (2015). Development of a candidate influenza vaccine based on virus-like particles displaying influenza M2e peptide into the immunodominant region of hepatitis B core antigen: Broad protective efficacy of particles carrying four copies of M2e. *Vaccine*, *33*(29), 3398–3406. <https://doi.org/10.1016/j.vaccine.2015.04.073>
- Turley, C. B., Rupp, R. E., Johnson, C., Taylor, D. N., Wolfson, J., Tussey, L., Kavita, U., Stanberry, L., & Shaw, A. (2011). Safety and immunogenicity of a recombinant M2e-flagellin influenza vaccine (STF2.4xM2e) in healthy adults. *Vaccine*, *29*(32), 5145–5152. <https://doi.org/10.1016/j.vaccine.2011.05.041>
- Tutykhina, I., Esmagambetov, I., Bagaev, A., Pichugin, A., Lysenko, A., Shcherbinin, D., Sedova, E., Logunov, D., Shmarov, M., Ataulakhanov, R., Naroditsky, B., & Gintsburg, A. (2018). Vaccination potential of B and T epitope-enriched NP and M2 against Influenza A viruses from different clades and hosts. *PLoS One*, *13*(1), e0191574. <https://doi.org/10.1371/journal.pone.0191574>
- Valkenburg, S. A., Mallajosyula, V. V. A., Li, O. T. W., Chin, A. W. H., Carnell, G., Temperton, N., Varadarajan, R., & Poon, L. L. M. (2016). Stalking influenza by vaccination with pre-fusion headless HA mini-stem. *Scientific Reports*, *6*, 22666. <https://doi.org/10.1038/srep22666>
- Varga, Z. T., & Palese, P. (2011). The influenza A virus protein PB1-F2: Killing two birds with one stone? *Virulence*, *2*(6), 542–546. <https://doi.org/10.4161/viru.2.6.17812>
- Vasin, A. V., Temkina, O. A., Egorov, V. V., Klotchenko, S. A., Plotnikova, M. A., & Kiselev, O. I. (2014). Molecular mechanisms enhancing the proteome of influenza A viruses: An overview of recently discovered proteins. *Virus Research*, *185*, 53–63. <https://doi.org/10.1016/j.virusres.2014.03.015>
- Walsh, G., & Jefferis, R. (2006). Post-translational modifications in the context of therapeutic proteins. *Nature Biotechnology*, *24*(10), 1241–1252. <https://doi.org/10.1038/nbt1252>
- Wan, H., & Perez, D. R. (2006). Quail carry sialic acid receptors compatible with binding of avian and human influenza viruses. *Virology*, *346*(2), 278–286. <https://doi.org/10.1016/j.virol.2005.10.035>
- Wan, Y., & Jeffrey, S. (2014). Does exposure to poultry and wild fowl confer immunity to H5N1? *Chinese Medical Journal*, *127*(18), 3335–3343.
- Wang, R., Song, A., Levin, J., Dennis, D., Zhang, N. J., Yoshida, H., Koriazova, L., Madura, L., Shapiro, L., Matsumoto, A., Yoshida, H., Mikayama, T., Kubo, R. T., Sarawar, S., Cheroutre, H., & Kato, S. (2008). Therapeutic potential of a fully human monoclonal antibody against influenza A virus M2 protein. *Antiviral Research*, *80*(2), 168–177. <https://doi.org/10.1016/j.antiviral.2008.06.002>

- Wang, T. T., Tan, G. S., Hai, R., Pica, N., Ngai, L., Ekiert, D. C., Wilson, I. A., García-Sastre, A., Moran, T. M., & Palese, P. (2010). Vaccination with a synthetic peptide from the influenza virus hemagglutinin provides protection against distinct viral subtypes. *Proceedings of the National Academy of Sciences of the United States of America*, *107*(44), 18979–18984. <https://doi.org/10.1073/pnas.1013387107>
- Wang, W., Li, R., Deng, Y., Lu, N., Chen, H., Meng, X., Wang, W., Wang, X., Yan, K., Qi, X., Zhang, X., Xin, W., Lu, Z., Li, X., Bian, T., Gao, Y., Tan, W., & Ruan, L. (2015). Protective Efficacy of the Conserved NP, PB1, and M1 Proteins as Immunogens in DNA- and Vaccinia Virus-Based Universal Influenza A Virus Vaccines in Mice. *Clinical and Vaccine Immunology: CVI*, *22*(6), 618–630. <https://doi.org/10.1128/CVI.00091-15>
- Watanabe, A., Chang, S.-C., Kim, M. J., Chu, D. W.-S., Ohashi, Y., & MARVEL Study Group. (2010). Long-acting neuraminidase inhibitor laninamivir octanoate versus oseltamivir for treatment of influenza: A double-blind, randomized, noninferiority clinical trial. *Clinical Infectious Diseases: An Official Publication of the Infectious Diseases Society of America*, *51*(10), 1167–1175. <https://doi.org/10.1086/656802>
- Watanabe, T., Watanabe, S., Maher, E. A., Neumann, G., & Kawaoka, Y. (2014). Pandemic potential of avian influenza A (H7N9) viruses. *Trends in Microbiology*, *22*(11), 623–631. <https://doi.org/10.1016/j.tim.2014.08.008>
- Webster, R. G., Bean, W. J., Gorman, O. T., Chambers, T. M., & Kawaoka, Y. (1992). Evolution and ecology of influenza A viruses. *Microbiological Reviews*, *56*(1), 152–179. <https://doi.org/10.1128/mr.56.1.152-179.1992>
- Wei, C.-J., Boyington, J. C., McTamney, P. M., Kong, W.-P., Pearce, M. B., Xu, L., Andersen, H., Rao, S., Tumpey, T. M., Yang, Z.-Y., & Nabel, G. J. (2010). Induction of broadly neutralizing H1N1 influenza antibodies by vaccination. *Science (New York, N.Y.)*, *329*(5995), 1060–1064. <https://doi.org/10.1126/science.1192517>
- Weis, W., Brown, J. H., Cusack, S., Paulson, J. C., Skehel, J. J., & Wiley, D. C. (1988). Structure of the influenza virus haemagglutinin complexed with its receptor, sialic acid. *Nature*, *333*(6172), 426–431. <https://doi.org/10.1038/333426a0>
- WHO. (2018). *Influenza (Seasonal)*. [https://www.who.int/news-room/fact-sheets/detail/influenza-\(seasonal\)](https://www.who.int/news-room/fact-sheets/detail/influenza-(seasonal))
- WHO. (2021a). *Global Influenza Programme*. <https://www.who.int/teams/control-of-neglected-tropical-diseases/yaws/diagnosis-and-treatment/global-influenza-programme>
- WHO. (2021b). *Human infection with avian influenza A(H10N3) – China*. [https://www.who.int/emergencies/disease-outbreak-news/item/human-infection-with-avian-influenza-a\(h10n3\)-china](https://www.who.int/emergencies/disease-outbreak-news/item/human-infection-with-avian-influenza-a(h10n3)-china)
- Wiley, D. C., & Skehel, J. J. (1987). The structure and function of the hemagglutinin membrane glycoprotein of influenza virus. *Annual Review of Biochemistry*, *56*, 365–394. <https://doi.org/10.1146/annurev.bi.56.070187.002053>
- Wiley, D. C., Wilson, I. A., & Skehel, J. J. (1981). Structural identification of the antibody-binding sites of Hong Kong influenza haemagglutinin and their involvement in antigenic variation. *Nature*, *289*(5796), 373–378. <https://doi.org/10.1038/289373a0>
- Wilkinson, T. M., Li, C. K. F., Chui, C. S. C., Huang, A. K. Y., Perkins, M., Liebner, J. C., Lambkin-Williams, R., Gilbert, A., Oxford, J., Nicholas, B., Staples, K. J., Dong, T., Douek, D. C., McMichael, A. J., & Xu, X.-N. (2012). Preexisting influenza-specific CD4+ T cells correlate with disease protection against influenza challenge in humans. *Nature Medicine*, *18*(2), 274–280. <https://doi.org/10.1038/nm.2612>
- Wilson, I. A., Skehel, J. J., & Wiley, D. C. (1981). Structure of the haemagglutinin membrane glycoprotein of influenza virus at 3 Å resolution. *Nature*, *289*(5796), 366–373. <https://doi.org/10.1038/289366a0>
- Wise, H. M., Foeglein, A., Sun, J., Dalton, R. M., Patel, S., Howard, W., Anderson, E. C., Barclay, W. S., & Digard, P. (2009). A complicated message: Identification of a novel PB1-related protein translated from influenza A virus segment 2 mRNA. *Journal of Virology*, *83*(16), 8021–8031. <https://doi.org/10.1128/JVI.00826-09>
- Wise, H. M., Hutchinson, E. C., Jagger, B. W., Stuart, A. D., Kang, Z. H., Robb, N., Schwartzman, L. M., Kash, J. C., Fodor, E., Firth, A. E., Gog, J. R., Taubenberger, J. K., & Digard, P. (2012). Identification of a novel splice variant form of the influenza A virus M2 ion channel with an antigenically distinct ectodomain. *PLoS Pathogens*, *8*(11), e1002998. <https://doi.org/10.1371/journal.ppat.1002998>
- Wong, K. K. Y., Rockman, S., Ong, C., Bull, R., Stelzer-Braid, S., & Rawlinson, W. (2013). Comparison of influenza virus replication fidelity in vitro using selection pressure with monoclonal antibodies. *Journal of Medical Virology*, *85*(6), 1090–1094. <https://doi.org/10.1002/jmv.23532>
- Woodland, D. L. (2003). Cell-mediated immunity to respiratory virus infections. *Current Opinion in Immunology*, *15*(4), 430–435. [https://doi.org/10.1016/s0952-7915\(03\)00067-0](https://doi.org/10.1016/s0952-7915(03)00067-0)
- Wu, N. C., & Wilson, I. A. (2018). Structural insights into the design of novel anti-influenza therapies. *Nature Structural & Molecular Biology*, *25*(2), 115–121. <https://doi.org/10.1038/s41594-018-0025-9>
- Wu, N. C., Zost, S. J., Thompson, A. J., Oyen, D., Nycholat, C. M., McBride, R., Paulson, J. C., Hensley, S. E., & Wilson, I. A. (2017). A structural explanation for the low effectiveness of the seasonal influenza H3N2 vaccine. *PLoS Pathogens*, *13*(10), e1006682. <https://doi.org/10.1371/journal.ppat.1006682>
- Xu, H., Bao, X., Wang, Y., Xu, Y., Deng, B., Lu, Y., & Hou, J. (2018). Engineering T7 bacteriophage as a potential DNA vaccine targeting delivery vector. *Virology Journal*, *15*(1), 49. <https://doi.org/10.1186/s12985-018-0955-1>

- Xu, R., Ekiert, D. C., Krause, J. C., Hai, R., Crowe, J. E., & Wilson, I. A. (2010). Structural basis of preexisting immunity to the 2009 H1N1 pandemic influenza virus. *Science (New York, N.Y.)*, *328*(5976), 357–360. <https://doi.org/10.1126/science.1186430>
- Xu, R., & Wilson, I. A. (2011). Structural characterization of an early fusion intermediate of influenza virus hemagglutinin. *Journal of Virology*, *85*(10), 5172–5182. <https://doi.org/10.1128/JVI.02430-10>
- Yamayoshi, S., & Kawaoka, Y. (2019a). Current and future influenza vaccines. *Nature Medicine*, *25*(2), 212–220. <https://doi.org/10.1038/s41591-018-0340-z>
- Yamayoshi, S., & Kawaoka, Y. (2019b). Current and future influenza vaccines. *Nature Medicine*, *25*(2), 212–220. <https://doi.org/10.1038/s41591-018-0340-z>
- Yamayoshi, S., Uraki, R., Ito, M., Kiso, M., Nakatsu, S., Yasuhara, A., Oishi, K., Sasaki, T., Ikuta, K., & Kawaoka, Y. (2017). A Broadly Reactive Human Anti-hemagglutinin Stem Monoclonal Antibody That Inhibits Influenza A Virus Particle Release. *EBioMedicine*, *17*, 182–191. <https://doi.org/10.1016/j.ebiom.2017.03.007>
- Yassine, H. M., Boyington, J. C., McTamney, P. M., Wei, C.-J., Kanekiyo, M., Kong, W.-P., Gallagher, J. R., Wang, L., Zhang, Y., Joyce, M. G., Lingwood, D., Moin, S. M., Andersen, H., Okuno, Y., Rao, S. S., Harris, A. K., Kwong, P. D., Mascola, J. R., Nabel, G. J., & Graham, B. S. (2015). Hemagglutinin-stem nanoparticles generate heterosubtypic influenza protection. *Nature Medicine*, *21*(9), 1065–1070. <https://doi.org/10.1038/nm.3927>
- Yoon, S.-W., Webby, R. J., & Webster, R. G. (2014). Evolution and ecology of influenza A viruses. *Current Topics in Microbiology and Immunology*, *385*, 359–375. https://doi.org/10.1007/82_2014_396
- York, I., & Donis, R. O. (2013). The 2009 pandemic influenza virus: Where did it come from, where is it now, and where is it going? *Current Topics in Microbiology and Immunology*, *370*, 241–257. https://doi.org/10.1007/82_2012_221
- Young, B., Sadarangani, S., Jiang, L., Wilder-Smith, A., & Chen, M. I.-C. (2018). Duration of Influenza Vaccine Effectiveness: A Systematic Review, Meta-analysis, and Meta-regression of Test-Negative Design Case-Control Studies. *The Journal of Infectious Diseases*, *217*(5), 731–741. <https://doi.org/10.1093/infdis/jix632>
- Zabel, F., Kündig, T. M., & Bachmann, M. F. (2013). Virus-induced humoral immunity: On how B cell responses are initiated. *Current Opinion in Virology*, *3*(3), 357–362. <https://doi.org/10.1016/j.coviro.2013.05.004>
- Zebedee, S. L., & Lamb, R. A. (1988). Influenza A virus M2 protein: Monoclonal antibody restriction of virus growth and detection of M2 in virions. *Journal of Virology*, *62*(8), 2762–2772. <https://doi.org/10.1128/JVI.62.8.2762-2772.1988>
- Zhang, Y., Zhang, Q., Kong, H., Jiang, Y., Gao, Y., Deng, G., Shi, J., Tian, G., Liu, L., Liu, J., Guan, Y., Bu, Z., & Chen, H. (2013). H5N1 hybrid viruses bearing 2009/H1N1 virus genes transmit in guinea pigs by respiratory droplet. *Science (New York, N.Y.)*, *340*(6139), 1459–1463. <https://doi.org/10.1126/science.1229455>
- Zhao, Y., Sun, F., Li, L., Chen, T., Cao, S., Ding, G., Cong, F., Liu, J., Qin, L., Liu, S., & Xiao, Y. (2020). Evolution and Pathogenicity of the H1 and H3 Subtypes of Swine Influenza Virus in Mice between 2016 and 2019 in China. *Viruses*, *12*(3), E298. <https://doi.org/10.3390/v12030298>
- Zheng, D., Chen, S., Qu, D., Chen, J., Wang, F., Zhang, R., & Chen, Z. (2016). Influenza H7N9 LAH-HBc virus-like particle vaccine with adjuvant protects mice against homologous and heterologous influenza viruses. *Vaccine*, *34*(51), 6464–6471. <https://doi.org/10.1016/j.vaccine.2016.11.026>
- Zhirnov, O. P., Ikizler, M. R., & Wright, P. F. (2002). Cleavage of influenza a virus hemagglutinin in human respiratory epithelium is cell associated and sensitive to exogenous antiproteases. *Journal of Virology*, *76*(17), 8682–8689. <https://doi.org/10.1128/jvi.76.17.8682-8689.2002>
- Zhou, D., Wu, T.-L., Lasaro, M. O., Latimer, B. P., Parzych, E. M., Bian, A., Li, Y., Li, H., Erikson, J., Xiang, Z., & Ertl, H. C. J. (2010). A universal influenza A vaccine based on adenovirus expressing matrix-2 ectodomain and nucleoprotein protects mice from lethal challenge. *Molecular Therapy: The Journal of the American Society of Gene Therapy*, *18*(12), 2182–2189. <https://doi.org/10.1038/mt.2010.202>
- Zhou, Y., Wu, C., Zhao, L., & Huang, N. (2014). Exploring the early stages of the pH-induced conformational change of influenza hemagglutinin. *Proteins*, *82*(10), 2412–2428. <https://doi.org/10.1002/prot.24606>
- Zhu, X., Guo, Y.-H., Jiang, T., Wang, Y.-D., Chan, K.-H., Li, X.-F., Yu, W., McBride, R., Paulson, J. C., Yuen, K.-Y., Qin, C.-F., Che, X.-Y., & Wilson, I. A. (2013). A unique and conserved neutralization epitope in H5N1 influenza viruses identified by an antibody against the A/Goose/Guangdong/1/96 hemagglutinin. *Journal of Virology*, *87*(23), 12619–12635. <https://doi.org/10.1128/JVI.01577-13>
- Zlotnick, A. (1994). To build a virus capsid. An equilibrium model of the self assembly of polyhedral protein complexes. *Journal of Molecular Biology*, *241*(1), 59–67. <https://doi.org/10.1006/jmbi.1994.1473>
- Zost, S. J., Wu, N. C., Hensley, S. E., & Wilson, I. A. (2019). Immunodominance and Antigenic Variation of Influenza Virus Hemagglutinin: Implications for Design of Universal Vaccine Immunogens. *The Journal of Infectious Diseases*, *219*(Suppl_1), S38–S45. <https://doi.org/10.1093/infdis/jiy696>

APPENDICES

Appendix 1. Examples of broadly protective influenza vaccine candidates in research and clinical trials

Influenza antigens*	Platform or vector	Protection against death	Stage	References
M1, NP, M2e	Synthetic polyepitope peptide	-	Phase 2b	(Pleguezuelos et al., 2020)
M1, NP	Modified replication-incompetent vaccinia virus Ankara (MVA) vector encoding conserved epitopes	-	Phase 2a	(Lillie et al., 2012)
4xM2e	M2e fused to <i>Salmonella typhimurium</i> flagellin	-	Phase 2	(Turley et al., 2011)
M2e, NP	Fusion protein	-	Phase 1b	(Dynavax, 2011)
A/H1/A/Idaho/07/2018 (H1N1), A/Perth/1008/2019H3N2), B/Colorado/06/2017, B/Phuket/3073/2013	Pentamer yeast <i>C. albicans</i> lumazine synthase displaying 20 HA molecules	-	Phase 1	NCT04896086
M1, NP, PB1	Modified replication-competent vaccinia virus Ankara (MVA) vector encoding conserved epitopes	Complete against H1N1	Animal models	(W. Wang et al., 2015)
NP, M2	Prime with plasmid DNA encoding NP or M2, or both, boost with replication-incompetent adenovirus encoding NP, M2, or both	Complete against H1N1 and H5N1	Animal models	(Lo et al., 2008)
NP	Prime with plasmid DNA encoding NP, boost with replication-incompetent adenovirus encoding NP	High against H1N1, complete against H3N2, No symptoms after sub-lethal H5N1	Animal models	(Epstein et al., 2005)
M2, NP, NP (B)	Replication-incompetent adenovirus vector encoding conserved epitopes	Complete against H1N1, H5N2, H9N2, high against H1N1, H3N2	Animal models	(Price et al., 2014; Tutykhina et al., 2018)
M2	Prime with plasmid DNA encoding M, boost with replication-incompetent adenovirus encoding M2	Complete against different H1N1 viruses, H5N1	Animal models	(Tompkins et al., 2007)
5xM2e	VLPs displaying M2e as a supplement for H1N1 split vaccine	Complete against H3N2 and rgH5N1	Animal models	(M.-C. Kim et al., 2014)
3xM2e	M2e fused to mucosal adjuvant CTA1-DD	Complete against H3N2	Animal models	(Eliasson et al., 2008)

5xM2e	VLPs displaying M2e	Slight symptoms after sub-lethal H1N1 infection, complete protection against secondary H5N1 infection	Animal models	(Y.-N. Lee et al., 2016)
3xM2e, NP	Replication-incompetent adenovirus encoding fusion protein of M2e and NP	High protection against different H1N1 viruses	Animal models	(D. Zhou et al., 2010)
M2e	M2e fused to tetrameric leucine zipper from the yeast transcription factor <i>GCN4</i>	Complete against H3N2	Animal models	(De Filette et al., 2008)
5xM2e	M2e epitope expressed on VLPs in Sf-9 insect cells	Complete against H1N1 or H3N2	Animal models	(M.-C. Kim et al., 2013)
M2e	M2e fused to rotavirus fragment NSP ₄₉₈₋₁₃₅	Complete against H1N1	Animal models	(Andersson et al., 2012)
4xM2e	M2e fused to decameric <i>Brucella abortus</i> lumazine synthase protein	Complete against H1N1	Animal models	(Alvarez et al., 2013)
M2e	M2e fused to keyhole limpet hemocyanin (KLH) or <i>Neisseria meningitidis</i> outer membrane protein complex	Complete against H1N1 or H3N1, no protection against H5N1	Animal models	(Fan et al., 2004)
Full-length HA	A prime-boost regiment with chimeric HAs consisting of H8 and H5 head domains combined with H1 stalk	-	Phase 1	(Nachbagauer et al., 2021)
Full-length HA	Nucleoside-modified mRNA encoding H1 HA enclosed in lipid nanoparticles	Complete homologous (H1), heterologous (H1), and heterosubtypic (H5)	Animal models	(Pardi et al., 2018)
Full-length HA	DNA encoding H5 HA as a prime for conventional vaccines	-	Phase 1	(Ledgerwood et al., 2011)
Full-length HA	DNA encoding H1 HA as a prime for conventional vaccines or replication-incompetent adenovirus 5 encoding HA	Complete heterologous (H1)	Animal models	(Wei et al., 2010)
Pre-fusion HA stalk	Headless-HA based on H1 and H3 HA	Complete homologous (H1)	Animal models	(Steel et al., 2010)
Pre-fusion HA stalk	H5-based headless HA stabilized fused to a synthetic trimerization motif "Foldon"	Complete heterologous (H1), heterosubtypic (H5), and cross-group (H3)	Animal models	(Valkenburg et al., 2016)
Pre-fusion HA stalk	H1-based headless HA stabilized with helical leucine zipper trimerization domain	Complete heterologous (H1) and heterosubtypic (H5)	Animal models	(Impagliazzo et al., 2015)
Pre-fusion HA stalk	H1-based headless HA on ferritin nanoparticles stabilized with HIV-1 glycoprotein 41 trimerization domain that was later removed	Complete heterosubtypic (H5) (mice), partial heterosubtypic (H5) (ferrets)	Animal models, Phase I	(Yassine et al., 2015); NCT03186781

Pre-fusion HA stalk	H5-based headless HA stabilized fused to a synthetic trimerization motif "Foldon"	Complete heterosubtypic (H1), limited cross-group (H3)	Animal models	(Mallajosyula et al., 2014)
HA stalk peptide, M2e	Synthetic H3 HA stalk glycopolypeptide and M2e fused to keyhole limpet hemocyanin	Complete homologous and heterosubtypic (H3, H1) (low dose), partial homologous and heterosubtypic (high dose)	Animal models	(Staneková et al., 2011)
Full length HA	Full-length H1 HA with hyperglycosylated head	Complete heterosubtypic (H9)	Animal models	(Eggink et al., 2014)
Full length HA	Full-length H5 HA with hyperglycosylated head	Complete heterologous (H5)	Animal models	(Lin et al., 2014)
Post-fusion HA stalk	H1-based headless HA	Complete homologous (H3), heterologous (H7)	Animal models	(Adachi et al., 2019)
Full-length HA	A prime-boost regiment with chimeric HAs consisting of H9, H5, and H6 (whole virus) head domains combined with H1 stalk	Complete heterologous (H1)	Animal models	(Nachbagauer et al., 2015)
Full-length HA	A prime-boost regiment with chimeric HAs consisting of H9 (whole virus or DNA), H6 or H1, and H5 or H1 head domains combined with H1 stalk	Complete homologous (H1), heterologous (H1) and heterosubtypic (H5, H6)	Animal models	(Krammer et al., 2013)

*Type A influenza if not unless stated otherwise

Appendix 2. Examples of native VLP vaccines against influenza in clinical trials

VLP antigens	Expression system	Development stage	References
A/Michigan/45/2015 (H1N1), A/Hong Kong/4801/2014 (H3N2), and B/Brisbane/60/2008 HA	Insect cells (Sf-9 cells)	Phase 1/2a	(Shinde et al., 2018)
A/Hong Kong/4801/2014 (H3N2) HA	Insect cells (Sf-9 cells)	Phase 1/2a	(Portnoff et al., 2020)
A/Indonesia/05/2005 (H5N1) HA	Plant (<i>Nicotiana benthamiana</i>)	Phase 2	(Pillet et al., 2018)
A/California/04/2009 (H1N1) HA and NA, A/Indonesia/05/2005 (H5N1) M1	Insect cells (Sf-9 cells)	Phase 2	(López-Macías et al., 2011)
A/California/07/2009 (H1N1), A/Victoria/361/2011 (H3N2), B/Brisbane/60/2008 (B, Victoria lineage), or B/Wisconsin/1/2010 (B, Yamagata lineage) HA	Plant (<i>Nicotiana benthamiana</i>)	Phase 3	NCT03739112
A/California/07/2009 (H1N1), A/Victoria/361/11 (H3N2), B/Brisbane/60/08 (B, Victoria lineage), and B/Massachusetts/02/2012 (B, Yamagata lineage) HA	Plant (<i>Nicotiana benthamiana</i>)	Phase 2	(Pillet et al., 2019)
A/Brisbane/59/07 (H1N1), A/Brisbane/10/07 (H1N1), B/Florida/04/06 (H3N2) HA and NA	Insect cells (Sf-9 cells)	Phase 2a	(Shirbaghaee & Bolhassani, 2016); NCT00754455
A/Brisbane/02/2018 (H1N1), A/Kansas/14/2017 (H3N2), B/Maryland/15/2016 (B, Victoria lineage), B/Phuket/3073/2013 (B, Yamagata lineage)	Insect cells (Sf-9 cells)	Phase 3	NCT04120194

Appendix 3. Examples of chimeric VLP vaccines against influenza in research and clinical trials

Modification approach	VLP platform	Display antigens	Expression system	Development stage	References
Modular	Q-VLPs	A/California/07/2009 (H1N1) HA (gH1 domain)	Bacteria (<i>E. coli</i>)	Phase 1	(Low et al., 2014)
Genetic	HBcAg	Influenza A M2e	Bacteria (<i>E. coli</i>)	Phase 1	NCT00819013
Genetic	HBcAg	Influenza A 4xM2e	Bacteria (<i>E. coli</i>)	Phase 1/2	(Tsybalova et al., 2015); NCT03789539
Genetic	HBcAg	Linear A/Shanghai/2/2013 (H7N9) HA stalk	Bacteria (<i>E. coli</i>)	Animal models	(Zheng et al., 2016)
Genetic	AP205 VLPs	Influenza A M2e	Bacteria (<i>E. coli</i>)	Animal models	(Schmitz et al., 2012)
Genetic	HBcAg	Linear A/Puerto Rico/8/1934 (H1N1) HA stalk	Bacteria (<i>E. coli</i>)	Animal models	(S. Chen et al., 2015)
Genetic	HBcAg	Linear A/Puerto Rico/8/1934 (H1N1) HA stalk and 3x M2e	Bacteria (<i>E. coli</i>)	Animal models	(Ramirez et al., 2018)
Genetic	Flock House virus VLPs	A/South Carolina/1/1918 (H1N1) HA A-helix	Bacteria (<i>E. coli</i>)	Animal models	(Schneemann et al., 2012)
Genetic	HBcAg	Influenza A 3xM2e and NP	Bacteria (<i>E. coli</i>)	Animal models	(X. Gao et al., 2013)
Genetic	T7 phage VLPs	Influenza A virus 3xM2e	Bacteria (<i>E. coli</i>)	Animal models	(Hashemi et al., 2012)
Genetic	M13 phage gpVIII VLPs	Influenza A virus M2e	Bacteria (<i>E. coli</i>)	Animal models	(Lotfi et al., 2019)
Modular	HPV VLPs	A/Aichi/470/68 (H3N1) M2	Yeast (<i>S. cerevisiae</i>) and <i>t</i> -Boc solid phase synthesis	Animal models	(Ionescu et al., 2006)